

UNIVERSITY
PENNSYLVANIA
LIBRARIES



CHARACTERIZATION AND ANALYSIS OF THE CALICHE WALLS OF
THE GREAT HOUSE, CASA GRANDE RUINS NATIONAL
MONUMENT, COOLIDGE, ARIZONA

ELISA MARIA DEL BONO

A THESIS


in

Historic Preservation

Presented to the Faculties of the University of Pennsylvania in
Partial Fulfillment of the Requirements for the Degree of

MASTER OF SCIENCE

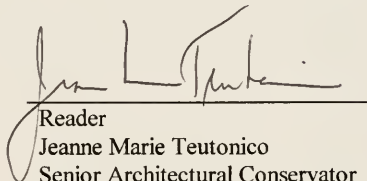
1999



Supervisor

Frank G. Matero

Associate Professor of Architecture



Reader

Jeanne Marie Teutonico

Senior Architectural Conservator
English Heritage



Acting Graduate Group Chair

David G. De Long

File Am/NA/02/1999.279

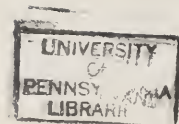


TABLE OF CONTENTS

ACKNOWLEDGMENTS	iv
LIST OF FIGURES	v
LIST OF TABLES	xi
CHAPTER 1: INTRODUCTION	1
1.1 Objectives and Methodology	2
CHAPTER 2: EXISTING CONDITIONS (PHASE 1)	5
2.1 Conditions of the Site	5
2.1.1 Local Geology and Soil Characteristics	5
2.1.2 Climate and Vegetation	11
2.2 Conditions of the Structure	15
2.2.1 Plan and Construction	15
2.2.2 Construction Material	22
2.2.3 Wall Construction Technique	25
2.2.4 Condition as a Ruin. The Shelter	30
CHAPTER 3: CHARACTERIZATION AND ANALYSIS OF THE GREAT HOUSE CALICHE AS A BUILDING MATERIAL (PHASE 2)	35
3.1 Caliche	35
3.1.1 Definition	35
3.1.2 Origins	36
3.1.3 Chemical Description	37
3.1.4 Genesis	39
3.1.5 Classifications	41
3.1.6 Uses Today	43
3.2 Testing Program	43
3.2.1 Previous Analyses	43
3.2.2 Sampling	45
3.2.3 Observations	48
3.2.4 Test Program	53
3.2.4.1 Bulk Mineralogy (X-Ray Diffraction)	54
3.2.4.2 Identification of Clays (X-Ray Diffraction)	58
3.2.4.3 Microscopic Observations (Polarized Microscopy and Scanning Electron Microscopy)	61
3.2.4.4 Acid-Soluble (Carbonate) Content	83
3.2.4.5 Particle Size Analysis (ASTM D422-63)	91
3.2.4.6 Particle Description	98
3.2.4.7 Atterberg Limits (Liquid Limit and Plastic Limit) (ASTM D4318)	101
3.2.4.8 Volumetric and Linear Shrinkage (ASTM D4943-89)	103

3.2.4.9 Determination of Moisture and Soluble Salt Content and Qualitative Analysis of Water-Soluble Salts	107
3.2.4.10 Compressive Strength (ASTM D1633)	111
3.2.4.11 Three-Point Bending (Modulus of Rupture) (ASTM D1635)	115
3.2.4.12 Water Related Tests: Wet/Dry Cycling (ASTM D559 modified), Water Resistance (Water Drop Test, CRATerre), and Capillary Water Absorption (NORMAL 11/85)	118
CHAPTER 4: DIAGNOSIS OF DETERIORATION AND PERFORMANCE ASSESSMENT OF THE GREAT HOUSE CALICHE AS A BUILDING MATERIAL (PHASE 3)	133
4.1. Processes of Deterioration of the Great House	133
4.1.1 Intrinsic Causes of Deterioration	137
4.1.1.1 Related to the Material	137
4.1.1.2 Related to the Construction Technique	143
4.1.1.3 Related to the Condition as a Ruin	147
4.1.2 Extrinsic Causes of Deterioration	149
4.1.2.1 Natural Factors	149
4.1.2.2 Human Factors	164
CHAPTER 5: INTERPRETATION OF DETERIORATION: NEW FINDINGS	167
5.1 Wall Construction Technique	167
5.2 Construction Sequence	171
CHAPTER 6: RECOMMENDATIONS AND CONCLUSIONS	187
6.1 Recommendations	187
6.1.1 Recommendations on Detachment and Falling Fragments of Caliche	188
6.1.2 Recommendations on Weathering of Friable Surface	193
6.1.3 General Recommendations	199
6.2 Conclusions	202
BIBLIOGRAPHY	207
APPENDICES	217
Appendix A: Previous Scientific Projects and Stabilization on the Great House and Casa Grande Ruins National Monument	218
Appendix B: Previous Analyses of the Caliche from the Great House	229
Appendix C: Observations and Tests	240
INDEX	277

ACKNOWLEDGEMENTS

The author wishes to express special gratitude to Frank G. Matero and Jeanne Marie Teutonico for their invaluable comments, constant support and encouragement.

Also, it is desired to express special appreciation to:

Jake Barrow, Exhibit Specialist, and Robert Hartzler, Architectural Conservator, from the Conservation Projects Program, Intermountain Support Office, National Park Service, Santa Fe, New Mexico;

Donald Spencer, Superintendent; Nathan Allen, former Ranger; and all personnel from Casa Grande Ruins National Monument, Coolidge, Arizona;

David Evans, Preservation Specialist, and James Rancier, former Archaeologist, from the National Park Service, Southern Arizona Group;

Gomar Omar, Eric Johansen and Elena Charola of the University of Pennsylvania;

Alex Radin and Xiu Chen from the “Laboratory for Research on the Structure of Matter”, University of Pennsylvania;

Karen Fix, Rynta Fourie, and all the persons that kindly gave their constant support and help for writing the present study.

LIST OF FIGURES

Figure 1: Map of location of Casa Grande Ruins National Monument	6
Figure 2: Typical pedon of Coolidge sandy loam	10
Figure 3: Present vegetation inside Casa Grande Ruins National Monument	14
Figure 4: Plan and west-east section (looking south) of the Great House	17
Figure 5: North view of the Great House	18
Figure 6: South view of the Great House	18
Figure 7: East view of the Great House	19
Figure 8: West view of the Great House	19
Figure 9: Example of water erosion in an area underneath a possible roof drain location (east elevation Tier D, right of the outer opening)	21
Figure 10: Painting (anonymous) that represents a channel dug by the Hohokams	23
Figure 11: Plan and west-east section of the Great House according to its present condition	32
Figure 12: The original shelter roof, constructed in 1903. Photo courtesy of Casa Grande Ruins National Monument	33
Figure 13: The second (present) shelter	34
Figure 14: Location on the west elevation from where the fragment of caliche fell in 1995	46
Figure 15: Close up Figure 14	46
Figure 16: Photograph showing the 1995 fragment divided in three smaller	

fragments upon impact on the ground	47
Figure 17: Dimensions of the caliche wall fragment	48
Figure 18: Caliche fragment during saw cutting	50
Figure 19: Orientation of each slab and location of different bands for samples	51
Figure 20: Caliche slab before (above) and after dividing in three bands (CAGR A, CAGR B and CAGR C)	52
Figure 21: X-ray diffraction of caliche fines (material passed sieve #200)	56
Figure 22: X-ray diffraction results of a caliche nodule (retained #4)	57
Figure 23: X-ray diffraction results of palygorskite as the clay mineral from the caliche	60
Figure 24: Material selection and sample preparation of caliche for thin-section	66
Figure 25: Microstructure of caliche	67
Figure 26: Anhedral quartz crystals of different grain size (2-10 μ m)	69
Figure 27: Subhedral microcline crystal (approximately 40 μ m long)	70
Figure 28: Elongated caliche nodule formed by calcite cryptocrystalline matrix (stained) enclosing and gluing together two quartz crystals	71
Figure 29: Subrounded nodule with porphyritic texture (stained)	72
Figure 30: Microcrystalline matrix of a nodule (stained) at high magnification	73
Figure 31: Subrounded nodule (stained) with porphyritic texture composed of poikilitic quartz crystals in a cryptocrystalline calcic matrix	31
Figure 32: Montaged microphotographs of caliche thin section (stained) showing a close porphyritic texture, composed of crystals (mainly quartz) and	

nodules of different shapes and sizes embedded in a cryptocrystalline calcic matrix (birefringence fabric)	76
Figure 33: SEM photographs showing caliche micromorphology, sample CAGR Ext (top) and CAGR Int (bottom)	78
Figure 34: SEM photograph of aggregate (probably sand grain) embedded in the caliche matrix	79
Figure 35: SEM Photographs of caliche micromorphology	80
Figure 36: SEM photographs of a palygorkite (clay) crystal (top) and back scattered image (bottom)	81
Figure 37: Percentage of calcium carbonate content by total acid digestion of samples	85
Figure 38: Separation of caliche sample by particle size using standard sieves and de-ionized water	88
Figure 39: Distribution of calcium carbonate content in the smaller grain size fractions (retained #30, #50, #100, #200 and passed #200) of sample CAGR B according to its total gross weight	88
Figure 40: Distribution of calcium carbonate content in the larger grains size fractions (#4, #16, #30 and passed #30) of sample CAGR C according to its total gross weight	89
Figure 41: Weight percentage of calcium carbonate content by particle size for samples CAGR B and CAGR C	91
Figure 42: Particle size analysis of the caliche without acid digestion	94

Figure 43: Particle size analysis of the caliche after total acid digestion	95
Figure 44: Comparative particle size analysis of the caliche with and without acid digestion	96
Figure 45: Comparative results of content of aggregates (gravel and sand) and fines (silt and clay) in the caliche with and without acid digestion (percentage by weight)	97
Figure 46: Particles retained on sieve #8 (2.36mm). Nodules of caliche, rounded in shape	99
Figure 47: Different sizes of caliche nodules of various shapes (subrounded to angular)	99
Figure 48: Sand (quartz-like) particles partially coated by calcium carbonate matrix	100
Figure 49: Particles retained on sieve #30 (600 μ m)	100
Figure 50: Linear and volumetric shrinkage of caliche with and without acid digestion	106
Figure 51: Caliche specimen during compression test	114
Figure 52: Caliche specimen after compression test	114
Figure 53: Caliche specimen during the three-point bending test (modulus of rupture)	117
Figure 54: Caliche specimen during the three-point bending test (modulus of rupture)	117
Figure 55: Percentage of total loss of samples of caliche after 12 cycles, wet-dry	

cycling test	120
Figure 56: Samples during first immersion cycle, wet-dry cycling test	121
Figure 57: Samples during last immersion cycle, wet-dry cycling test	121
Figure 58: Rate of loss of different caliche samples according to cycle, wet-dry cycling test	123
Figure 59: Caliche samples before wet-dry cycling test	124
Figure 60: Caliche samples after 12 cycles, wet-dry cycling test	124
Figure 61: Crater formed in caliche sample CAGR Int during water resistance (water drop) test	127
Figure 62: Samples of caliche after water resistance (water drop) test	127
Figure 63: Caliche samples during capillary water absorption test	130
Figure 64: Capillary water absorption of caliche samples	131
Figure 65: Intrinsic and extrinsic causes of deterioration	135
Figure 66: Section of wall showing movement of calcium carbonate in the caliche (case hardening) due to weathering (water movement) and exposure	139
Figure 67: Deterioration of caliche due to crust loss	141
Figure 68: Areas of wall where the calcium carbonate crust has been lost	142
Figure 69: A wall construction seam and drying cracks on the east elevation of the Great House	145
Figure 70: Deterioration and missing caliche near the parapet of the Great House probably caused by water (rain) deterioration	154

Figure 71: Deterioration (microhoodoos) caused by wind erosion	158
Figure 72: Close up of figure 71.	158
Figure 73: Proposed wall course construction	170
Figure 74: Crack on wall end (east elevation, north wall end) that suggests the proposed course construction	171
Figure 75: Different wall cold joints (interruption of continuity)	172
Figure 76: Course wall cross section showing different vulnerabilities due to cold joints (wall construction), movement of calcium carbonate (weathering), and various nature-related causes of deterioration	173
Figure 77: Loss of wall fragments	174
Figure 78: South elevation with evidence of tier construction	177
Figure 79: West elevation with evidence of tier construction	178
Figure 80: East elevation with evidence of tier construction	179
Figure 81: West wall end on the south elevation	180
Figure 82: Wall seam and north wall end, east elevation	181
Figure 83: Interior wall seams (corners) inside Tier A, looking west	181
Figure 84: Plan of the Great House with all wall seams and reconstruction of missing corners	183
Figure 84: Proposal of tier construction	184
Figure 85: Proposal of staging of construction within a single building episode	185

LIST OF TABLES

Table 1: Calcium carbonate content and distribution in samples CAGR A, CAGR B and CAGR C	90
Table 2: Liquid limit, plastic limit and plasticity index for caliche samples with and without acid digestion	103
Table 3: Wilcox and Shenk's results (1977) on soluble salts content of samples from a caliche fragment that fell off the west elevation of the Great House in 1975	108
Table 4: Results of moisture and soluble salts content for the caliche soil	108
Table 5: Presence of ions by semi-micro chemical reactions for the caliche soil	111
Table 6: Results for compressive strength of caliche samples	113
Table 7: Results of three-point bending (modulus of rupture) for a molded caliche sample	116
Table 8: Loss per cycle in relation to original weight of sample (percent)	123
Table 9: Average results of capillary water absorption of caliche samples	131

CHAPTER 1: INTRODUCTION

Casa Grande Ruins National Monument, located one mile south of the Gila River near Coolidge, Arizona, has long been considered a site of major significance in the cultural history of the American Southwest. Built during the fourteenth century¹ by the area's early inhabitants, known as the Hohokam, the site is a complex of various earthen structures, including buildings, walls and platforms arranged in compounds, constructed using "puddled caliche". The most dramatic structure at the site is the multistory earthen Great House (or Casa Grande).² This is the only remaining intact structure of its kind in the American Southwest and has intrigued visitors and scholars for nearly three centuries.

Casa Grande was the first archaeological site in the United States to be protected as a national preserve by Congress; Casa Grande Reservation was created on June 22, 1892 by order of President Benjamin Harrison. Cosmos Mindeleff, on behalf of the Smithsonian Institution, initiated stabilization of the Great House in 1891, the first such stabilization of an earthen structure in the United States.

In 1903 a shelter was erected over and within the structure to protect it from environmental deterioration. Later, in 1932, a second shelter was constructed, replacing the earlier roof.

¹ Wilcox and Shenk 1977, 58. Other authors, such as Clemensen (1992, 8) mention the thirteenth century as the time when structures similar to the Great House began to be constructed, that is during the Classic Period, which began about AD 1175.

² Father Francisco Eusebio Kino first named the structure "*Casa Grande*" (big house) in 1694 (Wilcox and Shenk 1977, 201). In the literature, the structure is referred to both as "*Casa Grande*" or "Great House". For the present study, it was decided to use the name "Great House" for the structure in order to differentiate it from the name of the monument.

The National Park Service has been concerned about the condition and structural stability of the Great House since the earliest days when the site became a monument and much more since 1956. Several scientific studies were initiated to determine the causes and possible remedies for deterioration. The structural analysis done by Kreigh and Sultan (1974) and the documentation of Wilcox and Shenk (1977), especially have contributed much to an understanding of the Great House.

In 1996 the National Park Service's Architectural Conservation Projects Program, Intermountain Support Office, Santa Fe, New Mexico and the Architectural Conservation Laboratory of the Graduate Program in Historic Preservation at the University of Pennsylvania began the development of a long-term conservation program to better understand the conditions, pathologies and potential interventions for the Great House. As a part of this program, the present thesis addresses the characterization and analysis of the caliche walls of the Great House.

1.1 Objectives and Methodology

As with all immovable cultural property, especially archaeological sites, the uncontrolled and open environment is the primary cause of physical deterioration. Exposed and uninhabited, earthen ruins are particularly vulnerable to the natural processes of weathering and to human and animal impact. For more than 500 years the Great House has withstood the processes of erosion that still threaten to destroy it today.

The main objective of this thesis is two-fold: (1) the analysis and characterization of the construction material—a caliche or calcareous soil—used in the construction of the Great House (microscale) and (2) the diagnosis of the major deterioration mechanisms based on the material analysis and characterization (macroscale) in order to provide recommendations for future preservation and maintenance.

The methodology followed in the present thesis has lead to the development of three phases:

Phase 1: Identification of the condition of the Great House and its site

Identification of the condition of the site, as well as that of the structure, was carried out both in the field and through the literature and archival research.

Phase 2: Characterization and Analysis of the Great House Caliche as a Building Material

Comprises a testing program developed to analyze and characterize the caliche from the Great House. Different tests and analytical techniques were selected in order to identify and compare physical , chemical and mechanical properties and/or alterations to the material overtime.

Phase 3: Diagnosis of Deterioration and Performance, and Assessment of the Great House Caliche as a Building Material

Archaeological sites are inextricably tied to their landscapes and must be addressed accordingly. Results obtained from the testing of the caliche were evaluated within the environmental and structural context of the Great House and its processes of deterioration

were identified. Site observations and data collected from the recent conditions survey produced new findings that serve as invaluable data for consideration of future intervention and maintenance. This phase includes a series of recommendations that will help National Park Service personnel in the future management of the Great House.

CHAPTER 2: EXISTING CONDITIONS (PHASE 1)

2.1 Conditions of the Site

2.1.1 Local Geology and Soil Characteristics

Casa Grande Ruins National Monument is located in Pinal County, Arizona. This area corresponds to the Basin and Range province, which is characterized by numerous mountain ranges¹ that rise abruptly from broad, plainlike valleys or basins. These features have resulted mainly from mid-Tertiary block faulting. Uplifted blocks eroded to form mountains and pediments, and the downfaulted blocks filled with sediment (United States Department of Agriculture 1991, 83).

In addition, this area is located in the Phoenix basin which is part of the Sonoran desert that covers most of southwestern Arizona and northwestern Mexico, and extends into the southeastern part of California (United States Department of Agriculture 1991, 83).

Formation of the major drainageways in the area is believed to have occurred prior to a major mountain building epoch 25 to 40 million years ago. These ancestral rivers were tributary systems that are now the Colorado River. The river flowed in a northwesterly direction through the area. The great canyons formed during the later Tertiary and early Quaternary periods gradually collected alluvial deposits from higher adjacent mountain slopes. Most of the parent material accumulated in this way, however, some resulted from eolian transport (United States Department of Agriculture 1991, 83).

¹ Mountain ranges are formed by Pre-Cambrian granites and schists. Some are cut by younger granitic rocks and flanked by Tertiary lava flows (United States Department of Agriculture 1991, 83).

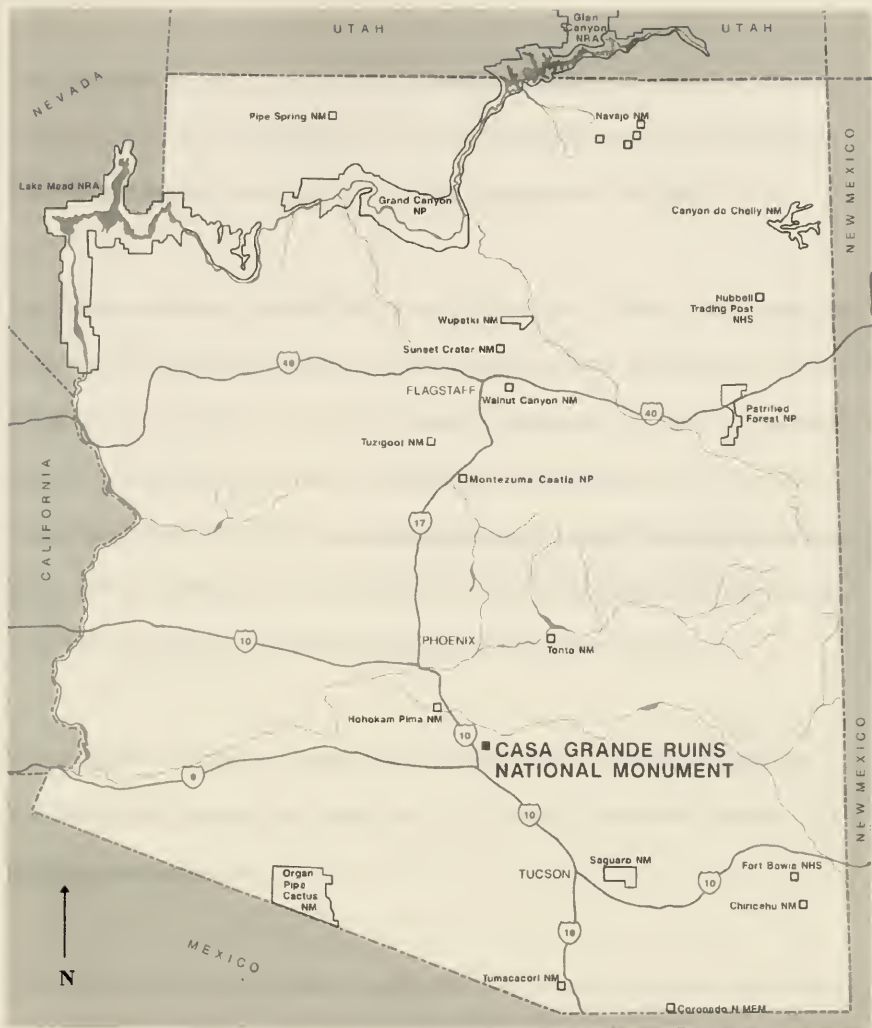


Figure 1: Map of Location of Casa Grande Ruins National Monument

The deposits of the Santa Cruz River contributed most of the stream alluvium. Stream alluvium can also be traced to alluvial deposits of the Gila River and the McClellan and Santa Rosa Washes (United States Department of Agriculture 1991, 83).

Fan alluvium in the area is derived from a variety of sources. Granite, gneiss, schist, and basalt are the dominant rock sources. Andesite, shale, quartzite, and limestone are present but they are not extensive. Fan alluvium appears to have occurred in two environments that are transitional to one another. Narrows belts of active erosion and sedimentation (channels) alternate with wide areas in which there was rather uniform sedimentation and little erosion (interfluves). Cross-bedding and cut-and-fill structures are common on the proximal end of fans (United States Department of Agriculture 1991, 83).

The monument is located on the drainage of McClellan Wash (a tributary of the Gila River) and has an elevation that ranges from 1,427 feet in the southeast corner to 1,414 feet on the northwest side.

The majority of the state of Arizona, specifically the area of the monument, is covered by Aridisols (dry soils) which are soils with a deficiency of water as their major characteristic (Brady and Weil 1996, 85).

Aridisols are characterized by an ochric epipedon² that is generally light in color and low in organic matter. The process of soil formation for Aridisols include a redistribution of soluble materials and their subsequent accumulation at a lower level in the soil profile. Thus, these soils may have an accumulation of calcium carbonate (calcic), gypsum (gypsic), soluble salts (salic), or exchangeable sodium (natric). In addition, they may have an argillic (clays) horizon as indication of a wetter period at some time during their soil formation (Brady and Weil 1996, 85).

The soils of Pinal County appear to have evolved as a result of a wide variety of past climatic conditions. Indeed, the development of argillic horizons, duripans, petrocalcic horizons, and probably most calcic horizons must have been different, cooler and wetter, than the present climate (United States Department of Agriculture 1991, 87).

According to the “Soil Survey of Pinal County, Arizona, Western Part” (United States Department of Agriculture, 1991) the soil map unit which corresponds to the location of Casa Grande Ruins National Monument is the “Denure-Laveen-Dateland series”. Specifically, the Monument lays on the “Coolidge series” (commonly referred as “Coolidge sandy loam”).

The Coolidge series consists of deep, somewhat excessively drained soil, located on fan terraces and stream terraces. These soils formed in fan and stream alluvium derived from

² Epipedon: “A diagnostic surface horizon that includes the upper part of the soil that is darkened by organic matter, or the upper eluvial horizons, or both” (Brady and Weil 1996, 703).

granite, schist, andesite, rhyolite, and some basalt. Its slope is 0 to 1 percent and its elevation is 1,140 to 2,000 feet. The average annual precipitation is about 6 to 8 inches, the average annual air temperature is 68°F to 72°F, and the average frost-free season is 240 to 325 days. According to the National Cooperative Soil Survey's system of soil classification, these soils are coarse-loamy, mixed, hyperthermic Typic Calciorthids³ (United States Department of Agriculture 1991, 63).

Ordinarily, the Coolidge Series has a light brown sandy loam surface layer about 7 inches thick. The subsoil is light brown sandy loam, 12 inches thick. This layer is slightly saline and moderately to strongly sodic. The next layer of the soil is pink, pinkish white, and light brown sandy loam about 25 inches thick. Below this to a depth of 60 inches or more is light brown sandy clay loam. Many soft masses of calcium carbonate are at a depth of 14 to 60 inches. A layer of calcium carbonate accumulation (commonly known as caliche) is found at a depth of 14 to 30 inches. Other characteristics of these soils are: moderately rapid permeability, moderate available water capacity, 60 inches or more of potential rooting depth, medium runoff, slight danger of water erosion, moderate danger of soil blowing, and less than 0.4% of organic carbon in the surface layer. Presently, this soil is mostly used for irrigated crops, rangeland, and homesite development. However, homesite development is limited by the high content of calcium carbonate and toxic salts (United States Department of Agriculture 1991, 63).

³ The system of soil classification used by the National Cooperative Soil Survey has six categories (order, suborder, great group, subgroup, family, and series) to classify a soil. Classification is based on soil properties observed in the field or derived from those observations or from laboratory measurements (United States Department of Agriculture 1991, 57).

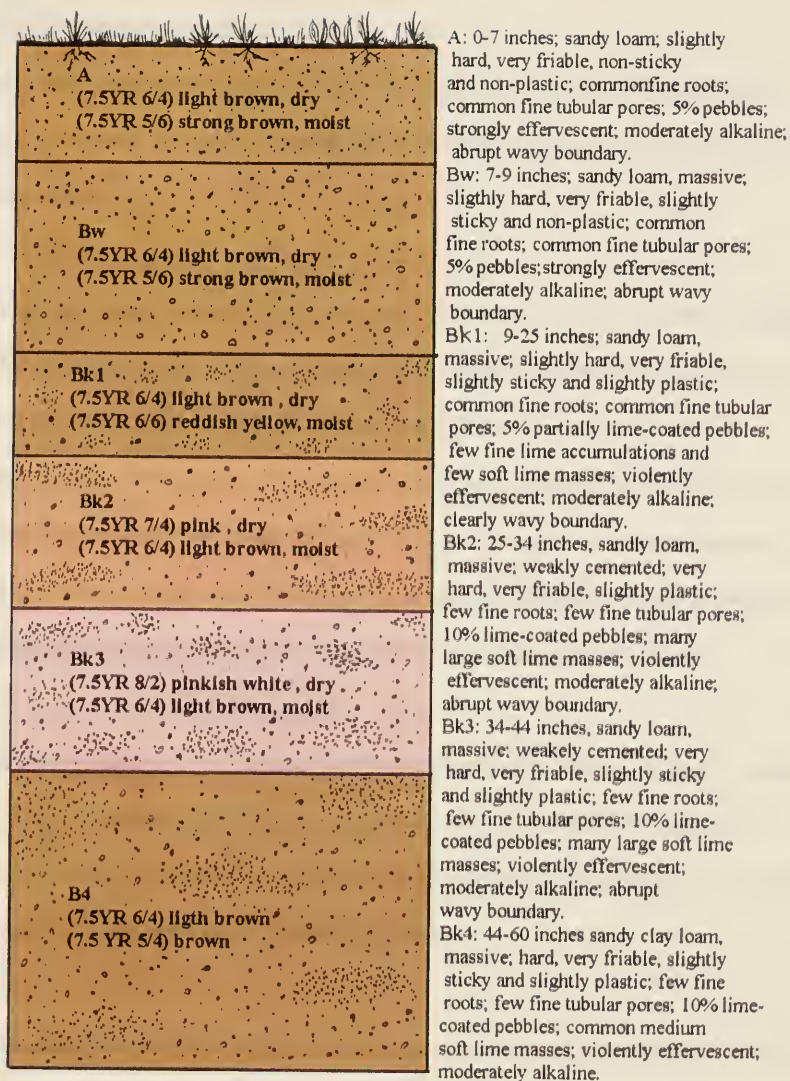


Figure 2: Typical pedon of Coolidge Sandy Loam.

Depth of the layer of calcium carbonate accumulation ranges from 14 to 30 inches. The content of rock fragments in the control section is as much as 15%. The calcium carbonate equivalent is 10 to 20%. The sodium adsorption ratio is as much as 40 or more. The electrical conductivity is as much as 8 millimhos per centimeter, especially in the lower horizons (Information from United States Department of Agriculture, *Soil Survey of Pinal County, Arizona, Western Part*, 1991, 63).

2.1.2 Climate and Vegetation

The desert environment of the area where the Monument is located is characterized by climatic extremes, such as low rainfall, very high evaporation rates, high temperatures, and strong winds.

Rainfall and temperatures are similar to those of low latitude or tropical deserts. Rainfall is thin, erratic, and influenced by subtropical high pressure air masses and trade winds flowing from the Gulf of California and the Gulf of Mexico. The average annual precipitation is 6 to 8 inches (8.5 inches at Casa Grande). Rainfall is characterized by a monsoon pattern with two distinct periods: (1) from November to February rains are gentle and longer lasting, and (2) during July, August and September, rains are brief and violent thunderstorms (United States Department of Agriculture 1991, 85).

Evaporation rates are 15 to 20 times the annual precipitation. Cloud coverage is minimal and normally clear skies predominate (70% of the time, exceeding 90% during the summer). Relative humidity is low, commonly 15 to 30% but 5% humidity is not unusual (United States Department of Agriculture 1991, 85).

Air temperatures are mild during the winter. December average temperature is 55°F and average temperature in July is 105°F.⁴ Diurnal temperature fluctuations typically are 20 to

⁴ Soil temperatures are usually 2 to 6 degrees warmer. In this arid environment, soil temperatures exceed 72° F, which approximates the boundary between the hyperthermic and thermic soil temperature regimes (United States Department of Agriculture 1991, 85).

30°F. Freezing temperatures are rare, and the annual frost-free period is 250 to 290 days (United States Department of Agriculture 1991, 85).

Strong and desiccating winds, which are common in spring and during summer thunderstorms, contribute to additions of eolian sodium, calcium carbonate and other sediments. Typical wind velocities range from 10 to 40 miles per hour. However, wind velocities up to 80mph have been registered at the Monument (United States Department of Agriculture 1991, 85).

As a result of the climate, the soil in the area has an aridic moisture regime which produces a desert-type vegetation. Desert plants have adapted to the limited available moisture resulting from low rainfall and high runoff, desiccating winds, high evaporation rates and high salt content (Fairbridge, 1972).

Along washes, streams, and areas where the water table is at a shallow depth, phreatophytes, such as saltcedar and mesquite, grow. Plants such as saltgrass, iodine weed, and canyon ragweed, occupy the areas where the soils are high in salts. The most abundant plants are the xerophytes. They are in upland areas and survive by using a variety of mechanisms. The nearly level plains between the mountain ranges contain Sonoran Desert shrub characterized by creosote bush (bursage vegetation) (United States Department of Agriculture 1991, 85-86).

During its period of occupancy and following abandonment of the Great House, native desert vegetation and grass covered the entire area. However, by the end of the nineteenth century the natural flora and fauna began to change due to an increment of human activity in the area.

By the early 1870s, ranchers started to settle in the area. Livestock wandering inside the monument not only affected the ruins but the surrounding vegetation. However, in the 1880s the development of irrigated land and an increase of human population led to a greater damage to the flora and fauna of the area (Clemensen 1992, 154-55).

The irrigated agricultural land surrounding the monument destroyed the outside native vegetation and reduced the animal's natural habitat. In addition, in 1934 the area of the monument was fenced to stop livestock damage to the ruins. However, the fence also prevented the free range of larger mammals. Hence, smaller mammals multiplied inside the monument and caused the destruction of young native plants (Clemensen, 1992, 154-57).

Further increases in irrigation and population almost exhausted the area's water supply after 1930. As a result, farmers and inhabitants began to drill wells to obtain water. Excessive pumping of ground water for irrigation had caused a tremendous decrease in the water table beginning in the 1940s. The decrease of water table had a great impact in the natural vegetation of the area (Clemensen 1992, 156).

During the 1930s, the destruction of natural vegetation became more noticeable with the death of the mesquite and decrease of salt bush. The situation with the mesquite persisted until 1953, and nearly all trees had died by the 1960s. Mesquite decline was attributed to a lowered water table and a mistletoe infestation. Age, insect infestation, high population of small mammals, and lack of reproduction of trees were considered secondary factors (Clemensen 1992, 159).



Figure 3: Present Vegetation inside Casa Grande Ruins National Monument. Notice the dead mesquite trees.

Human-related activities damaged the area's natural vegetation and wildlife equilibrium. The desert vegetation around Casa Grande has been replaced by crops such as cotton, alfalfa, grapes, and lettuce. As a result, Casa Grande Ruins National Monument has been left as an island in the midst of an agricultural community.

Today, the Monument land no longer contains an area of "typical" desert. Because of the intensive irrigation for agricultural development around its boundaries, Casa Grande's natural vegetation has been severely stressed.

2.2 Condition of the Structure

2.2.1 Plan and Construction

Originally, the Great House was a multistory rectangular structure approximately 42 feet wide by 59 feet long built on top of a solid earthen filled platform, partially above ground level.⁵ The structure is formed by five rectangular spaces; A, B, C, D, and E; called "tiers" (Wilcox and Shenk, 1977). Tier C, formerly three stories high above the platform, is located in the center of the structure with its longer axis oriented in the north-south direction; the remaining tiers, formerly two stories high above the platform, are laid out around Tier C (figure 4).⁶ Originally, the five tiers were divided into room spaces⁶, 11 in total, by roofs and floors across them (Wilcox and Shenk, 1977, 69).

⁵ This fill, originally about 3-4 feet high above grade, has oftentimes been confused with accumulated debris after abandonment of the Great House. Data presented by Pinkley (1938-1939) and by excavations during the 1891-92 stabilization works suggest that this fill was probably part of the original design.

⁶ The term "room space" refers to the physical box formed by a set of floors, the four walls of a tier, and the roof above (Wilcox and Shenk 1977, 69).

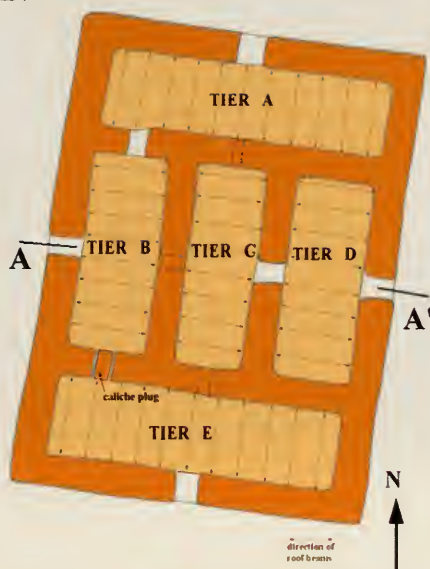
The Great House has a total of 18 existing openings that gave access to the different room spaces from the exterior and connected some of them from the inside. A set of two openings (one on the first level and the other one on the second level) were aligned in the center of each of the four elevations of the structure to give access from outside to the different room spaces of Tiers A, B, D and E. The central Tier (Tier C) had three openings, one for each of its three levels, aligned in the center of its east wall. In addition, the structure had two sets of paired interior openings, one on the first level and one on the second level, that connected some room spaces with each other.⁷ Later, plastered caliche plugs of the same wall thickness were inserted, sealing some openings.⁸ It is probable that the Great House originally had more openings (located on the roofs of the structure) that served to connect the different room spaces from the interior.

Wood lintels were inserted in the top of the openings to carry the weight of the wall above them. In addition to the openings that gave access to the different room spaces, the walls show a series of small openings and vent holes that probably had specific functions, including astronomical observation.

⁷ The locations of the interior openings were as followed: one set connecting Tier A and Tier B (on the south wall of Tier A, west end), one set connecting Tier A and Tier D (on the south wall of Tier A, east end), one set connecting Tier B and Tier E (on the north wall of Tier E, west end) and finally one opening on the second level connecting Tier D with Tier E (on the north wall of Tier E, east end).

⁸ Caliche plugs are located in the first and second story interior openings between Tiers B and D, and the second story exterior opening of Tier B located on the west elevation.

FLOOR PLAN



SECTION AA' LOOKING SOUTH

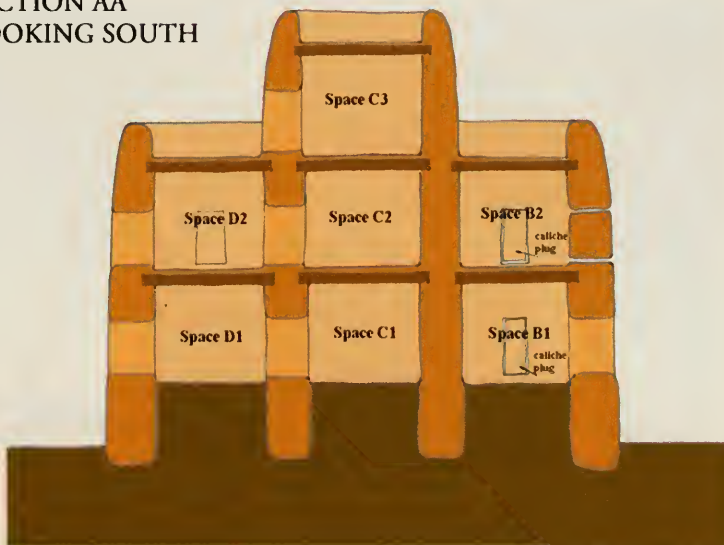


Figure 4: Plan and west-east section (looking south) of the Great House



Figure 5: North view of the Great House, 1997



Figure 6: South view of the Great House, 1997



Figure 7: East View of the Great House, 1997



Figure 8: West View of the Great House, 1997

The walls of the Great House, which are approximately 1.35m (4' 5") thick for the exterior walls and 1.07m (3' 6") for the interior walls, were erected in semi-continuous horizontal courses of caliche of variable height. All interior walls and the interior side of the exterior walls were plastered, forming a planar and almost perpendicular surface, which was smoothed and painted with a thin clay-based finish.

It is yet unknown if the exterior walls of the Great House were ever plastered. No visible physical evidence is left of an exterior finish or plaster. Most historical accounts express a different treatment for the structure's exterior in comparison to its interior (Wilcox and Shenk, 1977). Mindeleff (1896) suggested that while the walls were constructed the exterior surface was smoothed either by hand or with a tool. He added that the exterior finish was not as carefully executed as the interior nor was it treated like the latter with a separately applied material (plaster). Thus, a different treatment of the outer face of the wall in comparison to its interior face was likely.

Originally the Great House had eleven roofs which enclosed its different room spaces, although the earliest historical records of the Great House describe the structure without a roof (Wilcox and Shenk 1977, 8). These roofs probably followed the same configuration of some roofs found in other archaeological sites of the American Southwest. According to Ferguson (1959) the roofs were probably composed of four elements: (1) primary

beams, oriented across tiers; (2) secondary supports (Saguaro ribs), oriented along tiers; (3) a closing material on top (reeds or woven mats), and finally (4) a soil layering as



Figure 9: Example of water erosion in an area underneath a possible roof drain location (east elevation, Tier D, right of the outer opening

covering (caliche). Physical evidence, such as depth and diameter of beam holes and thickness of roofs, suggests that the roofs and floors of all tiers were probably identical in the way they were built and that all roofs belonging to a same level were laid simultaneously upon completion of each room space and tier (Wilcox and Shenk 1977, 77-81).

Considering the large area of the flat roofs, it is very unlikely that

the Hohokams did not plan a layout of a roof drainage system for the Great House.

Wilcox and Shenk (1977) suggested that the drains exited the roofs directly above prehistoric patches inside the outer wall of the uppermost room space in each tier.⁹ Later,

⁹ According to Wilcox and Shenk (1977, 162), the location of roof drains was as follows: in Tier C, in the middle of its west wall, upper area of wall; in Tiers A, B and D, to the right of the outer opening as one faces outside, upper area of wall. No location was estimated for Tier E due to collapse of wall portions.

Wilcox and Sternberg (1981) confirmed this hypothesis. All the suggested locations coincide with missing portions of parapets and show deep erosion in the areas located immediately underneath.

2.2.2 Construction Material

According to Hayden (1942 and 1957) a caliche soil was used in the construction of the Great House. As of yet no detailed and systematic studies of caliche borrow areas have been made for the Great House or the Monument, so the exact location of the source of the caliche soil is unknown, or if it was extracted from a single or several borrow areas.

Borrow area studies of other nearby Classic Hohokam sites, such as those by Burton, Knoob, Shrock, Spears and Phinney (1972) at Pueblo Grande in Phoenix, Arizona, provide valuable information on these issues. These data strongly suggest that the Hohokams preferred the purer caliche for its greater strength and hardness. In addition, certain characteristics of the Pueblo Grande borrow pits (ridges between pits, deep and sometimes undercut walls) seem to confirm that water was deliberately used to soften the caliche beds (Burton et al. 1972, 21-54).

Not enough evidence was found at Pueblo Grande to confirm if the caliche was ground on metates or if the poorer, gravely caliche was mixed with a given amount of pure caliche to get the desired consistency (Burton et al. 1972, 21).



Figure 10: Painting (anonymous) that represents a channel dug by Hohokams. Notice the use of water to help soften and extract the caliche. This method was probably similar to the one used for extraction of caliche for construction purposes. Painting courtesy of Casa Grande Ruins National Monument.

Hayden (1942 and 1957) gives other important details on the processing of caliche. He states that after its extraction, the caliche for the Great House was probably processed in “caliche mixing bowls” in the ground of an approximate size of 61cm (24”) in diameter and 25cm (10”) in depth (Wilcox and Shenk 1977, 117). Apparently, the caliche was puddled in the mixing bowls by adding water and then kneaded into a stiff dough.¹⁰

McGeorge (1937, 128) defines puddling as “the process that destroys the crumb structure [of the soil], bringing soil grains so close together that the movement of air and water is

¹⁰Thus the approximate volume of these mud mixing bowls was 0.073 cubic meters (1.6 cubic feet).

retarded". Vick (1973, 2) suggested that "... by puddling the volume of capillary pore space was reduced thus the material obtained its maximum density (this is practically without voids) and contained just the necessary amount of water which controlled shrinkage to a minimum".

Though more research on the extraction and processing of the caliche from the Great House is required, two important assumptions can be made based on the information previously discussed. These are:

- (1) It is probable that the caliche soil for the construction of the Great House walls came from different borrow areas. Calculations done by Wilcox and Shenk (1977) established that approximately 1545 cubic yards of caliche soil were used in the construction of the Great House walls. If all the caliche came from a single borrow area, a depression of about 3090 square yards would have been left after the extraction (Wilcox and Shenk 1977, 102). Such a depression size has never been found in the nearby area of the Monument. Another reason for this assumption is that the size of the Great House that would have demanded work extending over many months or perhaps years, which would have shifted the use of caliche from one borrow area to another. In addition, it seems that variations in the natural deposits of caliche were recognized by the Hohokams and only a caliche with special qualities may have been selected to be used in construction, leaving out the rest of the soil in the ground.

(2) Water may have been used to soften the dry caliche since, in its dry state, caliche is very difficult to extract as a material for construction. Burton and colleagues (1972, 54) proved that pouring water onto sun-hardened caliche, and letting it stand for a while softens the material and allows it to be easily scooped from a pit. If caliche was extracted while dried only stone tools were available for use, which would have made the process more labor intensive and time consuming.

2.2.3 Wall Construction Technique

Since 1694, there have been various hypotheses and opinions related to the construction technique used for the erection of the Great House. In general, these hypotheses followed two different speculations: (1) the use of a type of form or cast or (2) the erection of the walls without the use of forms or structural skeleton.

The first historical account on wall construction technique for the Great House dates from 1775, when Fathers Pedro Font and Francisco Garcés provided the first hypothesis. According to this account, the walls are described as “mud-walls made with boxes of various sizes” (Coues, 1900; Fewkes, 1912). Further historical descriptions come from: Emory and Kearny, 1846 (Kearny, 1848); Johnston and Stanley, 1846 (Emory, 1848; Fewkes, 1912); Bartlett, 1852 (Fewkes, 1912); Browne, 1864 (Browne, 1974); Grossman, 1871 (Fewkes, 1912); Hinton, 1871 (Hinton, 1954); Cushing, 1889 (Wilcox and Sternberg, 1981); Mindeleff, 1896 (Mindeleff, 1896); and Fewkes, (Fewkes, 1912).

Despite the disparity of these accounts, all observations concurred that a type of form or skeleton was used to build up the walls of the Great House.

The first reference to argue for a different wall construction technique for the Great House did not come until the beginning of this century from Frank Pinkley (Pinkley and Pinkley, 1926-1931). Referring to the Great House, Pinkley wrote:

“... putting this [caliche] in baskets or skin pack sacks, they carried it on their backs and heads to the site of the proposed building. The basket of mud was dumped on the wall and spread out by kneading it with the hands. Other baskets of mud were added until about two feet had been built up. Knowing that if they built higher at the time they would add so much weight as to squeeze the lower layers of freshly laid material; after getting the newly laid course about two feet high, they began carrying it forward horizontally along the wall. By the time they had built one of these courses around the walls, to the point of beginning, the first part of the course was dry and hard enough to bear the weight of another course or layer. Thus the walls were raised in what we might call monolithic courses, without the use of bricks, blocks or forms.” (Pinkley and Pinkley 1926-1931, 13).¹¹

Judd (1919, 5) suggested that supporting forms were unknown among the Pre-Hispanic cultures of the American Southwest, therefore, this technology was not available to the Hohokams. However, more modern hypotheses such as Steen (1965)¹² and DiPeso, Reinaldo and Fenner (1976) favored a mud concrete process¹³ for the construction of the Great House, thus implying the use of forms.

¹¹ A similar technique was previously described by Fewkes in 1912 (Fewkes, 1912). However, the description corresponds to the walls of Compound A and not specifically to the Great House.

¹² Steen referred to the construction of the foundations and not to the construction of the Great House walls.

¹³ “Mud concrete” or “poured adobe” is described by Feld (1965,4-40) as the method consisting of “a fluid mix poured into full-height forms or into movable forms, which are lifted as the work progresses”.

Kreigh and Sultan (1974) in their feasibility study for the preservation of the Great House assumed that the walls were built with the use of forms, according to an earthen-based construction technique known as "*pise de terre*" or "rammed earth".¹⁴

Finally, Wilcox and Shenk (1977) proved that there is no direct evidence that forms were used for the erection of the Great House walls¹⁵ and favored English cob as the construction technique used instead. Their hypothesis is based on: (1) the absence of regular or modular series of noticeable vertical joints commonly left by the use of forms¹⁶, and (2) irregularity of course height (Wilcox and Shenk 1977, 115).

According to Contreras (1970), when using forms the course height is very regular, which implies the continuous reuse of the forms while erecting the walls.¹⁷

Other signs such as curvature of the tops of the dried courses, dented appearance of the exterior surface of the walls probably due to palm impressions resulting from the batches of soil being pressed into place, and no form impressions help to support the assumptions

¹⁴ "*Pise de terre*" or "rammed earth" is described by Feld (1965, 4-40) as "a damp mix placed between sturdy wood forms, in layers of about 4 inches which are rammed to about 2 ½ inches"

¹⁵ The only places where form impressions were found are in the beam and reed holes, along the upper corners of doorways, and on the tops of the two door plugs in the south wall of Tier B. This evidence is related to construction of the openings and/or plugs and not to the wall construction (Wilcox and Shenk 1977, 115).

¹⁶ On the contrary, vertical or cold joints occur but they are not regularly spaced and in some courses they seem totally absent for a great distance (Wilcox and Shenk 1977, 115).

¹⁷ On the contrary, the height of the wall courses of the Great House vary as much as 15cm. (6 inches), and the variation between courses is 20-50cm (8 to 20") (Wilcox and Shenk 1977, 115).

that no forms were used. Further, the stiff consistency of the puddled caliche dough with hard caliche nodules probably did not require the use of forms.

Several archaeological structures from the American Southwest are known to have been constructed using English cob¹⁸ which prove that this earthen-based construction technique was practiced among the prehistoric cultures of the American Southwest.

Moquin (1992, 10-27) describes English cob¹⁹ as:

“... piling portions of moist mud along the course of the wall being built and compressing them into place. Each course is left to dry enough to hold its shape until the next is applied”.

The earliest report on this technique from the Southwest was done by Neil M. Judd (1919) at Paragonah, Utah. However, the most important and substantial information probably comes from Stubbs and Stalling (1953) whose architectural analysis of Pindi Pueblo, New Mexico, is one of the best reports on earthen construction in the literature on Southwestern archaeology. Additional information is provided by Kidder (1958), who analyzed Forked Lightning Ruin, New Mexico (Wilcox and Shenk 1977, 124; Moquin 1992, 10-27).

¹⁸ Some important examples of prehistoric structures of the American Southwest constructed with English cob are: Pindi Pueblo (1300-1350 AD) near Santa Fe, New Mexico; Bis Sá Ani Pueblo (1100-1190 AD) near Escavada Wash, New Mexico; Forked Lightning Ruin, (1250-1300 AD), located in Pecos, New Mexico; Taos Pit House (1190-1210 AD) located in the highlands area near Taos, New Mexico; Picuris Pueblo, (1400 AD), New Mexico; Nawthis Village Site (900-1200 AD) near the town of Salina in central Utah; Paragonah, in Utah; and Pendleton Ruin, (Animas Phase) in extreme southwestern New Mexico.

¹⁹ This method is similar to the method described by Pinkley (Pinkley and Pinkley 1926-1931; Pinkley, 1938-39). Also, Judd (1919), Stubbs and Stalling (1953), and Kidder (1958) name this method as “coursed adobe”. On the other hand, Feld (1965) and Wilcox and Shenk (1977) identify this method as “puddled adobe”.

Wilcox (1975a) and Wilcox and Shenk (1977) proposed a method of construction for the wall courses of the Great House based on the physical evidence found in the Reaves Trench (west profile of the east wall of the Great House). Thus, each wall course is composed of a layering or superposition of lens-shaped portions of caliche pressed in place by hand. Each portion of caliche has an approximate volume of 0.058m^3 (1.29 cubic feet)²⁰, which is very similar to the 0.073m^3 (1.6 cubic feet) capacity of the caliche mixing bowl described by Hayden (Wilcox and Shenk 1977, 117).

The wall courses of the Great House were not carried out continuously along the entire length of the walls. Instead, they were interrupted at variable intervals by vertical seams, also known as head or cold joints which are discontinuities of the wall course where a course stopped and was continued later when dried (Wilcox and Shenk 1977, 72).

Apparently, these seams were done without any interlocking method. Thus, when a course was stopped it was simply continued later, after drying.²¹

Based on direction of roof beams and uniformity of beam hole depths²², Wilcox and Shenk (1977, 81) suggested that the Great House was completed in a single building episode.

²⁰ The lenses of caliche from the courses placed on top of the walls are smaller; this is of less volume than their counterparts located in the courses of lower levels. (Wilcox and Shenk 1977, 117).

²¹ Some evidence found by Wilcox and Shenk (1977, 121) and Wilcox and Sternberg (1981, 19) suggests that Saguaro ribs might have been used for seams in order to improve the connection between the two courses and help reduce shrinkage. This evidence has not yet been corroborated.

²² All beams are oriented perpendicular to the longer wall of each tier. Thus, in Tiers A and E the orientation of beams is north-south and in Tiers B, C and D the orientation is west-east.

that is without latter additions. Also, they believe that several crews were working simultaneously on several sections. In their report, Wilcox and Shenk (1977, 121) mention some findings concerning a construction strategy. However, an attempt to completely reconstruct how the entire structure was put together has yet to be made.

2.2.4 Condition as a Ruin. The Shelter

Beginning with the first European that saw the Great House for the first time, most historical accounts describe the structure as a ruin, covered by cracks, breaks and faults, with its roofs and floors burnt and removed, and exhibiting erosion caused by natural forces and vandalism (Wilcox and Shenk, 1977).

The Oxford Encyclopedic English Dictionary defines a ruin as “a destroyed or wrecked state; the remains of a building that has suffered ruin”. Regarding ruins, Fielden expressed that “just as a skeleton is a more acceptable presentation of a decaying corpse, a ruin is a more sanitary state for a building when it is pronounced dead” (Fielden 1994, 248).

Thompson defines a ruin as a “roofless shell which could stand to roof height or exist only as an underground foundation” (Thompson 1991, 9). Therefore, a ruin is clearly distinguished from a roofed structure which provides shelter and is in a sense useful.

The Great House was probably designed for a specific function given its unique occurrence on the site and construction technique. When abandoned (loss of use) and

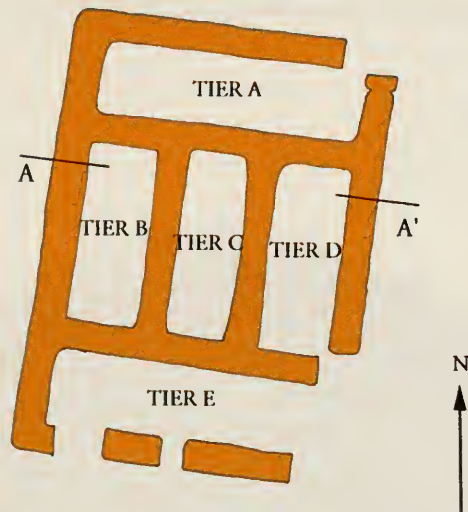
with the loss of its roof, the Great House did not function as a building any longer and became an interrupted system more vulnerable to the action of deterioration.

By the end of the nineteenth century, several requests were made for the addition of a shelter for the protection of the Great House. In 1890, Mindeleff's recommendations included a plan for such a shelter for the Great House. In 1893, 1895, and 1899, Custodian Isaac T. Whittemore repeatedly asked the Government for funds to be spent to protect the structure. Later, custodians H. B. Mayo and Frank Pinkley had concerns with the deterioration of the structure as well and also requested a roof for the protection of the Great House (Clemensen 1992, 40-50).

By 1903, S. J. Holsinger, General Land Office Agent, designed a covering for the ruins closely following Mindeleff's original plan. The contract for the construction of the roof was awarded to W. J. Corbett from Tucson, Arizona. The roof was made of galvanized, corrugated iron with a six-foot overhang and its framework was supported by redwood posts set 1.20m (4') in the ground within and around the structure. Anchor cables ran from the top of each corner to dead-men set twenty feet away to prevent uplift. The roof was completed on September 10, 1903 (Clemensen 1992, 51).

In 1915, James Bates, custodian of the monument, recommended a new roof for the Great House since the old galvanized roof had many holes and was leaking. By the mid-1920s it had become apparent that the roof of the Great House had deteriorated to the point that it

FLOOR PLAN (PRESENT CONDITION)



SECTION AA' LOOKING SOUTH

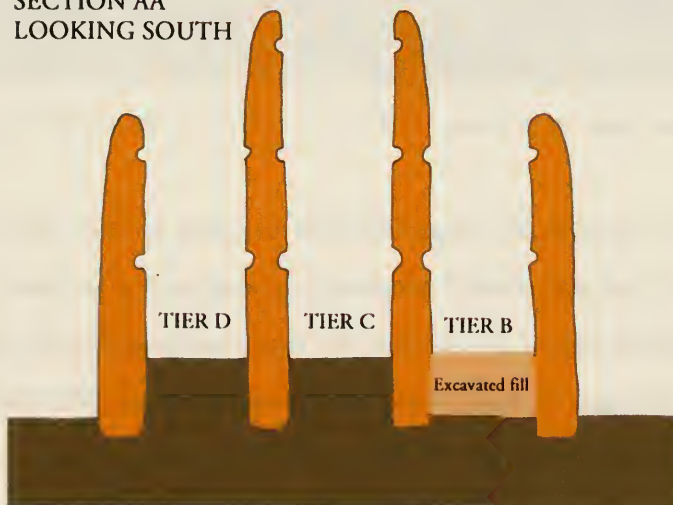


Figure 11: Plan and west-east section of the Great House according to its present condition as a ruin.

needed replacement. A competition was proposed for the new roof and a number of proposals were submitted. However, lack of funds prevented any action (Clemensen 1992, 78-79).



Figure 12: The original shelter roof, constructed in 1903 (Photo: courtesy of Casa Grande Ruins National Monument).

In 1932, funds to build the shelter were finally appropriated. The construction of the new roof was carried out by Allen Brothers of Los Angeles, California according to the design of Thomas Vint, chief landscape architect in the Park Service's San Francisco Field Headquarters. With only some exceptions, Vint followed the design suggested by Frederick Law Olmsted, Jr. The new shelter, formed by a hip roof on a steel frame that

stands forty-six feet from the ground to the eaves, was completed on December 12, 1932 (Clemensen 1992, 80).



Figure 13: The second (present) shelter.

CHAPTER 3: CHARACTERIZATION AND ANALYSIS OF THE GREAT HOUSE CALICHE AS A BUILDING MATERIAL (PHASE 2)

3.1 Caliche

3.1.1 Definition

The word “caliche”¹ is a Spanish term that derives from the Latin term “*calix*” which means lime or limestone. According to Corominas (1954) this term was first used in 1719, apparently originating as a variable of “*calizo*” (calcareous) from the Mozarabic. In the United States, the term caliche was first used by Blake (1902) in his study of caliche in Southern Arizona (Reeves 1976, 1-3).

In general, caliche has been used worldwide not only to identify calcareous-rich² but other types of deposits. Various other terms have also been proposed and used throughout the literature. Thus, confusion in terminology has resulted. Reeves (1976, 4-5) assembled a list of various terms (including caliche) commonly used for calcareous-rich deposits in various countries of the world. This list is extremely useful for identifying provenance and references to different terms associated with caliche.

Thus, caliche has been defined in various ways. However, the definition provided by Bates and Jackson (1980) has been selected for the present study. Accordingly, caliche is

¹ In Spanish language, “caliche” is used to name near-surface calcareous concretions or calcium-rich mineral associations (Real Academia Española, 1956).

² There are three major forms of calcareous-rich deposits occurring in nature: bedrock—including limestone, dolomite, chalk, calcareous clay and sand, and carbonate sediment; soil—including massive, indurated zones, and powdery caliches; and biological sources—including shells of mollusks, such as oysters and clams (Musick 1979, 5).

defined as:

“a term applied broadly in the Southwest of the United States, especially in Arizona, to a reddish-brown or white calcareous material of secondary accumulation, commonly found in layers on or near the surface of stony soils of arid and semiarid regions, but also occurring as a subsoil deposit in subhumid climates. It is composed largely of crusts of soluble calcium salts in addition to such materials as gravel, silt, and clay. It may occur as a thin porous friable horizon within the soil, but more commonly, it is several centimeters to a meter or more in thickness, impermeable, and strongly indurated. The cementing material is essentially calcium carbonate but it may include magnesium carbonate, silica, or gypsum. The term has also been used for the calcium-carbonate cement itself. Caliche appears to form by a variety of processes, e.g. capillary action, in which soil solution rises to the surface and on evaporation deposit their salt content on or in the surface materials. It is called hardpan, calcareous duricrust, or calcrete in some localities, and kankar in parts of India. Synonyms: soil caliche; calcareous crust; croute calcaire; nari; sabach; tepetate” (Bates and Jackson, 1980, 90).

3.1.2 Origins

Although caliche deposits are best known to be found in arid and semi-arid regions where they may strongly influence vegetation patterns, they exist in many other regions as well, some of which are characterized by rather high precipitation. Therefore, caliches occurring both as massive, indurated carbonate zones and as powdery soil carbonate, exist throughout many regions and climates of the world, including the Southwestern United States.³

The world’s diverse distribution of caliches seems to be related to their age. Most of the

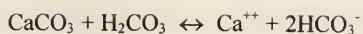
³ Specifically, in Arizona caliche exists both as indurated and soft discontinuous (Western Soil and Water Research Committee, 1964).

world's massive caliches seem to be of Tertiary age and poorly developed and incipient calcite zones in many areas are of both Tertiary and Quaternary age. Thus, caliches (calcium carbonate-rich zones) were formed in past climatic conditions, before most of the drastic changes had occurred over most of the earth's surface. Most caliches are fossils and are therefore representative of an ancient arid to semiarid climate (Reeves 1976, 5).

However, the ideal environment for caliche formation appears to be neither excessively arid nor excessively humid. Accumulation of calcium carbonate at and near the ground surface develops best in drier areas (with mean annual precipitation less than 50 cm. [20"] per year) though it can occur in regions with higher precipitation. The restriction of major calcium carbonate precipitation to dry areas results from two factors: (1) the calcium ion is highly soluble (ionic potential, 2.0) and little precipitation is required to leach the calcium from parent groundwater flow, (2) in areas of high rainfall, vegetation is very abundant. Thus, soil water is rich in carbon dioxide (CO_2) and organic acids from plant growth and decay, and carbonate ions are converted to HCO_3^- , which dissolves the calcium carbonate and prevents accumulation (Blatt and Tracy 1996, 235).

3.1.3 Chemical Description

Essentially, the origin of caliches could be illustrated by the following reversible chemical reaction:



As the reaction goes to the left (due probably to a rise in pH, a lowering of CO₂ partial pressure, or ionic saturation) calcium carbonate is precipitated while opposite conditions (i.e., lowering the pH, increase in the CO₂ pressure) will cause dissolution of calcium carbonate (Reeves 1976, 36).

Calcium carbonate profiles are very complex, not only because of the high solubility of the microcrystalline calcite crystals that compose the primary precipitate, but also because of the complex interrelationships among climate, parent material, topography, living organisms, and time. (Blatt and Tracy 1996, 235). Thus, the local relationships between precipitation, temperature, runoff and relief are critical for caliche formation. Basically it is the effectiveness in leaching of soil carbonate followed by the effectiveness of infiltration and precipitation of the carbonate which determines caliche formation (Reeves 1976, 84).

Worldwide, the chemistry of caliches varies considerably. Calcium carbonate accumulation is often associated with silica, calcium and magnesium carbonates, iron and aluminum compounds, and traces of other compounds including those of sulphur (Musick 1979, 8). Goudie (1972), who evaluated over 300 caliches, found that caliches are dominantly calcium carbonate and silica, with wide fluctuations in relative percentages.⁴ No dolomitic caliches (magnesium carbonate accumulation) have been recorded from the

⁴ As caliche ages both carbonate and silica contents increase (Reeves 1976, 37).

American Southwest. On a worldwide basis most caliches contain little magnesium carbonate, probably because of solubility factors⁵ (Reeves 1976, 36).

Caliches may contain minor amounts of organic debris, soluble salts, iron sulfide, glauconite, gypsum, phosphates, and aluminum, iron and manganese oxides (Goudie 1972; 1973; Ward et al. 1970). In addition, caliches may contain rare minerals such as radium, lithium, and thorium (Reeves 1976, 39-40).

3.1.4 Genesis

There is a controversy over the genesis of caliche due to the multiplicity of environments in which caliches are found (Reeves 1976, 88). Goudie (1973) suggests that caliche form by one of six possible models: 1) the fluvial model, 2) the lacustrine model, 3) the in situ model, 4) the capillary rise model, 5) the pedogenic model, and 6) the detrital model. The fluvial model relates to the distribution of caliches along stream valleys and channels, the lacustrine model explains caliche formation in ancient lakes, the in-situ model relates caliche formation to decomposition and accumulation of parent carbonate material, the capillary rise model refers to caliche formation by ascending soil water during dry periods, the pedogenic model involves the formation of caliche by pedogenic processes whereby soil water dissolves calcium carbonate at surface or at depth, and finally the detrital model relates caliche formation to solution, reprecipitation and cementation of fragments of calcium carbonate (Reeves 1976, 88).

⁵ The solubility of magnesium carbonate in the presence of CO₂, could be at least 12 times more than calcium carbonate (Reeves 1976, 36).

There have also been differing opinions on the sources of calcium in the world's massive caliches. Early studies (Blake, 1902; Theis, 1936; Pomel and Pouyanne, 1882) suggested that the calcium was brought from the depth to the surface by capillary rise of ground water. Other possible pedogenic carbonate sources for caliche mentioned in the literature include parent material, weathering of Ca^{++} -bearing aluminosilicate minerals, superficial accumulation by stream or lake waters, and such external calcium-rich sources as desert dust, eolian dust and clay deposits (also called loess⁶), vegetation (in the form of calcium carbonate-rich ashes and organic litter from arid areas), and precipitation (Reeves 1976, 98-110; McFadden and Tinsley 1985, 27). However, considerable evidence has been obtained which suggests that massive caliche profiles result from long-continued pedogenic development which includes solution, brecciation, re-crystallization and micritization of calcium coming from external sources such as eolian dust and precipitation (Reeves 1976, 108-109).

It has recently been generally accepted that most of the caliches of the American Southwest have been formed by calcium carbonate moving downward in solution during intermittent periods of wetting in a given (past) arid or semiarid climate (Gile et al., 1965). Some of the carbonates are released by weathering of the parent material, while others are derived from influx of carbonate-rich eolian dust or carbonates dissolved in rainwater.

⁶ Loess represents a deposit of eolian silt with grains predominantly in the 0.01 to 0.05mm range. It averages about 65% quartz and 35% feldspar, calcium and magnesium carbonates (Reeves 1976, 102).

The carbonates are precipitated at a particular depth by evapotranspiration processes (Beckwith and Hansen 1981, 19).⁷

3.1.5 Classifications

Caliches from different part of the world have been classified by Price (1933, 1958), Gillete (1934), Durand (1949, 1953, 1959 and 1963), Brown (1956), Gile (1961), Gile et al. (1965, 1966), Gile and Hawley (1966), Netterberg (1967, 1969, 1971), Multer and Hoffmeister (1968), Strakhov (1970), Reeves, Jr. (1971), Sehgal and Stoops (1972), Steel (1973), Harrison (1973, 1974), and Chapman (1971, 1974) among others. Most of these classifications are based on genetic factors, mineralogy, and soil fabric changes (Reeves 1976, 120-143).

Gile et al. (1965) developed a classification based on progressive carbonate accumulation and soil fabric, dividing caliche profiles into horizons. They proposed that soil horizons dominated by authigenic carbonate be named “K-horizons”⁸:

“The designation “K horizon” is proposed for soil horizons so strongly carbonate-impregnated that their morphology is determined by the carbonate. Though these horizons display a variety of macroscopic forms, and range in consistency from soft to extremely hard, they all have a peculiar and diagnostic soil fabric, the K-fabric. In material with K-fabric, fine-grained authigenic carbonate coats and engulfs skeletal pebbles, sand, and silt grains as an essentially continuous medium. The material breaks

⁷ A few exceptions to this process of formation are the Paleocene lake bed deposits in the Verde Valley in central Arizona. Also, it is probable that small lake bed or playa deposits and calcareous layers formed by groundwater are present in the parent material of some of these deposits (Beckwith and Hansen 1981, 20).

⁸ The term “K-horizon” was proposed for horizons of calcium carbonate accumulation at the meeting of the Association of Soil Classification and Cartography at Bonn, Germany, September 23-27, 1957.

down or is markedly softened by acid treatment. The designation K2 is proposed for carbonates horizons of 90% or more, by volume, of K-fabric, and K1 and K3 designations are proposed for upper and lower transitional horizons containing 50% or more of K-fabric" (Gile et al. 1965, 74).

Gile et al. (1966) and Hawley and Gile (1966) proposed another classification of caliche based on morphologic development due to increasing carbonate accumulation, both for gravels and non-gravelly materials. In the non-gravelly deposits, such as sand, "Stage I" is characterized by soft, discontinuous filaments and films of carbonate on sporadic grains. "Stage II" designation is applied when distinct nodules of sand cemented by carbonate exist. Carbonate filled root voids, animal borrows, and soil fractures also manifest during this stage. "Stage III" is used when the entire profile becomes carbonate impregnated, nearly all individual grains are impregnated by carbonate cement, and an abundance of indurated nodules exist. Finally, "Stage IV" is reached when a laminar horizon forms on top of the profile due to cementation and obstruction (Reeves 1976, 127).

On the other hand, Reeves (1971) suggested a classification based on progressive development and physical and chemical features. He suggested a terminology of: 1) young, 2) mature, and 3) old caliche, which resembles the classification terminologies of Gile et al. (1965), Gile (1966), Gile and Hawley (1966). Whatever the classification used, there is no doubt that a "caliche horizon" was the source of soil used to build the Great House walls (Hayden 1957, 1).

3.1.6 Uses Today

Caliche has been used commercially in many regions of the world for road construction and as source of calcium carbonate for various industrial applications (Reeves 1976, 144). In the United States, particularly in Texas and some other areas of the American Southwest, caliche has been used as a road base material and as a raw ingredient in the production of cement and lime (Musick 1979, 1).

There is hardly any reference in the caliche literature of its use for construction purposes. Musick (1979) produced a report on caliche in order to introduce calcium carbonate, particularly in the form of caliche deposits, as a practical masonry building material. He mentions indurated or rock-like caliche used as building stone in South Texas and several structures built with stabilized caliche, including one from the turn of the century, located in Wheeler County, Texas.

In the United States, early attempts to stabilize caliche were included as part of the research in the soil cement building industry which grew out of the developing science of road building, the housing problem in the United States associated with World War II, and the need for low cost housing in less developed countries (Musick 1979, 2).

3.2 Testing Program

3.2.1 Previous Analyses

The first recorded scientific analysis of the caliche from the Great House occurred in 1879,

when Professor George Cook⁹ took samples of the wall material.¹⁰ Chemical analysis of this soil showed 17% content of calcium carbonate. This discovery led to different speculations on how the Hohokams had obtained the lime for the soil. Some people suggested that it came from sea shells from the Gulf of California, others believed that the soil naturally contained a fair amount of calcium carbonate, but most decided that lime was burned with the building material (Hanks 1880, 104-105).

Since then, the caliche from the Great House walls has been analyzed by Littmann (1967), Vick (1973), Kreigh and Sultan (1974), Wilcox and Shenk (1977), O'Bannon (1978), and Roy (1980). Though for the most part, all these tests did not repeat or refer to the results of their predecessors, they have provided important and invaluable data for the present study. A detailed list of analyses and results is included in Appendix B.

Sample location is hardly mentioned in the previous analyses of the caliche and, when mentioned, the location varied from test to test. In addition, similar analyses performed by different researchers show great variability of results. This is probably due to variability of sample provenance and the different problems addressed by each researcher (different questions) rather than test method.

The majority of the researchers who have analyzed caliche samples from the Great House

⁹ Professor George Cook was part of an assemblage of New Jersey archaeologists led by Henry Hanks who set out to explore and document the Great House in 1879 (Clemensen 1992, 23).

¹⁰ The location where the sample was taken has not been specified.

have assumed that this material was homogeneous. However, this is not necessarily true. Though a single material was extracted from the nearby area to construct the walls of the structure, inconsistencies and differences should be expected, mainly in relation to soil source, size of the structure, construction technique, location in the structure, and time of exposure to the elements.

3.2.2 Sampling

For the purposes of this analysis, non-random sampling is the sampling method that was selected for the characterization of the caliche from the Great House. Non-random sampling is generally not advised as a sampling method to characterize materials, particularly earthen-based materials, for conservation purposes. However, the selection of this sampling method was based on the limitations of sample-taking and the availability of caliche material from a fragment that fell from one of the walls of the structure in 1995.

The sample obtained for the present characterization was part of a large caliche fragment which fell from the outer side of the west wall of Tier A (west elevation), close to the northwest corner during the summer of 1995. The fragment, which fell entirely from the second course above the 1891-92 stabilization work (base wall fill), broke into three smaller fragments upon impact with the ground. The caliche material was still intact and cohesive considering the great weight of the fragment and the height from which it fell (approximately 1.30 m.). Observations and notes were taken concerning the orientation of the pieces in the wall.

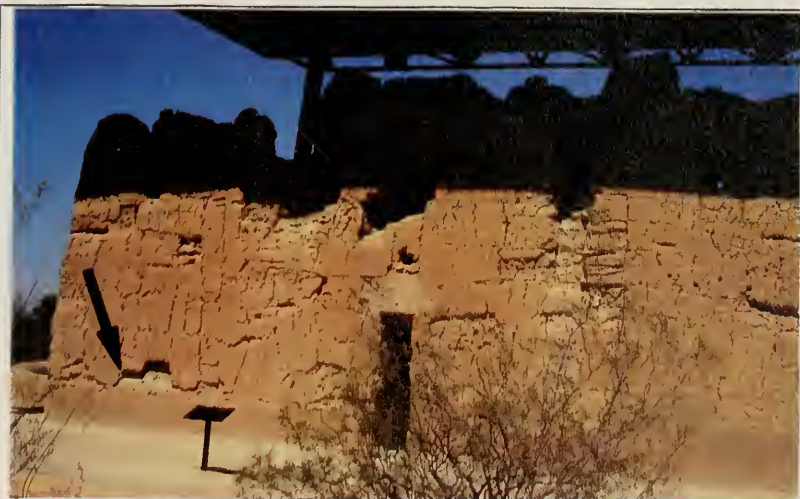


Figure 14: Location on the west elevation from where the fragment of caliche fell in 1995.
Figure 15: Close up of location.

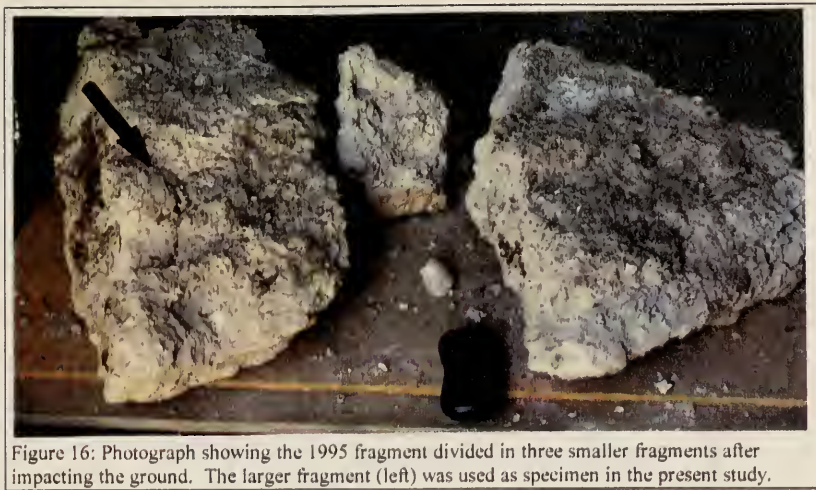


Figure 16: Photograph showing the 1995 fragment divided in three smaller fragments after impacting the ground. The larger fragment (left) was used as specimen in the present study.

One of the three pieces of caliche, the larger one with the characteristic reddish exposed surface, was sent to the Architectural Conservation Laboratory at the University of Pennsylvania for its characterization and analysis.

Because the caliche used for the present characterization came from an specific exterior location in the structure, it is representative only of that location. However, the results presented herein can be related to the general properties of the caliche from other sections of the Great House with the condition that inconsistencies in the material should be expected.

The caliche piece was first photographed and its dimensions¹¹ and observations were recorded (figure 17 and Appendix C).

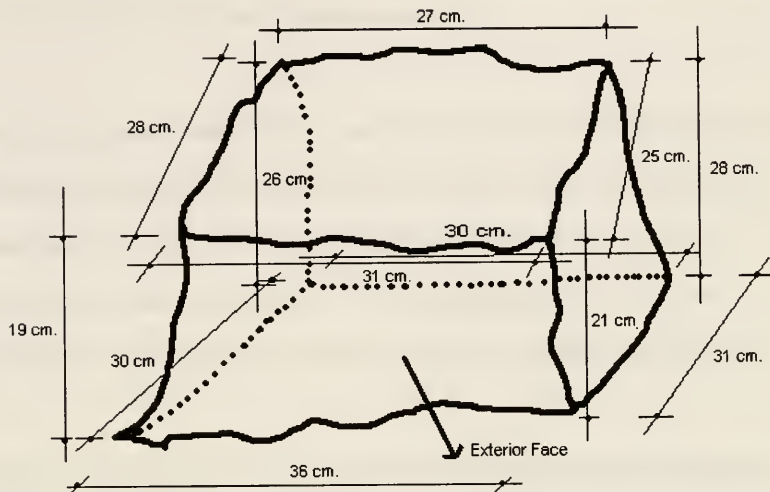


Figure 17: Dimensions of the caliche wall fragment.

This illustration reproduces the orientation of the fragment in the wall of the Great House. The exterior face corresponds to the outer side of the exterior wall.

3.2.3 Observations

The color of the caliche was determined by comparing the fragment surfaces with a set of 199 standard soil colors published by Munsell Color. The procedure followed the specifications of ASTM D1535.¹² The results obtained are:

¹¹ Due to its large size and weight, it was not possible to record the weight of the sample.

¹² ASTM D 1535, "Standard Test Method for Specifying Color by the Munsell System". ASTM: Philadelphia, 1993.

- Exterior (front) face: 5YR 6/6-6/8 (reddish yellow) for the material dry and 5YR 5/6-5/8 (yellowish red) for the material wet.
- Interior, Sides, Lower and Upper faces: 5YR 7/3-7/4 (pink) for the material dry and 5YR 6/3 (light reddish brown) for the material wet.

The caliche fragment showed different conditions on all its faces. The exterior face, with its characteristic exposed reddish surface, showed a flat, compact and dense surface with a smooth skin. Also, this face showed well dispersed constituents with only some superficial cracks and no insect activity. The large aggregates of this face were pronounced and well held by the matrix of soil; no loose aggregates were detected.

The rest of the faces (sides, top, lower and back) showed less compact, less dense and more irregular surfaces, without the reddish smooth skin characteristic of the exterior. Large aggregates were completely embedded in the soil matrix. The caliche from all these faces was very crumbly, particularly the caliche from the back face of the piece which greatly lacked cementation. In addition, all these faces showed more cracks (in several dimensions and orientations) and quite an amount of webs, nests, and dead insects, probably associated with past intense insect and animal activity. Additional photographs and detailed observations are included in the Appendix C.

Consistency differences in outer (exposed) and inner caliche from the Great House exterior walls were also reported by Wilcox and Shenk (1977). They concluded that these

differences were due to a chemical alteration of the outer surface probably caused by extreme temperature fluctuations¹³ and the action of rainwater seeping into the material and dissolving the carbonates in the caliche.

Based on this it was decided to analyze the caliche from different areas of the original sample (front, middle and back) in order to explain the differences in texture and consistency observed during initial examination. Fortunately, the caliche fragment was large enough to allow extraction of samples from different depths (10, 20 and 30cm).

After photography and observations were completed, the caliche fragment was cut into slabs for testing. Each slab, approximately 10cm (4") thick, was cut perpendicular to the

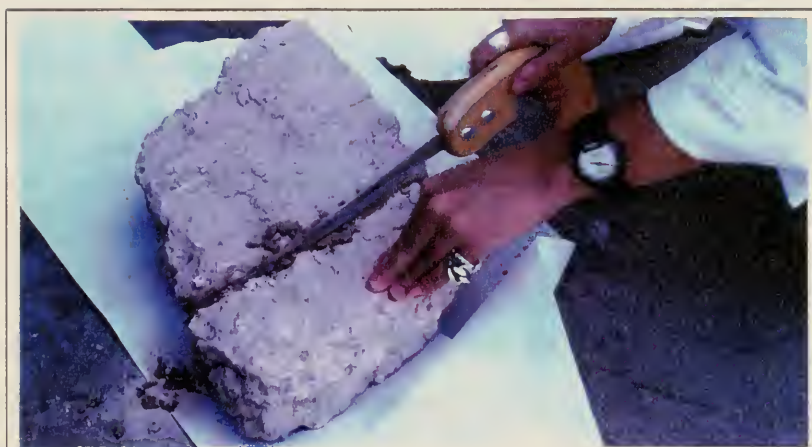


Figure 18: Caliche fragment during saw cutting

¹³ Temperature fluctuations within the caliche were reported by Kreigh and Sultan (1974).

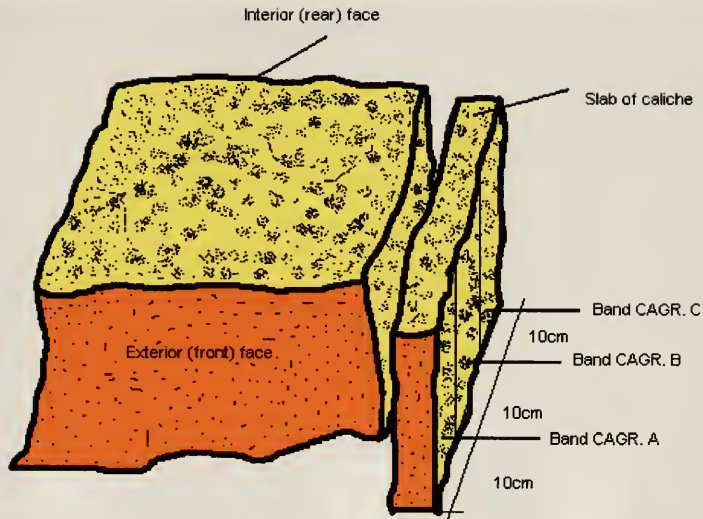


Figure 19: Orientation of each slab and location of different bands for samples. Four slabs were cut from fragment

exterior (front face), that is, parallel to the side faces.¹⁴ A hand bow saw (Popular Mechanics TM) with a 30" raker tooth hard point blade was used for the cuts. In order to get compact and regular slabs, de-ionized water was poured along the groove during the cuts to soften the caliche and avoid crumbling of the soil by movement of large aggregates.

After cutting several slabs, each one was divided into three parallel bands, approximately 10cm in thickness (figures 19 and 20) named:

¹⁴ The decision on the orientation of the slabs was based upon the great differences found in the caliche from the front and rear faces of the fragment.

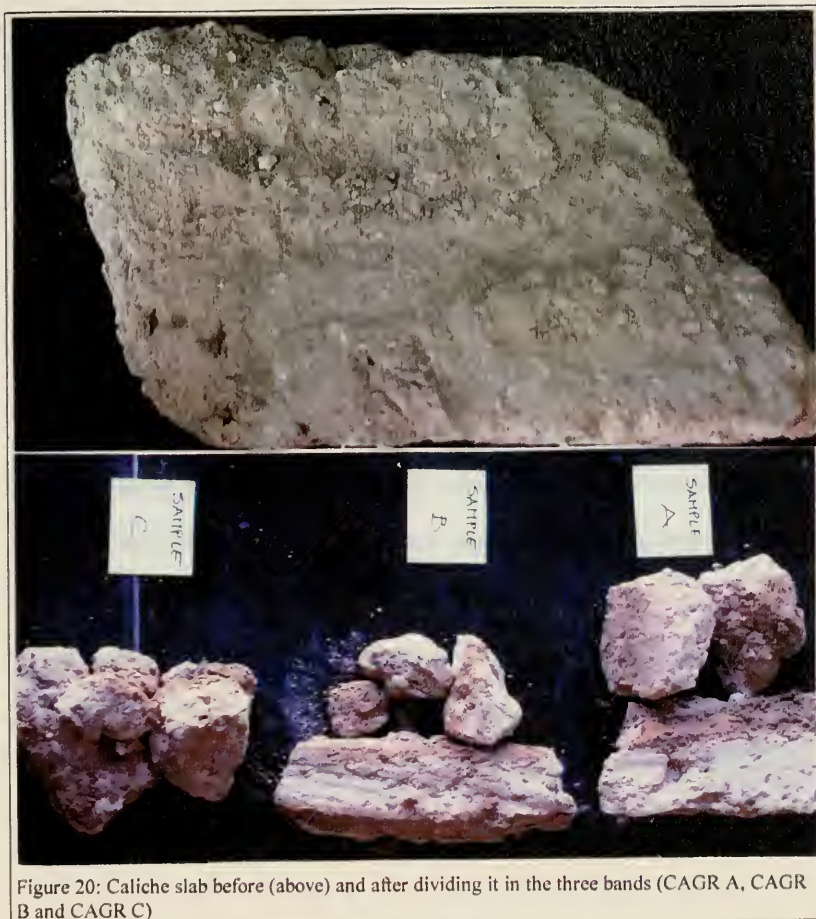


Figure 20: Caliche slab before (above) and after dividing it in the three bands (CAGR A, CAGR B and CAGR C)

- CAGR A: This band corresponded to the outer 10 cm of caliche material from the exterior face of the Great House exterior walls, therefore, it contained the reddish exposed surface with the smooth skin.
- CAGR B: This band, corresponded to the caliche material roughly located 10 to 20cm in depth from the exterior face of the Great House exterior walls.

- CAGR C: This band corresponded to the caliche material roughly located 20 to 30cm in depth from the exterior face of the Great House exterior walls. (this is the point at which the fragment detached from the wall).

Various samples were obtained from each band of caliche to be used in the different tests. Thus, caliche material from the exterior walls of the Great House were represented by samples CAGR A, CAGR B and CAGR C.

3.2.4 Test Program

A specific testing program, which started in January 1997, was developed for the characterization of the caliche from the Great House in order to address specific questions regarding existing conditions and alteration and deterioration through time. Two groups of testing procedures were assembled in order to: (1) characterize the caliche as a soil by means of geo-technical soil tests, and (2) characterize the caliche as a solid material, by cutting samples of various shapes and sizes using a water-cooled masonry saw¹⁵ and subjecting them to physico-chemical tests.

The caliche as a soil was characterized according to the following tests:

- Bulk Mineralogy (X-ray Diffraction)
- Identification of Clays (X-Ray Diffraction)
- Microscopic Observations (Polarized Microscopy and SEM)

¹⁵ Water was controlled and kept to a minimum while cutting these samples.

- Acid-Soluble (Carbonate) Content (Channey et al. 1981; Teutonico 1988, Experiment 21)
- Particle Size Analysis (ASTM D422)
- Particle Description (Stereo Microscope Observations)
- Atterberg Limits (Liquid and Plastic Limits) (ASTM D4318)
- Volumetric and Linear Shrinkage (ASTM D4943)
- Determination of Moisture and Soluble Salt Content (Charola, 1997) and Qualitative Analysis of Water-Soluble Salts (Teutonico 1988, Experiment 16)

The caliche as a composite material was analyzed according to the following tests:

- Compressive Strength (ASTM D1633)
- Three Point Bending (Modulus of Rapture) (ASTM D1635)
- Wet/Dry Cycling (ASTM D559 modified)
- Water Resistance (Water Drop Test - CRATerre)
- Capillary Water Absorption (NORMAL 11/85)

3.2.4.1 Bulk Mineralogy (X-Ray Diffraction)

In x-ray diffraction the wavelengths of x-rays are approximately the same as the internal spacing of the atomic particles within the crystals, which results in diffraction of the x-rays when they pass through the crystalline material (Alva Balderrama and Teutonico 1983, 11). The significant peaks obtained are compared with a master database called the Powder Diffraction File Database, containing a list of all identified minerals.

The caliche¹⁶ from the monument has been analyzed by Kreigh and Sultan (1974) and Roy (1980) using x-ray diffraction. Kreigh and Sultan's results include: calcite and quartz (major minerals), dolomite, plagioclase, orthoclase and illite (minor minerals), and kaolinite, chlorite and amphibolite (trace minerals) (Kreigh and Sultan 1978, 22). Roy obtained results for the fine fraction (material passed sieve #200) as well as for selected aggregates.¹⁷ The minerals found in the fine fraction are: calcite, quartz, anorthic-rich feldspar and illite. The minerals found in the aggregates (sand, volcanic rock fragments and gypsum) are: quartz, feldspar and gypsum (Roy, 1980, 56-57). Roy concluded that quartz and feldspars detected in the fine fraction of the caliche are due to contamination of this fraction by aggregates during sample preparation.

A caliche sample (away from the calcium carbonate enriched crust, i.e.; interior caliche) was selected for x-ray diffraction. In addition, a nodule of calcium carbonate was also selected. The caliche sample was sieved (using a de-ionized water) through a #200 sieve and oven dried (110°C) until constant weight. The mineralogical composition obtained is: calcium carbonate (calcite), silicon oxide (quartz), manganese sulfide, and hydrated magnesium aluminum silicate hydroxide (palygorskite, clay mineral) (Figure 21). On the other hand, the selected nodule was analyzed as a whole (that is without grinding of the sample). The results obtained for the nodule are: silicon oxide (quartz), calcium carbonate

¹⁶ The sample analyzed by Kreigh and Sultan (1978) came from a wall of Compound A and not from the Great House.

¹⁷ No calcium carbonate nodules were selected.

Z08666.RAW

CAS6 C FINES NO DIG. 5-65@10PM

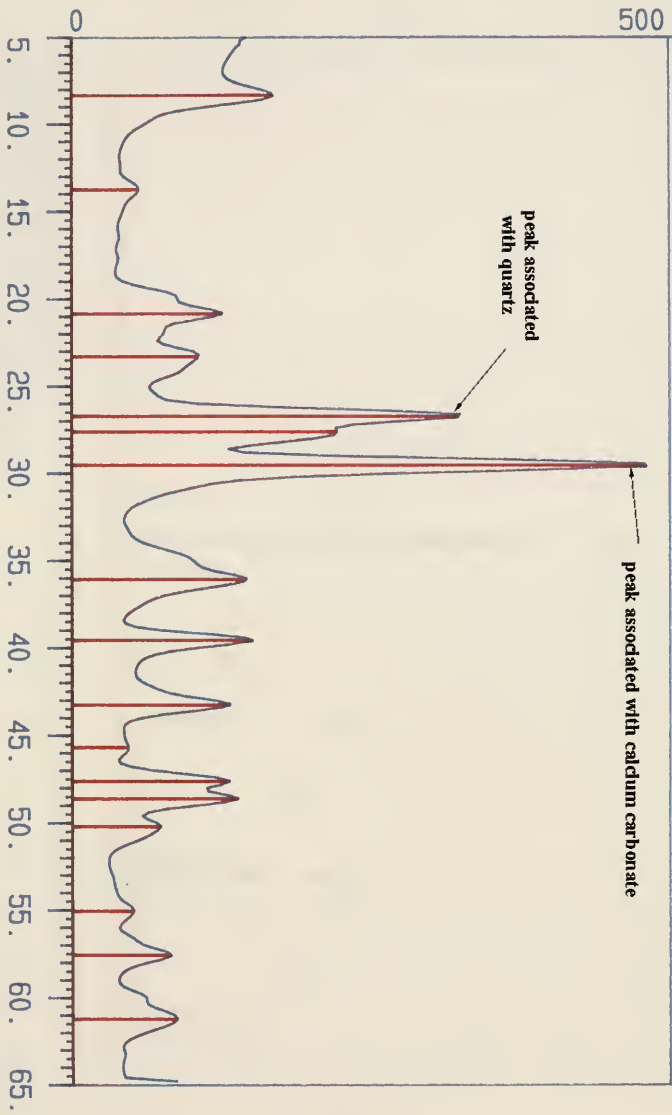


Figure 21: X-ray diffraction of caliche fines (material passed sieve #200)

Casa Grande caliche

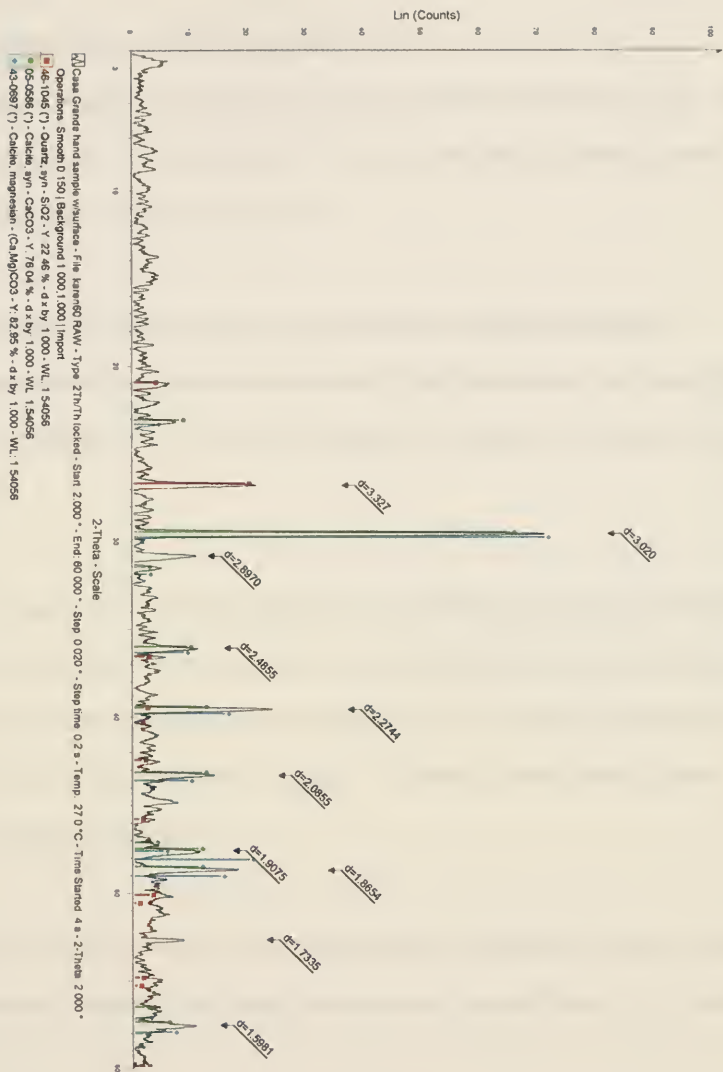


Figure 22: X-ray diffraction results of a caliche nodule (retained sieve #4)

(calcite) and calcite magnesian (Ca,Mg)CO₃ (Figure 22).

3.2.4.2 Identification of Clays (X-ray Diffraction)

Little data is available on clays found in caliches from different parts of the world. The type of clays found locally in a caliche will depend on geography and lithology as well as on the parent material (Reeves 1976, 37).

Clays such as chlorite, illite, kaolinite, montmorillonite, sepiolite and attapulgite (palygorskite) have been found in caliches in the United States and in other parts of the world (Vanden Heuvel 1966, Gile 1967, Gardner 1968, Aristarain 1970 and 1971, Frye et al. 1974).

The only known clay mineral identification by x-ray diffraction previously performed in the caliche from the Great House was done by the “Soils and Water Testing Laboratory at the University of Arizona, Tucson (Wilcox and Shenk 1977) in a sample that came from the backdirt of the Reaves trench (below grade).¹⁸ The results obtained showed a small amount of montmorillonite.¹⁹

A sample of material passed sieve #200 was prepared for identification of the clay mineral. The procedure followed is the standard procedure used for identification of clay minerals

¹⁸ Outside the east entrance on the east elevation of the structure.

¹⁹ The results also included a large amount of mica (phyllosilicate mineral). However, no type is specified in the results.

based upon their reaction to air, ethylene glycol, and heat (520°C). The clay identified by X-ray diffraction (Figure 23) is hydrated magnesium aluminum silicate hydroxide (palygorskite) $[(\text{Mg Al})_4 \text{Si}_8\text{O}_{20} (\text{OH})_2 \cdot 8\text{H}_2\text{O}]$.²⁰

Palygorskite²¹ is a complex clay mineral that contains some substitution of aluminum, iron and other ions and balancing exchangeable cations. Because of its structure, palygorskite is typically fibrous, rather than scaly like the other clay minerals (layer silicates) and may form flexible matted sheets that are sometimes called “mountain leather” (Nesse 1991, 242).²²

The chemical environment required for palygorskite formation is one of high pH and a high concentration of silica and magnesium. Thus, it is not surprising that lacustrine sediments in the intermittent lake basins of the semi-arid lands often contains this type of clay mineral in great quantity (Reeves 1976, 37-38).

It appears that palygorskite, along with sepiolite, are commonly found in caliches in many widespread localities, including Arizona. Therefore, they must be considered minerals

²⁰ This clay mineral was also found in the bulk mineralogy of the caliche fines.

²¹ Also known as attapulgite, however, this mineral is a very compact variety from Attapulgus, USA. The clay mineral was originally referred to descriptively as mountain cork, leather, paper and fossil skin. Palygorskite is now named after “Palygorsk”, a mining district in the Ural Mountains (Luenlaad and Hayes 1978, 105).

²² Oftentimes, palygorskite appears with attached calcite crystals that look like interwoven glass beads (Luenlaad and Hayes 1978, 105).

Casa Grande

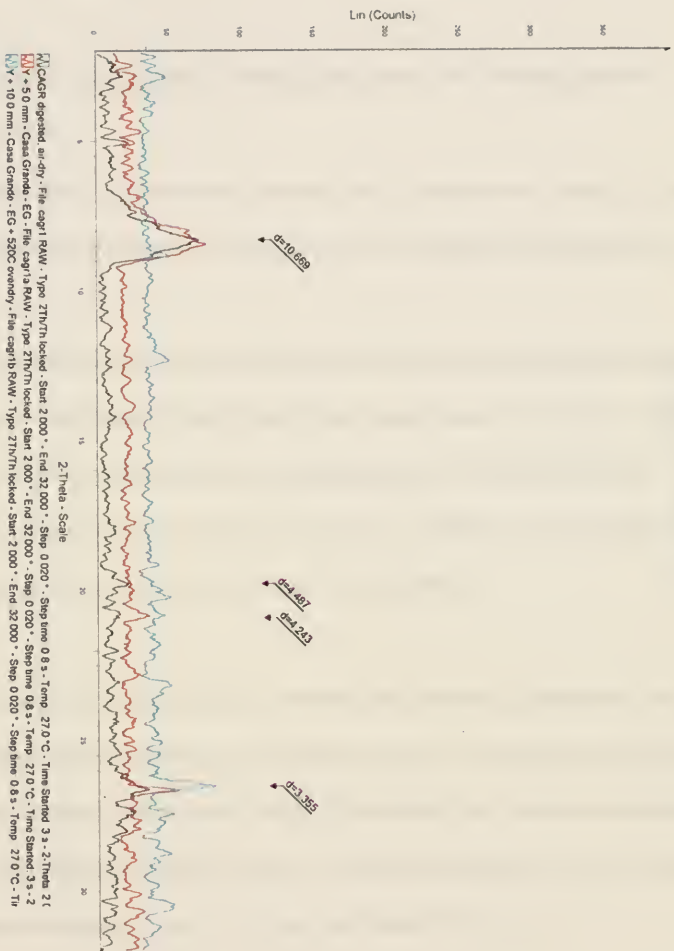


Figure 22: X-ray diffraction results of palygorskite as the clay mineral from the caliche. The black line represents the straight air-dry sample; the reddish line represents the sample treated with ethylene glycol; and the blue line is after the sample was heated to 520°C oven for one hour.

directly related to the peculiar geographic environments or the chemistry of caliche formation (Reeves 1976, 39).

3.2.4.3 Microscopical Examination: Polarized Microscopy and Scanning Electron Microscopy (SEM)

Microscopical studies of earthen-based materials used in architecture is related to fields such as micropedology and micromorphology (Courty, Goldberg and Mcphail 1990, 1).

The study of undisturbed soil samples with the aid of microscopical techniques is called micropedology, which helps to identify the different constituents of a soil and to determine their mutual relations in space and, as far as possible, in time. This technique was developed from the work of the Austrian scientist W. L. Kubiěna, who is considered the spiritual father of micropedology (Stoops and Eswaran 1986, 1).

On the other hand, micromorphology is concerned with the study of undisturbed soils, loose sediments and other materials, such as bricks, mortars, earthen-based architectural materials, and ceramics at a microscopic scale. This relatively new science employs both microscopic and ultramicroscopic techniques to examine and analyze a diversity of man-made and natural materials (Courty, Goldberg and Mcphail 1990, xvii).

The microscopical study of earthen-based construction materials does not differ much from what is normally carried out on undisturbed soils, archaeological soils and sediments. It comprises the description of coarse constituents (petrological identification, sorting, particle-size composition, proportion of organic to mineral matter), the fine fraction in which coarse elements are embedded, void pattern, and the geometrical relationships or arrangement of these three components (Courty, Goldberg and Mcphail 1990, 119).

Most plutonic, metamorphic, sedimentary and pedological features are reasonably well understood and their identification is possible by comparison with available reference texts. On the other hand, only a few records and descriptions of archaeological materials (such as the caliche under study), have only recently entered the literature. Many of these materials have either never been discussed or have not yet been interpreted (Courty, Goldberg and Mcphail 1990, xvii).

Interesting and important studies of microscopical observations of caliche have been done by Sehgal and Stoops (1972) and Brewer (1972) among others. However, such studies are more applicable to a caliche as a natural soil and not so much to a caliche used in construction which probably underwent some type of manipulation during its extraction and/or preparation stages.

The method proposed by Courty, Goldberg and Mcphail, (1990) provides a good working guide for describing and interpreting the micromorphology of the caliche in thin section.

Microscopical observations of the caliche involved the examination of thin sections under the polarized light and the examination of caliche samples with the aid of the scanning electron microscope.

The polarized microscope, which can examine mounted thin-sections ground to approximately 30 microns, allows the passage of polarized light rays through the material itself. This makes it possible to identify mineral grains through their characteristic optical properties under plane-polarized and cross-polarized light, and to reveal textural and chemical variations of the grains and binding matrix. This technique is also useful in determining quantitative relationships between the constituents of heterogeneous material in the caliche, such as the volume of percentage of aggregates to the binding matrix.

The scanning electron microscope offers the opportunity to study the three-dimensional aspects of objects at a continuous range of magnifications that varies typically from 100x to 60,000x. The surface of a specimen²³ is scanned by a focused beam of high-energy electrons. When bombarded with electrons, substances emit a large number of signals, the most common of which are: secondary and back-scattered electrons, r-ray, photonic radiation and transmitted electrons. Detection and imaging of secondary electrons is one of the basic functions of the standard scanning electron microscope. Secondary electrons are captured and their energies are transformed into an electric current that produces an

²³ In order to make the samples electrically conductive, they are coated with a thin, continuous film of metal (gold, platinum) or carbon.

electric image of the surface of the sample, thus permitting the study of the surface structure. As there are no lenses between the sample and display screen the SEM produces images with great depth of field at all magnifications (100 to 500 times greater than the microscope (Courty, Goldberg and Mcphail 1990, 50).

SEM was chosen to resolve questions regarding the process or processes of cementation of calcium carbonate in the caliche soil matrix and find existing differences in the cementing media of the caliche from different locations in the caliche piece.

Thin-Section Observations (Polarized Microscopy)

Observations were carried out using a Nikon polarizing microscope. Due to limitation problems concerning low magnification, several areas of the sample were selected and photographed under 4x magnification (the lowest magnification available for this study) and then montaged together for respective observations (see figures 25 and 32). Several observations, mainly regarding large aggregates, were performed under higher magnifications (20x and 40x).

Due to the differences encountered in the caliche during the examination of the caliche fragment, it was decided to make thin sections of caliche from different parts (front, middle and back) of the fragment in order to make comparative observations.

A slab of caliche material was obtained from the original sample following the procedure explained previously. A band of caliche of approximately 6cm (width) by 25cm (length) and 3cm (thickness) was cut from the center of the slab. Thus, the caliche material selected for the thin sections was representative of the whole thickness of the original sample (figure 24).

In order to fit all the material in 5cm by 7.5cm (2"x 3") glass slides, the caliche band was cut into four pieces which were named: 1F (belonging to the front face of the fragment), 2, 3, and 4B (belonging to the back face of the fragment).

Thin section were mounted on glass slides. The names of the samples and an arrow was carved on the glass slide (left side) for identification and orientation of the sample in order to maintain a known sequence. Each thin section was partially stained (left side) using alizarin red to reveal calcareous aggregates and patterns of calcite deposition.

Microstructure of the caliche refers to the size, shape and arrangement of its fine grains, aggregates and voids, in other words, the internal geometry of the soil components (Courty, Goldberg and Mcphail 1990, 70). According to the geometrical pattern relating its coarse and fine constituents, the caliche is characterized as a close porphiric (embedded) microstructure, that is, the coarser particles (unsorted) occur in a fabric of very fine material (microsparitic or micritic) related to pedogenic accumulation of calcium

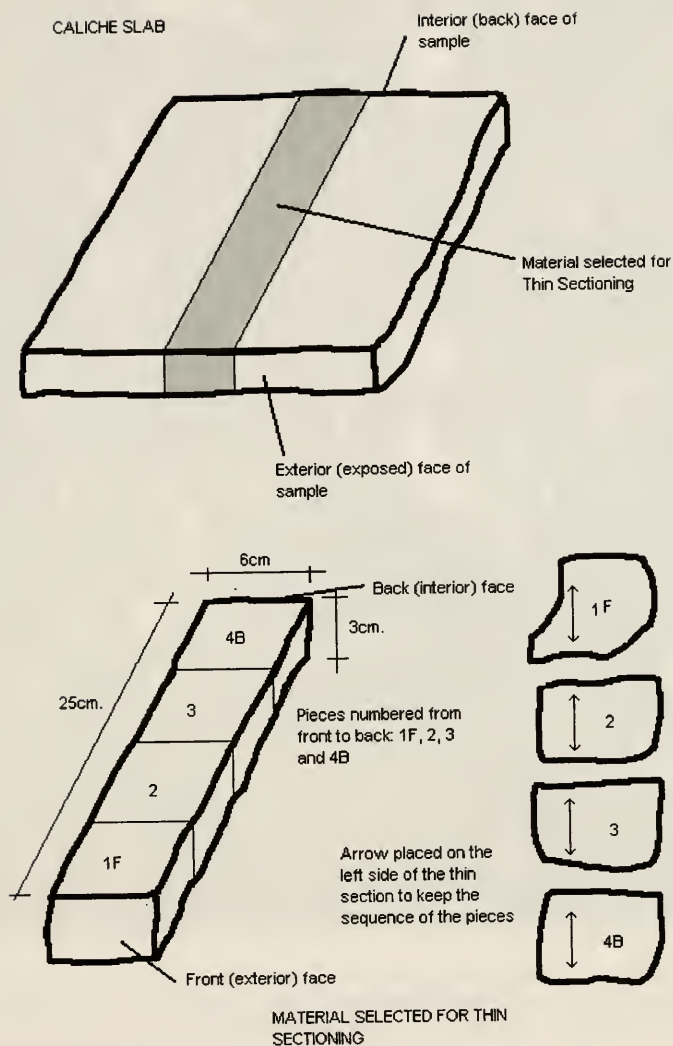


Figure 24: Material selection and sample preparation of caliche for thin-section

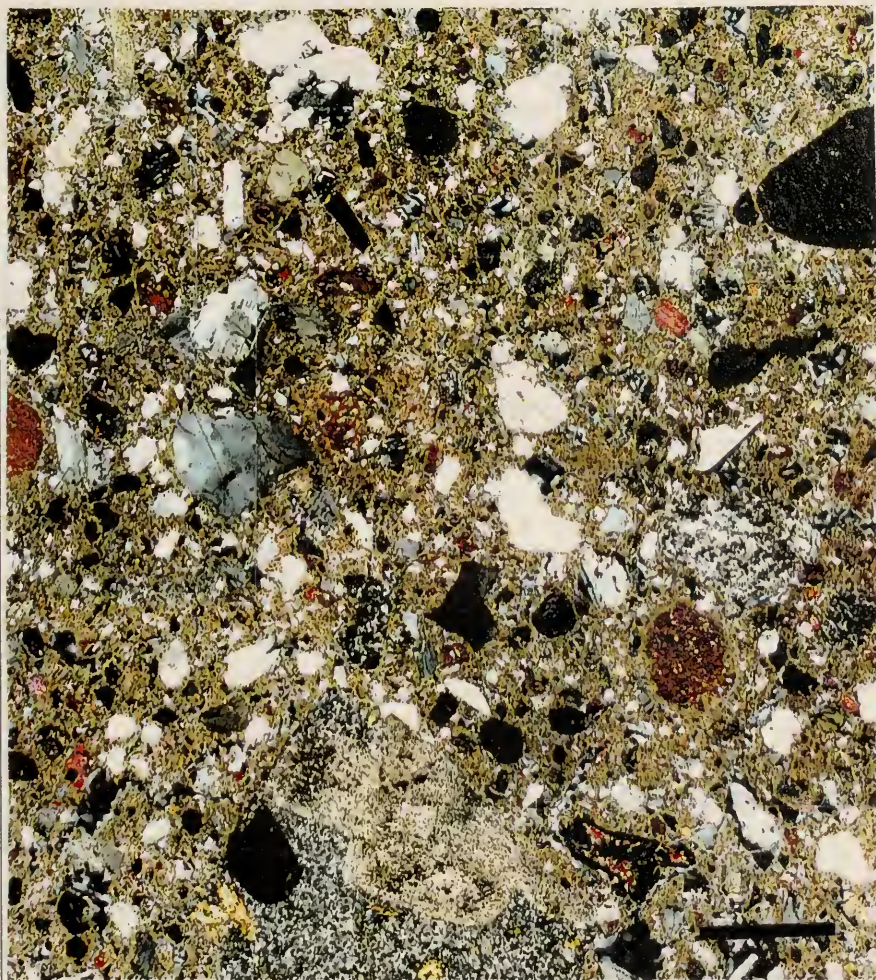


Figure 25: Microstructure of caliche. Bar is 10 μ m. Mag: 14X, crossed polars. The caliche shows a close porphyritic texture, that is, mineral grains (single and compound minerals) with various shapes and sizes embedded in a matrix of finer material (cryptocrystalline), mainly calcic.

carbonate.²⁴ No banding or preferential arrangement of the coarse aggregates was detected in any of the four thin sections (1F, 2, 3 and 4B) of the caliche under study.

- Aggregates

The aggregate portion of the caliche soil is composed of (1) single mineral grains, which are individual grains of certain minerals that have been derived from sediments or rocks (mainly quartz and feldspars), and (2) compound mineral grains which are composed by more than one mineral, for example reworked fragments of rocks (lithic fragments) of various origins and nodules of calcium carbonate, derived from pedogenic processes.²⁵

All aggregates are non-homogenous in shape, size and mineralogical composition. No prevalent orientation was found in the aggregates of the caliche, that is, all aggregates are oriented randomly. The content of aggregates is fairly uniform in all thin sections.

Due to the high density of aggregates in the caliche soil and magnification limitations in the polarized microscope (4x, the lowest magnification available was too high) the quantitative distribution of particle size was not performed through microscopical observations (modal analysis). Only rough estimates of percentages by type of aggregate are given.

²⁴ According to petrological observations, cryptocrystalline matrix.

²⁵ Two other types of soil aggregates, one of each, were found in the caliche. One was probably an inorganic aggregate of biological origin (phytolith or a fossil) found in thin section 4B, and the other one was an unidentified fiber found in thin section 3. Due to their low number, it was decided not to identify these two aggregates or record them through microphotographs. No other type of soil aggregate was identified in the caliche under study.

Approximately 80% of the single mineral grain aggregate is composed of quartz grains, irregularly angular in shape and with undulatory extinction. Eighteen percent was identified as feldspar crystals with distinct crystal faces. Several types of feldspars were identified and include plagioclase, perthitic feldspar and microcline. Both quartz and feldspar crystals show grain boundaries slightly pitted. Some feldspar crystals showed replacement by secondary minerals parallel to cleavage directions. The remaining 2% of single mineral grains is composed of muscovite laths and some rounded hornblende crystals.

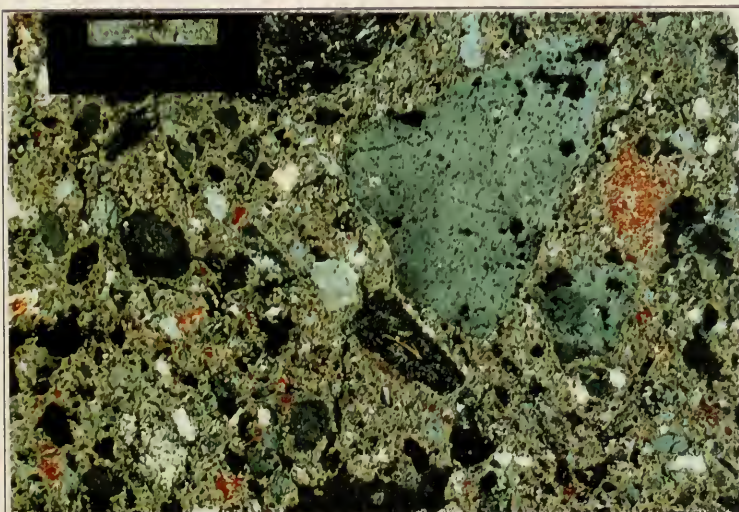


Figure 26: Anhedral quartz crystals of different grain size (2-10 μm in diameter) Most quartz particles show cracks and pitting, probably due to sedimentation or metamorphic processes. Bar is 10 μm . Mag.: 35X, crossed polars.

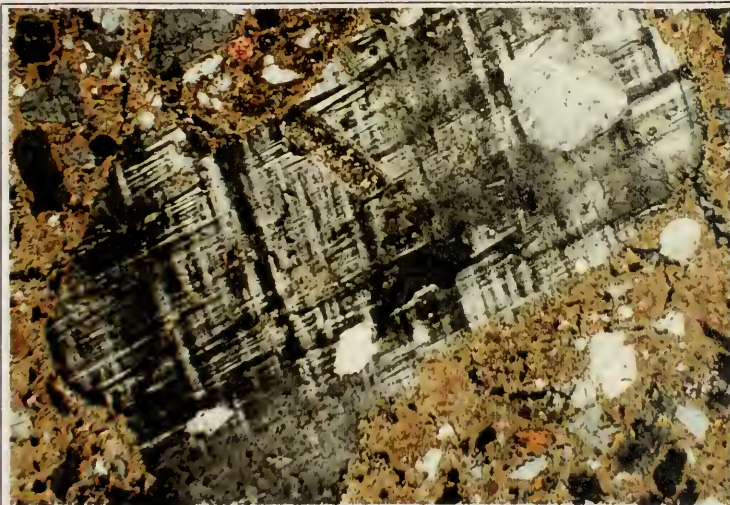


Figure 27: Subhedral microcline crystal (approximately 40 μ m long). Mag.: 50X, crossed polars.

Roughly 85% of the compound mineral grains aggregate is composed of calcium carbonate nodules of different sizes and shapes (mostly rounded, anhedral). The rest (15%) is composed of irregularly shaped (rounded to angular) lithic fragments of igneous and sedimentary origins.

Holmes (American Geological Institute, 1957) defines a nodule as “a general term for rounded concretionary bodies, which can be separated as discrete masses from the formation in which they occur”. Also, nodules have been defined on the basis of shape, surface, and structure (Reeves 1976, 54).

All the nodules identified in the caliche from the Great House seem to correspond to what Weider and Yaalon (1974) identified as disorthic nodules, which are nodules with clear recognizable boundaries and rims, and which have experienced displacement, that is, they have not been formed in place. Allothic nodules or nodules that are relics from another soil²⁶ where not identified in the caliche (Reeves 1976, 66)

The nodules from the caliche under study are related to pedogenic accumulation of calcium carbonate in the caliche as a natural material. Thus, repeated cycles of dissolution and reprecipitation had produced nodules with a complex internal fabric.²⁷

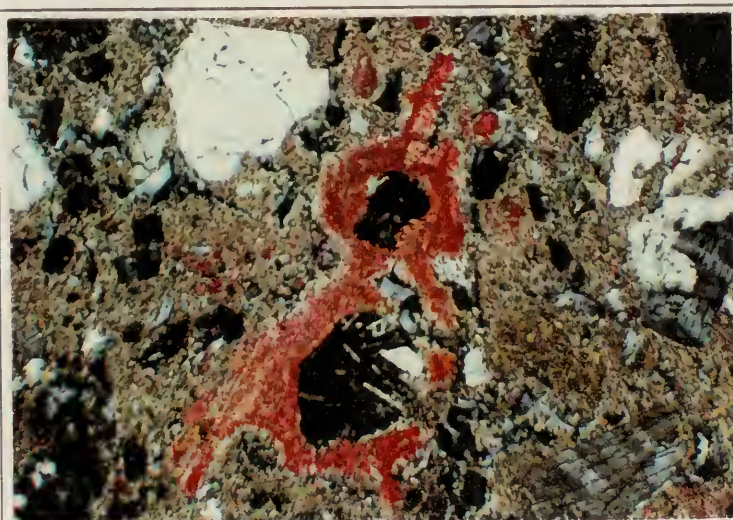


Figure 28: Elongated shape caliche nodule formed by calcitic cryptocrystalline matrix (stained) enclosing and gluing together two quartz crystals. Mag.: 35X, crossed polars.

²⁶ Allothic nodules exhibit different cement patterns, biorelicts, and types of skeletal grains (Wieder and Yaalon, 1974).

²⁷ In addition, calcium carbonate nodules are sensitive to changes in soil conditions and can be good indicators of past environmental conditions.

There is a great variability in the microstructure of the nodules. Some nodules present a cryptocrystalline calcic matrix with some poikilitic mineral grains (figure 31). Others have a porphyritic texture composed of various crystals of different shapes, sizes and mineralogical composition embedded in a cryptocrystalline matrix (figure 29), and other ones present a microcrystalline matrix with no mineral inclusions (figure 30). The majority of the large nodules show a rim (identified by a deeper color of alizarin red in the stained half of the thin section) which could probably be associated with the dissolution and recrystallization processes of the previously formed nodule (figures 29 and 32).

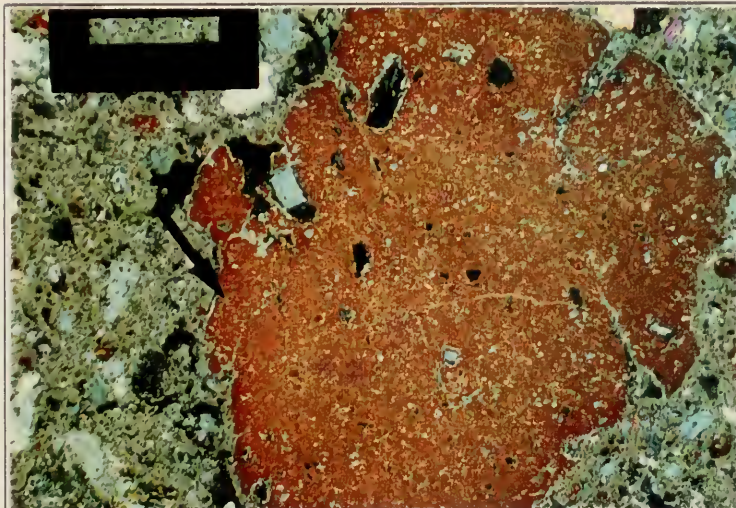


Figure 29: Subrounded nodule with porphyritic texture (stained). Note the more intense reddish staining along the left rim of the nodule (probably associated to calcium carbonate dissolution and migration). Bar is 10 μ m. Mag.: 35x, crossed polars.

Results obtained from Content of Calcium Carbonate by Particle Size tests, showed a tendency toward greater softness in nodules of small size. According to Reeves (1976,

54), slicing of numerous nodules had revealed a progressive development that shows that the smaller nodules tend to be softer (composed of a powdery carbonate), contain a high percentage of sand, and have a very irregular shape. On the other hand, the larger nodules display a greater degree of lithification, contain less sand, and have a more spherical shape. In addition, nodules which may be slightly harder than surrounding carbonate, or thoroughly lithified, develop best in sands and sandy parent material. This information seems to be very applicable to the caliche from the Great House.

David Hendricks, soil scientist from the University of Arizona who studied a specimen of caliche from the Great House, stated that nodules found in the caliche from the Great House are evidence that an original K-horizon (petrocalcic horizon) was powdered to produce the material for the walls (Wilcox and Shenk 19977, 103) However, the



Figure 30: Microcrystalline matrix of a nodule (stained) at high magnification. Bar is 10 μm . Mag.: 50X, crossed polars.

relationship between sizes and shapes of the aggregates (unsorted) and their mineralogical constitution inside the matrix of caliche revealed in thin section tends to disprove Hendricks' assumption (figure 32). It is very unlikely that the nodules in the caliche are a product of manipulation of the soil for construction purposes. On the other hand, it is very probable that nodules were naturally present in the caliche²⁸ before it was used in the construction of the Great House.

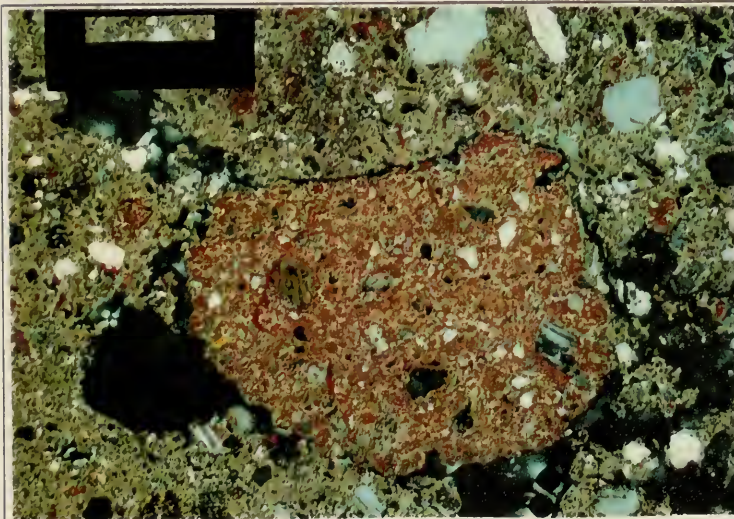


Figure 31: Subrounded nodule (stained) with porphyritic texture composed of poikilitic quartz crystals in a cryptocrystalline calcic matrix. Bar is 10 μ m. Mag.: 35X, crossed polars.

²⁸ According to Gile et al. (1966) and Hawley and Gile (1966), nodules are present in stages II and III of caliche development.

Unfortunately, it was very difficult to study the void pattern of the caliche in thin section because of the high density of aggregates and unavailability of lower magnifications (less than 4x).

Some voids or irregular spaces that have not been filled with matrix were observed in all thin sections with less found in 1F (outer caliche). Difficulties in thin section preparation were reported. Particularly, the material for 3 and 4B (inner caliche) which was very crumbly and very difficult to grind without suffering disintegration. Therefore, it is possible that the sample preparation method of thin section may have altered the natural void pattern of the caliche by creating new ones.

- Fine fraction (fabric) or birefringence fabric

Small particles, such as the fine fraction of a soil, cannot actually be observed individually under the polarizing microscope. Rather, one sees the manifestation of this fabric under crossed polars as represented by the interference colors and birefringence of the fine material and its inclusions. Thus, the expression of the internal geometry of the fine fraction of a soil or material is called the birefringence fabric (also called the b-fabric) (Courty, Goldberg and Mcphail 1990).

The caliche soil presents a crystallitic birefringence fabric, very grainy due to high density of fine crystals, and mottled gray to yellow to brown under plain polarized light.²⁹

²⁹ Cryptocrystalline according to petrology terminology.



Figure 32: Montaged microphotographs of caliche thin section (stained) showing a close porphyritic texture, composed of crystals (mainly quartz) and nodules of different shapes and sizes embedded in a cryptocrystalline calcic matrix (birefringence fabric). Note the large subrounded nodule (upper area) with porphyritic texture (poikilitic quartz crystals in a cryptocrystalline matrix). The nodule show a micritic rim of CaCO_3 (lower and right), identified by a more intense reddish color, probably related to dissolution of previously cemented CaCO_3 . Bar is 10 μm . Mag.: 14X, crossed polars.

According to Courty, Goldberg and Macphail (1990) these qualities may refer to a pure micritic fabric, a term that refers to a fabric composed of calcitic crystals less than 10 μ m in size.

Under crossed polars, the b-fabric shows extinction and high birefringence typical of carbonate material. No differences or banding of the b-fabric were detected in any of the four caliche thin sections under 40x magnification. In addition, no color change in the alizarin red stained-side of all thin sections (associated to migration or depletion of carbonate content in the matrix) was detected.

The outer edge of thin section 1F (outer caliche) was closely observed under high magnification (40x) in order to detect any micromorphological change that could explain the color alteration observed on all exterior faces of the Great House walls (outer face of fragment). In addition, Wilcox and Shenk (1977) reported a chemical alteration of 3mm in thickness on the exposed caliche. No micromorphological change of the caliche b-fabric was visible under the highest magnification available (40x). Therefore, the questions regarding the color alteration of the exposed caliche and the chemical alteration reported by Wilcox and Shenk (1977) remain still unanswered. Microscopical observations of the caliche under higher magnification (higher than 40X) are highly recommended for the future.

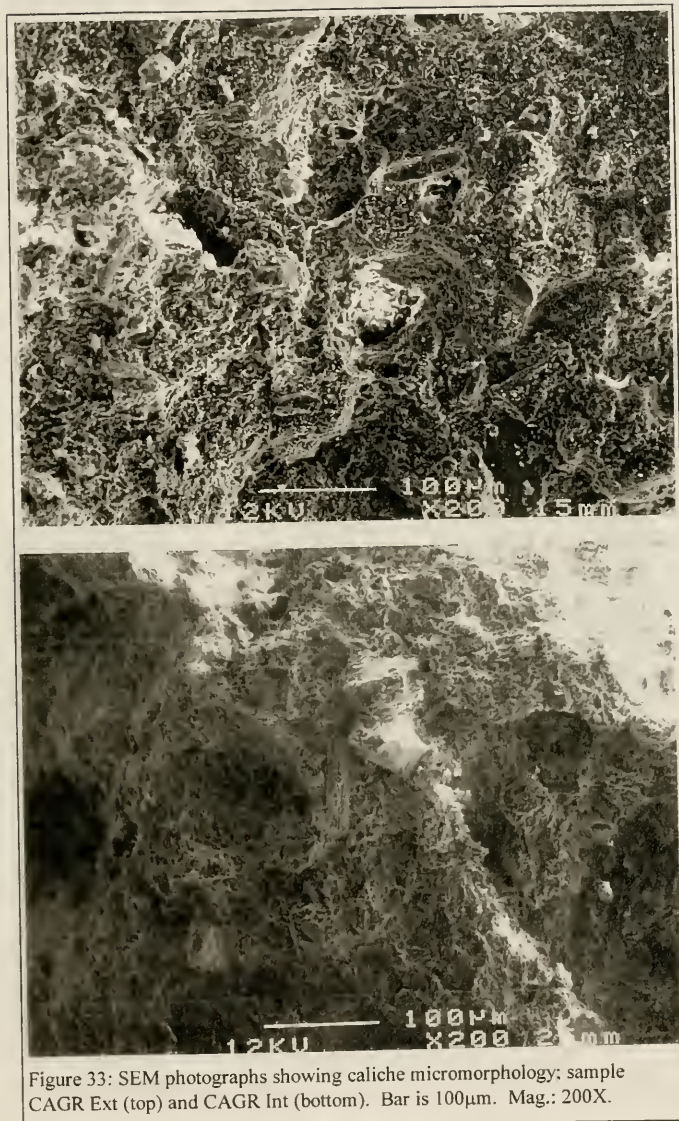


Figure 33: SEM photographs showing caliche micromorphology; sample CAGR Ext (top) and CAGR Int (bottom). Bar is 100µm. Mag.: 200X.

its characteristics surface on top.

Scanning Electron Microscopy (SEM)

Two samples,

CAGR Ext (outer
caliche with the

characteristic
reddish surface)

and CAGR Int

(inner caliche

approximately 20

to 30 cm deep into
the fragment) were

observed using

SEM at

magnifications

ranging from 200x

to 1,500x. Sample

CAGR Ext was

placed on the

sample holder with

The microstructure of the caliche under low magnification (200x) is characterized by a porous and crystalline fabric in which a variety of aggregates are embedded. Zoned or layered fabric/aggregate interfacial regions were not observed under this magnification. In addition, no micro- morphological differences between samples were encountered (figure 33).

It was decided to increase the magnification of SEM (800x and 1,500x) to observe the shape and size of the micritic particles that compose the birefringence fabric of the caliche.

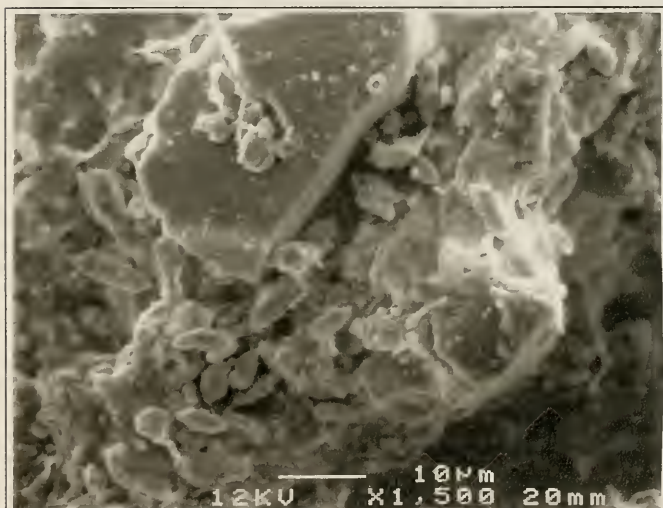


Figure 34: SEM photograph of an aggregate (probably sand grain) embedded in the caliche matrix. Rice-shaped calcium rich particles (calcite) appear to be growing from the pits of the aggregate's surface. Bar is 10 μ m. Mag.: 1,500X.

Under higher magnification (1,500x) the aggregates in the samples appear slightly to moderately etched, and small (less than 5 μ m), rice-shaped calcium rich particles, probably

calcite, appear to be growing from the pits in the aggregate surfaces (Figure 34).

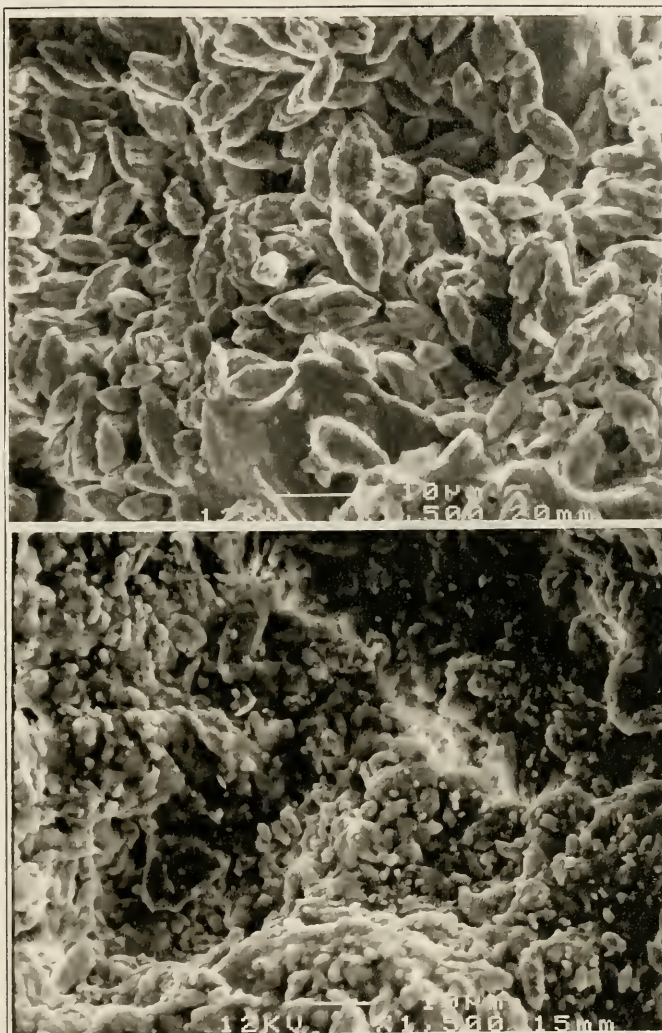
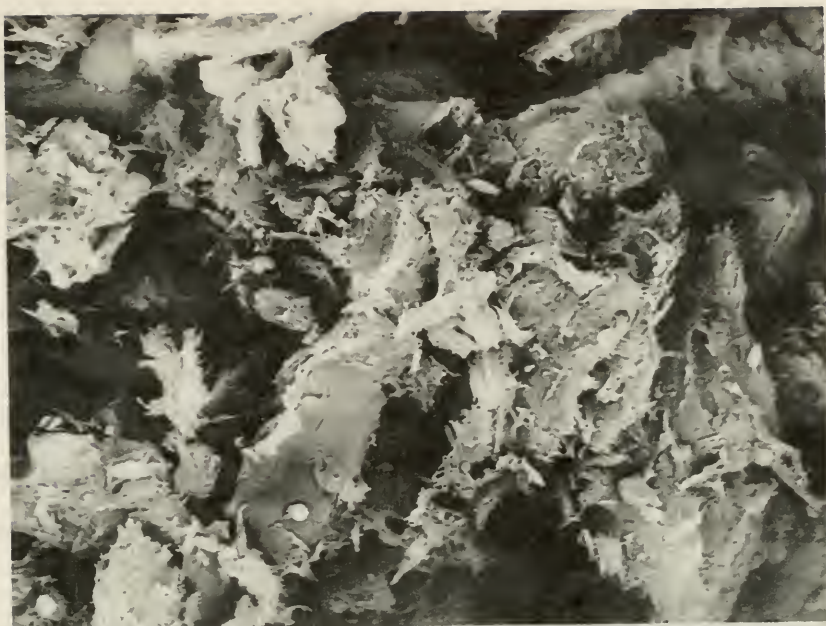


Figure 35: SEM Photographs showing caliche micromorphology. Notice the difference in size of calcium rich particles from the caliche matrix of sample CAGR Ext (top) and CAGR Int (bottom). Bar is 10µm. Mag.: 1,500X.

Micro-morphological differences between samples were found under 800x and 1,500x magnifications, especially in the fabric (fine fraction) of the caliche (figure 35). Sample CAGR Int presents a fabric formed by micritic calcic particles, rounded, rice-like shaped (lozenge), less than 5µm in length and 1µm in

thickness. Larger particles are embedded in this matrix. Sample CAGR Ext also shows a fabric formed by similar shaped calcic particles. However, the size of these particles is



Casa Grande

5 μ m

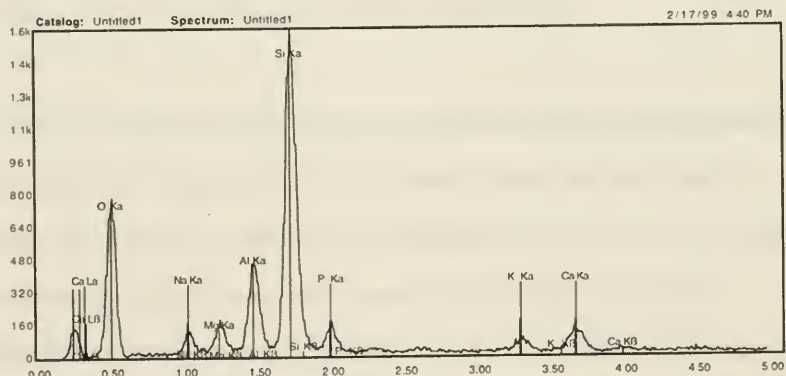


Figure 36: SEM photograph of a palygorskite (clay) crystal (top) and back scattered image (bottom). Bar is 5 μ m. Mag.: 20,000X.

larger (approximately 5 to 12 μ m and 2-3 μ m in thickness) than in the other sample, thus, the fabric of sample CAGR Ext is formed by both micritic and some microsparitic particles (between 10 and 50 μ m). The larger size and more abundance of calcic particles in CAGR Ext makes its fabric much more denser than that of CAGR Int. This micromorphological feature explains the stronger cementation of the outer caliche.

Electron dot mapping of both samples was done in order to obtain visual images of ions (Mg, Al, Si, K, Ca, Fe) present in the different particles (aggregates and finer fraction). Results and microphotographs are shown in Appendix C. In addition, SEM was used to confirm x-ray diffraction results of palygorskite as the clay mineral present in the caliche. Fortunately, using high magnifications (3,500X and more) it was possible to find and photograph palygorskite particles (figure 36). Identification was completed by comparisons with a standard palygorskite SEM microphotograph.

The difference found in the fabric of both caliche samples under high magnifications (800x and 1,500x) may be associated to lateral movements of water enriched in dissolved calcium carbonate and reprecipitation or recrystallization of the carbonate due to repetitive wetting and drying cycles. As a result, a cementation from calcium carbonate accumulation probably associated with osmosis seems to have formed in the outer zone of caliche of the Great House (see chapters 4 and 5 for more details).

3.2.4.4 Acid-Soluble (Carbonate) Content³⁰

Calcium carbonate (CaCO_3) is a primary mineral component of calcareous soils (caliche). A number of laboratory procedures have been developed to determine the amount of calcium carbonate in a soil specimen. Basically, these different procedures can be divided in two groups: (1) those that determine the calcium ion (Ca^{+2}) concentration, and (2) those that determine the concentration of carbonate ions (CO_3^{-2}) (Chaney et al. 1981, 6). The type of procedure to be used depends upon many factors, such as: accuracy required, amount of sample, analytical speed, costs, operator skills, and environmental conditions (Channey et al. 1981, 4-6).

It was decided to use an acid-soluble weight loss method³¹ (also called acid digestion) to determine the concentration of carbonate ions in the caliche soil from the Great House. This selection was based on availability of funds and technical resources.

The basis of an acid-soluble weight loss method is the treatment of a calcareous soil with diluted hydrochloric acid (HCl) which digests all carbonate material and some other minor constituents, thus giving a rough index of carbonate content.

³⁰ Acid-Soluble Weight Loss Method (Chaney et al. 1981, 10), Mortar Analysis Simple Method (Modified) (Teutonico 1988, 113).

³¹ According to Chaney et al. (1981), the acid-soluble weight loss methods are classified with a “rough” relative accuracy ($>\pm 5$ percent), “high” analytical speed according to specimens/day, and “low” initial equipment/cost.

Many calcareous soils of the Southwestern United States contain nodules or concretions strongly cemented by calcium carbonate inside a relatively uniform cemented matrix containing less calcium carbonate(Beckwith and Hansen 1981, 24). This is true for the caliche soil from the Great House. Thus, calcium carbonate is present not only as cementation on fine particles of soil (soil matrix) but also as cementing particles of various sizes and shapes (gravel, sand, silt and clay), forming nodules that play a very important role in the characteristics of the caliche under study.

For this reason, it was decided to perform two forms of the acid-soluble weight loss test: (1) complete acid digestion of a caliche sample in order to obtain a total content of calcium carbonate, and (2) acid digestion of the caliche first separated into different particle size fractions in order to obtain the content of calcium carbonate of each. All procedures and results are described in detail in the Appendix C.

Acid (HCl) Digestion of the Complete Sample³²

The purposes of this test are (1) to determine the total content of calcium carbonate in the caliche, and (2) to compare total content of calcium carbonate in the caliche according to the different depths of the caliche fragment.

A set of three samples, CAGR A, CAGR B and CAGR C was selected for this test. The samples were obtained according to the sampling procedure previously explained.

³² Teutonico, J. M., Experiment #21 modified, (1988), p.113 and Chaney et al., (1981), pp. 10-11.

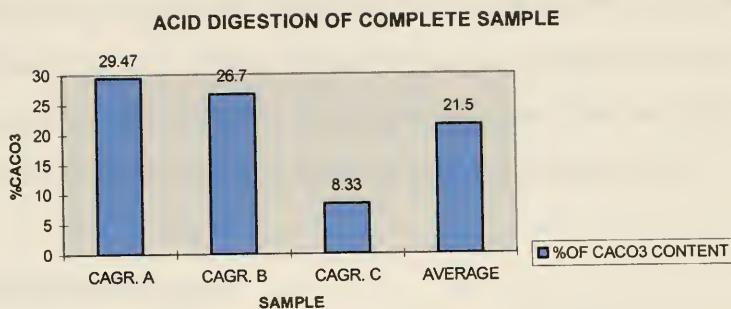


Figure 37: Percentage of CaCO_3 content by total acid digestion of samples

The results obtained (figure 37 and Appendix C) show a different content of calcium carbonate in each of the three samples. The difference of calcium carbonate content is most obvious between sample CAGR C (8.33%), near the core, and CAGR A (29.47%), the outer 10cm face of the wall. The percentage for sample CAGR B (26.70%) is similar to CAGR A, though slightly lower.

The content of calcium carbonate in the fragment decreases as the depth increases, that is, the caliche that has been more exposed to the weather (outer 10-20cm) possesses more calcium carbonate than the one deeper in the wall (between 20 and 30cm) which has been depleted of calcium carbonate.³³ The differences in results could be interpreted as an enrichment of calcium carbonate at the surface due to increased exposure to the weather

³³ The deepest caliche tested (CAGR C, approximately 30cm deep) is not considered as part of the core of the wall. CAGR C caliche has suffered transformation due to migration of its calcium carbonate toward the outside, and the caliche core (deeper than 30cm) probably did not suffer any transformation.

and a migration-depletion from calcium carbonate from the area located immediately behind the outer enrichment zone. The calcium carbonate enriched layer, or crust, varies in thickness and calcium carbonate content (as demonstrated by variation of results in samples CAGR A and CAGR B) and can be visually distinguished by its outer reddish color.³⁴ This process has been observed in nature in caliche soils (Lattman 1977).

Acid Digestion by Particle Size³⁵

The purpose of this test is (1) to determine the calcium carbonate content of various particle size fractions of the caliche, and (2) to compare calcium carbonate content by particle size in the caliche soil from different depths of the caliche fragment.

Only samples CAGR B and CAGR C were selected for this test. Sample CAGR A was omitted due to its high content of calcium carbonate which cemented the sample and made it impossible to break down into fractions.

The hypotheses for this test are: (1) calcium carbonate content in the caliche decreases as its grain size decreases (this explains the different hardness of the nodules), and (2) variation of calcium carbonate content (migration and depletion) probably occurs in the smallest fraction of the caliche (<75 μ m, matrix). For this reason, CAGR B will show more calcium carbonate content within this grain size than CAGR C.

³⁴ Munsell reading at the site: 5YR 6/4 - 7/4, and Munsell reading of sample in the laboratory: 5YR 6/6 - 6/8.

³⁵ Teutonico (1988, 113) Experiment #21 (modified) and Chaney et al. (1981, 10-11).

Each sample was sorted according to particle size with the use of standard sieves and de-ionized water (Figure 38) (see Appendix C for detailed procedure and results).

Sample CAGR B was divided according to the following sieves:

#30 ($\geq 600\mu\text{m}$)

#50 (300-600 μm)

#100 (150-300 μm)

#200 (75-150 μm)

pan ($< 75\mu\text{m}$).

Sample CAGR C was sorted according to the following sieves:

#4 ($\geq 4.75\text{mm}$)

#8 (2.36-4.75mm)

#16 (1.18-2.36mm)

#30 ($< 600\mu\text{m}$).

Thus, sample CAGR B gave a good indication of calcium carbonate content of the smaller particles ($< 600\mu\text{m}$) and CAGR C gave the content of calcium carbonate of the larger fractions ($> 600\mu\text{m}$).

Figure 39 shows the distribution of calcium carbonate content in the smaller grain size fractions (retained #30, #50, #100, #200, and passed #200) of sample CAGR B according to its total gross weight. These results show a slight difference in the content of calcium

carbonate for #50, #100 and #200 (0.82%, 1.15%, and 1.28% respectively), and a very high content for the smallest particles (passed #200 or particles $< 75\mu\text{m}$) which is 9.24%.

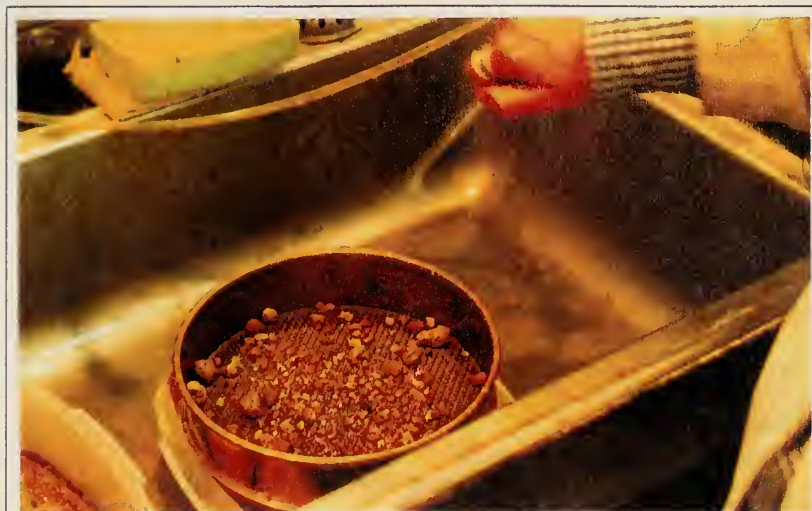


Figure 38: Separation of caliche by particle size using standard sieves and de-ionized water.

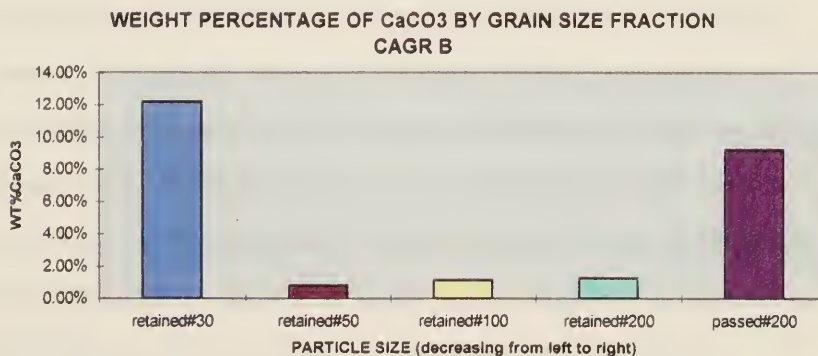


Figure 39: Distribution of calcium carbonate content in the smaller grain size fractions (retained #30, #50, #100, #200, and passed #200) of sample CAGR B according to its total gross weight.

Note: "Retained #30" includes all particles which passed sieves #4, #8, and #16.

Therefore, sample CAGR B shows a very good cementation of the caliche matrix represented by a high content of calcium carbonate in the smallest particles (smaller than 75 μ m, silt and clay fractions).

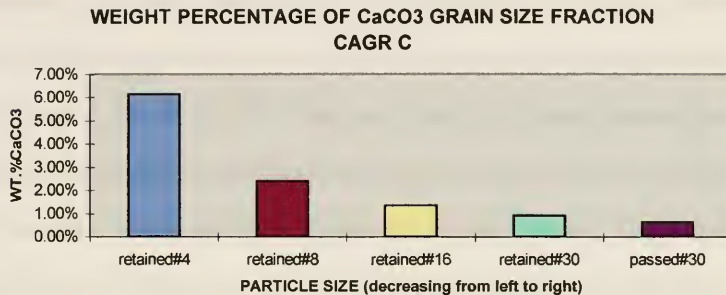


Figure 40: Distribution of calcium carbonate content in the larger grain size fractions (#4, #8, #16, #30 and passed #30) of sample CAGR C according to its total gross weight.

Figure 40 shows the distribution of calcium carbonate content in the larger grain size fractions (#4, #8, #16, #30 and passed #30) of sample CAGR C according to its total gross weight. These results show that the larger the particle size, the higher the calcium carbonate content (6.15% for #4, 2.41% for #8, 1.36% for #16, 0.93% for #30, and 0.65% for passed #30), and explains the difference in hardness of the nodules, which tend to be softer as their sizes decrease. In general, these results could be applicable to the rest of the samples (CAGR A and CAGR B), and for the entire caliche fragment.

The results obtained for sample CAGR. B cannot be compared to samples CAGR A or CAGR C because each of these samples will show a difference of calcium carbonate content in their smaller grain size fraction, especially that portion of less than 75 μ m, due to calcium carbonate enrichment (CAGR A) or depletion (CAGR C).

In conclusion, the results obtained for the two samples (figure 41 and table 1) not only reveal a difference in total content of calcium carbonate for each sample (24.70% for CAGR B and 11.50% for CAGR C)³⁶ but also a variation of calcium carbonate content by particle size, particularly in the small particle fraction (particles >600 μ m or passed #30) which resulted in 12.49% for CAGR B and only 0.65% for CAGR C. There is only a small difference of calcium carbonate content in the large particles of both samples (particles >600 μ m, or retained on sieve #30), 12.21% for CAGR B and 10.85% for CAGR C. These, together with the previous results, clearly indicate that migration (CAGR B) and depletion (CAGR C) of calcium carbonate occurs in the matrix of the caliche. In addition, the results verify the micromorphological changes in the matrix of the caliche visible in SEM.

Sample	B	C
Wt.% CaCO ₃ content of total sample	24.70%	11.50%
Wt.% CaCO ₃ content of particles retained 30 (>600 μ m) (sieves #4, #8, #16 and #30)	12.21%	10.85%
Wt.% CaCO ₃ content of particles passed 30 (<600 μ m) (sieves #50, #100, #200 and pan)	12.49%	0.65%

Table 1: calcium carbonate content and distribution in samples CAGR B and CAGR C.

³⁶ Both results are very similar to the ones previously obtained from acid digestion of the complete sample.

**CAGR B - WEIGHT PERCENTAGE CaCO₃
CONTENT BY PARTICLE SIZE**



**CAGR C - WEIGHT PERCENTAGE CaCO₃ CONTENT BY
PARTICLE SIZE**

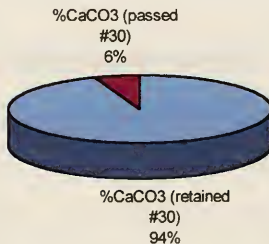


Figure 41: Weight percentage of calcium carbonate content by particle size for samples CAGR B and CAGR C.

3.2.4.5 Particle Size Analysis (ASTM D422-63)³⁷

Particle size analysis is “the method that covers the quantitative determination of the distribution of particle sizes in soils” (ASTM 1993, 91). The distribution of particle sizes

³⁷ D 422-63 (Re-approved 1972) “Standard Method for Particle-Size Analysis of Soils”, Philadelphia: ASTM, 1993, pp. 91-97.

larger than $75\mu\text{m}$ (retained on the #200 sieve) is determined by sieving, while the distribution of particle sizes smaller than $75\mu\text{m}$ is determined by a sedimentation process.

The caliche of the Great House consists of a mixture of discrete particles of various shapes and sizes. These are: gravel (2-60mm), sands (2mm- $60\mu\text{m}$), silts ($60\mu\text{m}$ - $2\mu\text{m}$), and clays ($<2\mu\text{m}$). The types and relative proportions of these particles give the caliche a particular character and behavior. In addition, nodules or concretions (sands, silts and clays cemented by calcium carbonate) of various shapes and sizes also play a very important role in the particle size distribution of the caliche from the Great House. Beside the nodules, calcium carbonate particles are present among the silt and clay particles.

Due to the presence of calcium carbonate in the matrix of the caliche ($<2\mu\text{m}$) it was very difficult to obtain accurate results from sedimentation without acid digestion of this particle fraction.³⁸

Three major decisions were made concerning particle size analysis:

1. To eliminate the sedimentation component of particle size analysis and just obtain a weight percentage of silts and clays from the sieving procedure.

³⁸ Ideally, particle size analysis of the caliche should have involved: (1) separation of the caliche by particle size, (2) acid digestion of the silt and clay fractions (particles smaller than $75\mu\text{m}$ or passed #200), and (3) sedimentation of silts and clays. This process was very time consuming and the caliche proved to be very difficult to sort by particle size, especially the sample coming from the outer 10cm of the original fragment (CAGR A), which is more cemented by calcium carbonate.

2. To perform particle size analyses in samples CAGR B and CAGR C. Sample CAGR A was not included for particle size analysis because of the difficulties it presented in its preparation due to its highly cemented condition.
3. To perform different particle sizes tests: in samples without acid digestion and in samples with total acid digestion. This decision was taken in order to determine the percentage of nodules in relation to the rest of the caliche particles.

These tests were performed according to the procedure detailed in “A Laboratory Manual for Architectural Conservators”, experiments 18A (Teutonico 1988, 73). All details and results are presented in Appendix C.

Particle Size Analysis Without Acid Digestion

The results obtained from this test (figure 42 and Appendix C) show great similarity of particle content for both samples. The most noticeable difference is in the silt and clay fraction. Such difference could be related to a larger amount of calcium carbonate particles in this fraction in sample CAGR B (as proved in acid digestion by particle size).

According to the “Standard Test Method for Classification of Soils for Engineering Purposes”³⁹, both samples classify as a coarse-grained soil since more than 50% of the

³⁹ D 2487-85 “Standard Method or Classification of Soils for Engineering Purposes”, Philadelphia: ASTM, 1993, pp. 301-302.

PARTICLE SIZE ANALYSIS WITHOUT ACID DIGESTION

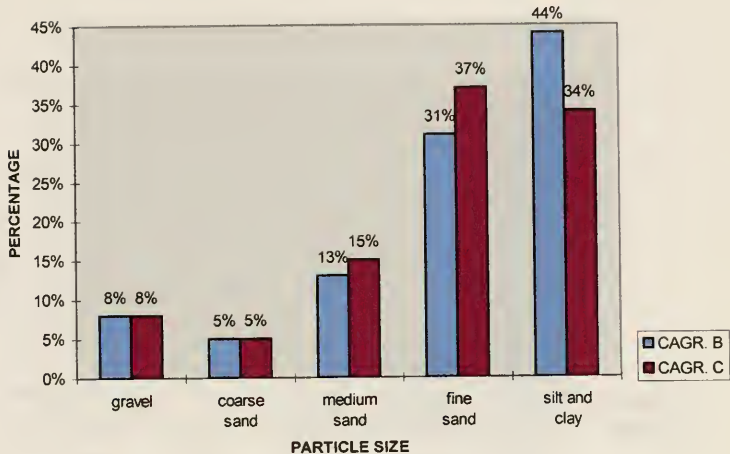


Figure 42: Particle size analysis of the caliche without acid digestion

particles were retained on the #200 sieve, and as “sand” (since more than 50% of the coarse fraction passed #4 sieve). In addition, the samples classify as “coarse-grained with fines” (since more than 12% of the test specimen passed # 200 sieve), and the fines as “silty clayey”⁴⁰

Particle Size Analysis with Total Acid Digestion

Like the previous test, the results obtained in this test show great similarity for both samples (figure 43, Appendix C).

⁴⁰ The fines are determined to be either clayey or silty based on the plasticity index versus liquid limit. D 2487-85 “Standard Method of Classification of Soils for Engineering Purposes”, Philadelphia: ASTM, 1993, pp. 301-302.

PARTICLE SIZE ANALYSIS WITH TOTAL ACID DIGESTION

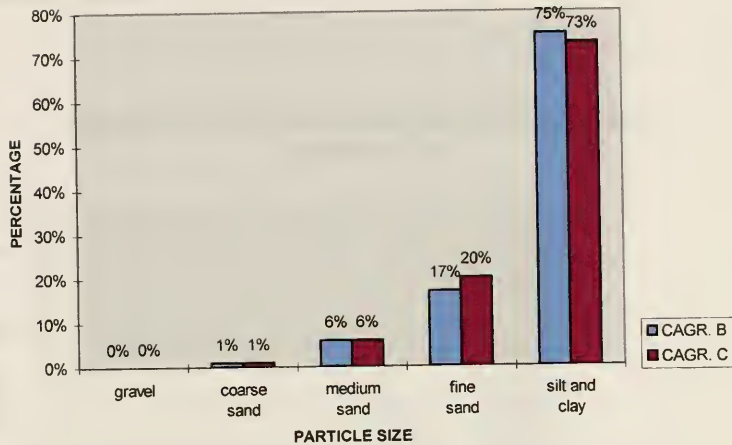


Figure 43: Particle size analysis of the caliche after total acid digestion

According to the “Standard Test Method for Classification of Soils for Engineering Purposes”⁴¹, the caliche with total acid digestion classifies as a fine-grained soil (since more of the 50% of the particles passed #200 sieve). In addition, this soil is classified as “silty clayey”⁴² with sand” (since less than 30% and more than 15% of the particles were retained on the #200 sieve).

Averages of particle size analyses for both samples of caliche with and without acid

⁴¹ D 2487-85 “Standard Method or Classification of Soils for Engineering Purposes”, Philadelphia: ASTM, 1993, pp. 301-302.

⁴² This is related to the plastic limit and plasticity index of this soil fraction.

digestion were obtained in order to make comparisons (figure 44).

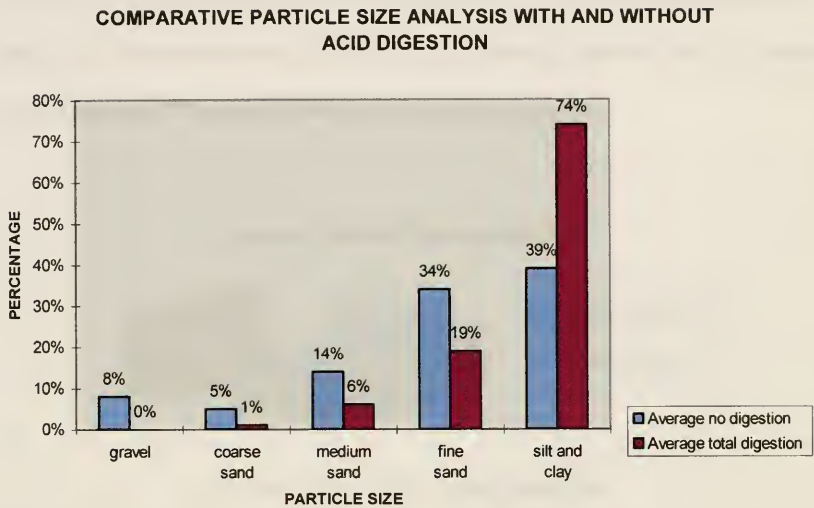


Figure 44: Comparative particle size analysis of the caliche with and without acid digestion

These results show a large reduction of coarse particles (gravel and sands) and a great increase of silt and clay particles after acid digestion of the caliche. Thus, the majority of the larger particles of caliche (particularly gravel and coarse sand) are composed of acid-soluble nodules which disappeared after acid digestion and released previously cemented silts and clays. Thus, most of the material left from the disintegration of the nodules is

composed of silts and clays which adds to the quantity of silts and clay naturally present in the caliche, increasing the percentage.

The dissolution of nodules greatly affects the percentage of coarse material (gravel and sand) in relation to the percentage of fines in the caliche. In its natural form the caliche contains 61% coarse material and 39% fines. After total acid digestion, these percentages are transformed to 26% coarse material and 74% fines (figure 45).

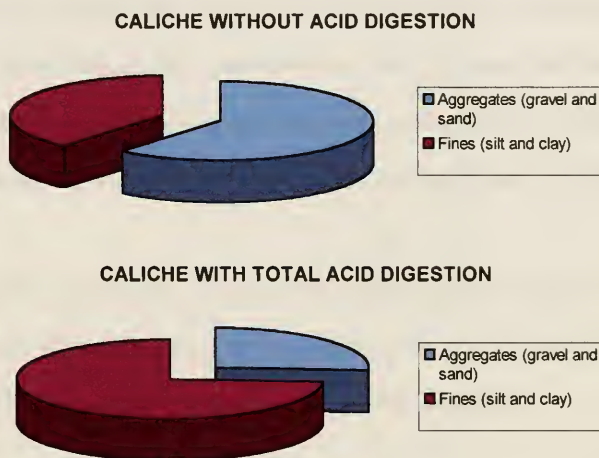


Figure 45: Comparative results of content of aggregates (gravel and sand) and fines (silt and clay) in the caliche with and without acid digestion (percentages by weight)

It can be concluded from these tests that the caliche from the Great House is composed of unsorted particles of gravel and sands and a fair amount of silts and clays. Most of the larger particles are represented by various sizes of nodules, mainly composed of silt and

clay particles bound by calcium carbonate, which probably played an extremely important role in the selection of the caliche as a material for construction purposes. According to Gile (1966) and Hawley and Gile (1966), nodules of caliche are a natural characteristic of different stages of development in gravelly and non-gravelly caliches. Therefore, it is very unlikely that these nodules are the result of grinding a petrocalcic horizon.

3.2.4.6 Particle Description (Stereo-microscope)

The fraction of caliche soil particles larger than 75 μ m (retained on sieve #200) obtained from particle size separation was examined under a Nikon SMZ-U stereo microscope with a Foster 8345 quartz halogen fiber optic light source, and 1:10 zoom lens. General observations were recorded, including particle shape, roundness, color, organic matter content and presence of calcium carbonate by nodule content (Bullock et al. 1985, 30-32).

As per the results of particle size analyses, there is a high content of nodules of various sizes and shapes. The nodules, which are very light in color, are composed of a calcium carbonate matrix enclosing other particles of various sizes and shapes.

The shape of the nodules varies from rounded (mainly the larger ones, retained in sieve #4) to subrounded and subangular. Most of the sharper edges of the nodules are formed by gravel and sand particles enclosed or partially enclosed by calcium carbonate matrix.



Figure 46 (top): Particles retained on sieve #8(2.36mm). Nodules of caliche, rounded in shape. Stereomicroscope. Mag.: 14X
 Figure 47 (bottom): Different sizes of caliche nodules of various shapes (subrounded to angular). Stereomicroscope. Mag.: 14X

Some nodules, mainly the most subangular ones, are formed by two or more large particles partially embedded in the calcium carbonate matrix or simply adhered together by the calcium carbonate matrix with only a thin coating covering the particles (figure 28).

The non-nodule particles, mainly quartz or quartz like particles, are white, light gray and yellowish in color and tend to increase in



Figure 48 (top): Sand (quartz-like) particles partially coated by calcium carbonate matrix. Stereomicroscope. Mag.: 14X

Figure 49 (bottom): Particles retained on sieve #30 (600µm).

Approximately similar proportions of nodules and sand (quartz-like) particles compose this fraction of caliche. Stereomicroscope. Mag.: 14X

number as the particle size decreases. Like the nodules, these particles have various shapes, rounded to angular. In general, these particles tend to have sharp edges and corners, particularly the small ones.

Color of caliche soil particles was determined by comparing them with the Munsell soil color chart.⁴³ In general, the results obtained show a high value (8-7) and a low chroma (3-1).

⁴³ D1535, "Standard Test Method for Specifying Color by the Munsell System". Philadelphia: ASTM, 1993.

These results are probably due to the high content of caliche nodules which are closer to white due to their high calcium carbonate content. In addition, these results show a general tendency of a slight decrease in value and increase in chroma as the size of the particles decreases. This is probably due to the fact that the quantity of caliche nodules decreases with a decrease in particle size and the color is mostly provided by the quartz or quartz-rich particles of the caliche soil fraction.

3.2.4.7 Atterberg Limits (Liquid Limit and Plastic Limit)(ASTM D4318)

The liquid limit and plastic limit of soils (along with the shrinkage limit) are collectively known as the Atterberg Limits in recognition of their formation by the Swedish soil scientist, A. Atterberg. These limits distinguish the boundaries of the several consistency states of plastic soils.⁴⁴

The liquid limit of a soil is defined as “the water content, expressed as a percentage of the mass of the oven-dried soil, at the boundary between the liquid and plastic states” (Teutonico 1988, 102).⁴⁵

The plastic limit of a soil is defined as “the water content, expressed as a percentage of the mass of the oven-dried soil, at the boundary between the plastic and semi-solid states”

⁴⁴ D 4318-84, “Standard Test Method for Liquid Limit, Plastic Limit, and Plasticity of Soils”, Philadelphia: ASTM, 1993, p. 591.

⁴⁵ The liquid limit is determined by using a Casagrande device, which repeatedly drops a sample of wet soil scored with a groove until the soil flows and closes the groove. The moisture content of the soil is then calculated. The device is calibrated and the test is methodical so that the arbitrarily defined liquid limit can be calculated from repeated performances (ASTM D4318-84).

(Teutonico 1988, 96).⁴⁶

A third characteristic, the plasticity index (PI) can be calculated from the plastic and liquid limit. The plasticity index (PI) is obtained by subtracting the liquid limit value from the plastic limit value. Higher values for the PI usually predict greater expansion when the soil is saturated with water (Young and Warkentin 1975, 62).

The plastic limit, liquid limit and plasticity index tests were performed on caliche soil samples from the front (CAGR A), middle (CAGR B) and rear (CAGR C) sections of the caliche fragment. All tests were carried out on the samples with their calcium carbonate content (without acid digestion) as well as on the samples without their calcium carbonate content (after digestion in acid).⁴⁷

The results obtained from these tests are shown in table 2. In general, both the liquid limit and plastic limit are lower in the samples without digestion (with calcium carbonate) and they increase in the samples digested (without calcium carbonate). According to Reeves, (1976, 146-49) oftentimes the liquid limit of most caliches, which ranges between 10 and 60%, is higher than expected from the plasticity index and shrinkage due to predominance of powdery calcium carbonate.

⁴⁶ It is determined by repeatedly rolling a soil sample into 3.2 mm. threads, until the soil crumbles, and then calculating the water content of the soil. For range of soils, the plastic limit varies less than the liquid limit, and is somewhat related to the surface area of the clay particles, though not in direct proportion (Young, Raymond N. and Benno P. Warkentin 1975, 66).

⁴⁷ Acid digestion of the prepared samples for these tests (material passed sieve #40 - 425 μ m) followed the procedure described in Appendix C.

WITHOUT ACID DIGESTION				WITH ACID DIGESTION			
Sample	Liquid Limit	Plastic Limit	Plasticity Index	Sample	Liquid Limit	Plastic Limit	Plasticity Index
CAGR. A	22	29	NP	CAGR. A	43	35.24	7.76
CAGR. B	34	24.89	9.11	CAGR. B	35	37.26	NP
CAGR. C	40	26.32	13.68	CAGR. C	Indeterminate	40.91	Indeterminate

Table 2: Liquid limit, plastic limit and plasticity index for caliche samples with and without acid digestion.

The plasticity index (PI) for both sets of samples (with and without acid digestion) is very low which indicate little expansion when the caliche is saturated with water. The plasticity index of most caliches ranges between 0 and 20% (Reeves 1976, 148).

The tests described herein were performed only on the portion of a soil which passed sieve #40 (425 μm)⁴⁸, so the relative contribution of this portion of soil to the properties of the caliche as a whole must be considered when using these tests to evaluate the caliche properties (ASTM D4818-84).

3.2.4.8 Volumetric and Linear Shrinkage (ASTM D 4943-89)⁴⁹

An important characteristic of a soil used for architectural purposes is the ability to dry with an acceptable degree of shrinkage. The shrinkage limit is useful to evaluate the shrinkage, crack development and swell potentials of earthen structures involving cohesive soils.

⁴⁸ However, a #30 (600 μm) sieve was used instead.

⁴⁹ D 4943-89 Standard Test Method for Shrinkage Factors of Soils by the Wax Method, Philadelphia: ASTM, 1993.

“The term shrinkage limit, expressed as a moisture content in percent, represents the amount of water required just to fill the voids of a given cohesive soil at its minimum void obtained by oven-drying” (D 4943-89, 991).

Shrinkage is also related to the amount of water in the wet soil mix. High water content results in considerably increased shrinkage (Alva Balderrama and Teutonico 1983, 49).

The amount of shrinkage is a practical measurement of soil performance, and that performance is determined by the constituents of the soil, including sand, silt, and clay. Sand experiences very little linear shrinkage, and silt is only slightly more active than sand. Clay minerals in the smectite family (montmorillonite, bentonite) are particularly water sensitive. They swell when wet and shrink (and therefore crack) when dry (Head 1992, 107-109). Thus, the clay fraction is by far the most active.⁵⁰ According to the results obtained from x-ray diffraction, palygorskite is the clay mineral identified for the caliche of the Great House. This type of clay is oftentimes associated with calcite and is not as water sensitive as are the clays from the smectite group.

Shrinkage of a soil is measured both linearly and volumetrically. Similar to the liquid and plastic limits, shrinkage is performed only on the portion of a soil which passes a # 40

⁵⁰ Kaolinite-type clays have a linear shrinkage rate of 3% to 10%; illites, 4% to 11%; and smectites/montmorillonites, 12% to 23% (Houben and Guillaud 1994, 31).

sieve (425 μm)⁵¹, so the relative consistency of this portion needs to be compared to the properties of the caliche as a whole.

Shrinkage tests were performed on caliche samples CAGR A, CAGR B and CAGR C. The tests were conducted on samples with their calcium carbonate content (without acid digestion) as well as those without (after digestion in acid).⁵² The procedures followed for this test were according to ASTM D 4943-89. The results obtained from this test are shown in figures 50 and Appendix C.

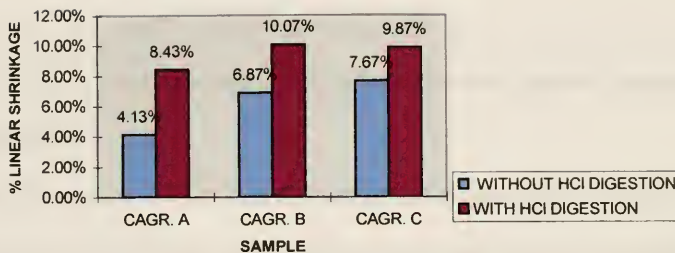
In general, the results obtained from this test show more volumetric and linear shrinkage in the soil samples with their calcium carbonate content removed. The results obtained for linear shrinkage are within 0 and 10%, which is the range of linear shrinkage of most caliches (Reeves 1976, 146).

Samples CAGR B and CAGR C with calcium carbonate show similar volumetric and linear shrinkage. Similar results were obtained for the same samples without calcium carbonate. Sample CAGR A, both digested and undigested, show less shrinkage compared to CAGR B and CAGR C digested and undigested. Therefore, these results show that calcium carbonate plays a very important role in controlling shrinkage.

⁵¹ However for this case #30 (600 μm) sieve was used instead.

⁵² Acid digestion of the prepared samples for these tests (material passed sieve #30 - 600 μm) followed the procedure described in Appendix C.

LINEAR SHRINKAGE



VOLUMETRIC SHRINKAGE

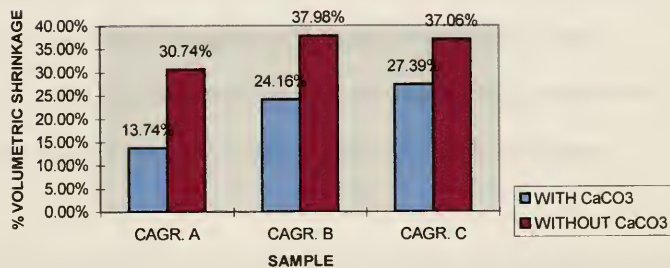


Figure 50: Linear and volumetric shrinkage of caliche with and without acid digestion.

Shrinkage results obtained in this test are only representative of a portion of the caliche (passed sieve #40), that is, the portion without the larger particles or aggregates. The caliche contains a large proportion of large sized particles that probably play a very

important role in decreasing or controlling shrinkage. In addition, calcium carbonate acts as a stabilizer, controlling shrinkage. Therefore, the shrinkage of the caliche soil as a whole, with all its particle sizes, should be lower.

3.2.4.9 Determination of Moisture and Soluble Salt Content and Qualitative Analysis of Water-Soluble Salts⁵³

Water-soluble salts, mainly sulfates, chlorides, nitrites and nitrates, are the product of chemical reaction of water, pollution compounds present in the water or the atmosphere, construction materials, and sometimes, the contribution of micro-organisms and animal activity (Teutonico 1988, 58).

Soluble salt content analysis provides information on the percentage of soluble salts present in the sample material. In addition, this analysis (combined with semi-microchemical reactions) provides information about the types of ions present in the sample and gives an indication of the maximum quantity of single ions present.

In the past, Wilcox and Shenk (1977, 94-95)⁵⁴ obtained soluble salts content of caliche samples taken from the backdirt of the Reaves trench outside the east door of the Great

⁵³ Charola, E. Determination of Moisture and Soluble Salt Content (1997); Teutonico, J. M. Qualitative Analysis of Water-Soluble Salts and Carbonates (1988, 58).

⁵⁴ Kreigh and Sultan (1978) obtained some salt content from a caliche sample from the monument. However, the sample was obtained from a wall of Compound A and not from the walls of the Great House. Their results are included in Appendix B.

House and from a fairly large fragment that fell off the west elevation (1975).⁵⁵ Wilcox and Shenk's results (table 3) show high concentration of soluble salts in the caliche.

Sample Separation	Analysis of separate fragments from each sample	Analysis of sub-samples from ground-up primary sample	
Sample Provenance	West Wall	West Wall	West Wall
Soluble Salts in Saturation Extract			
pH	7.7	7.8	7.6
ECe x 10 ³	9.5	6.7	8.4
Total Sol. Salts	6650	7482	9841
ESP/e	2.0		
Ca (ppms)	840	1220	1940
Mg (ppms.)	148	188	88
Na (ppms.)		880	928
Cl (ppms.)		1775	1405
SO ₄ (ppms.)	540	1930	3411
HCO ₃		275	305
NO ₃	148	1214.4	1764.4
PO ₄	540		
1:5 H O Routine			
pH	8.1	7.5	7.6
ECe x 10 ³	1.29	1.35	1.50
Total Sol. Salts	1208.7	851.18	997.68
Ca (ppms)	390	122	152
Mg (ppms.)	75	14	10
Na (ppms.)	112	108	136
Cl (ppms.)	138	152	136
SO ₄ (ppms.)	145.0	172	239
HCO ₃	45.1	23.18	17.08
NO ₃	303.6	264.0	303.6
CaCO equiv. <2mm	22.0%	26.0%	24.0%
Total		31.50%	34.6%

Table 3: Wilcox and Shenk's results (1977) on soluble salts content of samples from a caliche fragment that fell off the west elevation of the Great House in 1975.

SAMPLE	MOISTURE % W/W	SOLUBLE SALT % W/W
CAGR. A	1.56%	1.36%
CAGR. B	1.50%	0.94%
CAGR. C	1.48%	1.01%
AVERAGE	1.51%	1.10%

Table 4: Results of moisture and soluble salts content for the caliche soil.

⁵⁵ The fragment's location on the west elevation is contiguous to the original location of the fragment under study.

Three samples of the caliche, CAGR A, CAGR B and CAGR C, were selected for determining moisture and soluble salt contents.

The solid samples were weighed and then oven dried for 24 hours. Then, samples were weighed again and their moisture content was calculated. The soluble salt content was calculated by grinding the sample and soaking it in de-ionized water. Each sample was then filtered and oven dried for 24 hours. After drying, each sample was weighed and the content of soluble salt was calculated.⁵⁶ The results of this test are presented in table 4 and Appendix C.

The results are reflective of only the area where the samples were taken (west wall, near northwest corner). In addition, the caliche from which the testing sample was obtained was stored for more than a year at Casa Grande National Monument, and almost another year went by until the various tests were performed. Thus, the moisture content results obtained through this test are not entirely representative of the standing exterior walls of the Great House. What is significant from this analysis is that the salt content is relatively low.

Important variations of moisture and soluble salts content in different areas and heights of the Great House walls should be expected. Principally, soluble salts should be

⁵⁶ This test is explained in detail in Appendix C.

more concentrated in areas closer to ground level. Depending on the height of the capillary rise, it is possible that much of the salt infested basal zone was removed and stabilized by the 1891-92 repairs and maintained stable by the significant dropping of the water table. In addition, Wilcox and Shenk (1977, 93) associate the difference of salt content to movement of water inside the caliche. According to them, accumulation of soluble salts would tend to concentrate along the lens boundaries of the material due to high evaporation of water between lenses. Thus, this phenomenon makes the comparability of results questionable from one sample to another.

Three possible sources of soluble salts in the caliche of the Great House are: (1) soluble salts naturally present in the caliche, (2) soluble salts accumulated through groundwater (capillary action), and (3) salts from repairs, possible cement.

Soluble salts identification present in the caliche was performed by semi-microchemical reactions according to “Qualitative Analysis of Water-Soluble Salts and Carbonates” (Teutonico 1988, 58). The test was performed on the salts obtained by boiling the liquid obtained from soaking the samples for salt content until all water was evaporated. This test showed the presence of sulfates, chlorides, nitrites and carbonate salts as the major soluble salts in all three samples (CAGR A, CAGR B and CAGR C). The results of the qualitative analysis of water-soluble salts and carbonates are shown in table 5.⁵⁷

⁵⁷ Semi-micro chemical analysis of nitrates and phosphates were not possible to be performed at the time of the testing.

ANION	CAGR. A	CAGR. B	CAGR. C
Sulfates (SO_4^{-2})	++	+++	+++
Chlorides (Cl^{-1})	++	+++	+++
Nitrites (NO_2^{-1})	+	++	++
Carbonates (CO_3^{-2})	++	++	+++

+ = presence of the ion

++ = presence of the ion in notable quantity

+++ = presence of the ion as the principal component.

Table 5: Presence of ions by semi-micro chemical reactions for the caliche soil (According to the procedure explained in "Qualitative Analysis of Water-Soluble Salts and Carbonates (Teutonico 1988, 58).

Like the results obtained by Wilcox and Shenk (1977), the results obtained from soluble salts identification are high in sulfates and chlorides.

The results presented in this study, obtained both through moisture and soluble salt content and qualitative analysis of water-soluble salts, are only preliminary and not conclusive. More research needs to be accomplished in the future. In situ or laboratory testing should be carried out involving caliche from different locations in the walls, especially behind the brick-pinning, in order to make a comparative study of salts present in the caliche from the Great House. However, it is very important to understand that results obtained from soluble salt analysis will be only representative of a specific location in the structure; care must be taken when comparing results from location to location.

3.2.4.10 Compressive Strength (ASTM D1633)⁵⁸

The test was conducted at the Laboratory for Research on the Structure of Matter at the University of Pennsylvania on March 25th, 1997. Alex Radin, from LRSM performed the

⁵⁸ ASTM D1633, Standard Test Method for Compressive Strength of Molded Soil-Cement Cylinders. ASTM: Philadelphia, 1993.

testing. The results were analyzed and processed by engineering students from the Engineering Department, University of Pennsylvania, under the direction of Eric Johansen.

The test specimens of caliche were cut from the interior portion of the caliche fragment (CAGR B and C), i.e.; away from its exposed side. The cutting was done with a wet diamond saw.⁵⁹ Three specimens were cut and left to dry for 1 week at room temperature. Specimens were then dried in an oven at 100°C for 24 hours. Moisture content and weight of specimens were recorded.

A stroke control ramp test was performed on all three specimens using an Instron Testing machine 1331. The displacement speed used was 0.08 in/min. Observations and photographs were performed during and after the testing of specimens.

In specimen 1 the cracking symptomatic of failure was limited to one side of the specimen. This indicated that the load was concentrated on that side. This load concentration resulted from the fact that the specimen's top and bottom edges were not parallel. Therefore, the compressive strength is probably higher than the value calculated from testing this specimen.

In specimen 2 cracking was better distributed than in specimen 1, although not an ideal distribution.

⁵⁹ The use of water was controlled to a minimum.

The following are considerations for further testing:

Specimen	Width 1 (cm)	Width 2 (cm)	Height (cm)	Weight (g) after drying	Moisture content (%) after drying
1	5.5	6.0	9.0	530.52	2
2	5.5	5.8	10	566.82	4
3	5.5	5.5	9.7	542.56	5
Specimen	Maximum Load (lb)		Compressive Strength (psi)		
1	585		114.4		
2	780		157.8		
3	950		202.6		

Table 6: Results for compressive strength of caliche samples

- Specimens cut with a wet saw should be allowed to dry for longer than a week.
- Ensuring that the top and bottom edge of the specimens are parallel is a critical factor in the accuracy of testing.
- Specimens of different sizes and height should be tested to see variation of results.
- If possible, test specimens from separate sections of the walls to get a sense of variation of results.

In conclusion, the compression testing yielded a reasonable allowable range for compression stress, but further testing is needed to obtain conclusive results. For the present thesis, dry caliche will be assumed to have a compressive strength of 150 psi

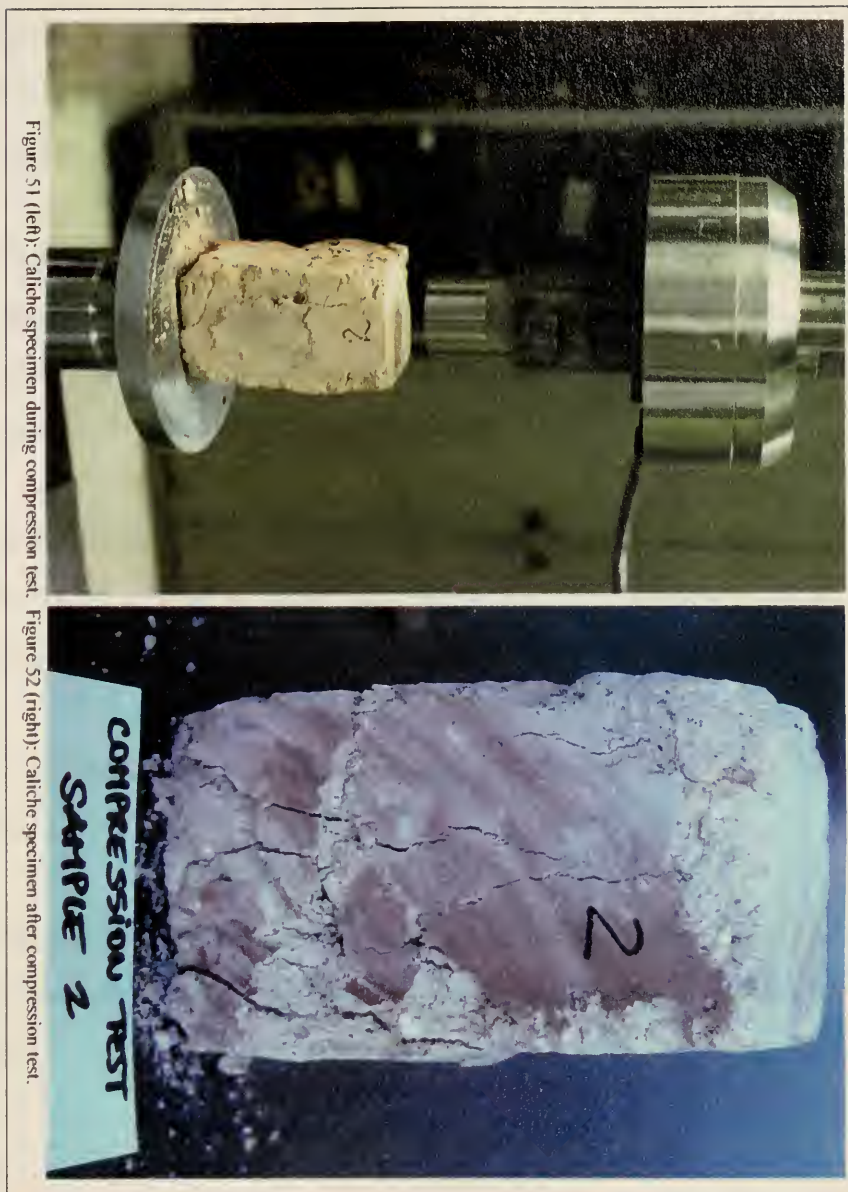


Figure 51 (left): Caliche specimen during compression test. Figure 52 (right): Caliche specimen after compression test.

which appears to be a conservative estimate. Compressive strength of wet caliche should be considered significantly lower. This is important in the diagnosis of pre-shelter conditions as basal saturation would have caused potential failure under load.

3.2.4.11 Three Point Bending (Modulus of Rupture) (ASTM D1635)⁶⁰

A specimen was molded for this test after several unsuccessful attempts to cut a sample with the diamond saw.⁶¹ The material used came from the interior of the caliche fragment (CAGR B and CAGR C), that is away from the outer carbonate enriched crust.

The specimen measured 4.8cm. (width) x 5.0cm. (height) x 17cm. (length), weighed 723.50 g and had a moisture content of 6%. After molding, it was allowed to dry for two weeks at room temperature. Then, it was oven dried at 100°C for 24 hours.

The specimen was repositioned so three tests were conducted. The results are shown in Table 6.

In the three tests cracking originated where the knife came in contact with the specimen and extended to the bottom of the specimen at an angle $\geq 45^\circ$ from the specimen's top edge.

⁶⁰ ASTM D1635, Standard Test Method for Flexural Strength of Soil-Cement Using Simple Beam with Third-Point Loading, ASTM: Philadelphia, 1993.

⁶¹ During cutting the material developed cracks.

The following are considerations for further testing:

Use of a more sensitive scale (psi) is needed. Such a scale will be slower and give more accurate results.

Test	Maximum Load (lb)	Allowable Bending Stress (psi)
1	170	45.7
2	135	36.3
3	160	43.0

Table 7: Results of three-point bending (modulus of rupture) for a molded caliche sample.

- Use of a longer gage length is needed to lessen the chance of failure caused by the knife pushing into the material.
- It is better to cut the specimens from the caliche rather than forming them. However, the limited availability of material and the presence of nodules of calcium carbonate make this task very difficult. Therefore, molding of specimens is probably the best recommended for this case. If molding is selected for this test, the drying period at room temperature should be longer - at least one month.

In summary, the three point bending test was inconclusive for two reasons: (1) there was only one specimen and it was hand-formed; (2) the failures seemed to result from the knife digging into the soft material of the specimen. However, the results obtained could give an idea of the behavior of the caliche under shear stress, and set the bases for improving further testing in the future.

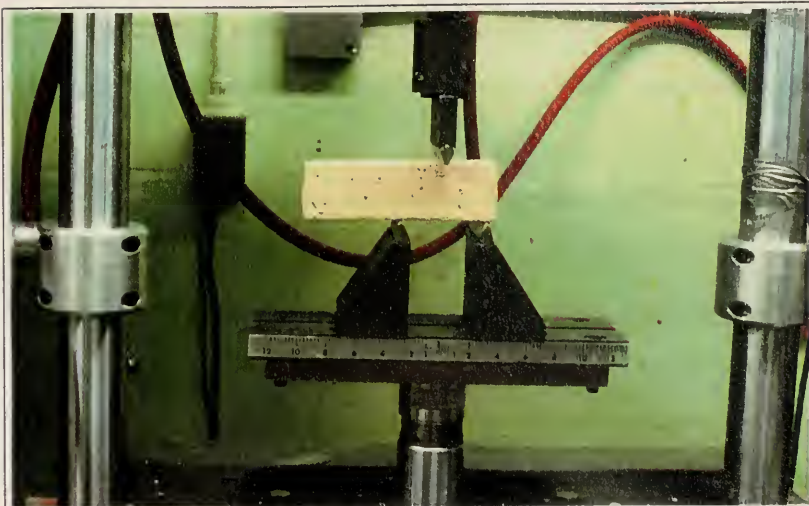


Figure 53 (top): Caliche specimen during the three-point bending test (modulus of rupture).
Figure 54 (bottom): Caliche specimen after the three-point bending test (modulus of rupture).

3.2.4.12 Water Related Tests: Wet/Dry Cycling (ASTM D559 modified), Water Resistance (Water Drop Test, CRATerre), and Capillary Water Absorption (Normal 11/85)

Water has long been associated with deterioration processes affecting porous building materials. Its presence within the interior pore structure of a material can result in physical destruction, especially if it undergoes wet/dry cycling. This is particularly relevant to the caliche from the Great House. Indeed, water has played a very important role in the erosion of the Great House walls during centuries of exposure. In addition, all but indurated caliches tend to absorb unusual quantities of water. This is due to the high porosity and permeability of most caliches (Reeves 1976, 149).

The presence of water, or just moisture, is necessary for triggering numerous deterioration processes such as the ones related to soluble salts, biological organisms, wind, pollution, and mechanical stress from wet-dry cycling and shrinkage.

Due to these factors, the permeability, resistance and behavior of the caliche when exposed to the action of water are very important since they are directly related to the durability of the material.

Three tests involving wet/dry cycling, water resistance, and capillary water absorption were selected to be carried out in the caliche from the Great House. These are:
Wet/Dry Cycling (ASTM D559 modified)

Water Resistance (Water Drop Test CRATerre)

Capillary Water Absorption (NORMAL 11/85)

Samples from the front side of the caliche fragment (CAGR Ext, containing the reddish surface) and samples from the back of the caliche piece (CAGR Int) were cut for these tests.

Wet/Dry Cycling (ASTM D559 Modified)⁶²

The purpose of this test is to observe and evaluate the resistance to wet/dry cycling of the caliche coming from different depths of the caliche fragment. Samples were cut into regular cubes and their dimensions and weights were recorded. The dimensions of the samples were:

- CAGR. Ext. 1 (6cm. x 6cm. x 6cm.)
- CAGR. Ext. 2 (5cm. x 5cm. x 5cm.)
- CAGR. Int. 1 (6cm. x 6cm. x 6cm.)
- CAGR. Int. 2 (5cm. x 5cm. x 5cm.).

A fifth sample, named CAGR. Ext-Int., (17 cm. long)⁶³, which was obtained as leftover from the various cutting of the caliche piece, was added to the test in order to visually record any differences in loss within the length of the sample.

⁶² ASTM D559. "Standard Test Methods for Wetting and Drying Compacted Soil-Cement Mixtures". ASTM: Philadelphia, 1993.

⁶³ This sample was not cut into a regular shape. One end of the sample was formed by the exposed caliche (10cm deep) and the other end by the caliche within 20-30cm deep.

All samples were oven dried at 110°C for 24 hours until constant weight. Results and descriptions collected during each cycle are presented in Appendix C. The resistance to wet/dry cycling is expressed by both (1) the rate of loss of material during the experiment (see table 8 and figure 58) and (2) the percentage of material loss after the experiment (as is shown in Appendix C and figure 55).

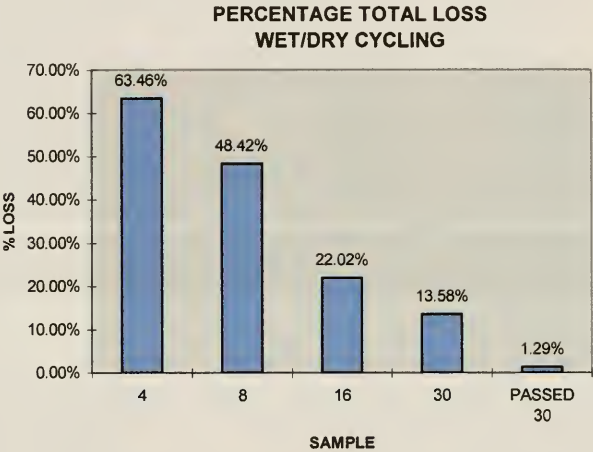


Figure 55: Percentage of total loss of samples of caliche after 12 cyles, wet-dry cycling test

According to the results obtained for total loss, samples CAGR Ext. 1 and CAGR Ext 2 lost 2.92% and 34.99% of their respective original weights after 12 cycles of immersion. Samples CAGR Int 1 and CAGR Int 2 lost 50.66% and 100% respectively. Though these

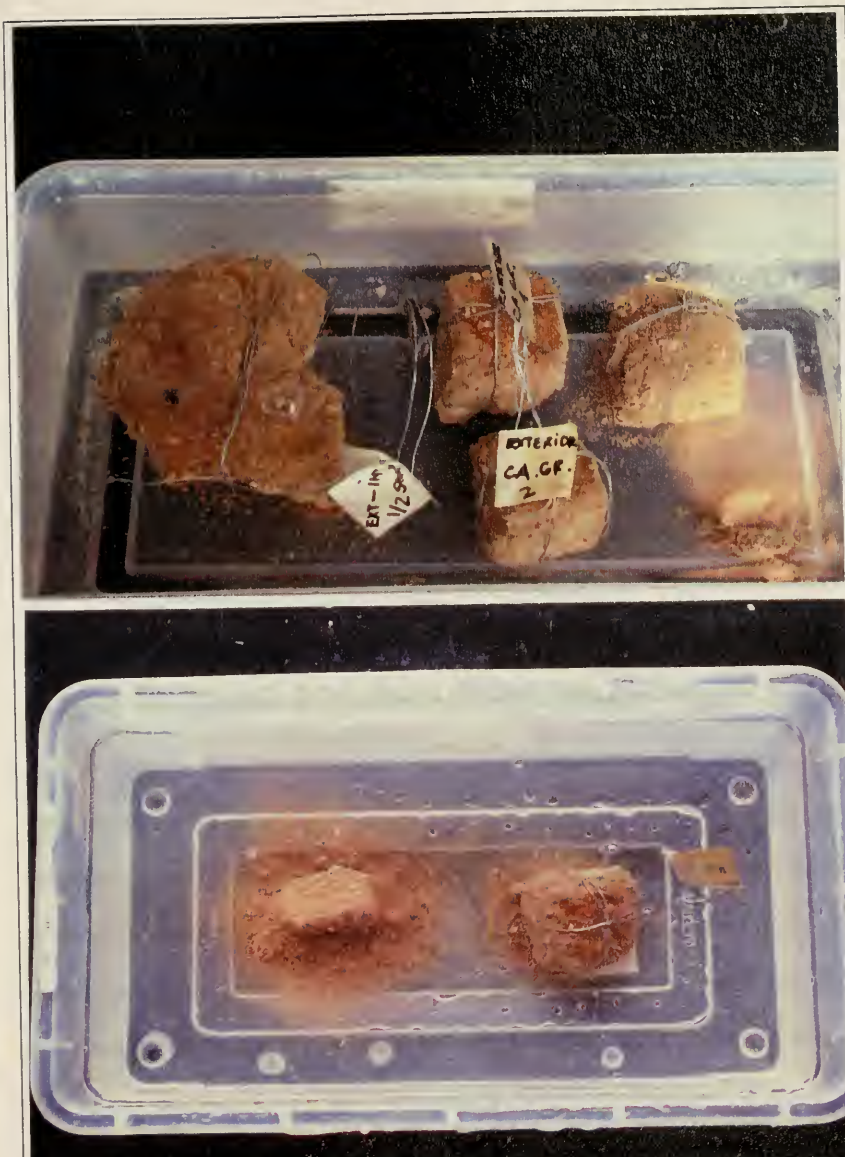


Figure 56 (top): Samples during first immersion cycle, wet-dry cycling test.

Figure 57 (bottom): Samples during last immersion cycle, wet-dry cycling test. Notice the different loss of sample CAGR Ext (left) compared to CAGR Int (right).

results show a wide difference in material loss between samples of the same set, CAGR Ext samples showed less percentage of total loss than the interior samples.

During immersion, the loss of samples CAGR Ext 1 and CAGR Ext 2 was concentrated on their bottom; the loss was uniform and from all faces for CAGR Int 1 and CAGR Int 2. Sample CAGR Int-Ext suffered loss along its back, that is, away from the reddish surface (crust).

According to the results obtained (table 8 and figure 58), all samples suffered little loss after the first wet/dry cycle (between 0 and 10%). However, after the first cycle all samples show different rates of loss. Sample CAGR Ext-Int experienced most of its material loss between cycles 2 and 3. Then, loss rate of this sample became uniform until the end of the experiment. Sample CAGR Ext 1 showed almost no loss throughout the entire experiment, and some water retention during cycles 4, 6 and 10. Sample CAGR Ext 2 experienced most of its loss between cycles 2 and 4. Then, loss rate of this sample became uniform until the end of the experiment. Sample CAGR Int 1 showed a fairly uniform rate of material loss (nonetheless, more pronounced than samples CAGR Ext until the last cycle of the experiment when great amount of material was suddenly lost. Sample CAGR Int 2 lost most of its material during cycle 2; the rate loss of this sample continued pronounced until its disintegration during cycle 8.

MATERIAL SAMPLE (BY WEIGHT PERCENT) REMAINING AFTER EACH WET/DRY CYCLING					
SAMPLE	CAGR. Ext-Int.	CAGR. Ext. 1	CAGR. Ext. 2	CAGR. Int. 1	CAGR. Int. 2
CYCLE 1	90.80	99.33	97.66	97.79	94.87
CYCLE 2	71.91	98.49	89.17	95.03	25.81
CYCLE 3	52.12	98.07	79.90	91.81	15.94
CYCLE 4	46.47	98.15	73.19	88.79	11.36
CYCLE 5	42.92	98.07	71.12	86.19	9.56
CYCLE 6	39.30	98.57*	70.04	85.64	9.06
CYCLE 7	37.74	97.82	68.06	82.87	sample disintegrated
CYCLE 8	35.93	97.65	66.68	79.32	
CYCLE 9	35.93	97.15	66.09	75.69	
CYCLE 10	34.18	97.82	66.09	74.67	
CYCLE 11	33.52	97.82	66.09	73.72	
CYCLE 12	30.03	97.07	65.00	49.33	

*Water retention

Table 8: Loss per cycle in relation to original weight of sample (in percentage)

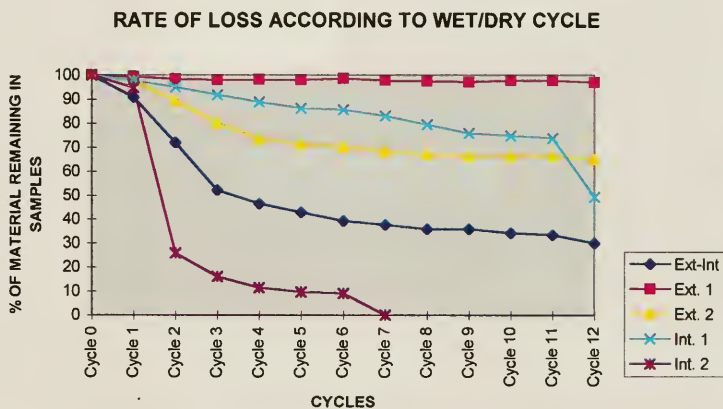


Figure 58: Rate of loss of different caliche samples according to cycle, wet-dry cycling test.

It can be concluded from this test that there is a general tendency of more resistance to wet/dry cycling of samples CAGR Ex. (with a mean value of total material loss of 18.95%) compared to samples CAGR Int (with a mean value of total material loss of

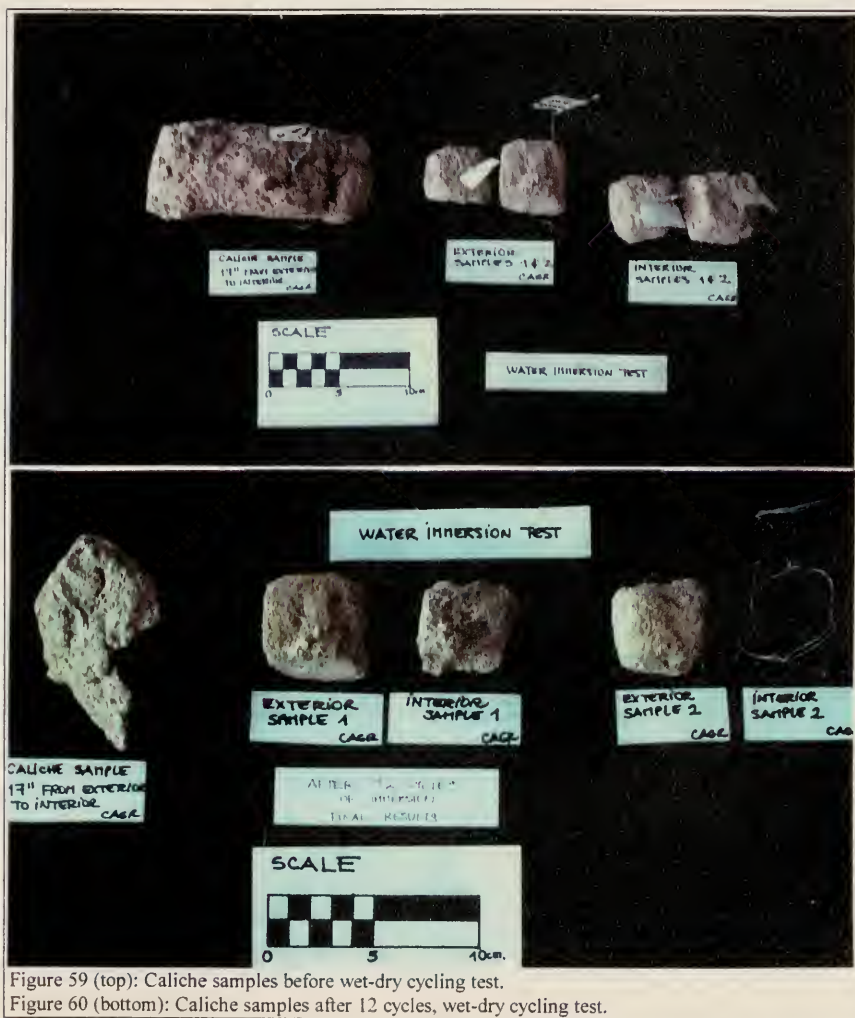


Figure 59 (top): Caliche samples before wet-dry cycling test.

Figure 60 (bottom): Caliche samples after 12 cycles, wet-dry cycling test.

75.33%). This is very visible in the sample CAGR Ext-Int (66.96% of loss) in which all the loss of the sample occurred from the area away from the outer reddish surface.⁶⁴

As outlined in the results previously discussed for percentage of total loss, the material loss shows variations among the samples within the same set. However, a general pattern of loss in the majority of the samples can be observed. Very little material loss was recorded during the first wet/dry cycle. Most of the loss was registered within cycles 2 and 4. In general, after the third or fourth cycle the rate of loss of the samples became more constant.

The differences in behavior registered throughout the test of samples cut from the same caliche could be attributed to two main factors: (1) the nature of the construction technique used to build the walls of the Great House (puddled earth) and (2) the variation in thickness of the calcium carbonate enriched crust that has been formed on the outer face of the caliche fragment through calcium carbonate dissolution and surface enrichment. This would render the exterior zone more resistant to water-related deterioration mechanisms.

⁶⁴ Sample CAGR Ext-Int measured 17cm. in length and after the wet/dry cycling (12 cycles in total) measured 3.5cm in length.

Water Resistance (Water Drop Test - CRATerre)⁶⁵

The purpose of this experiment is to observe and evaluate the resistance of the caliche to the mechanical action of continuous water drops. Samples CAGR Ext and CAGR Int 1 were cut for this test in order to obtain comparative results. The samples measured approximately 5.5cm x 5.5cm x 4cm (height).

After oven drying at 110°C for 24 hours (until constant weight), each sample was subjected to 1 drop of deionized water per second, from a height of 2.5 meters, impacting upon an area approximately 1cm² for a timed period of 1 hour (approximately 3600 drops). Samples CAGR Ext 1 and CAGR Ext 2 were placed to receive the impact of the water drops on the reddish surface.

From the beginning of this test, a great difference in behavior was noticed between the two sets of samples. After one hour of test, no changes in color or water absorption were observed in samples CAGR Ext 1 and CAGR Ext 2. No crater was formed by the impact of the water drops and a film of water was formed on the surface of both samples (pooling). In order to record any difference of behavior, it was decided to continue the experiment for an additional hour. However, no visible changes were recorded after the second hour of the experiment. Both samples showed great stability after two hours of the experiment.

⁶⁵ Douline, A. *Batiments en vouler et compoler en adobe, Niger*. Memoire de CEAA-Terre. Grenoble, France: CRATerre-EAG, 1990.

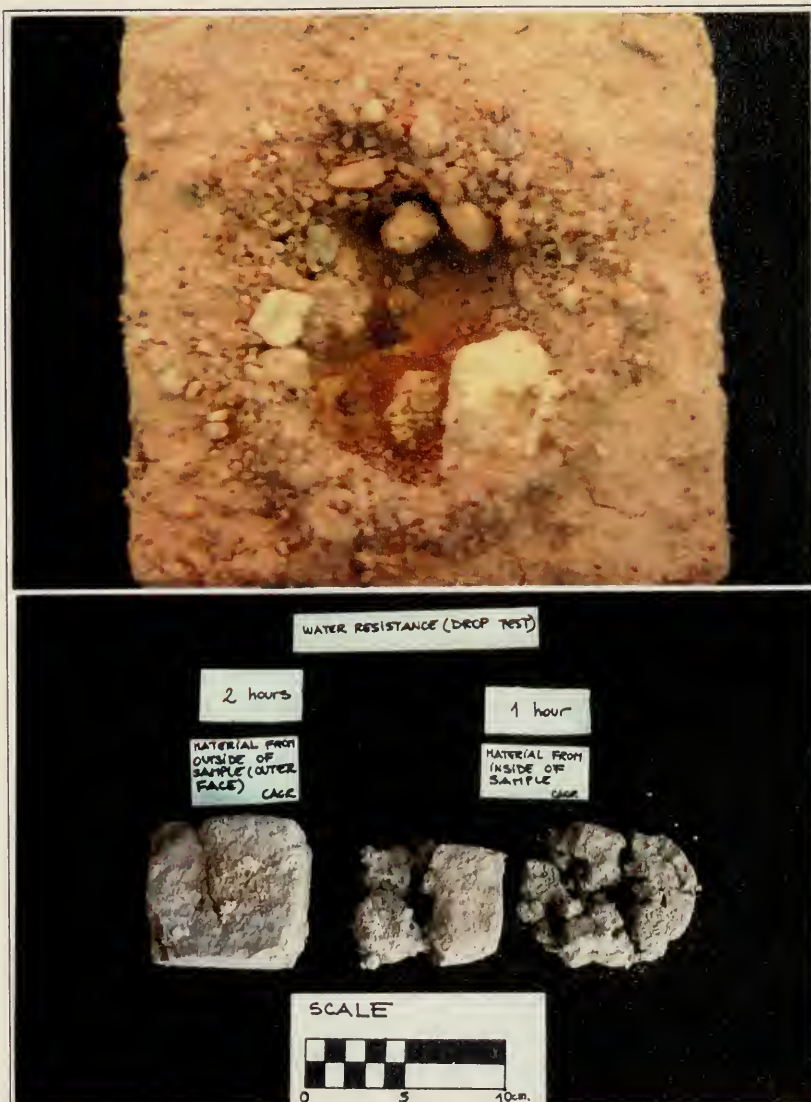


Figure 61: Crater formed in caliche sample CAGR Int during water resistance (water drop) test.
 Figure 62: Samples of caliche after water resistance (water drop) test.

Conversely, samples CAGR Int 1 and CAGR Int 2 showed rapid absorption of water and immediate cratering. Both samples rapidly started to swell without retaining much of their structural cohesion. The samples were destroyed by the impact of the water drops before the end of the experiment (approximately after 30-40 minutes). Unfortunately, due to the extreme difference in behavior of the samples (no change versus complete destruction), it was not possible to take timed and final measurements to record rate of penetration and size of the craters formed on the samples by the impact of the water drops. No water resistance indicator factor, given by the width (diameter) of erosion, could be obtained for any of the samples. Photographs are included in order to better illustrate the results of this test.

The results obtained from this test again confirm differences in behavior between samples cut from the exterior of the caliche and samples from the interior of the caliche (original fragment). The exterior caliche (outer 10cm in the caliche fragment) showed the highest water resistance with no apparent absorption (observable as color change) and significant pooling. All samples of this material resisted cratering. On the other hand, samples from the inner caliche (within 20-30 cm. deep in the caliche fragment) showed the greatest water absorption with significant swelling that resulted in the disintegration of the samples during the test.

Capillary Water Absorption (NORMAL 11/85)⁶⁶

The purpose of this test is to measure and compare the capillary rise of the caliche enriched by calcium carbonate and the capillary rise of the caliche depleted of calcium carbonate.

Capillary water absorption is defined as “the amount of water absorbed per unit surface [g/cm^2] as a function of time at room temperature and pressure, by a sample which has its support surface in contact with de-ionized water” (NORMAL 11/85, 1).

Frye (1945), Harper (1957), and Stuart and colleagues (1961) emphasize that in fine-textured soils, solubles such as calcium carbonate are concentrated at the interface (underlying coarser sand or gravel lenses), resulting in caliche development. Certainly, a caliche horizon impedes the movement of both infiltrating and capillary water (Reeves 1976, 110).

Two sets of three samples (exterior caliche and interior caliche) were cut into cubes.⁶⁷

The dimensions of the samples are:

- CAGR Ext 1 (3.80cm x 3cm x 3.08cm)
- CAGR Ext 2 (3.5cm x 3.5cm x 3.5cm)
- CAGR Ext 3 (4cm x 4cm x 4cm)

⁶⁶ This test was developed for stone materials, but has been adapted for use here.

⁶⁷ Samples were cut as regular as possible. However, due to the characteristics of the material, it was impossible to obtain perfect cubes.

- CAGR Int 1 and 2 (4cm x 4cm x 4cm)
- CAGR Ext. 3 (3.5cm x 3.5cm x 3.5cm).⁶⁸

The test procedure is described in Appendix C. Results are presented in table 9. Average values of capillary water absorption of each set of samples were calculated and plotted in a graph as a function of \sqrt{t} where time t (time) is given in minutes (figure 64).



Figure 63: Caliche samples during capillary water absorption test.

This test again proved the extreme difference in behavior between samples CAGR Ext and CAGR Int. Samples CAGR Int displayed high water absorption with significant swelling that resulted in the disintegration of the samples after 4 hours (240 minutes) of testing.

⁶⁸ The samples were cut with the objective of obtaining like sizes as much as possible.

Only three readings, which show high capillary water absorption, were recorded before disintegration. On the other hand, samples CAGR Ext showed high capillary water

AVERAGE CAPILLARY WATER ABSORPTION RESULTS M/S (10^{-2} g/cm ²)		
TIME vt (IN MINUTES)	CAGR. EXT. (g/cm ²)	CAGR. INT. (g/cm ²)
15	1.05	2.22
45	1.65	2.61
120	1.66	2.78
240	1.70	Complete disintegration of samples due to excessive and rapid absorption.
1020	1.76	
2460	1.81	
3900	1.84	
5340	1.89	
6780	1.88	
8220	1.95	
9660	1.95	

Table 9: Average results of capillary water absorption of caliche samples. The first column of numbers refer to the time (in minutes)

CAPILLARY WATER ABSORPTION

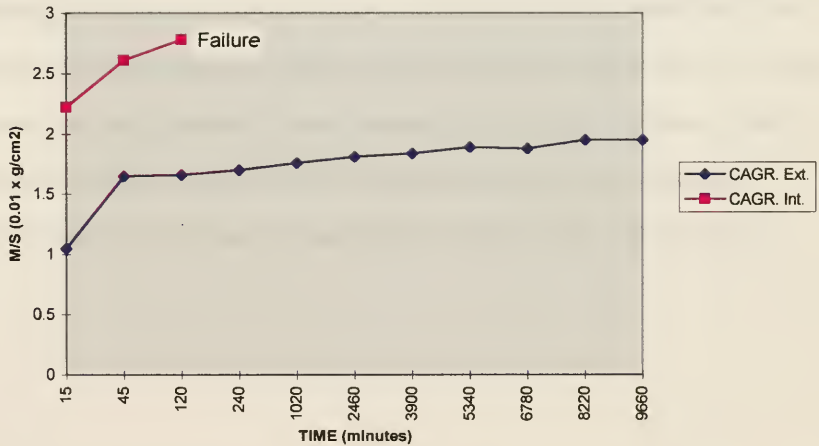


Figure 64: Capillary water absorption of caliche samples

absorption after the first 15 minutes. Then, the samples showed stability and consistency during the entire test which lasted 161 hours (9660 minutes) and provided 11 different readings.⁶⁹

Both groups of samples showed high capillary water absorption between 45 minutes and 120 minutes. Afterwards, capillary water absorption decreased in samples CAGR Ext but continued increasing in samples CAGR Int until failure. Samples CAGR Ext showed a more or less constant and low capillary water absorption until the end of the test.

These results clearly indicate that capillary water absorption is higher in the caliche from the inner zone (20-30cm) (CAGR Int) and is lower in the caliche from the outer 10cm zone (CAGR Ext). This is probably related to calcium carbonate enrichment of the outer caliche, which has changed the pore structure of this caliche and has transformed it into a denser, more stable material and made it more impermeable to water infiltration or escape. On the other hand, depletion of calcium carbonate from the inner zone has also probably changed its capillary structure and has transformed this caliche into a more porous material making it, therefore, more susceptible to water movement and water attack.

⁶⁹ Because of a lack of change in capillary water absorption in the last two readings (after 8220 and 9660 minutes), it was decided to stop the test.

CHAPTER 4: DIAGNOSIS OF DETERIORATION AND PERFORMANCE ASSESSMENT OF THE GREAT HOUSE CALICHE AS A BUILDING MATERIAL (PHASE 3)

4.1 Processes of Deterioration of the Great House

For many centuries the Great House has withstood the processes of deterioration that still threaten to destroy it today. For this reason, it is fundamental to know not only the nature, causes and consequences of deterioration but also to know which processes of deterioration existed in the past, and are still active today, and what new processes have developed. These issues will allow an understanding of the changes or differences in behavior of the structure over time and to take actions in order to delay or reduce the action of deterioration.

Deterioration is seldom the result of one set of circumstances alone. It may be the result of a whole series of unrelated situations or of a chain reaction. In general, it is a combination of both, with very complex relationships between causes and effects.

Like other archaeological remains, the deterioration of the Great House is of two kinds: intrinsic and extrinsic. Intrinsic causes of deterioration could structure-related (the inherent flaws), or site-related. On the other hand, extrinsic causes of deterioration are related to external agents or forces, both natural and human-related which, acting upon the susceptibility or inherent flaws of the Great House, result in damage.

Materials, layout and construction technique are all intrinsic causes of deterioration related to the structure. Their actions and influences should be considered when evaluating the condition of the ruin of the Great House and its exposure to the uncontrolled environment for hundreds of years.

All the characteristics of the site, climate, vegetation, soil, geology, location, are grouped as intrinsic causes of deterioration related to the site of the Great House.

Causes of Deterioration	Intrinsic	Structure (Great House)	Materials (caliche) Layout Construction Technique (English Cob) Condition of Ruin
		Site	Soils/Geology Hydrology Location Climate Vegetation
	Extrinsic	Nature Related	Natural Forces of deterioration Natural Disasters
		Human Related	Direct (when the structure is the target of deterioration) Indirect (when the structure is not the target of deterioration)

Extrinsic causes of deterioration can be natural or human-related. Both, nature and man have been considered the major agents of deterioration of the Great House.

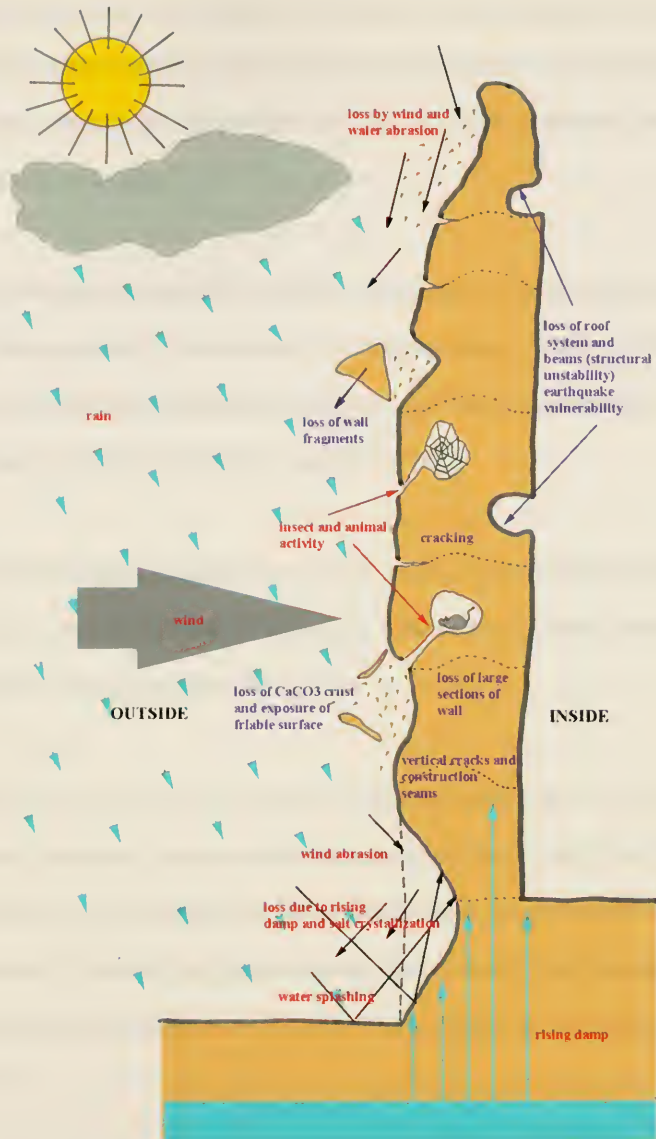


Figure 65: Intrinsic and extrinsic causes of deterioration. Extrinsic causes are in red and intrinsic causes are in blue.

The natural environment is a combination of physical, chemical, biological and micro biological forces of deterioration that can alter, age and/or destroy the Great House. These agents' influences are very complex since they can act independently or in connection with each other.

Natural disasters are also extrinsic, naturally occurring causes of deterioration of the Great House. Earthquakes are the most destructive of natural disasters. Cushing (1890) believed that earthquakes significantly contributed to the failure of some sections of the caliche walls from the structure (Wilcox and Shenk 1977).

Over the centuries, humans and their actions have affected the Great House. Vandalism, looting, graffiti, past stabilization and other direct human actions proved to be the cause of various degrees of deterioration to the structure.

The 1996-97 documentation of the existing and past conditions of the Great House suggests that the majority of the deterioration noticed today in the walls of the Great House is inactive. It is probably related to the abandonment and uncontrolled weathering of the structure in the past (roof destruction and beams removal), which happened well before the first photo-documentation in the 1870's and the erection of the first protective roof in 1903.

For the purpose of the present study, this section will focus only on the decay mechanisms that played or still play a very important role in the deterioration processes of the Great House. In this case, only the interaction between inherent flaws of the structure (materials and construction technique, condition of ruin) with the action of some natural and human-related agents of deterioration will be discussed. In addition, all new data provided by the testing phase of the present study will be used to explain the processes of deterioration.

4.1.1 Intrinsic Causes of Deterioration

4.1.1.1 Related to the Material

Like other porous building materials, caliche experiences deterioration processes when exposed to the aggressive action of the environment. The rate and symptoms of such processes are influenced by a number of variables, partly depending upon the properties of the material itself and partly upon several environmental factors, acting separately or in various combinations.

The caliche of the Great House is formed by numerous particles of sand, silt and clay cemented by calcium carbonate which give special characteristics to the material. However, exposure, mainly in the form of water and water evaporation (wetting and drying cycles), has resulted in changes to the caliche on the structure. As reported in the testing section of this thesis, the caliche from the Great House has developed a zone of calcium carbonate enrichment on its outer (exposed) surface (variable depth,

approximately 10-20cm) and an interior calcium carbonate impoverished zone (about 20-30cm deep).

This natural phenomenon, which is related to the interaction of calcium carbonate soils (caliche) with weathering processes, is also common in porous limestones, sandstones and some granites, and is known as case hardening.

Winkler (1979, 55) defines case hardening or surface induration of a material surface as “the process or processes which lead to a surface reinforcement and hardening”. Any migration of solution assumes porosity and adequate permeability of the original material substance. Solutions tend to move inward (by capillary absorption) and outward (by evaporation). The moisture in the material tends to be pulled to the surface by the sun, high summer temperatures, low relative humidity, and drying winds, which accelerate the process.

As a result of case hardening, the exposed caliche material has developed zones from the surface inward, as follows: (1) calcium carbonate enriched crust, (2) less calcium carbonate enriched zone, and (3) calcium carbonate impoverished zone (figure 66). This alteration has only happened where the caliche is exposed to the elements, that is, on the exterior side of the exterior walls and probably interior side of parapets. Therefore, the caliche located deeper in the wall (core) or on its interior surface have not suffered any alteration.

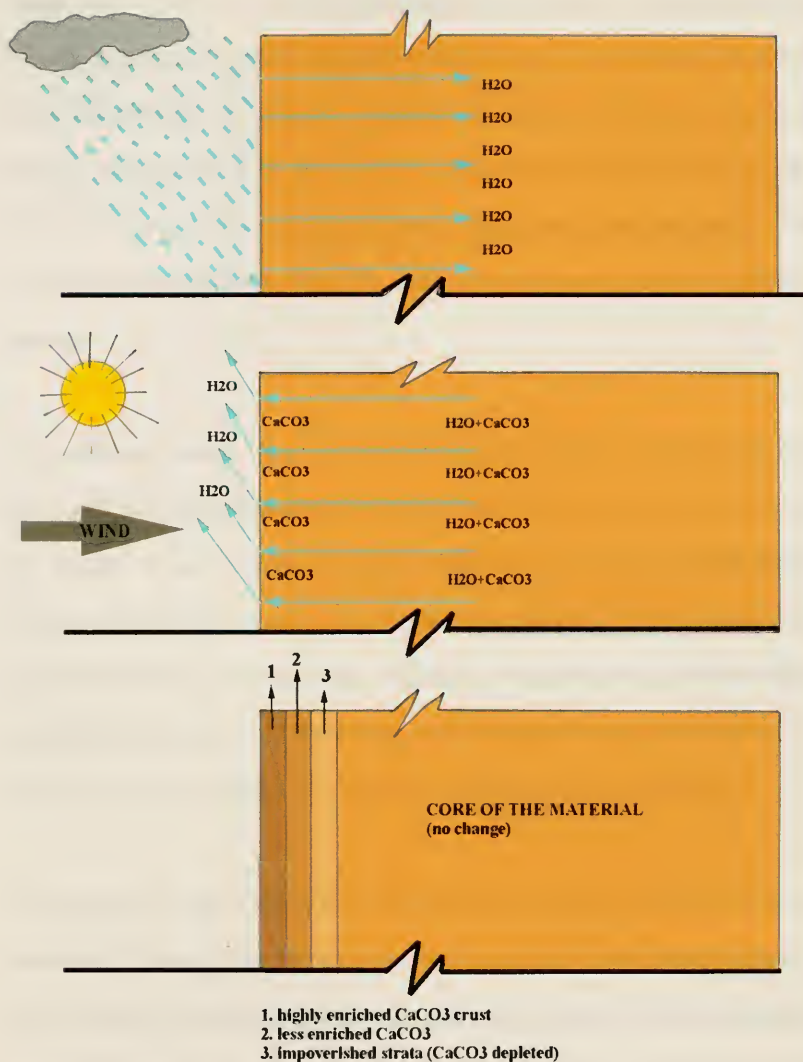


Figure 66: Section of wall showing movement of calcium carbonate in the caliche (case hardening) due to weathering (water movement) and exposure

Lattman (1977, 221-231) who did some studies with weathering of caliche in Southern Nevada, found that petrocalcic and laminar layers of caliche are not subject to solution attack and are highly impermeable. These layers weather predominantly by mechanical breakup when exposed at the surface. On the other hand, the softer calcic horizons of Southern Nevada show weathering by solution effects due to their permeability. When exposed, these horizons are affected by wind and water abrasion due to the friability of the material.

The weathering patterns observed in Southern Nevada caliche are probably very similar to the weathering of the different caliche bands located in the exposed side of the Great House walls. Thus, the enriched calcium carbonate crust will weather by mechanical breakup (cracking) and the calcium carbonate impoverished zone will be more subject to deterioration effects caused by water. In addition, the friable condition of this band will also make it vulnerable to wind abrasion, insect and animal activity, and other nature-related processes of deterioration, all acting in conjunction or independently.

The calcium carbonate enriched crust of the caliche is variable in thickness and is seldom continuous because cracks frequently traverse it, creating points of access to decay. Thus, deterioration can continue behind the crust taking advantage of incoherent, desegregated material. Damage can thus proceed rapidly under the deceptive appearance of a well

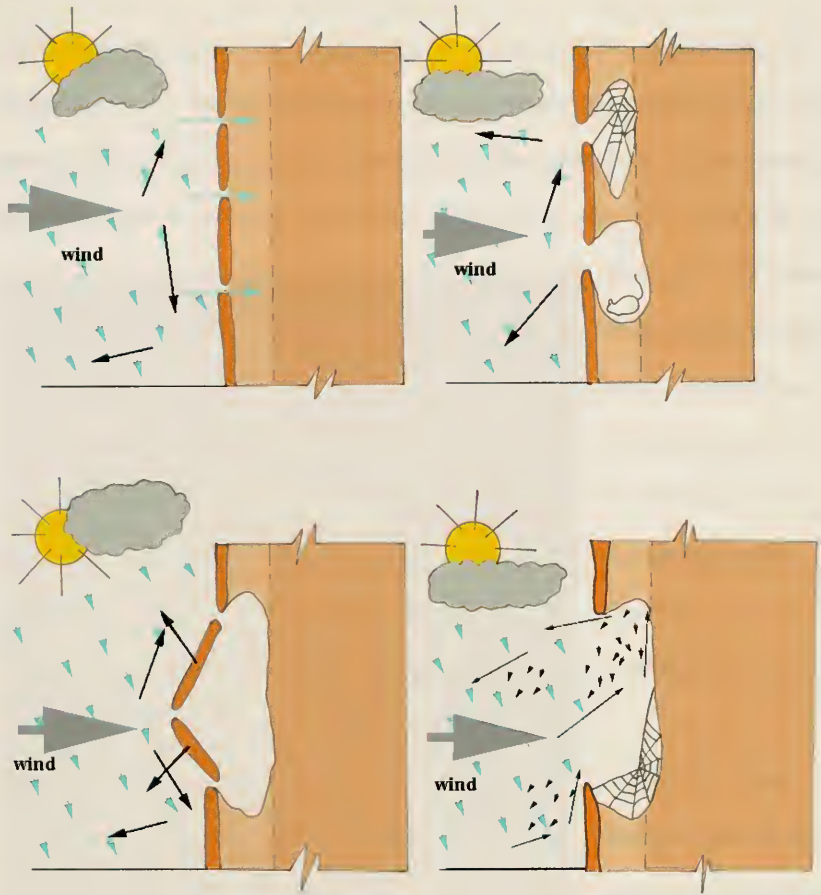


Figure 67: Deterioration of caliche due to crust loss. In the first stage, the crust weathers by mechanical break up (cracks) and the CaCO_3 depleted zone weathers by dissolution caused by water. Weather and insect/animal activity take advantage of the soft material behind the crust. Further deterioration cause the loss of the crust. The exposed friable surface behind the crust is exposed after crust loss and deterioration happens more quickly.

preserved surface. Once the crust is lost, the interior and more friable surface is exposed to environmental forces and deterioration occurs more rapidly (Figure 67).

This type of deterioration could be observed in many areas on the exposed side of the Great House walls. However, it is more evident in sections where portions of parapets are missing (Figure 68) and on specific construction courses. Perhaps after abandonment the unattended water drains of the roofs became obstructed, causing water penetration. Soon

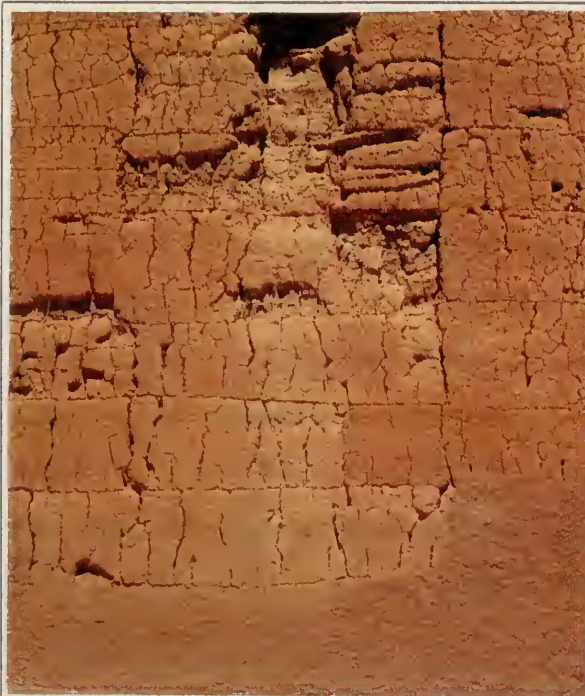


Figure 68: Areas of wall where the CaCO_3 crust has been lost.

water, along with other natural-related decaying agents, started to destroy the weak material, causing the later failure of the surface and further deterioration of wall material due to exposure.

In addition to case hardening, the caliche has suffered color alteration (2-3mm in thickness) in the

same areas associated with this natural phenomenon. This color alteration is more noticeable (darker) on the west elevation and on the surface mostly intact from erosion.¹

¹ Munsell readings for the west elevation are: 5YR 6/4 (light reddish brown) for the surface of the wall and 2.5YR 7/4-8/3 (pink) for eroded areas. For the rest of the elevations is 5YR 7/4 (pink) for the surface of the wall and 5YR 8/3 - 8/2 (pinkish white, pink) for eroded areas. Readings were taken in the afternoon in sunny conditions.

Wilcox and Shenk (1977) associated the color change of the caliche to a chemical alteration due to extreme temperature fluctuations and water penetration.

Laboratory thermal experiments done on caliche (Lintz, 1989) proved that the material suffers discoloration when exposed to high temperatures. In addition, the color alteration could be related to fine reddish material (loess, clays, silts) blown onto the wet surface and cemented by CaCO_3 . However, the cause of discoloration has not been established yet for the caliche from the Great House.

4.1.1.2 Related to the Construction Techniques

The construction technique of the Great House has been considered by many researchers, observers and explorers as a very advanced and refined technique. However, like other earthen prehistoric and historic structures, the Great House presents defects related to its methods of construction. These flaws in the structure, combined with the lack of roofs and the action of other decay mechanisms, cause different types of deterioration that have resulted in cracking and spalling of large of pieces of caliche from the walls.

Therefore, cracks, losses and detachment are the manifestation of the interaction of various deterioration phenomena, all associated with the construction techniques used in the structure.

As previously explained, the walls of the Great House were erected in a series of horizontal courses formed by lens-shaped units of puddled caliche. Such construction technique produced a series of discontinuities: (1) horizontal (seams or course boundaries), (2) vertical (head joints or cold seams) and (3) interior (lens profiles produced during shaping of each course).

Cold joints are no more than interruptions of continuity during the construction of a course, several courses, or an entire tier wall. Each discontinuity was formed by a period of drying of the caliche in place followed by addition of more wet caliche afterwards. Such discontinuity created a weakness in the material due to an imperfect bond between the dry and wet caliche, and created a vulnerability in the wall to the future action of decaying agents.

In addition, during and after construction, other types of discontinuities were formed in the walls of the Great House due to different stresses that caused the splitting of the caliche. In this manner, cracks formed during initial drying and by exposure to repetitive cycles of wetting and drying of the caliche (drying cracks)², stresses due to construction seams, walls joints (spécially at corners), and loss of roofs, combined with the action of natural and human agents of deterioration.

² Drying cracks are those vertical cracks contained between the boundaries of a wall course.



Figure 69: A wall construction seam and drying cracks on the east elevation of the Great House

The combination of seams and cracks with the action of deterioration have been causing losses of caliche of various shapes and sizes, even of entire pieces of walls. Two type of losses can be identified according to their sizes, causes and rates. These are: (1) losses of discrete fragments and (2) losses of wall sections.

1. Losses of discrete fragments coming from a single wall course are probably the result of the interaction of different agents of

deterioration with the construction technique used to erect the wall course. Thus, these pieces usually detach usually following

course seams, head joints and drying cracks (figure 69). The pieces could weigh several hundred pounds and could fall from different heights up to 30-35 feet. Losses of this type are likely to have occurred for centuries at a low but continuous rate. Historical photographic documentation and the conditions survey of the walls of the Great House from 1996-97 have dated losses of this type from the south, west and north elevations as

early as 1891 and as late as 1995.³ At present, this type of loss is still active, though at a rather slow rate.

1. Losses of wall sections, usually of columnar shape, are the result of the interaction among sudden stresses in the structure (such as during an earthquake or stabilization), structural instability of walls, different agents of deterioration, and wall discontinuities, either produced by stresses (cracks) or construction technique (vertical cold joints and wall abutments). Thus, after a section of wall fell, it naturally tended to break in fairly sharp, clean planes following vertical cracks and vertical construction seams. These pieces are extremely massive, usually the height of an entire wall. Example of these losses are visible on different areas of the south, east and north elevations. Historical photographic documentation and the conditions survey of the walls of the Great House from 1996-97 have dated three losses of this type. The earliest, located on the north elevation, east wall end, is dated after 1878 and before 1903. The latest, located on the south elevation, is dated from 1891 and happened during the stabilization work of 1891-92. The general conditions of these collapses are unsupported “broken” edge and parallel vertical discontinuities as cracks or head joints. At present, this type of loss could be considered as inactive as long as any suddenly applied forces happen in the structure. In the event of an earthquake or other type of soil movement (such as caused by ground water table variation), entire wall sections could fall. Since no roofs

³ Location and date of losses of this type are as follows. South elevation: piece from the second course above 1891-92 repair, east wall end, dated 1902, 338-pound piece from upper part, 1955; west elevation: pieces from the fourth course above 1891-92 repair, near south end of wall, dated 1891-92 and 1932, piece from first course above 1891-92 repair, left of entrance, dated 1945, and pieces from first course above 1891-92 repair, near north end of wall, dated 1975, 1981 and 1995; north elevation: pieces along wall top near northeast end dated from 1896, 1940 and 1977.

connects the walls inadequate structural ties exist throughout the structure. Current research on this matter is underway by Johansen, King and Matero.

4.1.1.3 Related to the Condition as a Ruin

Among immovable cultural property, ruins are probably more vulnerable to accelerated deterioration since they exist in a fragmented state open to the environment. Natural agents of deterioration, natural disasters, abandonment, vandalism, and lack of maintenance, all contribute to the degradation of ruins (GCI Newsletter 1992, 47).

Earthen architecture is inherently weather-sensitive due to the nature of the material. Its deterioration is typically related to moisture infiltration, a situation which becomes more precarious when the structure lacks a roof (Jerome 1995, 36).

In the Great House, so long as the roofs remained and the wall tops were protected and maintained, deterioration proceeded slowly. However, when the roofs failed or were removed and lintels were removed after abandonment, water and wind combined with alternate wetting and drying cycles and the action of other agents of deterioration attacked the exposed walls which gradually eroded, cracked and suffered the loss of material.

In addition, the loss of the roofs, which has produced a different structural condition in the Great House, may have been responsible for crack formation, especially along weaker planes produced by vertical cold joints due to unrestricted movement. As a result of this,

columnar sections of walls have been left free standing by their own weight, vulnerable to further cracking and deterioration.

The roofs and floors system of the Great House served not only to create a suitable environment protected from the elements but also played a very important structural role. Thus, the roof and flooring system composed of vigas (lintels), Saguaro ribs, reeds, and mud (caliche), which exhibited unique strength/stiffness characteristics when acting together, was probably capable of providing diaphragm action under seismic conditions (Johansen, 1998).

Since 1903 with the first shelter addition, followed by the present roof completed in 1932, the Great House has been protected from exposure to the direct effects of rain, and to some extent from solar heat. However, the roof does not protect against wind, wind-driven rain and animal/insect activity.

In addition, the roof has minimized and practically eliminated the movement of precipitation water in the caliche material. Therefore, the natural phenomenon of protective crust formation (case hardening) is presently inactive. This could be a threat for those areas of material without the protective crust which are exposed to wind and wind-driven rain.

4.1.2 Extrinsic Causes of Deterioration

4.1.2.1 Natural Factors

As with other earthen structures, water and wind have been the most harmful natural agents of deterioration for the Great House. Both have triggered other types of deterioration involving the action of wetting and drying cycles, salt crystallization, dissolution of mineral matter and rising damp which have resulted in the creation and enlargement of cracks, basal and wall top erosion, and fragment losses.

Water

Caliche, as any other porous building material, is permeable to water and water vapor to a degree determined by its pore structure and mechanical strength. Since the material has been modified by the creation of zones with different physical and chemical properties on its exposed side, water permeability in the caliche is extremely variable; from very low where the crust has formed to very high right beneath the crust. Such phenomena have produced differential erosion of the caliche due to water attack.

Deterioration caused by water is produced by different processes. The most important are:

- Wetting and Drying Cycles

Wetting and drying cycles can cause chemical and mechanical damage both (1) during the wet phase, mostly due to swelling of clays, acid attack, and mineral dissolution, and (2)

during the dry phase, mostly due to mechanical shrinkage of clays and salt crystallization (Torroca 1988, 42).

Wet phase: swelling of clays and mineral dissolution

Clay are present in different types of soils and in a wide variety of sedimentary rocks. They are produced by the weathering of feldspars, micas, and other silicates. Clays, particularly from the smectite group (montmorillonite, bentonite) are specially water sensitive, swelling when wet and shrinking when dry (Head 1992, 107-109). Repetitive swelling and shrinkage of clays produces stresses in the caliche and forms cracks. X-ray diffraction results have identified palygorskite, as the clay mineral present in the caliche. Fortunately, this type of clay is not as water sensitive as montmorillonite or bentonite are. Therefore, the problem of swelling and shrinkage of the caliche due to clay presence is not so severe.

Water, either coming from precipitation or from the ground (rising damp) contains carbon dioxide and therefore reacts as a dilute solution of carbonic acid. Under such conditions, calcium carbonate (from calcite) is transformed into calcium bicarbonate and slowly dissolved.⁴ This process is responsible for altering the binder (calcium carbonate) of the exposed caliche which results in a transformation of its pore structure and mechanical strength.

In addition, silicate minerals undergo incongruent dissolution, that is, their dissolution is accompanied by a phase change. When such a reaction takes place, some ions, such as calcium, aluminum, potassium, and sodium are leached out.

⁴ Any further dissolution is then determined by more carbon dioxide (dissolved in water) entering the equilibrium system (Stambolov and van Asperen de Boer 1976, 8).

Most of the material remains insoluble but is transformed into clay minerals, which are more vulnerable to water attack (Stambolov and van Asperen de Boer 1976, 8; Torroca 1988, 40).

Dry phase: mechanical shrinkage of clays and salt crystallization

During the drying phase, the caliche shrinks, due to loss of water. Drying cracks are produced by this mechanical shrinkage which is perhaps attributable to the collapse of the clay matrices as water is lost. Cracking is also related to the amount of water present in the caliche at the moment of construction.

In addition, during this phase water is transported through the capillary system to the surface where evaporation takes place, resulting in the deposition of salts either coming from the caliche itself or from exterior sources (ground water).

Depending on the solubility of the salts and the rate of water evaporation, precipitation and crystallization are observed at different points in the pores: on the surface of the material (efflorescence) or inside of its pores (subflorescence or cryptoflorescence). Both kinds of salt deposition can exist next to each other and are often interconnected (Torroca 1988, 34-36). Salt damage is produced by mechanical shattering of the soil particles and by chemical destruction of the cohesive properties of the material and its further disintegration (UNESCO, 1964). The majority of deterioration phenomena can be explained by cyclic humidity changes in the presence of soluble salts. In such cases, the damage is proportional to the number of cycles and not to the concentration of salts. Frequent cycles of drying and wetting thus cause an oscillating front accompanied by periodic

crystallization and dissolution of salts (Stambolov and van Asperen de Boer 1976, 21).

Testing for soluble salts in the caliche material from the Great House proved positive for presence of sulfates, chlorides, nitrites and carbonates. Chlorides and nitrates are very harmful because they tend to pulverize the caliche. On the other hand, sulphates could make the caliche more permeable to air, more vulnerable to volume expansion, and can also break it apart through the formation of gypsum (Stambolov and van Asperen de Boer 1976, 9).

Salts crystallization was initially cited as responsible for undercutting the walls of the Great House (Hayden 1954, 105). Though salt deterioration seems to be inactive now due to significant drop in the water table from agricultural overburden since the 1930's, it could become a problem in the future with a rise in the water table, which could contribute to activating the salt concentration of the walls through rising damp.

- Rising damp

Walls may become wet not only if they are in actual contact with the water table, but also by suction from the ground, which is known as capillary rise or rising damp. Its deteriorating action is concentrated near the base of the walls.

The height that water can actually reach in a structure is influenced mainly by the balance between the water intake and the evaporation from the wall surfaces, temperature and

⁵ The soils of the area of the monument contain salts naturally.

relative humidity, ground water table depth and thickness of walls, materials porosimetry, salt content, and presence of surface treatments.

The deteriorating action of rising damp combined with salt crystallization was responsible for the severe basal erosion of the walls of the Great House and probably produced fragment loss. In 1891, Mindeleff thought that the greatest destruction of the walls within the first foot above ground level was due to water raised by capillary action which softened the caliche and made it vulnerable to mechanical deterioration, mainly from wind abrasion (Clemensen 1992, 36).

A decrease in the ground water table level due to intensification of agriculture in the area during the present century has apparently stopped any rising damp deterioration of the walls from the Great House. Further, the fills of fired brick and cement mortar (1891-92 stabilization) which were placed in the cavities left in the walls by basal erosion appear to have improved the stability of the walls. However, this may be more cosmetic than structural.

- Rain

Henry Foth (1990, 102) has described several types of erosion caused by the action of rainwater in soils which are applicable to rainwater deterioration of earthen structures, in particular the Great House. These are: splash, (caused by raindrop), sheet, rill, gully and channel erosions. Usually, these types of rain erosion act in conjunction with each other.



Figure 70: Deterioration and missing caliche near the parapet of the Great House probably caused by water (rain) deterioration.

Raindrops falling on bare walls detach particles and splash them up into the air. Then when there is enough water collected at the wall surface, the water tends to run down the surface of the material as a thin sheet, causing more detachment of particles (sheet erosion). While moving down the wall, water acquires more energy which causes damage to the caliche in the form of rills and gullies. Finally, water has the tendency to collect into small rills that converge to

form large channels and produce channel erosion (Foth 1990, 102). For this reason, the deteriorating effect of rainwater in the walls is more harmful at their base due not so much to splashing but to total water runoff, with the addition of saturation and salt attack. While there are various formulas to grade the erosive factor of rainwater in soils, the

rainfall factor is the most applicable to earthen architecture. The rainfall factor⁶ is a measure of the erosive force of a specific rainfall. Such erosive force, or available energy, is related to both the quantity and intensity of the rainfall (Foth 1990, 102). This is particularly important for the Great House due to the severity of the short but intense storms in the area of the Monument, mainly during the monsoon season in late summer. Oftentimes, such severity of rainfall is increased by hail and strong winds which causes more deterioration of the structure.

The harmful deteriorating action of rainfall to the Great House has been almost stopped since 1903 with the addition of the roof. Only the sections of walls located on the east elevation and near the southeast and northeast corners (facing the prevailing winds from the east) are still vulnerable to deterioration from wind driven rainfall, verified by the current eroded conditions of soil wash and microhoodoos.

- Water Condensation

Besides wetting and drying cycles, rising damp, and precipitation, another water-related deterioration effects for the Great House is the effect of water condensation combined with cyclical contraction and expansion of the caliche. This natural phenomenon may have been responsible for the formation of micro-cracks which have played and still play an important role in the detachment of the previously formed crust. Water condensation

⁶ The rainfall factor is the product of the total kinetic energy of the storms times the maximum 30 minutes intensity of fall and modified by any influence of snow melt. Rainfall factors have been computed for many locations of the country, with values ranging from less than 20 in the western United States to 550 along the Gulf Coast of the southeastern United States. The rainfall factor in the area of Arizona where the monument is located is between 35 and 50, which is considered a low value (Foth 1990., 102).

effects are still active in the Great House since the roof offers no protection from this agent of deterioration.

Finally, moisture content in general has played an important role in decreasing the tensile and compressive strength of the caliche, in particular, at the bases of the walls. That is the section where the material has to support all the weight of the wall. For this reason, the caliche from that area tends to be more vulnerable once saturated with water (Stanley Price, 1984).

Wind

Wind plays a very important role in the erosion of earthen structures, especially when located in desert environments. Such is the case of the Great House in which wind has been a persistent agent of deterioration for centuries.

On almost any warm day, tall, whirling columns of dust spiral against the sky in the area of the Monument. Large dust storms, caused by a combination of high surface temperatures and downdrafts from decaying thunderstorms, sweep north from Mexico to the Phoenix area on an average of 3 ½ times per year (Chronic, 1983). The winds, which prevail from the east direction, can reach up to 80 mph, particularly during the monsoon season.

One of the most typical deterioration processes caused by wind is the blowing of particles which cause abrasion of the caliche and can produce detachment of loose pieces from the walls. According to Foth (1990, 110) the majority of soil particles carried by wind moves

by a process called saltation. During this process, fine soil particles (0.1 to 0.5mm in diameter) are rolled over the surface of the walls by direct wind pressure. When striking the surface, the particles could rebound into the air or hit other particles into the air before coming to rest. Very fine particles (such as silts, clays, calcium carbonate) could be thrown into the air by the impact of larger particles moving in saltation. Once in the air, their movement is governed by wind action and they could be carried very far away.

Wind erosion in combination with water is visually detected on the walls by small protruding stalks of earthen wall material that are formed by wind and wind-driven rainfall striking the structure. These stalks, or “microhoodoos”, are oriented parallel to the prevailing wind, and usually are supported by an erosion resistant particle (nodule) at the tip.⁷ This type of deterioration is more visible on wall tops, wall ends and in interior walls located near the opening of the structure (figure71 and 72).⁸

Differences in air pressure caused by wind and its prevailing direction influence rain penetration in the caliche located in more exposed areas (east elevation). Thus, wind plays an important role in water deterioration caused by wind-driven rain because it may increase rain penetration.

⁷ Graduate Program in Historic Preservation, University of Pennsylvania. *Condition Assessment Definitions*. Winter Field School, Casa Grande Ruins National Monument, Arizona, December 1996-1997, 3.

⁸ Such as: on the south wall of Tier A, southeast corner which is exposed to wind drafts entering the structure by the northeast corner opening, in Tier D, especially around its southeast corner and, in Tier E on its south and north portions of wall near the east missing wall.

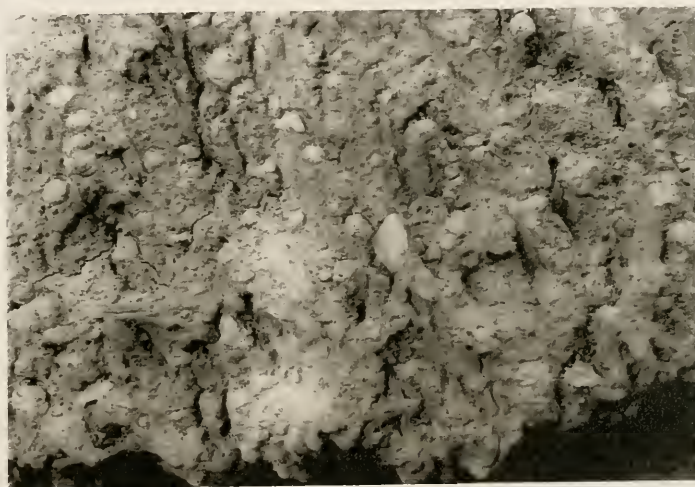


Figure 71 (top): Deterioration (microhoodoos) caused by wind erosion, east elevation.
Figure 72(bottom): Close up

Influence of wind pressure on the horizontal transport of water is very important in the case of cracks, crevices and other openings facing the direction of the wind (Stambolov and van Asperen de Boer 1976, 18-19).

In addition, wind plays a very important role in salt crystallization. It increases surface evaporation speed which cause evaporation to take place immediately below the surface, in the pores of the caliche already weakened by loss of calcium carbonate. Therefore, the disruptive effect of salt crystallization is at its maximum, creating alveolar erosion by differential loss of material.

Wind blows toward the structure and penetrates it through openings creating vortices that strongly affect the caliche of the walls. Missing wall sections and the lack of roofs and floors have increased the vulnerability of the Great House to wind-related deterioration.

The modern roof added to the structure may be responsible for changes in wind pattern and the subsequent creation of wind whirlpools may have increased wind velocities. The most vulnerable areas to the action of wind are wall tops, wall ends, inner and outer areas of wall located near openings (south, southeast and northeast sections), and areas that lack the calcium carbonate enriched crust (mainly located on walls facing the wind direction).

Animal/Insect Activity

Though animal and insect activity may have contributed to the deterioration of the Great House to some extent, the overall results of such activity are consider of minor importance compared to the action of other nature-related agents of deterioration.

For centuries, the area of the monument blended with the surrounding area to provide an ecological niche for many insects, birds and animals. In 1934 the area of the monument was fenced to stop the damage to the cultural resources from livestock.⁹ Such a protective measure affected the natural balance of the monument's wildlife and caused overpopulation of small mammals because large free range mammals were kept outside the monument by the fence (Clemensen 1990, 163).

The intensification of agriculture and increase of human population in the area during the twentieth century produced the last and greatest changes in what was left from the monument's natural ecosystem. Such changes affected the animal and insect activity of the area and of the monument as well but caused only a low impact in the Great House.

In the 1940s, an infestation of Mexican Free-tail bats (probably produced by an overpopulation of insects) affected the walls of the Great House by stains caused from its

⁹ By the later part of the 19th Century, livestock wandering over open range, may have caused some deterioration to the Great House. However, livestock proved to be more harmful to the natural vegetation of the monument than to its cultural resources (Clemensen 1992, 154).

droppings.¹⁰ Bats also contributed to crack enlargement and attracted other animals such as black and red racer snakes (Clemensen 1990, 164) Spraying the area cotton fields reduced the insect population in the monument so bats moved to other areas or died from ingesting insecticide-contaminated insects.¹¹

The bird population of the monument was also affected by the insecticide sprayed on nearby agricultural fields. The most harmful effect for the Great House was caused by a decrease in the population of owls and a consequent increase in the sparrow population. In 1968, Roy Reaves estimated that sparrows were greatly responsible for knocking down caliche material from the walls. In addition, an increase in stains from bird dropping was registered, especially in the interior walls of the Great House (Clemensen 1992, 164). At the moment, sparrow population seems to be controlled and no major wall material shows signs of destruction due to their presence.

The protective shade created by the shelter provides a microclimate attractive to certain animals, mainly birds and insects. However, this seems to represent a minor threat of deterioration to the Great House walls at the moment.

At present, animal and insect activity in general is associated with cracks greater than 10cm which can provide shelter for birds, bats, insects, and birds. In addition, voids

¹⁰ Bat guano is highly acidic and in contact with rain water may have contributed to some calcium carbonate dissolution in the caliche. However, such effect has not been mentioned in the literature.

¹¹ By 1956, bats no longer lived in the monument (Clemensen 1992, 164).

produced by detached fragments of caliche material become the home to rodents, birds and insects; this can lead to detachment of further fragments.¹² While animals may not be the initial cause of damage, opportunistic use of cracks and voids causes fragments to detach, resulting in material loss.

Natural Disasters: Earthquakes

The Great House probably experienced damage from earthquakes which may have resulted in wall splitting, displacement and fracturing, and the loss of large columnar sections of walls. Such is the case of a cracked column of wall located on the north elevation, near the east end of the wall (showed in an historical photograph taken in 1878) which possibly was a casualty of the Sonoran earthquake of 1887.¹³

Based on mathematical analysis of earthquake forces applied on the walls, Krieger and Sultan (1974) established that an earthquake was the most dangerous threat of deterioration and destruction of the Great House. They calculated the earthquake forces on the walls of the Great House according to a mathematical analysis in accordance to the Uniform Building Code Requirements (Zone II). The results obtained from such analysis showed a greater overturning moment for the walls comparing to their resisting moment.¹⁴

¹² Clearly, recent detachment of fragments have shown rodent activity behind them.

¹³ Architectural Conservation Laboratory, Graduate Program in Historic Preservation, University of Pennsylvania. Wall Condition Documentation and Assessment, Casa Grande Ruins National Monument, Coolidge, Arizona, 1996-97 (unpublished).

¹⁴ When this study was done the Uniform Building Code classified the area of the Monument as Zone II (Krieger and Sultan 1974, 14). However, current buildings codes now classify southern Arizona as one of the areas in the United States least in danger from earthquakes and Sternberg 1981, 17) so Krieger and Sultan calculated a damage five times as great as the one suggested by the present regulations (Wilcox and Sternberg 1981, 17).

Such results, together with the great potential of a large earthquake, led to the conclusion that there is a potential that the Great House could be completely demolished. In addition, because of the obvious leaning of some of the walls, in particular the south wall portions, a concern existed as to their structural stability (Kreigh and Sultan 1974, 19-20).

The major issue in the Great House concerns the lack of roofs and the stability of the walls in seismic loading. The original lateral resistive system (vigas, Saguaro ribs, reeds and caliche floor/roof) provided horizontal load transfer through the structure as well as adequate lateral support to the walls. Further, the complex manner in which the diaphragm system interacted with the wall system, could have resulted in additional energy dissipation which would have facilitated the overall structural integrity of the system. Given that the Great House has lost its lateral resistive system over time it has minimal seismic resistance (Johansen, 1998).

While historical evidence shows little indication that earthquakes are a major cause of deterioration of the Great House, threats of earthquake damage to the structure should not be overlooked. The lack of lateral supports (mainly due to lack of roofs and floors) lack of wall interlocking at corners, and through-wall long, vertical cracks and construction seams have transformed the walls of the structure into large, free-standing columnar sections which in the event of an earthquake could fall and have the potential for great damage and further instability of the Great House.

4.1.2.2 Human

Direct

The removal of roofs and floors beams for their re-use in other structures was probably the first major direct human-related action of deterioration that the Great House suffered immediately after its abandonment.

The desert environment helped to shelter the Great House from the deteriorating action of man for many centuries. Therefore, deterioration of the structure caused by direct human agency was limited only to some vandalism in the form of excavations, graffiti, and some wall material removal.

Greater opportunity for looting and vandalism of the Great House and other cultural resources of the monument occurred after the Southern Pacific Railroad completed a line through the area in the winter of 1879-80. Soon a stagecoach line, which ran within a few feet of the Great House, opened to connect Florence with the new railroad station located 20 miles to the west of the monument. At this time it was common practice for passengers to stop and dig among the ruins, leading to further deterioration of the Great House. The protective actions against vandalism during the end of the nineteenth century and beginning of the twentieth century helped to control and practically stop this type of deterioration (Clemensen 1992, 25).

Fortunately, other human interventions in the Great House such as stabilization works and addition of the protective roofs, have contributed more to the preservation of the structure than to its further deterioration.

At present, the threat caused by direct human-related deterioration is minor. Visitor's use is controlled. No access is allowed inside the Great House and visitors are restricted to walking around the structure. The monument's staff has developed an effective surveillance system that has practically stopped vandalism, graffiti and other type of human-related physical damage to the structure.

Indirect

Human-related activities in the area, such as ranching during the nineteenth century followed by twentieth century farming and population growth, not only have helped to destroy the desert ecosystem of the area but also have isolated the monument in the midst of an area of fast human development.

Such changes have produced variations in the ground water table, increases in vibrations, pollution and other indirect human-related causes of deterioration that could be the cause of past, present or future damage of the Great House.

Damages caused by indirect human action are very difficult to assess because (1) the structure is not the direct target of such deterioration, and (2) usually these damages are

not immediately visible. For these reasons, indirect human actions could cause far greater damage to the Great House than direct ones because of the unknown nature of the problem.

The already discussed processes of deterioration analyzed in the context (condition) of the Great House, along with results obtained from the present characterization of the caliche, have provided additional data in wall course construction and the construction sequence of the Great House. In addition, the invaluable data provided by previous research (Stubbs and Stalling, 1953; Wilcox and Shenk, 1977, Wilcox and Sternberg, 1981), and results obtained from the wall conditions survey carried out by the University of Pennsylvania have greatly contributed to the formulation of new theories of wall course construction and construction sequence.

5.1 Wall Course Construction Technique

Analysis of the shape and form in which caliche fragments fall from the wall, together with site observations from cracking patterns and results obtained from migration of calcium carbonate in the caliche, have provided new data to establish that the wall course construction technique proposed by Wilcox and Shenk (1977)¹ may be only applicable to the construction of the foundation or fills of the Great House.²

The preparation technique of the caliche (puddling) and the units or lenses of caliche probably were the same for the foundations as well as for the wall courses. However, it is probable that a different method of assembling caliche units above ground may have been

¹ Already explained in chapter 2.

² Indeed, this assumption is based on evidence found in the Reaves trench, that is underground.

used for the wall courses.

Wilcox and Shenk's proposal applies to the foundation construction, where piling up caliche lens-shaped units might have been a rather easy task since the walls and bottom of the trench served as a form that gave the final shape to the mass of caliche.³

Since no forms were used for the erection of each wall course, Wilcox and Shenk's proposal might have been extremely difficult to carry out. Therefore, this author proposes the following wall course construction sequence:

1. First, onto the ground, the wet lens-shaped units of puddled caliche described by Wilcox and Shenk were dumped and pressed into place by hand. The material was piled up in layers all at once, without letting them dry, to form a cone shape mass. The height of the pile was determined by the slump height, that is, the maximum height at which the pile maintained its shape.⁴
2. After some drying took place and the cone-shaped mass had acquired enough consistency, additional units of caliche were added to both sides of the course which then were carefully shaped, smoothed and leveled until obtaining a flat planar surface approximately 90° with the ground level. The top of each course was probably left convex⁵ to contribute not only to the stability of the wall course while drying but also

³ This same process might have been followed for the erection of the fill above ground level.

⁴ The slump height is also related to the amount of water present in the material; this is the stiffness of the mix. In the case of the caliche, the presence of hard aggregates (caliche nodules and stones of different size and shape) and the kneading of the material while in the caliche mixing bowl might have contributed to increasing the slump height by a decrease in content of water.

⁵ Convexity of the top of wall courses was found by dissecting the walls at Pindi Pueblo (Stubbs and Stalling, 1953) and at Fork Lightening ruin (Kidder, 1958).

to the stability of all the courses in the wall, therefore improving the interlocking capacity of the course with each other (figure 73).

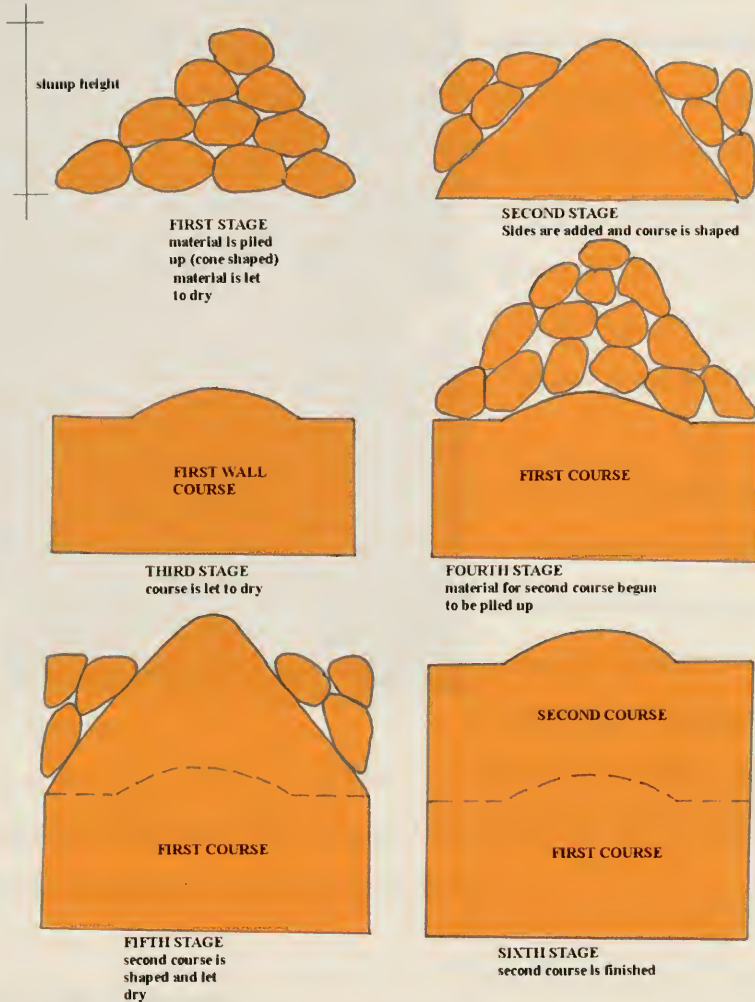
3. Once the course was completely dried, another was started on top following the same procedure. The last wall course, this is the parapet, was probably raised at once since the wall thickness in that section is thinner. Also, they were nearly continuous across tiers as a bond beam. As with the rest of the courses, the top of the parapets were left convex.

On the north end of the east elevation (the section of wall facing north) there is a crack that arches through the wall section creating a mounding profile suggestive of the built-up construction technique already described (figure 74).

The results obtained from different calcium carbonate content showed from testing the caliche fragment that fell from the west elevation of the Great House (1995) provides additional data that could further explain the falling of large fragments of caliche. In this sense, the depletion of calcium carbonate found in the back of the piece has created another internal weakness in the wall.

Zones created by different calcium carbonate content due to migration and depletion processes may be only associated to the outer portions of lens-shaped units of caliche that were added to the core of the course once dry. The caliche from the inner cone-shaped mass of the course may have not been affected by this natural phenomenon due to (1) lack

PROPOSED WALL COURSE CONSTRUCTION



* top of course is left concave to improve interlocking of courses in the wall

Figure 73: Proposed wall course construction



Figure 74: Crack on a wall end that suggests the proposed course construction

of enough exposure to wetting and drying cycles, and (2) interruption of continuity of the outer and this inner mass caused by course construction cold joints (figure 75). These help clarify the reason why the caliche material from the core of the wall may not be affected by case hardening.

The falling of pieces of caliche can now be explained as a combination of the following phenomena: (1) patterns of cold joints (exterior and interior) left in the wall by the

course construction technique, (2) the friability of the material due to calcium carbonate impoverishment along the plane of contact of an internal cold joint, and (3) a combination of nature-related processes of deterioration (figure 76).

5.2 Construction Sequence

As previously explained in chapter 1⁶, Wilcox and Shenk (1977, 121) made an attempt to

⁶ Chapter 2, section 2.2.3 (Wall Construction Technique).

DIFFERENT COLD JOINTS (INTERRUPTIONS OF CONTINUITY) IN THE WALLS

FRONT WALL (DETAIL)

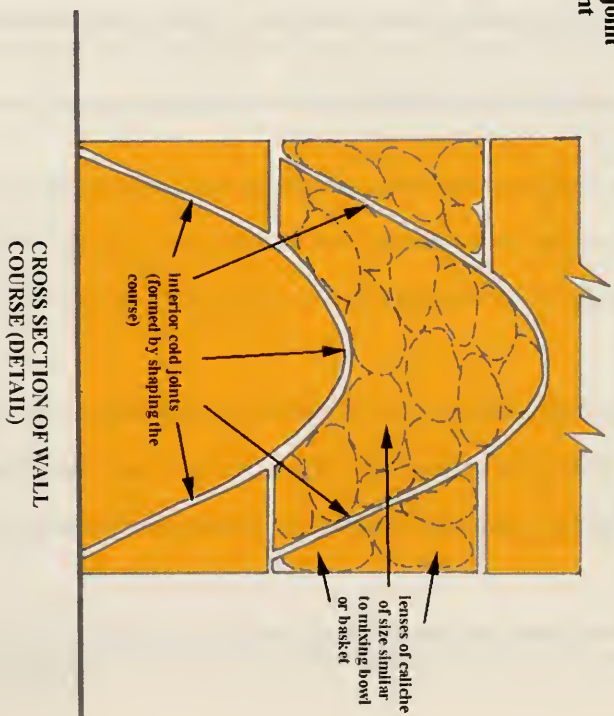
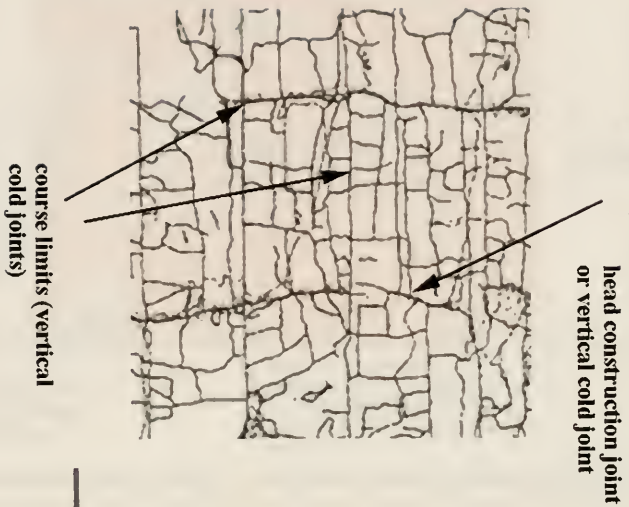
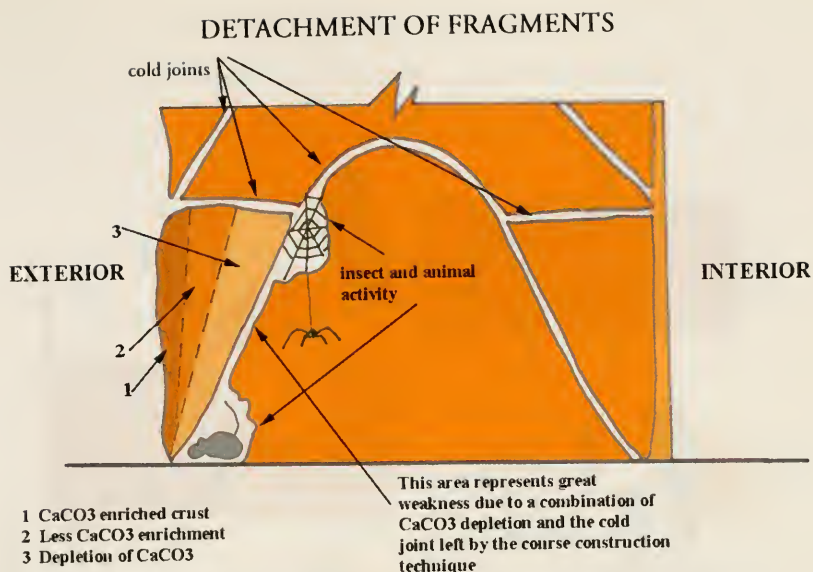


Figure 75: Different wall cold joints (interruption of continuity)



Detachment of fragments is mainly caused by a combination of internal cold joints (construction technique), movement of CaCO_3 (weathering), and various nature-related causes of deterioration

Figure 76: Course wall cross section showing different vulnerabilities of the course to deterioration

explain the actual construction sequence (strategy) as to how the Great House was put together. However, this construction sequence for the structure is not complete. No other attempts to order construction sequence have been made for the Great House yet.

Field observations and preliminary results obtained from the conditions survey of the Great House walls (interior and exterior)⁷, have provided new data which allow identification of a possible strategy used to build such a large structure. The process

⁷ The condition survey was carried out by students from the Graduate Program in Historic Preservation, University of Pennsylvania, during the winter field schools at the monument carried out in December 1996 and December 1997.

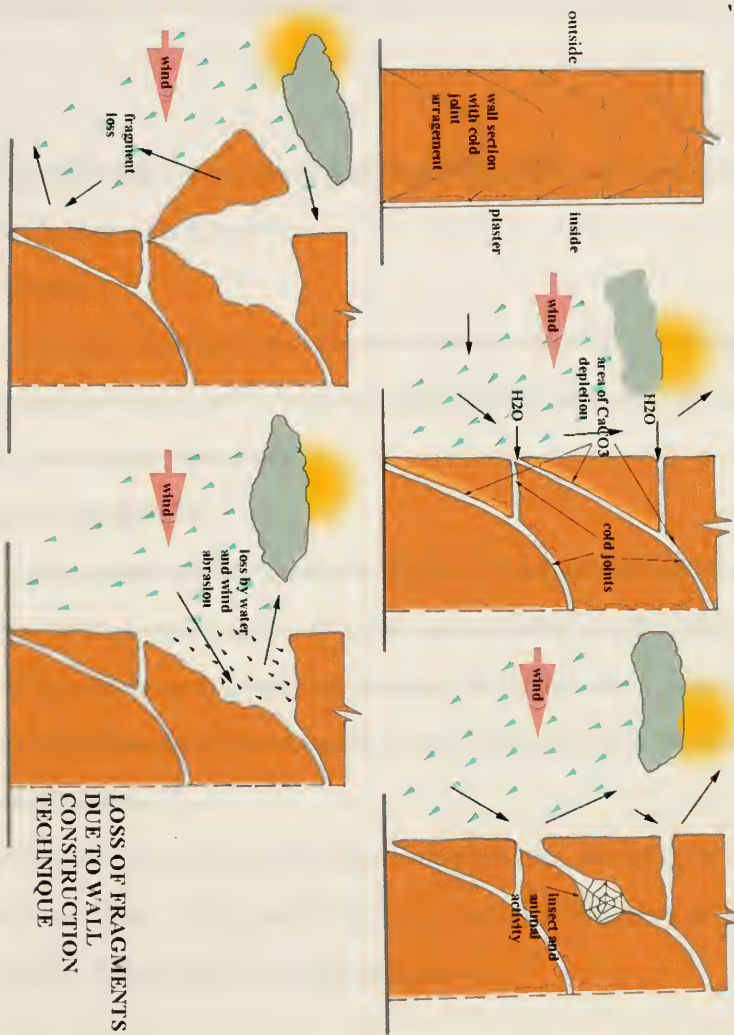


Figure 77: Loss of wall fragments

LOSS OF FRAGMENTS
DUE TO WALL
CONSTRUCTION
TECHNIQUE

followed to determine a proposal of construction strategy was: (1) identify several features and conditions of the walls in search of a pattern or similarities in construction; and (2) connect these features and conditions to the layout of the Tiers by plotting them on a floor plan.

The following findings can be drawn from the identification of features and conditions found on the walls of the Great House:

North Elevation

- Analysis of wall junctures suggests that this wall (north wall of Tier A) was originally construction-butted against the west wall of Tier B and the east wall of Tier D (west and east elevations respectively).

South Elevation (figure 78)

- The most-western wall end appears to be the limit of an integrally constructed corner, that is the southwest corner is formed by the west wall which turns 90° without any interruptions. The uniform thickness and straight edge of this wall end suggests a wall construction seam formed by the alignment of the head joints of all the courses of the
- wall at that point.
- The most-eastern wall end could also be a construction seam, although not as uniform as the western one. This is probably due to exposure to prevailing winds and rainfall since the southeast corner of the structure is missing.

West Elevation (figure 79)

- Two distinctive through-wall vertical cracks bisect the northern end of this wall and appear to be related to the intersection of the north and west walls of Tier A into the west wall of Tier B. These cracks traverse the full height of the wall and are accompanied by erosion and animal activity.
- There is another distinctive vertical through wall crack near the southern end of the wall (aligned with the south wall of Tier B) which seems to be related to the intersection of the west wall of Tier E into the west wall of Tier B.

East Elevation (figure 80)

- All of the south end of the east wall (east wall of Tier D) is missing so all physical evidence of construction of the southeast corner and the intersection of the south and east walls of Tier D has been lost.
- A distinctive vertical through-wall crack is located near the northern end of the wall (aligned with the south wall of Tier A) which seems to be related to the intersection of the east wall of Tier A into the east wall of Tier D.
- The north wall end (north of the lower spur of the north end) also presents a uniform thickness and straight edge which suggests a part of a wall seam (where the east wall of Tier A butted the east wall of Tier D).

Interior Walls (inside Tiers)

Several vertical through-wall cracks along walls are viewed in the interior of the Great House. The location of these cracks are as follows:

SOUTH ELEVATION

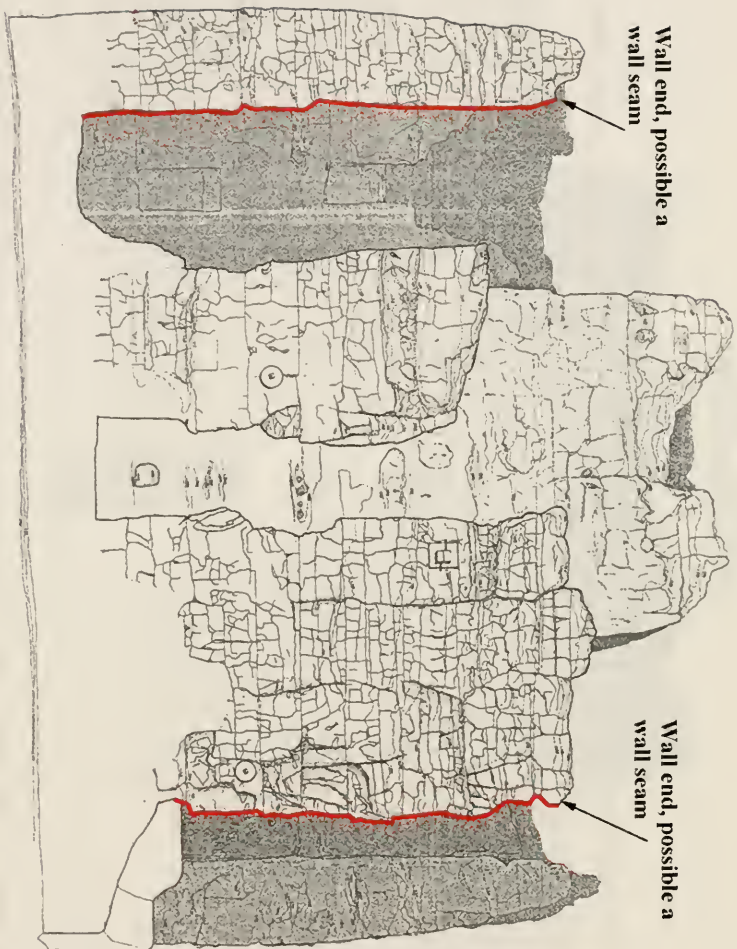


Figure 78: South elevation with evidence of tier construction (Myra, P and E. Borchers, Terrestrial photogrammetry of the Great House, 1979. Courtesy Casa Grande Ruins National Monument)

WEST ELEVATION

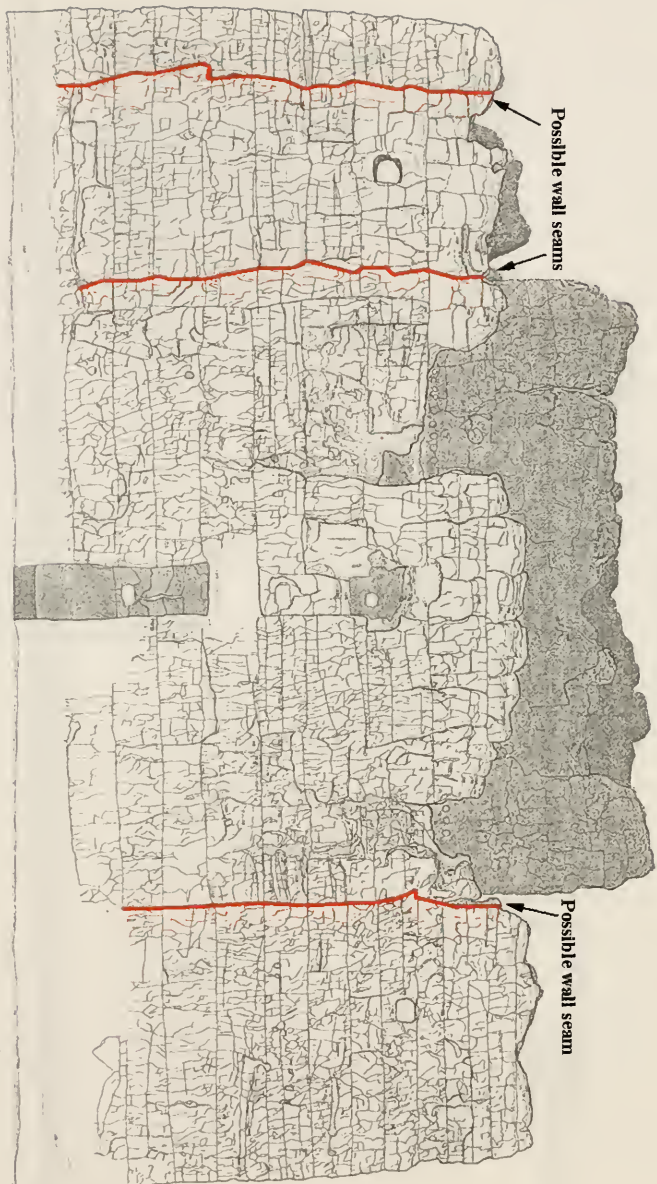


Figure 79: West elevation with evidence of tier construction (Myra, P and E. Borchers, Terrestrial photogrammetry of the Great House, 1979. Courtesy Casa Grande Ruins National Monument)

EAST ELEVATION

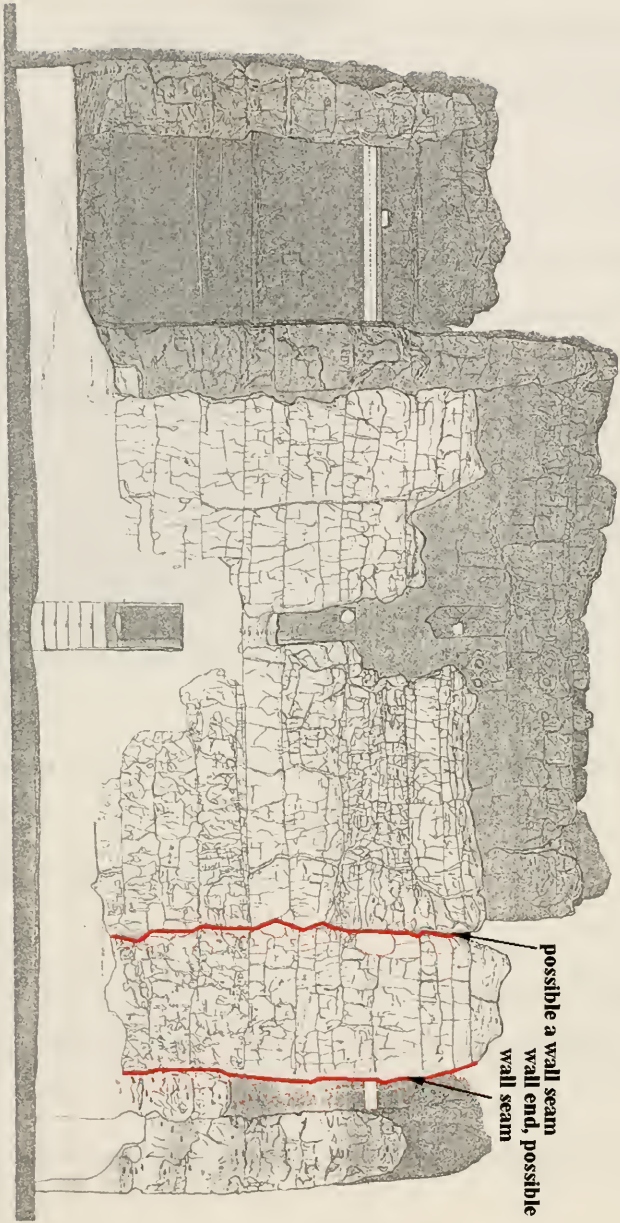


Figure 80. East elevation with evidence of tier construction (Myra, P and E. Borchers, Terrestrial photogrammetry of the Great House, 1979. Courtesy Casa Grande Ruins National Monument)



Figure 81: West wall end on the south elevation.

- Tier B: northwest, northeast, southwest and southeast corners.
- Tier D: northwest, northeast and southwest corners. The southeast corner of Tier D is missing.
- No vertical through-wall cracks were found in any of the four interior corners of Tier C (except two in the parapet course).

Figures 84 plot all the above information in the floor plans of the Great House. Figures 85 proposes a tier by tier construction in floor plan which hypothesizes the stages of construction within a single building episode.

All vertical through-wall cracks detected on the east and west elevations as well as in the interior corners of Tiers B and D seem to be directly related to Tier construction.

The most western and eastern ends of the south elevation and the northern end of the east



Figure 82: Wall seam and north wall end, east elevation. Figure 83: Interior wall seams (corners) inside Tier A, looking west

elevation seem to represent what is left from wall seams.

The two corners of the structure, northwest and southwest, which still exist are evidence of different methods of corner construction. Additional evidence found near the missing corners, northeast and southeast, help to suggest that these two exterior corners of the structure may have followed one of the two methods of corner construction of the two remaining corners. Probably the northeast corner was similar to the existing northwest corner (since both belong to Tier A) and the southeast corner was similar to the existing southwest corner (since both belong to Tier E)

The absence of through-wall cracks in any of the interior corners nor on the interior walls of Tier C and the almost intact condition of the wall plasters suggest that the construction of Tier C may have been carried out as a whole, in contrast to the rest of the tiers.⁸ Thus, the wall courses may have been continued around the four corners without stopping so Tier C is formed by a series of concentric loops similar to the coiling system used in pottery. The location of course seams is obscured by the wall plasters.

Based upon the assumption by Wilcox and Shenk (1977) that several crews were working in several areas of the structure, figure 85 represents a proposal of staging of construction for the first story of the Great House, and figure 86 represents a proposal of staging of construction of the entire structure during a single building episode.

⁸ However, these conditions may be due to the fact that the walls of Tier C are structurally the most stable and protected since Tier C is located in the middle of the structure.

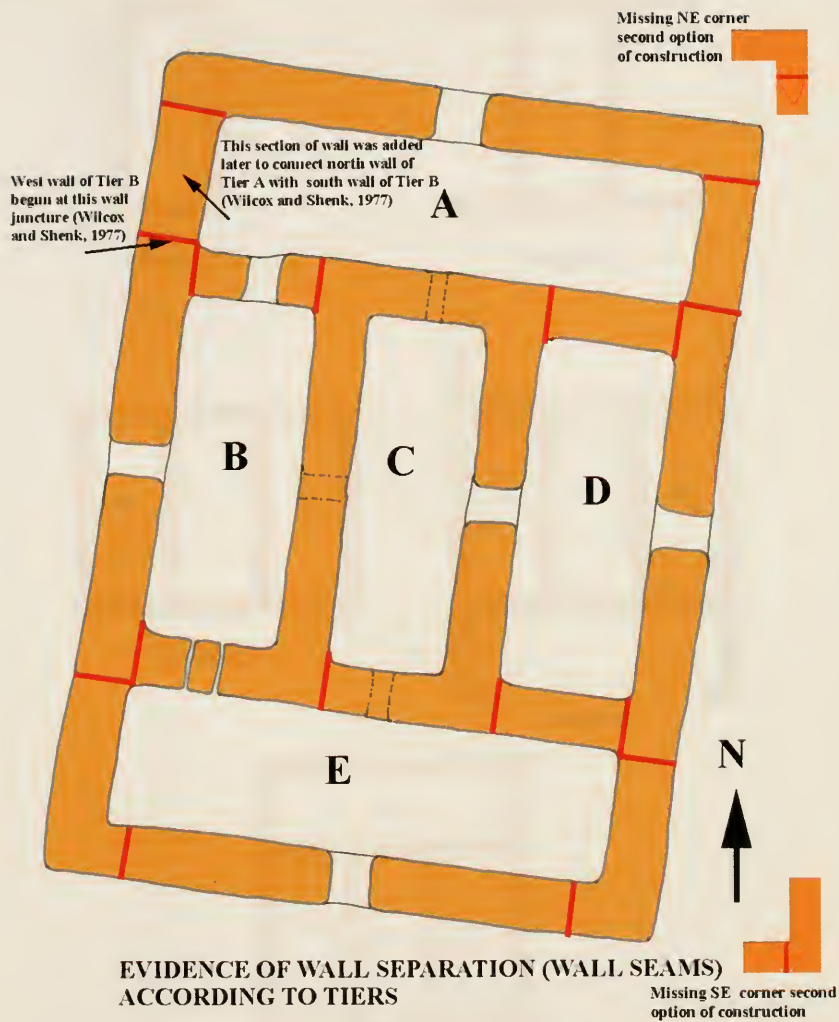


Figure 84: Plan of the Great House with all wall seams and reconstruction of missing corners

PROPOSAL OF TIER CONSTRUCTION FOR THE GREAT HOUSE

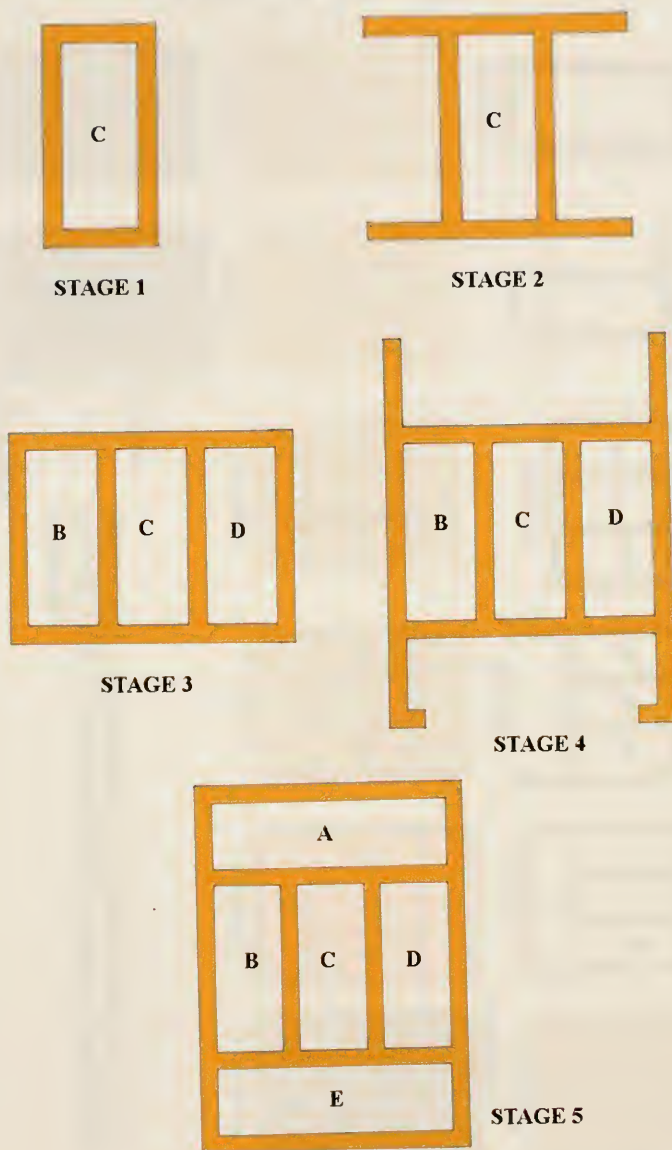


Figure 85: Proposal of tier construction

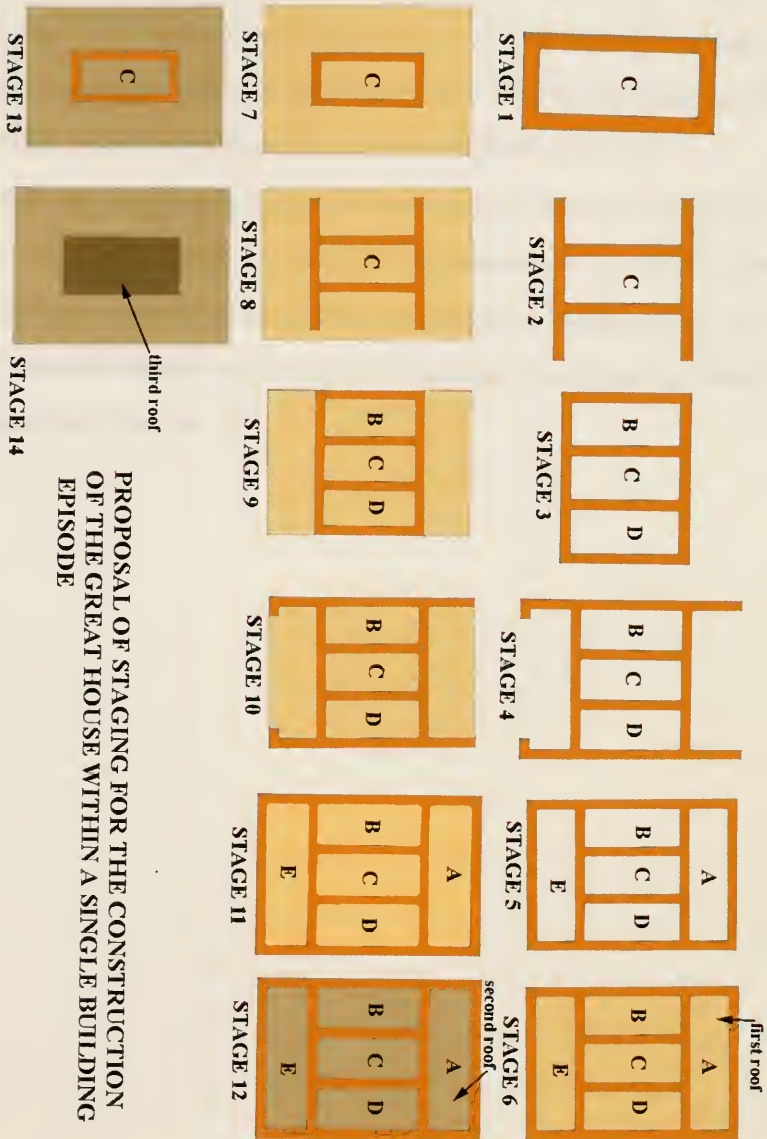


Figure 86: Proposal of staging of construction within a single building episode

The proposal suggests that the structure was started from its core, Tier C, toward the outside. Thus, the four walls of the first story of Tier C were laid simultaneously (stage 1). Once completed, the walls of the first story of Tiers B and D followed (stages 2 and 3), and finally the first story walls of Tiers A and E were added (stages 4 and 5).

Immediately after completing the first story of the structure, the floors were added to the Tiers and the sequence of stages was repeated for the stories above. Once all Tiers' roofs of the second story were completed, the drains and wall parapets were laid (Tiers A, B, D and E). Afterwards, the third story of Tier C was completed, its roof added, and finally its parapets and roof drains were laid.

6.1 Recommendations

The identification, documentation and explanation of the processes of deterioration of the Great House are a necessary prelude to any conservation and management strategy.

Fortunately, since the first stabilization of 1891-92 until the present, continuous care and maintenance have significantly reduced deterioration of the Great House. From 1903 with the addition of the first protective roof until the present, several processes of deterioration, mainly rainwater-related, have become greatly reduced in the Great House. However, deterioration has continued. Unfortunately, no final solution is likely to be available for earthen structures, more so for earthen ruins.

Recommendations will concentrate on the caliche material from the Great House since that is the focus of the present study. However, some general recommendations will also be included at the end of this section.

The most active deterioration of the caliche from the Great House walls is related to the material itself and the method of wall construction used in the structure which has resulted in (1) detachment and falling fragments of caliche, and (2) exposure of friable surface due to loss of the protective calcium carbonate enriched crust. Both problems, which are intrinsic in nature, cannot be stopped but can be retarded with the aid of different methods

of stabilization. In addition to these two problems, the Great House has suffered losses of large section of walls which are connected to the instability of the structure due to lack of roofs during earthquakes and the 1891-92 stabilization.

6.1.1 Recommendations on Detachment and Falling Fragments of Caliche

There are two different stabilization problems to address related to falling fragments of caliche: (1) fragments, generally small in size, though detached are still adhered to the wall, and (2) large fragments of caliche completely detached and too heavy to be supported.

Detachment of caliche fragments

The conditions survey is a very important tool to detect areas of detachments or loose fragments so they can be monitored. If the monitoring shows potential danger of falling, the fragment should be re-attached using techniques and materials compatible with the caliche. This practice will prevent sudden unpredictable loss of fragments and further loss of the protective calcium carbonate enriched crust.

Research needs to be conducted concerning the formulation of a material to be used in the re-attachment of caliche pieces as well as to be used as void and crack filler in order to improve the mechanical resistance of the material and close all possible access routes of water to the inner parts of the caliche.

Lime-based mortars, cement, grouts of organic and inorganic binders, and various resins have been commonly used to solve this type of problem.

In the past, Kreigh and Sultan (1974) developed an epoxy resin compound to be used in the Great House to bond the fragmented and cracked wall pieces together and to fill voids in order to restore and maintain the structural continuity of the walls. The epoxy formula was the result of laboratory testing of selected epoxy resins blended with various curing agents and fillers in order to obtain a material with properties and strength as close as possible to the original caliche. However, the epoxy formula was never tested in the Great House walls because Kreigh and Sultan's strategy of epoxy injection was considered too invasive for the Great House.

Most recent research in stabilization of earthen structures seems to focus on the use of a variety of soil-based grouts which have proved successful for filling voids, cracks and material separation. For this reason, the formulation of a caliche-based grout could be a very effective and promising method of stabilization for detached caliche pieces from the walls of the Great House.¹

¹ Around 1903, S. J. Holsinger recommended to Frank Pinkley to use original material (caliche) for repairs and fills of wall cracks. He indicated that a suitable source of caliche could be found in the immediate area around the Great House at 7-8 feet deep in the ground (Clemensen 1992, 50).

Sources of caliche should be tested in order to establish compatibility with the original caliche.² Mineralogical composition, especially the amount of calcium carbonate content, and physical properties should be analyzed and compared to the ones from the original caliche. In addition, concentration of soluble salts of the caliche source should be tested before making any decision.

When formulating a caliche grout, the use of additives (such as fillers) and different binders (organic or inorganic) should be explored. However, in the case of binders, emphasis should be put on the use of calcium carbonate (lime) in order to obtain a product as similar as possible to the caliche from the walls.

A laboratory testing of different grouts should be developed in order to test physical properties such as shrinkage, viscosity, expansion and contraction, adherence, setting time, water resistance, compression resistance. Furthermore, recommendations related to site application (injection methods, handling and mixing of materials) and any other important site specification should not be disregarded. The grout should be tested at the site in order to obtain an accurate evaluation of its application and performance. Further monitoring should be carried out for a period of time to test the effectiveness of the treatment in time.

² The practice of excavation to obtain soil to be used in repairs and stabilization of ruins is not allowed inside National Park's property in the present. Therefore, the caliche from inside the Monument cannot be used for stabilization of the Great House.

Complete detachment of large heavy caliche fragments

Fragments that suddenly fall should be carefully collected and photographed. An inventory of records should be made with the dimensions and weight of the fragments, the date and approximate time of detachment, weather conditions at that time, exact location and orientation of the fragment in the section from where it fell, and any other important details.

Once a fragment has been properly recorded, it should be put back in the exact location from which it fell. This is most applicable to large fragments and fragments containing the calcium carbonate enriched crust.

In the case of small fragments, the reattachment technique should follow the same technique used for re-adhering detached fragments that are still in the walls. However, in the case of reattachment of large fragments, further research related to the use of compatible materials and reattachment methods is needed.

Falling fragments weighing over a hundred pounds represent a great hazard for visitors if they fall from the exterior walls of the structure. Therefore, the reattachment technique must provide a strong bond in order to prevent them from detaching again.

For reattaching large fragments, it is necessary to have a material that flows and locks the fragment in place, providing a continuous bond that will increase the effectiveness of the reattachment.

Soil-based grouts generally tend to have low capacity of bonding while under pressure and set slowly which could represent a great problem when reattaching large fragments.

In general, thermosetting resins, such as epoxy compounds are the high strength adhesives of choice used commonly for the reattachment of stone. Kreigh and Sultan (1974) tested various epoxy compounds with caliche. However, this research is outdated due to advances in the adhesive industry. In addition, epoxies are not compatible with caliche because they are not water-based.

The extensive experience of using different types of pins in the reattachment of masonry could be applicable for reattaching large caliche fragments. However, vibration from drilling during the installation of the pins in the caliche could seriously jeopardize the stability of the entire walls and cause cracking in the material due to nodule deflection.³ For this reason, low vibration drilling techniques for pin insertion or manual drilling

³ Krieger and Sultan (1974, 120-123) proved that several drilling techniques were not safe for the Great House due to vibration effects from resulting jolting or shock effects experienced when hitting nodules and excessively loose material. For their study, they proposed the use of a rock-melting penetration technique. However, the details and specifications of such technique were never developed for the project.

methods with the use of water to soften the caliche⁴ and lower vibration (caused by movement of aggregates), can only be considered, if at all.

Hydraulic limes offer a good option of compatibility with low impact in the reattachment of large fragments of caliche. However, further research and testing is needed.

The effectiveness of the materials and techniques to reattach large fragments of caliche should be tested in the laboratory as well as in situ in order to obtain sufficient data for future specifications. Both materials and technique performance could be tried in the existing testing walls⁵ on the site using the remaining material from the fragment that fell in 1995 from the exterior side of the west wall.⁶ Further monitoring should be carried out for a period of time to test the effectiveness of the treatment in time.

6.1.2 Recommendations on Weathering of Friable Surface

More than any other building material, the treatment of disintegration of earthen-based materials has been of great concern for conservators, engineers, archaeologists, scientists, and architects for many years. An endless list of different products, either by themselves or mixed with water or solvents, have been used as hardening chemicals for earthen structures in order to increase the water repellence and improve the mechanical properties

⁴ During cutting of caliche for testing, it was found that water softens the material reducing vibration to a minimum.

⁵ Twenty-eight testing walls were constructed at the Monument between 1977 and 1978 in order to carry on different chemical soil amendments and develop a durable overcoat mortar (Clemensen 1992, 123).

⁶ The rest of caliche from the piece that fell in 1995 is still stored at the monument.

of the soil material. The long history of water-proofing agents applied to prehistoric and historic earthen structures has been one failure after another, and the damage caused by loss of the treated surface has been often greater than that from natural weathering.

More than any other site, Casa Grande Monument has served as a field laboratory to experiment with various products for the stabilization of its resources. Experimentation with chemical preservatives occurred in the 1930s, 1940s, 1970s, and 1980s in an attempt to harden the soil material of the ruins against deterioration (Clemensen 1992, 107).⁷ All these trials resulted in failure, sometimes with disastrous consequences for the cultural resources. Fortunately, the Great House was never selected for the application of these products.

Kreigh and Sultan (1974, 1) in their study recommended the need for the formulation of a sealing chemical compound that could be sprayed and/or painted on the exposed walls of the Great House without altering their color or natural look. They specified a product resistant to sunlight, rainfall, and raindrop impact, moisture migration, wind, wind-blown sands and temperature variations.

The problem of selecting the most suitable consolidant for an specific case of earthen-based material deterioration is not easy to solve. Selection should be done on the basis of comparative weathering tests carried out in the material, and the choice of the process

⁷ A Stabilization Chronology is included in Appendix A.

should depend upon the type of material and its chemical and physical properties.

It is not the purpose of the present study to analyze and evaluate the performance of consolidation products in soil-based materials⁸ but to suggest alternative consolidation methods appropriate for the caliche from the Great House.

As demonstrated during the testing of the caliche, the friable caliche is the one lacking the calcium carbonate enriched crust formed naturally while the material was drying during construction and by exposure to repetitive wetting and drying cycles. Due to the addition of a protective roof to the Great House (1903), this natural phenomenon has been interrupted and once the crust is lost it cannot form again and deterioration could occur more rapidly. Thus, a feasible alternative of consolidation of the friable caliche would try to reproduce this natural crust in order to protect the caliche from the weathering action of wind and wind-driven rain.

The reproduction of the caliche crust could be achieved by two methods: (1) by exposure of the friable caliche to repetitive wetting and drying cycles or (2) by applying a solution of calcium carbonate using an external source so it can be deposited in the caliche pores and bind the loose particles of the material.

⁸ The results of extensive research on this topic and experiences from field applications have been published in the extensive literature of earthen-based materials and by numerous adobe conferences and seminars since the early 1970s.

The formation of a caliche crust by means of exposure of the friable caliche to wetting and drying cycles is not recommended. Such an endeavor could probably be very difficult to achieve at the site, could be very time consuming, and may be impractical due to the size of the structure. However, the main reason for not recommending this practice is because the process of crust formation by wetting and drying cycles uses a source of calcium carbonate from the inner caliche (not exposed), causing a depletion of binder from this caliche contiguous to the crust (underneath). If the processes of crust formation and crust loss happened repetitively in the same area, it might result in more rapid and deeper losses of caliche, and more deterioration.

On the other hand, the formation of a calcium carbonate enriched crust on the friable caliche using an outside source of calcium carbonate (in solution) is highly recommended to be researched as a possible method of consolidation. A similar method has been used to increase the cohesion and compressive strength of calcareous stones by saturating it with a solution of calcium hydroxide (limewater) which resulted in some success in the field.⁹ Calcium hydroxide deposits upon the surface of the pores as the solution evaporates, carbonates expand in volume, theoretically strengthening the material, both through increasing particle-to-particle cementation (cohesion) and interlocking calcium carbonate inside the pores (Fidler 1995, 52).

⁹ Consolidation of stone using a solution of calcium hydroxide (limewater) was very popular in the 19th century and probably early (Lazzarini L. and Marisa Laurenzi Tabasso 1986, 185). However, the earliest documented use of a lime-based technique used for consolidation of stone dates to 1960, when an English professor named Robert Baker formulated a group of procedures known collectively as the “Baker” or “Wells” method. This method has been used in England to treat limestone from church facades, for example the facade of Merton College Chapel in Oxford, and the facades of Wells and Exeter cathedrals.

All this experience and results could serve as the basis for future research and could lead to application of this technique in the Great House. The use of limewater in the consolidation of friable caliche could be very suitable because it would reduce the caliche's diffusivity (movement of water). This is caused not only by an increment of calcium carbonate particles in the pores of the caliche but also by the small size of the particles deposited once the water evaporates from the limewater.¹⁰

Consolidation using limewater is still widely debated as to its efficacy, largely due to the lack of penetration of the calcium carbonate. For this reason, it is necessary to carefully develop research and testing methods that would give results for the caliche.

Several aspects should be taken in consideration for future research, among the most important are: sources of limewater (use of different types of lime) and their influences, effect of temperature in the concentration of calcium hydroxide in suspension¹¹, methods of application of limewater (in the laboratory and most important in the field), methods of protecting the limewater from the atmosphere during application¹², number of applications to achieve good consolidation, and depth of the deposits.

¹⁰ Diffusivity is not only related to the amount of calcium carbonate but also to the size of its particles. The finer the particles the lower will be the diffusivity of the material. If particles of calcium carbonate are too coarse, diffusivity will be increased (Soil Resources, Management and Conservation Service. Land and Water Development Division 1979, 30).

¹¹ Limewater at 15°C contains 1.4% of calcium hydroxide in suspension. This percentage seems to slightly increase at cooler temperatures (Ashurst, 1984).

¹² When the limewater is protected from the atmosphere during application, it deposits the maximum amount of calcium hydroxide (Larson 1982, 222).

Techniques such as SEM, environmental SEM, or radioactive "tagging" of the calcium hydroxide should be considered for quantifying or recording the results from limewater application in the caliche since deposits of calcium carbonate are minute enough for detection through thin-section microscopic observations. In addition, some of the tests presented in this thesis (water drop test, water absorption by total immersion, capillary water absorption) could be applied to ascertain changes in the caliche before and after consolidation with limewater. In addition, air abrasion tests could also be used for hardness evaluation. Some caliche material or caliche debris left from the piece that fell in 1995 could be used for this testing.

Results and effectiveness obtained from limewater consolidation of the caliche should be compared with other consolidants that proved successful in the consolidation of calcareous stones or other earthen-based materials.

The consolidant selected for the caliche should be tested both under the conditions of the laboratory and at the site in order to obtain an accurate evaluation of its application and performance. Further monitoring should be carried out for a period of time to test the effectiveness of the treatment in time. At the site, it is very important to consolidate only areas that have lost the natural calcium carbonate protective crust. If proved to be satisfactory, the consolidation method could be adopted as a form of continuous maintenance by monument personnel.

6.1.3 General Recommendations

Maintenance

Like other earthen ruins, the Great House cannot survive without continuous maintenance. Therefore, its preservation requires periodic inspection and maintenance of all its protective systems. Failures in these protective systems, if detected in time, can be repaired before more aggressive decay develops. For this reason, it is very important to keep an effective maintenance plan to avoid the outbreak of deterioration processes which, unattended, can result in excessive stabilization campaigns.

Finally, the periodic inspection and maintenance of the shelter is extremely important for the Great House since a failure in the shelter can result in great damage of the structure.

Monitoring

Intermittent observations of the Great House for nearly 300 years has served to monitor the condition of the structure over time, providing the opportunity to assess the processes of deterioration that have transformed the structure from what it once was into the structure of today. The detailed material based computerized conditions survey of the walls of the Great House (completed by the University of Pennsylvania) is an important tool for monitoring the structure and for comparing its condition over one hundred years ago as well as establish a baseline for the future. For this reason, the update of the conditions surveys should continue in order to chart damage over time.

The following are possible issues for establishing a monitoring system in the future.

- The effect of salt in the mechanical properties of the caliche should be determined. Capillary rise and crystallization of soluble salts are still major dangers for the Great House, mainly with the possibility of rising of the groundwater levels in the future.
- Soil settlement due to decrease of groundwater table level. It is important to monitor if the settlement is differential.
- The groundwater table level should be measure at various times of the year and should be compared with moisture content of the wall of the structure (especially at the base of the walls). Variations in the groundwater table are likely to be involved in any gradual deterioration of the fabric.
- A wind study related to the roof (circulation of air) should be part of a monitoring plan in order to detect areas most affected by wind, therefore, more vulnerable to wind erosion. An assessment of the seriousness of erosion of the structure by wind should be carried out and the effect of the roof in enhancing or mitigating this erosion should be evaluated.
- Past stabilization treatments in the structure, especially base wall fills and bitumen floors inside the structure should be inspected and monitored. The fired-brick and cement mortar wall fills were added to the base of the walls during the stabilization of 1891-92 in an effort to improve the stability of the walls. It is necessary to monitor the performance of such fills since they could be hiding active deterioration (such as rising damp and salt crystallization). In addition, if the groundwater levels rise in the future, the fills could increase the capillary rise of the caliche walls since capillary rise

in fired-brick is much higher than in earthen-based materials (such as caliche), which in general does not surpass 30-40 cm.

- Insect and animal activity should be monitored in the Great House. In the present, birds, insects and other type of animals seem not to be a problem, probably due to changes in the area (use of pesticides, increase of urban population).
- Vibration caused by traffic, trains, machinery at the monument and by any other source should be monitored in order to analyze their effects in the stability of the walls from the Great House.

Evaluation of Earthquake Resistance

There are several basic factors which must be considered when evaluating the structural integrity of the Great House. One of these is the chemical and physical properties of the caliche from which the structure was constructed (mineral content, unit weight, compressive strength, tensile strength, coefficient of thermal expansion, and others). Besides material properties, consideration must be made of the loads which can exert forces on the structure (wind loads, seismic loads, sonic wave loads, thermal loads and gravity loads). This information must be combined with the structural shape, size of walls and wall interlocking to complete an evaluation of the structural integrity of the Great House (Kreigh and Sultan 1974, 15). Also, as Wilcox and Shenk (1977, 210) suggested, a stress analysis of the Great House should be completed.¹³

Human-related Activity

Casa Grande Ruins National Monument can no longer be considered an island preserve

¹³ This is currently underway by King, Eric Johansen and Roy Wilson.

but part of a fast growing area where changes are happening more rapidly than during the previous centuries. As part of a large context, the monument must be studied and considered as such. Therefore, any changes to the context in which the monument exists will produce changes in its resources. Large, medium and small development plans for the area should consider the possible impacts to the Great House as well as to the rest of the cultural resources of the monument and its plant and animal life. Protection of the natural resources of the monument should be as important as the protection of its cultural resources since both share and interact in the same environment and influence each other.

6.2 Conclusions

Hayden (1957) determined that caliche was the material used in the construction of the Great House. Caliche refers to accumulations of authigenic carbonate common in soils of arid regions, where the accumulation forms prominent layers in which the morphology is determined by the impregnating carbonate (Gile et al., 1965, p. 74).

Caliche was obtained from borrow areas and then processed and puddled in caliche mixing bowls (Hayden, 1942, 1957). By breaking up the natural caliche, and puddling it, the Prehistoric builders of the Great House were able to improve, in the form of walls, the natural properties of this particular soil.

Many speculations in relation to the construction techniques used in the Great House have been made since it was first viewed by Europeans during the seventeenth century. Most implied the use of forms in the construction. However, Wilcox and Shenk (1977) finally proved that no forms were involved and that, a system best described as “English cob” was used instead. This system involves the construction of wall courses by piling portions of moist caliche and compressing them into place. Each course is left to dry until the next is applied.

The caliche from the Great House was first analyzed by Cook in 1879, who proved content of calcium carbonate in the soil. Since then, scientific studies of the caliche have been carried out by Littman (1967), Vick (1973), Kreigh and Sultan (1974) Wilcox and Shenk (1977), O-Bannon (1978), and Roy (1980).

The present characterization was performed on a fragment that fell from the west elevation of the structure in 1985. An extensive testing program (ASTM, NORMAL) using various analytical techniques (Microscopy, SEM, XRD) was put together to analyze the caliche both as a soil and as a solid material. Different samples coming from different areas of the caliche fragment were tested in order to compare any physical and/or chemical changes.

The caliche from the Great House is composed of a combination of gravel, sands, silt and clay cemented by calcium carbonate. In addition, a high percentage of nodules or

concretions of calcium carbonate of different sizes and shapes were found as the main component of the coarse particles of the caliche. Therefore, calcium carbonate is naturally present in the caliche in two forms: as binder of the caliche fabric (fine particles) and also binding various particles of different sizes and shapes to form calcic nodules. These probably play a very important role in the caliche as construction material, as does gravel in concrete.

The caliche from the Great House has developed a calcium carbonate enriched crust on its exposed surface and a calcium carbonate depleted area located immediately behind the crust (20-30cm deep). Surface crusting is a quality of calcareous soils which is related to both chemical reaction of carbonates with water and water movement in the soil. Water, either migrating through the material during drying or from exterior sources, changes the cementing media of the caliche. Thus, the caliche loses some of its calcium carbonate which being dissolved, is transported to the surface, and then during evaporation is precipitated. Accordingly, close to the outer surface the pores are gradually filled with calcium carbonate at the expense of internal depletion and weakening. In this manner, the crust containing calcareous matter develops only on the exposed side (exterior of the structure). The relocation of material from inside the caliche outward changes its density, porosity and strength. Hence, an increment of calcium carbonate content in the form of very fine particles within capillary tubes of the caliche has reduced the difussivity (water movement) of the material. This caliche proves to have a high resistance to water, wet/dry cycles, relatively low capillary water absorption, and shows controlled shrinkage.

Conversely, the zone of caliche that suffered impoverishment of calcium carbonate shows more shrinkage, high porosity (capillary water absorption), friability and low strength. This material had very low resistance to water impact, wet/dry cycles, and capillary water absorption.

Physical and chemical changes in the caliche have produced differential weathering of the material when exposed to the action of various processes of deterioration. Thus, the calcium carbonate-enriched zone has functioned as a protective crust more resistant to water and wind erosion due to its highly cemented condition. This exposed caliche has only been subject to deterioration caused by mechanical breakup (cracks). On the other hand, interior carbonate-depleted zones have been greatly affected by water (dissolution) and wind abrasion combined with other processes of deterioration.

However, differential deterioration is not only due to physico-chemical changes in the caliche. Other intrinsic causes of deterioration are construction-related (internal flaws of the material) combined with roof removal. In addition, the large size of the structure and the great thickness of its walls have produced differential exposure of the caliche according to location (wall core vs. outer wall area; exterior walls vs. interior walls). Extrinsic deterioration has been responsible for aggravating existing intrinsic problems resulting in the various detachment of fragments and cracking of the Great House.

Site observations based on patterns of deterioration, along with results obtained from the wall conditions survey and the present characterization of the caliche have provided additional data in wall course construction and construction sequence of the Great House. Such findings have allowed interpretation of the interpret the differential deterioration of the structure, especially in relation to the large fragment detachments that have been happening from various wall courses.

Various preliminary recommendations, mainly toward alleviating the deterioration of the caliche, have been developed in order to be the subject for future studies of the caliche from the Great House. General recommendations have also been included in order to help direct the management of the structure in the future.

In conclusion, a combination of intrinsic factors (manufacture/manipulation techniques of the caliche, construction methods and physico-chemical transformations of the caliche) with natural and human-related processes of deterioration have been responsible for the differential weathering and present deterioration phenomena of the Great House.

BIBLIOGRAPHY

- Alva Balderrama, Alejandro and Jeanne Marie Teutonico. "Notes on the Manufacture of Adobe Bricks for the Restoration of Earthen Architecture", *Adobe: International Symposium and Training Workshop on the Conservation of Adobe, Lima-Cuzco, Peru, 10-22 September 1983*, Rome: UNDP/UNSECO/ICCROM, 1983, 41-54.
- American Geological Institute. *Glossary of Geology and Related Sciences*, Washington DC.: American Geol. Inst., 1957.
- Annual Book of ASTM Standards (1993)*. (Various volumes). Philadelphia: ASTM, 1993.
- Architectural Conservation Laboratory, Graduate Program in Historic Preservation, University of Pennsylvania. *Wall Condition Documentation and Assessment*, Casa Grande Ruins National Monument, Coolidge, Arizona, 1997-98 (unpublished).
- Aristarain, L. F. "Chemical Analyses of Caliche Profiles from the High Plains, New Mexico", *Journal of Geology*, v. 78, 1970, 201-212.
- _____. "Clay Minerals in Caliche Deposits of Eastern New Mexico", *Journal of Geology*, v. 79, 1971, 75-90.
- Ashurst, John. "The Cleaning and Treatment of Limestone by the "Lime Method". Part I. *Monumentum*, Vol. 27, No. 3, September, 1984.
- Bates, Robert L. and Julia A. Jackson. *Glossary of Geology*. Second Edition, Falls Church, Virginia: American Geological Institute, 1980.
- Beckwith, G. H. and L. A. Hansen. "Calcareous Soils of the Southwestern United States". *Geotechnical Properties, Behavior, and Performance of Calcareous Soils*, K. R. Demars, The University of Connecticut and R. C. Chaney, Humboldt State University editors, Philadelphia: ASTM Special Technical Publication 777, 1981, 117-35.
- Blake, W. P. "The Caliche of Southern Arizona. An Examination of Deposition by Vadose Circulation, *Trans. Amer. Inst. Min. Met Eng.*, v 31, 1902, 220-226.
- Blatt, Harvey and Robert Tracy. *Petrology. Igneous, Sedimentary, and Metamorphic*, Second Edition, New York: W. H. Freeman and Company, 1996.
- Brady, Nyle C. and Ray R. Weil. *The Nature and Properties of Soils*. Eleventh edition, New Jersey: Prentice Hall, 1996.

- Brewer, R. "The Basis of Interpretation of Soil Micromorphological Data", *Geoderma*, v. 8, 1972, 81-94.
- Brown, C. N. "The Origin of Caliche on the Northeastern Llano Estacado, Texas", *Journal of Geology*, v. 64, 1956, 1-15.
- Browne, J. R. *Adventures in the Apache County, a Tour Through Arizona and Sonora, 1864*, Tucson, Arizona: University of Arizona Press, 1974.
- Bullock, P. N. Fedoroff, G. Stoops, A Jongerious, and T. Tursina. *Handbook for Soil Thin Section Description*, Wolverhampton, UK: Waine Research Publications, 1985.
- Burton, R. J., N. E. Knoob, M. Shrock, C. D., Spears, and C. Phinney. *1972 Excavations at Pueblo Grande, Arizona U:9:1 (PGM), A report on Caliche Pits at Pueblo Grande*, Phoenix, Arizona: Pueblo Grande Museum, 1972.
- Chaney, R. C., S. M. Slonim, and S. S. Slonim. "Determination of Calcium Carbonate Content in Soils." *Geotechnical Properties, Behavior, and Performance of Calcareous Soils*. K. R. Demars, The University of Connecticut and R. C. Chaney, Humboldt State University editors, Philadelphia: ASTM Special Technical Publication 777, 1981, 3-15.
- Chapman, R. W. "Climatic Changes and the Evolution of Landforms in the Eastern Province of Saudi Arabia", *Geol. Soc. America Bull.*, v. 82, 1971, 2713-2728.
- _____. "Calcareous Duricrust in Al-Hasa, Saudi Arabia". *Geol. Soc. America Bull.*, v. 85, 1974, pp. 119-130.
- Charola, A. Elena. *HSPV 656 - Advanced Architectural Conservation. Laboratory Notes*. Graduate Program in Historic Preservation, University of Pennsylvania: Spring 1997 (unpublished).
- Chronic, Halka. *Roadside Geology*, Missoula: Mountain Press Company, 1983.????
- Clemensen, Berle A. *A Centennial History of the First Prehistoric Reserve: 1892-1992*. Washington DC.: United States Department of the Interior, National Park Service, 1992.
- Contreras, W. E. "Restauraciones en Casas Grandes", 1969-70, Mexico, *INAH Bulletin* 40, 1970, 4-11.
- Corominas, J. *Diccionario Crítico Etimológico de la Lengua Castellana*, Bern, Switzerland: Franke, Ed., 1954.

- Coues, E. *On the Trail of a Spanish-Pioneer: The Diary and Itinerary of Francisco Garces in His Travels Through Sonora, Arizona, and California 1775-1776*, Vol. 1, New York: Francis P. Harper, 1900, 92.
- Courty, Marie Agnes, Paul Goldberg, and Richard Macphail. *Soils and Micromorphology in Archaeology*, Cambridge: Cambridge University Press, 1990.
- DiPeso, C. C., J. B. Reinaldo, and G. J. Fenner. *Casas Grandes, a Fallen Trading Center of the Gran Chichimeca*, Vol. 4, Flagstaff, Arizona: Northland Press, 1976.
- Douline, A. *Batiments en Vouter et Compoler en Adobe, Niger*. Memoire de CEEA-Terre, CRATerre-EAG, Grenoble, France: CRATerre, 1990.
- Durand, J. H. "Essai de Nomenclature des Croûtes", Tunisia, *Soc. Des Sciences Naturelles de Tunisie*, Bull. 3-4, 1949, pp. 141-142.
- _____. *Etude Geologique, Hydrogeologique et Pedologique des Croûtes en Algerie*, Algeria: Algerie Direction du Service de la Colonisation et de l'Hydraulique Clairbois-Birmandreis, 1953.
- _____. *Les Sols Ronges et les Croûtes Calcaires en Algeria*, Algeria: Direction du Service de la Colonisation et de l'Hydraulique Clairbois-Birmandreis, 1959.
- _____. "Les Croûtes Calcaires et Gypsenses en Algerie: Formation et Age" France, *Soc. Geol. France Bull.* Ser. 7, v. 5, 1963, pp. 959-968.
- Emory, W. H. *Notes of a Military Reconnaissance from Fort Leavenworth, in Missouri, to San Diego, in California, including parts of Arkansas, Del Norte, and Gila rivers*, Washington DC.: 30th Congress, 1st Session, (House) Ex Doc 41, 1848.
- Engelhardt, Wolf, v. *Sedimentary Petrology. Part III. The Origin of Sediments and Sedimentary Rocks*, Stuttgart, Germany: Schweizerbart'sche Verlagsbuchhandlung (Nagele u. Obermiller), 1977.
- Fairbridge, R. W. "Climatology of a Glacial Cycle", *Quaternary Research, A Review Volume for the 7th Congress of the International Association for Quaternary Research*, 1977, 283-302.
- Feld, J. "Soil Mechanics and Foundations". *Building Construction Handbook*. Second edition, edited by F. S. Merritt,. New York: McGraw-Hill, 1965.
- Fewkes, J. W. "Excavations at Casa Grande, Arizona, in 1906-1907." *Smithsonian Miscellaneous Collections*, Washington DC.: Smithsonian Institution 50, 289-329, 1907.

Casa Grande, Arizona. 28th Annual Report of the Bureau of Ethnology, 1906-07, Washington DC.: National Park Service, 1912.

Fidler, John. "Lime Treatments: Lime Watering and Shelter Coating of Friable Historic Masonry" *The Association for Preservation Technology* (Bulletin) Vol. XXVI No. 4, 1995, 50-55.

Fielden, Bernard M. *Conservation of Historic Buildings*. Bury St. Edmunds, Suffolk, Great Britain: St. Edmundsbury Press Ltd., 1994.

Foth, Henry D. *Fundamentals of Soil Science*. New York: John Wiley and Sons, 1990.

Frye, J. C., H. D. Glass, A. B. Leonard, and D. D. Coleman. *Caliche Development and Clay Mineral Zonation of the Ogallala Formation in Central-eastern New Mexico*, New Mexico: Bureau of Mines and Mineral Resources Circ. 144, 1974.

Gardner, L. R. *The Quaternary Geology of the Moapi Valley, Clark County, Nevada*, Ph.D. Dissertation, Pennsylvania State University, University Park, PA., 1968.

Gile, L. H. "A Classification of Ca Horizons in Soils of a Desert Region, Dona Ana County, New Mexico", *Soil Sci. Soc. America Proc.*, v. 25, 1961, 52-61.

Gile, L. H. "Soils of An Ancient Basin Floor Near Las Cruces, New Mexico", *Soil Science*, v. 103, 1967, 262-276.

Gile, L. H., E. F. Peterson, and R. B. Grossman. "The K-horizon: A Master Soil Horizon of Carbonate Accumulation", *Soil Science*, Vol. 99, No.2, 1965, 317-60.

"Morphological and Genetic Sequences of Carbonate Accumulation in Desert Soils", *Soil Science*, v. 101, 1966, 347-360.

Gile, L. H. and J. W. Hawley. "Periodic Sedimentation and Soil Formation on an Alluvial Fan Piedmont in Southern New Mexico" *Soil Sci. America Proc.*, v. 30, 1966, 261-268.

Gillete, H. S. "Soils Tests Useful in Determining Quality of Caliche", *Public Roads*, v. 15, 1934, 237-242.

Goudie, A. S. "The Chemistry of World Calcretes Deposits", *Journal of Geology*, v. 80, 1972, 449-463.

Duricrusts in Tropical and Subtropical Landscapes, Oxford, England: Clarendon Press, 1973.

Graduate Program in Historic Preservation, University of Pennsylvania. *Condition Assessment Definitions*. Winter Field School, Casa Grande Ruins National Monument, Coolidge, Arizona, December 1996-97, 3 (unpublished).

Hanks, Henry Garber, "Casa Grande", *Californian* 2 (August 1880), 101-106.

Harrison, R. S. "Caliche Profiles of Barbados (West Indies). Processes, Products, and Controlling Parameters", *Geol. Soc. America abstracts*, 1973, 653.

_____. *Near-surface Subaerial Diagenesis of Pleistocene Carbonates, Barbados, West Indies*. Ph.D. Dissertation, Brown University, 1974.

Hayden, J. D. "Plaster Mixing Bowls", *American Antiquity*, 7 (4), 1942, 405-407.

_____. "Excavations, 1940 At University Indian Ruin, Tucson, Arizona", *Southwestern Monuments Association, Technical Series*, Vol. 5. Gila Pueblo, Globe, Arizona, 1957.

Head, K. H.. *Manual of Soil Laboratory Testing, vol. 1, Soil Classification and Compaction Tests*, London: Halstead Press, 1992.

Hennessy, J. T., R.P. Gibbens, J. M. Tromble, and M. Cardenas. "Water Properties of Caliche", *Journal of Range Management: A publication of the Society for Range Management*, v. 36, no. 6, (November, 1983), 723-726.

Hinton, Richard J. *The Hand-book to Arizona: Its Resources, History, Towns, Mines, ruins and Scenery*, Tucson, Arizona: Arizona Silhouettes, 1954.

Houben, Hugo and Hubert Guillaud. *Earth Construction*, London: Intermediate Technology Publications, 1994.

Jerome, Pamela. "Proposed Permanent Shelter for Building 5 at the Bronze Age Site of Palaikastro, Crete", *Conservation and Management of Archaeological Sites*, Volume 1, Number 1, 1995, 35-42.

Johansen, G. Eric. *Report Concerning Calculations of the Casa Grande Project*, E. T. Techtonics: P. O. Box 40060, Philadelphia, PA. 19106, 1998 (unpublished).

Judd, Neil M. *Archaeological Investigations at Paragonah, Utah*, Washington DC.: Smithsonian Miscellaneous Collections 70(3):1-22 and pl., 1919.

Kidder, Alfred Vincent. *Pecos, New Mexico: Archeological Notes*, Papers of the Robert S. Peabody Foundation, vol. 5, 1958.

- Kriegh, James D. and Hassan A. Sultan. *Feasibility Study in Adobe Preservation. Casa Grande National Monument and Fort Bowie National Historic Site*, Tucson, Arizona: College of Engineering, The University of Arizona, 1974.
- Larson, J. H. "A Museum Approach to the Techniques of Stone Conservation", *Proceedings of the Fourth International Congress on the Deterioration and Preservation of Stone Objects*, K. L. Gauri, J. A. Larson, and J. H. Gwinn. Louisville, KY, July 7-9, 1982. University of Louisville: KY., 1982, 219-237.
- Lattman, Laurence H. "Weathering of Caliche in Southern Nevada", *Geomorphology in Arid Regions. A Proceedings Volume of the Eighth Annual Geomorphology Symposium, State University of New York at Binghamton, September 23-24, 1977*. Fort Collins, Colorado: Donald O. Doehring editor, 1977, 221-231.
- Lazzarini Lorenzo and Marisa Laurenzi Tabasso. *Il Restauro della Pietra*, Padova: CEDAM, Casa editrice dott. Antonio Milani, 1986.
- Lintz, Christopher. "Experimental Thermal Discoloration and Heat Conductivity Studies of Caliche from Eastern New Mexico". *Geomorphology: An International Journal*, Volume 4, Number 4, (New York: John Wiley and Sons, Inc.), 1989, 319-346.
- Littmann, E. R. n.d. Southwestern Mortars and Plasters from Casa Grande, Moctezuma Castle and Walnut Canyon, CAGR: 571 LI Box., WACC: Arch. 913.08 U5a no.3, Tucson, Arizona, 1967.
- Luenlaad, D. J. and M. H. B. Hayes, ed. *The Chemistry of Soil Constituents*, New York: John Wiley and Sons, 1978.
- McFadden, L. B. and J. C. Tinsley. "Rate and Depth of Pedogenic-Carbonate Accumulation in Soil: Formulation and Testing of a Compartment Model", *Geological Society of America*, Special Paper 203, 1985.
- McGeorge, W. T. "Studies of Soil Structure: Some Physical Characteristics of Puddled Soils.", *Agricultural Experiment Station Technical Bulletin 67*, Tucson, Arizona: University of Arizona College of Agriculture, 1937.
- Mindeleff, C. "Casa Grande Ruin", *13th Annual Report of the Bureau of American Ethnology*, Washington DC.: National Park Service, 1896, 289-319.
- Moquin, Michael. "From Bis Sá Ani to Picuris. Early Adobe Technology of New Mexico and the Southwest", *Traditions. The Adobe Journal*, Issue 8, Winter 1992, 10-27.

- Multer, H. G. and J. E. Hoffmeister. "Subaerial Laminated Crusts of the Florida Keys". *Geol. Soc. America Bull.*, v. 79, 1968, 168-169.
- Munsell Soil Color Charts*. Baltimore, MD: Macbeth Division of Kollmorgen Instruments Corp., 1988.
- Musick, Steven P. *The Caliche Report. Second Edition. The Distribution and Use of Caliche as a Building Material*, Austin, Texas: Center for Maximum Potential Building Systems, 1979.
- Nesse, William D. *Introduction to Optical Mineralogy*, Second Edition. New York: Oxford University Press, 1991.
- Netterberg, F. "Some Roadmaking Properties of South African Calcretes", *Proceedings of the 4th Regional Conference in Soil mechanics and Foundation Engineering, Cape Town, South Africa*, 1967, 77-81.
- _____. "The Interpretation of Some Basic Calcrete Types", South Africa, *South African Arch. Bull.*, v. 24, 1969, 117-122.
- _____. "Calcrete in Road Construction". South Africa: *Natl. Inst. Road Research Bull.* 10, 1971, 73.
- Pinkley, E. T. *Casa Grande, The Greatest Valley Pueblo of Arizona*, Tucson, Arizona: Arizona Archaeological and Historical Society, 1926.
- Pinkley, F. and E. T. Pinkley. *The Casa Grande National Monument in Arizona*. Tucson, Arizona: Arizona State Museum Library, University of Arizona, 1931.
- Pomel, A. and J. Pouyanne. *Texte Explicatif de la Carte Geologique au 1:800,000 des Provinces d'Alger et d'Aran, Algeria*, 1882.
- Price, W. A. "Reynosa Problem of South Texas, and Origin of Caliche", *American Association Petroleum Geologists Bulletin*, v. 17, 1933, 488-522.
- _____. "Sedimentology and Quaternary Geomorphology of South Texas". *Trans. Gulf Coast Assoc. Geol. Soc.*, 1958, 47-75.
- Real Academia Española. *Diccionario de la Lengua Española*, Madrid, Spain: Real Academia Española, 1956.
- Reeves, C. C. Jr. "Relations of Caliche to Small Natural Depressions, Southern High Plains, Texas and New Mexico", *Geological Society of America Bulletin*, v. 82, 1971, 1983-1988.

-
- Caliche. *Origin, Classification, Morphology and Uses*. Lubbock, Texas: Estacado Books, 1976.
- Roy, D. M. *Longevity of Borehole and Shaft Sealing Materials: Characterization of Cement-Based Ancient Building Materials*, University Park, Pennsylvania: Pennsylvania State University, 1980.
- Schlesinger, William H. "Carbon storage in the caliche or arid soils: a case study from Arizona", *Soil Science*, Vol. 133, No. 4, April 1982, 247-255.
- Sehgal, J. L. and G. Stoops. "Pedogenic Calcite Accumulation in Arid and Semi-Arid Regions of the Indo-Gangetic Alluvial Plain of Erstwhile Punjab (India). Their Morphology and Origin", *Geoderma*, v. 8, 1972, 59-72.
- Soil Resources, Management and Conservation Service Land and Water Development Division. *Soil Survey Investigations for Irrigation*, Rome: Food and Agriculture Organization of the United Nations, 1979.
- Stanley Price, Nicholas. *Conservation on Archaeological Excavations*, Rome: ICCROM, 1984.
- Stambolov, T. and J. R. J van Asperen de Boer. *The Deterioration and Conservation of Porous Building Materials in Monuments. A Review of the Literature*. Rome: International Centre for the Study of the Preservation and the Restoration of Cultural Property, 1976.
- Steel, R. J. "Cornstone (Fossil Caliche). Its Origin and Some Features of Its Stratigraphic and Sedimentological Importance in the New Red Sandstone Rocks of Western Scotland", *Journal of. Geology*, v. 82, 1973, 351-369.
- Steen, Charlie R. "Excavations in Compound A, Casa Grande National Monument, 1963", *Kiva* 31 (December 1965), 59-82.
- Stoops, Georges and Hari Eswaran. *Soil Micromorphology*. New York: Van Nostrand Reinhold Soil Science Series, 1986.
- Strakhov, N. H. *Principles of Lithogenesis, Vol. 3*. New York: Plenum Pub. Co., 1970.
- Stubbs, Stanley and W. S. Stallings. *The Excavation of Pindi Pueblo, New Mexico*, Santa Fe, New Mexico: Archaeological Institute of America, School of American Research Monographs No. 18, 1953.

- Teutonico, Jeanne Marie Teutonico. *A Laboratory Manual for Architectural Conservators*, Rome: ICCROM, 1988.
- Theis, C. V. "Possible Effects of Ground Water in the Ogallala Formation of the Llano Estacado, Texas", *Washington Academy of Science Journal*, v. 26, 1936, 390-392.
- The Oxford Encyclopedic English Dictionary*. Second Edition, Edited by Judy Pearsall and Bill Trumble. New York: Oxford University Press, 1995.
- Thompson, M. W. *Ruins. Their preservation and display*, British Museum Publication: London, 1981.
- Twenhofel, W. H. and Tyler, S. A. *Methods of Study of Sediments*, McGraw-Hill, New York, 1941.
- Torroca, Giorgio. *Porous Building Materials*, Rome: ICCROM, 1988.
- UNESCO: International Centre for the Study of the Preservation and the Restoration of Cultural Property, Rome. *Preservation of the Monument of Mohenj Daro, Pakistan*, Prepared for UNESCO, 1964.
- United States Department of Agriculture. *Soil Taxonomy: A basic system of Soil Classification for Making and Interpreting Soil Surveys*, Washington DC: U. S. Dep. Agricultural Handbook 436, 1975.
- United States Department of Agriculture, Soil Conservation Service in Cooperation with Arizona Agricultural Experiment Station. *Soil Survey of Pinal County, Arizona, Western Part*, Washington DC: National Cooperative Soil Survey, United States Department of Agriculture, 1991.
- Van Heuvel, R. C. "The Occurrence of Sepiolite and Attapulgit in the Calcareous Zone of a Soil Near Las Cruces, New Mexico", *13th National Conference on Clays and Clay Minerals*, Proc., Oxford, England: Pergamon Press 1966, 193-207.
- Van Valkenburgh, Sallie. "The History of Casa Grande Ruins National Monument", *The Kiva* 27 (February 1962), 10.
- Vick, E. L. *Investigation and Study of Materials*, Tucson, Arizona: Southern Arizona Testing Laboratory, 1973.
- Ward, W. C., R. L. Folk, and J. L. Wilson. "Blackening of Eolianite and Caliche Adjacent to Saline Lakes, Isla Mujeres, Quintana Roo, Mexico, *Journal of Sedimentary Petrology*, v. 40, 1970, 548-555.

- Weider, M and D. H. Yaalon. "Effect of Matric Composition on Carbonate Nodule Crystallization", *Geoderma*, v. 11, 1974, 95-121.
- Western Soil and Water Research Committee. *Soils of the Western United States*, Washington State: Washington State University, 1964.
- Wilcox, David R. "The Relationship of Casa Grande Ruin to Compound A: Research Potential of the In Situ Deposits", *Arizona State Museum Archaeological Series* 83, Tucson, Arizona: University of Arizona, 1975a.
- Wilcox, David R. and Lynette O. Shenk. *The Architecture of the Casa Grande and Its Interpretation*, Tucson, Arizona: Arizona State Museum, University of Arizona, 1977.
- Wilcox, David R. and Charles Sternberg. *Additional Studies of the Architecture of the Casa Grande and Its Interpretation*, Phoenix, Arizona: Archaeological Series No. 146, 1981.
- Winkler, E. M. "Effect of Case Hardening in Stone.", *Deterioration and Conservation of Stones. Proceedings of the Third International Congress, Venice 24-27 of October, 1977*. Venice, Italy, 1979, 55-63.
- Young, Raymond N. and Benno P. Warkentin. *Soils Properties and Behavior*, New York: Elsevier Scientific Publishing Company, 1975.

Appendix A: Previous Scientific Projects and Stabilization on the Great House and Casa Grande Ruins National Monument¹

1879: First real scientific investigation of the ruins led by Henry Hanks and a group of New Jersey geologists including professor George Cook. Cook took samples from the Great House for analysis of calcium carbonate content. The results obtained showed the content of 17% calcium carbonate.

1889: Alexander L. Morrison of the Santa Fe Division of the General Land Office made an inspection and report on repairs and protection of the ruins. He concluded that vandalism, natural weathering, and wall undermining were the main dangers to the ruins. Morrison's recommendations were: 1) brick pinning of the walls, 2) addition of a shelter, 3) removal of debris from the entire building, and 4) construction of a fence around the monument.

1890: Victor and Cosmos Mindeleff made a report on the ruins. Their recommendations were very similar to Morrison's. However, visitors were added as a main cause of deterioration of the Great House. Cosmos Mindeleff's final recommendations included: 1) brick pinning of walls, 2) removal of material from top of walls and cap them with

¹ Condensed from: Clemensen, Berle A. *Casa Grande Ruins National Monument, Arizona: A Centennial History of the first Prehistoric Reserve, 1892-1992* (1992); Van Valkenburgh, Sallie. *The History of Casa Grande Ruins National Monument* (1962); Kriegh, James D. and Hassan A. Sultan. *Feasibility Study in Adobe Preservation. Casa Grande National Monument and Fort Bowie National Historic Site* (1974).

concrete, 3) reinforce the structure with tie rods and beams, 4) replace broken and missing lintels, and fill cavities above lintels. Mindeleff included a plan of a roof for the Great House. In December 1890, Cosmos Mindeleff completed the first most detailed survey of the Great House (elevation, floor plans, height of debris accumulation inside the structure. Mindeleff thought that much of the damage of the Great House came from treasure hunters. He also observed that the northeast and southeast corners of the structure had fallen and portions of the south wall were unstable and likely to fall. He thought that most of the destruction of the walls occurred at ground level, caused by capillary action.

1891: The contract for stabilization work on the Great House was given to Theodore Louis Touffer and Frederick Emerson White of Florence. The repairs were completed in 4 months. The repairs included: brick pinning of wall bases and largest lower wall holes, cement stucco over brick repairs, replacement of lintels above openings and filling of cavities above them, installation of three interior braces: a wooden tie beam across full length of structure and two iron tie rods across width of Tier E.

1892-99: Whittemore mentioned several times the need of a roof to protect the walls, specially from the upper story. He asked for funds to fence 40 acres of the monument.

1901: Custodian H. B. Mayo requested a roof for the structure, concrete patchwork in crumbled or undermined portions of the walls and a fence for better security.

1902: Custodian Frank Pinkley requested a need of repairs for the Great House. He identified 5 openings with missing lintels, three large cavities that required brick and mortar fill and the ruins to the south and to the east of the Great House needed underpinning.

1903: S. J. Holsinger inspected the Great House. He secured the necessary data for a shelter design. He stated that no more brick or concrete should be used on the ruins and proposed that any future stabilization and repairs should be done with as much original material as possible (caliche). Holsinger instructed Pinkley to make a mixture from the debris and apply it to several cracks. According to Holsinger the effort was a success. He also indicated a source for future repairs, a stratum of caliche similar to the original located at 7-8 feet below ground level. Holsinger also proposed the use of reservation's mesquite to replace lintels.

Holsinger designed a shelter for the Great House. It had galvanized corrugated iron roof with a 6 feet overhang set on redwood posts. W. J. Corbett from Tucson was awarded the contract of the roof on June 22, 1903.

1906-1908: Walter Fewkes from the Bureau of Ethnology arrived to the monument to conduct an inspection of the roof. He excavated Compound A, including Center Building located at southwest corner of the Great House, which previously looked like a mound of debris. He also installed the drainage system of Compound A and stabilized walls with soil and cement.

1926: Custodian James Polk Bates' annual report express that locals have constantly been removing mesquite for wood and fence post construction. Another problem he mentioned was the cattle and horses left to graze all over the reservation. Bates asked for a fence
First roof is damaged on west side and patched with a lighter material. Bates recommended a new galvanized iron roof for the Great House because the existing one had holes in it.

1927-1928: Jackson applies new stucco over original stucco applied to brickwork by Mindeleff.

1932: Congress appropriated money to construct a new shelter roof over the Great House. On September 19, 1932 the old shelter was removed and a temporary and a temporary shelter was constructed over the Great House to protect it during construction of the new roof. The second (current) shelter was completed on December 12, 1932.. The east and north boundaries of the Monument were fenced.

1931-1935: During this period a new emphasis was placed on finding a material capable of permeating the surface of the caliche walls and provide resistance to erosion instead of capping or stuccoing the walls. Several products were tested both in the laboratory and the field, however, none of them proved to be successful.

The west and south boundaries of the monument were fenced. Compound A was graded to facilitate proper drainage, and concrete curtain walls were built at the bases of some walls in the compound.

1935-1943: During this period an attempt of forming a moisture barrier around and under the walls was made by digging trenches and waterproofing with cement stabilized soil plaster in Compound A. The results were not encouraging in both efforts.

1940: Water continued to be a problem in the 1940s. Water table started to drop rapidly due to the drilling of a large number of irrigation wells.

Monitoring equipment was installed for the first time in the Great House during the summer of 1940. Brass rods were installed across corners of the building to monitor wall movement (these were later removed [n. d.]). Monel metal rivets were installed in the tops of the center walls of the structure to measure wind erosion.

1946: R. Gordon Vivian supervised Charlie Steen in treating caliche blocks and walls with different water repellents (not on the Great House) at the monument. In order to use methods of application in the interior of the block wall he tried to drill holes in the caliche, but frequently the blocks would break due to aggregate movement caused by vibration while drilling. Several materials were including waxes, oils, silicates, and emulsified asphalt were tested. The results were generally not encouraging or successful.

1948: Steen began stabilization work on Compound A. He tried to remove all previous wall capping and replaced them with a 2 inch thick caliche cap. After drying, the caliche caps cracked so Steen brushed them with a caliche grout using a straw broom. He successfully filled the cap cracks.

A. T. Bricknell settled for stabilizing the Great House floors by using a caliche base with a top finish of bituminous oil. The work was done by CCC workers and it was completed in September 1948.

1955: John Davis, General Superintendent of the Southwestern Monuments, reported that despite the shelter protection, the upper are of the Great House had continued to crumble and the wind-exposed side had suffered from wind erosion caused by blown sand. He requested to enclose the ruins with steel reinforced plastic or glass.

1956: Vivian and Richert removed concrete steps from north doorway and filled the lower part of the opening.

1958: Funds to stabilize Compound B were approved. Vivian and Richert decided to preserve the walls by enclosing them with new walls. For the stabilization, they use a mixture of caliche and concrete, which they poured in forms. The caliche came from a Coolidge Sand and Rock Company pit about 5 miles east of the monument. After the forms were removed, they sprayed the new walls with Daracone. Impression marks left by the forms were removed not until 1972.

1960-1963: Richert inspected previous work. He felt that the hand-mixed, concrete-stabilized soil used for a veneer in Compound A walls in 1955 was not holding up as well as that produced in a cement mixer the following year. Consequently, he thought that area should be replaced in 1962. Both Compound A and Compound B walls needed to be sprayed with another covering of Daracone.

The asphalt floor in the Great House needed to be replaced.

Gordon Vivian experimented on a part of a wall (no location specified) with an electro-chemical soil hardening technique. It seems that the experiment proved a failure.

In 1963, Vivian sprayed 34 gallons of “Texas Refining Company” sand and adobe preservative on both sides of the largest east-west wall of Compound B. This epoxy solution darkened the wall and formed a glaze which continued to look wet although it had set up very hard.

1967: A major stabilization project focused on Compound A with some work done on Compound B. Martin Meyer performed maintenance work on all walls and buildings including the Great House. He patched and/or replaced disintegrated soil-cement caps and veneer on all walls and treated them with silicone. In the Great House, Meyer plastered the lintels over seven doorways, replastered loose and missing concrete stucco on the structure’s base, and repaired minor breaks and holes and walls in walls. A new product Daraweld-C, was mixed with the soil-cement to help new patches bond better. In

Compound B Mayer sprayed silicone on the compound walls and stabilized rooms 3 and 4.

1969-70: During the winter of 1968-69 a caliche fragment fell in the north room. In 1969, Meyer inspected the room and repaired sections of the walls. The next year, he stabilized an upper pair of holes in the east room, as well as the cracks at the top of the walls. Mayer also rebuilt the east doorway and recess stairs of the east room.

1972: W. E. Sudderth came to Casa Grande to continue with the stabilization work. He patched cracks in the compound walls and a number of rooms of Compound A. Sudderth experimented with different finishes on walls to find one that would harmonize with the Great House for uniformity of color and texture. He used a commercial product called Daraweld-C mixed with caliche and sand to produce an "Ammended Mud" which then applied to the ruin walls with whisk brooms. This treatment is still current at the monument (every 2 years).

Late this year, the structural stability of the Great House came into question. It was feared that entire wall sections could collapse. A contract was given to James Kriegh and Hassan A. Sultan of the University of Arizona, College of Engineering to study the Great House walls. Their study extended through 1973-74. They were to evaluate the stability of the Great House walls, and study and assess techniques to stabilize and maintain structural integrity.

1973: Compound B was backfilled.

The interior access to the Great House was closed. It has never been re-opened to the public.

Field Applications of chemicals on caliche walls of Compound B by Kreigh and Sultan.

Nine chemicals were selected for field application in order to provide a moisture barrier to caliche. Each chemical was mixed separately and poured through a hose onto the wall surface until saturation (run off). Treated wall surface was exposed from 15 months, between August 73 and November 74.

1974: Kreigh and Sultan found that the walls of the Great House were unsafe since they were not tied together. They believed that an earthquake represented the greatest danger to the structure. Consequently, they thought that the Great House needed both vertical and horizontal ties to improve its structural integrity. They recommended that pipes be placed in vertical holes drilled through the walls after which each pipe and hole would be filled with epoxy. The additional pipes would make the building more rigid. Kreigh and Sultan were also asked to find or formulate a sealing chemical which could either be sprayed or painted on the walls. They tested 20 chemicals and found one to be superior to the others. However, they suggested to continue with experimentation. In addition, Kreigh and Sultan called for the installation of a moisture barrier which sloped away from the base of the walls as a mean to stop capillary action.

Kriegh and Sultan stabilization's recommendations for the Great House were not carried out because they were considered too invasive and drastic. In addition, the chemical experimentation suggested by Kreigh and Sultan was also not carried out.

1977: David Wilcox and Lynette Shenk (Cultural Resource Management Section of the Arizona State Museum) completed a study of the Great House at Casa Grande Ruins National Monument. Funding was provided by the National Park Service.

Two earlier excavations on the south and east sides of the Great House were re-opened and detailed profiles were drawn of all exposed deposits, including the first complete and extensive condition survey of both interior and exterior walls of the structure. In addition, the report includes a review of the literature of the Great House, caliche testing, analysis of wall construction technique and recommendations.

A three-phase chemical research plan was developed by the Western Archaeological Center. The plan involved the testing of chemical soil amendments to find one that would effectively protect badly eroded walls and development of durable overcoat mortar for soil cement walls which would give a more natural appearance. Twenty eight testing walls were constructed at Casa Grande from soil taken from the prehistoric Escalante Ruins. The testing walls were allowed to weather for nine months (between March 1977 and January 1978) before they were treated with 10 water-based chemicals. The effectiveness of these chemicals was monitored over a period of one year with unsuccessful results. No overcoat mortar was tested.

The last phase of the chemical testing on the experimental walls came about through a contract with the Arizona State University, College of Engineering. Its purpose was to determine the effectiveness of electro-chemical treatment of earthen walls in terms of compressive strength, decreased capillary action, appearance, and weathering. The Arizona State engineers recommended the use of aluminum sulfate for electro-chemical treatment, due to that it increased the compressive strength and reduced capillary action of the walls. Thus, walls suffered less weathering. Also, the treatment had less effect on wall color than other treatments. No action was taken to implement this study's recommendation.

1980: A plan was prepared by Wilcox which urged that the walls be stabilized by filling all the second-story beam holes, roof grooves, and erosion grooves with caliche. Such course of action meant covering one-third of the culturally significant features on wall surfaces. Howard Chapman, Western Regional Director, decided not to follow this plan.

1984: Crack gauges were installed at several wall intersections to measure wall movement. These gauges are still in place.

Appendix B: Previous Analyses of the Caliche from the Great House²

Cook (1879)

An assemblage of New Jersey geologists, including professor George Cook, was part of a scientific investigation of the Great House led by Henry Hanks in April 1879. Professor Cook took caliche samples from the Great House. The results from analysis of the caliche are the following:

Results

Provenance of Sample	Unspecified
Calcium carbonate content (CaCO₃)³	17%
Speculations on sources of CaCO₃	<ul style="list-style-type: none">• from sea shells from the Gulf of California• Naturally present in the soil• Lime was burned with the caliche for building purposes.

² Condensed from: Clemensen 1992, Littmann 1967, Vick 1973, Krieger and Sultan 1974, Wilcox and Shenk 1977, and Roy 1980.

³ No data was found related to the analytical technique/s used by Cook.

Littmann (1967)

Littmann was interested in comparing methods for manufacturing mortar and plaster used by Southwestern societies with those used by the Mayas. He studied some plasters and wall material from the Great House, and plaster and mortar from Montezuma Castle and Walnut Canyon. Since the Mayas used burned lime to make their mortar, he studied the effects of fire upon caliche, finding that burning tends to destroy the ability of the caliche to form a curable plaster.

Sample Provenance	Piece of plaster and wall material from debris removed from the Great House
Conclusions:	<ul style="list-style-type: none">• Plaster and mortar are essentially the same material.• Material is a form of clay with small amount of calcium mineral content and appreciable amount of sand.• Both plaster and wall material were cured under the same conditions, apparently without previous burning.• Natural hardening or cementation of both materials similar to sun-baked clay

Results

Sample Number	CG-1P	CG-1B	CG-2B	CG-3B
Loss on Ignition	10.8	11.9	9.0	13.7
Acid Insoluble Material	69.4	68.9	77.9	65.5
Ca	7.4	8.2	5.4	8.4
Mg	0.1	0.1	0.1	0.7
CaCO	18.5	20.5	13.5	21.0
MgCO	0.3	0.3	0.3	2.4
Acid Soluble Material+CaCO+MgCO	88.2	89.7	91.7	88.9
Calculated Loss on Ignition	8.3	9.2	6.1	10.5

Vick, Southern Arizona Testing Laboratory (1973)

Results

Sample provenance	Two samples of material obtained from a wall fragment that collapsed. No exact specification of location in the structure or year of the collapse.		
Material characteristics	<ul style="list-style-type: none"> • caliche-earth, with varies slightly in consistency. • Variation of clay content • Material Decomposes when saturated with water 		
Physical properties	Unit weight Specific Gravity Dry Compressive Strength	130-138 pounds/cu. 2.567 450 psi	
Mechanical Analysis (particle size)	Sieve Size 6" 432 1½ 1 ¾ ½ 3/8 ¼ #4 8 10 16 30 40 50 100 200 pan	%Retained (Indiv.) 0.0 1.6 1.0 3.8 2.4 4.8 2.1 3.8 7.2 4.1 4.8 10.3 7.6 46.5	%Passing (Cumul.) 100.0 98.4 97.4 93.6 91.2 86.4 84.3 80.5 73.3 69.2 64.4 54.1 46.5
Liquid Limit Plastic Limit Plasticity Index Soil Classification	42% 25% 17% Sand-clay mixture		

Vick, Southern Arizona Testing Laboratory (1973) (Continued)

Conclusions	<ul style="list-style-type: none">• The portion sampled was built by a bud dough method, by taking a portion of wet material and kneading it until it became a stiff dough. While the material was in the plastic state it was placed on the wall and pressed, formed and smoothed with the palmed hand. By this method, the material obtained its maximum density (virtually free of void) and it contained the minimum amount of water (reducing shrinkage to a minimum).• Remaining structure is deteriorating or crumbling rapidly during stormy weather.• The remaining of the structure will stand as long as it is dry and undisturbed. Should a portion become saturated it may crumble during its weakened, wet condition or it may crumble during the drying season due to shrink of the previously wet and expanded particles.• The bracing is protection only if the structure or foundation becomes saturated. Present bracing should not be removed unless strain is checked.• The covering cover the Great House has preserved this portion to a great extent, while walls away from the main structure continue to erode and crumble.• Erosion is evident where rain has been able to blow in against the exterior, unprotected walls.
Recommendations	<ul style="list-style-type: none">• Provide additional cover to prevent any direct contact of water to the structure.• Improve drainage around the structure so water will not stand near the walls• During prolonged cold, wet seasons provide some means of heat for drying (heat lamps).• The structure may be returned to a similar and usable state by using methods and materials which approximate those originally used. Mechanical means may be employed for mixing, placing and pressing new materials in place.

Kriegh and Sultan (1974)

Kriegh and Sultan physical and chemical analysis of caliche were part of a feasibility study in adobe preservation at the Casa Grande. The study included a comparison of some physical and chemical properties of soil-based materials from Casa Grande Ruins National Monument and Escalante Ruins, and caliche blocks (untreated and treated with different chemicals) weathering tests in order to compare performance of treatments. Only results obtained from the monument and untreated caliche sample weathering results are listed.

Results

Sample Provenance	Blocks of caliche were obtained from walls in Compound A , Casa Grande Ruins National Monument*	
Density (ρ)	116.7 lb/ft ³	
pH	7.3	
Soluble Salts, ppm	2450	
Nitrates (NO_3), ppm	7.0	
Phosphates (PO_4), ppm	0.15	
Sodium (Na), ppm	1000	
Potassium (K), ppm	8500	
Calcium (Ca), ppm	11,400	
Magnesium (Mg), ppm	1200	
Sulfates (SO_4)	2050	
X-Ray Diffraction	Major Minerals:	Calcite, Quartz
	Minor Minerals:	Dolomite, Plagioclase, Orthoclase, Illite-mica
	Trace Minerals:	Random mixed layer, Kaolinite, Chlorite, Amphibole

*The caliche material for samples did not come the Great House walls

Results on weathering of untreated caliche blocks

Sample Provenance	Compound A and Escalante Ruins	
Tests	Observations	Rating
Freeze-thaw cycles (after 6 cycles)	Absorbed water fast, broke to pieces, efflorescence	unsatisfactory
Rainfall dry cycles, erosion loss: 91.0%	Complete erosion except for few gravels.	Unsatisfactory
Surface abrasion, brushing loss: 1.3%; rain loss: 93.0%	Complete erosion (rain), except few gravels	Unsatisfactory
Heating-Cooling cycles (after 6 cycles) rain loss: 89%	Complete erosion (rain) except few gravels	Unsatisfactory
Soaking Test, material loss:100%	Complete slaking within 2 minutes	Unsatisfactory

Wilcox and Shenk (1977)

Three samples of caliche soil material from the Great House were submitted by Wilcox and Shenk for their analysis to the Soils and Water Testing Laboratory at the University of Arizona. One of the sample came from the backdirt in the Reaves trench outside the east door of the structure. The other two were portions of a fairly large fragment that fell from the west wall of the Great House on May 18, 1975.⁴

Conclusions (west wall samples)	<ul style="list-style-type: none">• Differences in caliche soil color and consistency.• West wall (exterior) show that the wall surface has been chemically altered, probably due to the extreme temperature fluctuations experienced in that area. The depth of the modification is about 3mm.• On the contact between the soil lenses that make up the wall, along a 26-51 mm wide zone extending inward from the exterior , but no more than 1 to 2mm thick, the soil lacked cementation, was very frothy, vesicular, and friable in appearance. This condition is possibly due to the effects of rainwater seeping along the contacts (lens edge). As rain water is often slightly acidic, it may have reacted with carbonates in the wall, producing the condition observed.• It was concluded that the caliche soil from the structure is not homogeneous and each sample is representative of an specific location.
--	---

Results of Analysis of Separate Pieces from Each Sample

Sample Provenance	Reaves Trench Backdirt	West Wall
Mechanical Analysis (particle size)		
Sand (2-0.05mm)	39.5%	39.1%
Silt (0.05-0.002mm)	35.0%	41.0%
Clay (<0.002mm)	25.5%	19.9%
Classification	Loam	Loam
Color (Munsell)	7.5YR 5/3 (wet) 7.5YR 7/3 (dry)	5YR 6/3 (wet) 7.5YR 8/2

⁴ From adjacent location to sample analyzed in the present study.

(Wilcox and Shenk (1977) (Continued)

Soluble Salts in Saturated Extract of Separate Pieces from Each Sample and of Sub-Samples from Ground-up Primary Sample

Sample Separation	Analysis of Separate Pieces from Each Sample		Analysis of Sub-Samples from Ground-up Primary Sample		
Sample Provenance	Reaves Trench	West Wall	Reaves Trench	West Wall	West Wall
Soluble Salts in Saturation Extract					
pH	7.9	7.7	7.6	7.8	7.6
ECe x 10 ³	7.56	9.5	4.8	6.7	8.4
Total Sol. Salts	5292	6650	6229	7482	9841
ESP/e	9.0	2.0			
Ca (ppms)	890.0	840	1180	1220	1940
Mg (ppms.)	3321.0	148	200	188	88
Na (ppms.)			400	880	928
Cl (ppms.)			576	1775	1405
SO ₄ (ppms.)	1500.0	540	2450	1930	3411
HCO ₃			85	275	305
NO ₃	891	148	1337.6	1214.4	1764.4
PO ₄	15	540			
1:5 H O Routine					
pH	7.9	8.1	7.6	7.5	7.6
ECe x 10 ³	0.97	1.29	1.09	1.35	1.50
Total Sol. Salts	587.0	1208.7	657	851.18	997.68
Ca (ppms)	44.0	390	85	122	152
Mg (ppms.)	7.0	75	16	14	10
Na (ppms.)	99.0	112	87	108	136
Cl (ppms.)	83.2	138	56	152	136
SO ₄ (ppms.)	146.0	145.0	194	172	239
HCO ₃	48.8	45.1	12.20	23.18	17.08
NO ₃	159.0	303.6	206.8	264.0	303.6
CaCO equiv. <2mm	25.88%	22.0%	24.5%	26.0%	24.0%
Total			30.7%	31.50%	34.6%
X-ray Diffraction on the Clay Fraction	Montmorillonite Mica Vermiculite Chlorite Kaolin Interstratified		2 (small amount)		
From Sample: Reaves Trench Backdirt			4 (large amount)		
			0		
			0		
			0		
			0		

Arizona State University - Charles O'Bannon (1978)

Results

Compressive strength	Fc=2150, psf=14.93 psi
Dry density	90pcf
Specific gravity	2.72
Plasticity Index	2

Roy (Pennsylvania State University) (1980)

Results of Various Tests

Sample Provenance	Not Specified.	
Microscopic Observations	Aggregates Quartz sand 0.1-2mm, clear to yellowish Undifferentiated Igneous Sand small rock fragments up to 0.5cm caliche fragments up to 0.5cm	Binder Crumbly, poorly coherent, carbonate-containing (Munsell: 5YR 7/2)
Density	Bulk Density 2.627	Percentage Pore Space 15%
Polarized Microscope Observations	Aggregate Very fine grained and mottled gray to yellow to brown. Patches within the matrix are coarser grained and show typical carbonate extinction and high birefringence.	Binder (particles passed #200 sieve) Irregular angular quartz grains, 0.25 to 0.6mm in diameter, which show undulatory extinction and feldspar crystals with distinct crystal faces. Muscovite laths and a few rounded hornblende crystals were also observed.
Scanning Electron Microscope	Microstructure characterized by a porous, crystalline matrix in which a variety of aggregates are embedded. The morphology of the matrix ranges from pseudo-hexagonal to rhombohedral crystals to massive and its typical of calcite. Aggregates in this sample are slightly to moderately etched, and small discrete crystals, probably calcite, appear to be growing from the pits in the aggregate surfaces. These crystals are less than about 5µm in size and appear to be coating the aggregates. Zoned or layered matrix/aggregate interfacial regions were not observed. The well crystallized, porous matrix suggests that the material is friable and have relatively low compressive strength. Calcium carbonate (CaCO ₃) and not lime (CaO) is the calcium contained in the sample.	
X-Ray Diffraction	Matrix or Binder (particles passed sieve #200) Calcite Quartz Feldspar (anorthite rich) Illite	Aggregates (non-nodule particle) Quartz Feldspar Gypsum
Differential Thermal Analysis (DTA)	50-100°C = dh. EW, 140°C = dh. I, 200°C (?); 860°C = dc. C	

Roy (198) (Continued)

Results of Quantitative Chemical Analyses

Sample Provenance	Casa Grande Ruins National Monument (no specific location)
SiO ₂ %	44.4
Al ₂ O ₃ %	8.27
TiO ₂ %	0.51
Fe ₂ O ₃ %	2.80
CaO %	16.72
MgO %	2.91
MnO %	0.038
Na ₂ O %	1.21
K ₂ O %	2.07
Ba, ppm	710
Cr, ppm	40
Cu, ppm	60
Ni, ppm	25
Sr, ppm	600
V, ppm	85
Zr, ppm	230
Cl, ppm	---
SO ₃ , ppm	0.35
CO ₂ , ppm	13.4
H ₂ O 110°C	2.8
Total	6.4

Appendix C: Observations and Tests

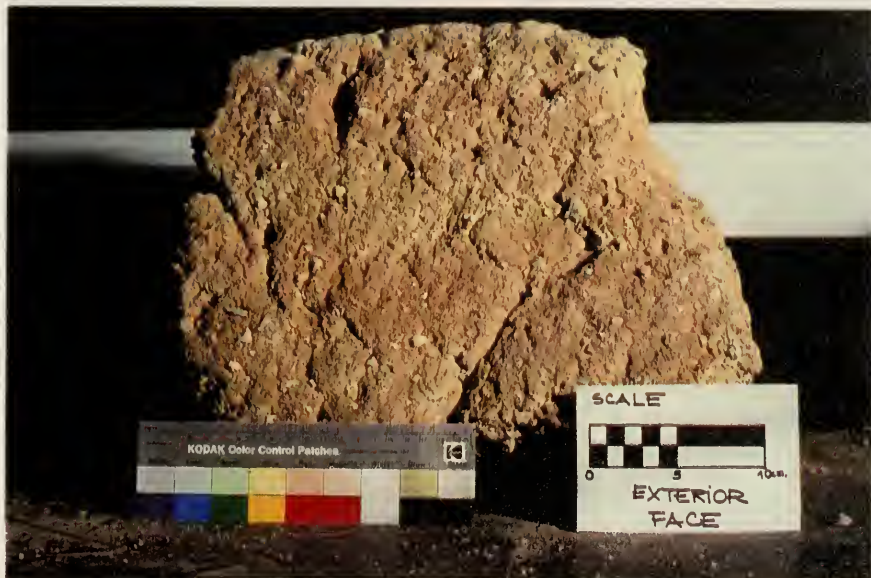
C1: Data and Observations from Caliche Fragment

CALICHE FRAGMENT - EXTERIOR (FRONT) FACE

OBSERVATIONS

Munsell Color: 7YR 6/4

Very compact and dense surface. Not crumbly to the touch. Homogeneous in constituents all over the surface. Surface even in color. No detected areas that look different. Some superficial cracks. Smooth, regular surface, it looks like it has a skin. Skin is hard when tapped with fingers. Nodules and aggregates exposed and cleaned on surface. Nodules and aggregates very well hold by the soil matrix. No insect activity detected on this face.



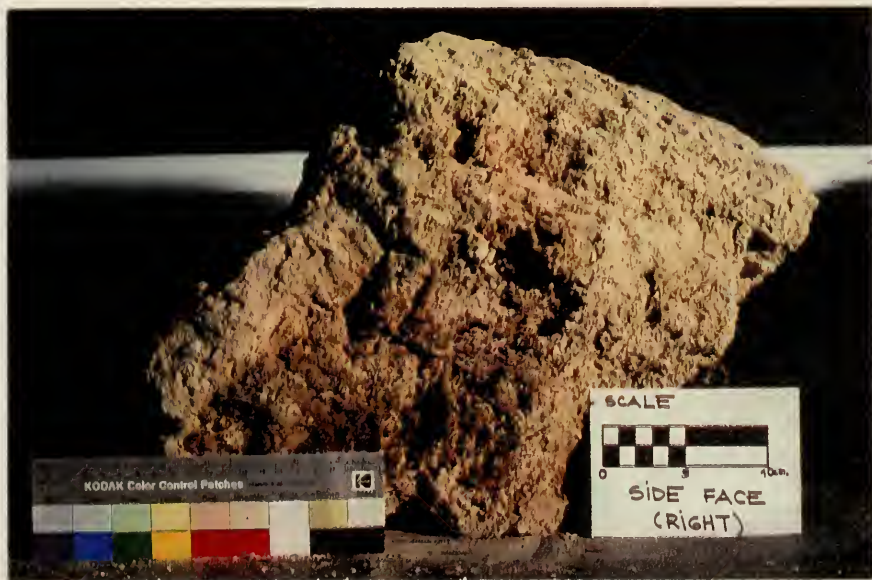
CALICHE FRAGMENT - SIDE (RIGHT) FACE

OBSERVATIONS

Munsell: 5YR 7/4

Surface is not smooth and is very irregular. Several cracks; probably this fragment broke along one of its cracks. Material is very crumbly, specially in areas of insect activity. Surface is even in color. Nodules and aggregates completely embedded in the soil matrix.

Great Amount of inactive insect and animal activity (webs, cocoons, insect nests, insects skeletons).



CALICHE FRAGMENT - SIDE (LEFT) FACE

OBSERVATIONS

Munsell: 5YR 7/4

Surface is not smooth and is very irregular. Several cracks. Material is very crumbly, specially in areas of insect activity. Powdery surface. This face has a depression in its middle. Surface even in color. Nodules and aggregates completely embedded in the soil matrix.

Great Amount of inactive insect and animal activity (webs, cocoons, insect nests, insects skeletons, animal excrement), concentrated specially along cracks.



CALICHE FRAGMENT - INTERIOR (REAR) FACE

OBSERVATIONS

Munsell: 5YR 7/4

Surface is not smooth and is very irregular. Several cracks. Surface is even in color. Material hard to the touch. Nodules and aggregates completely embedded in the soil matrix.

Great Amount of inactive insect and animal activity (webs, cocoons, insect nests, insects skeletons) spread all on the surface. White stain (efflorescence) located in the center of the face.



CALICHE FRAGMENT - LOWER FACE

OBSERVATIONS

Munsell: 5YR 7/4

Surface is not smooth and is very irregular. Several cracks. Surface is hard to the touch and even in color. Nodules and aggregates completely embedded in the soil matrix.

No insect activity on this face. This face has a depression in its central area.



CALICHE FRAGMENT - UPPER FACE

OBSERVATIONS

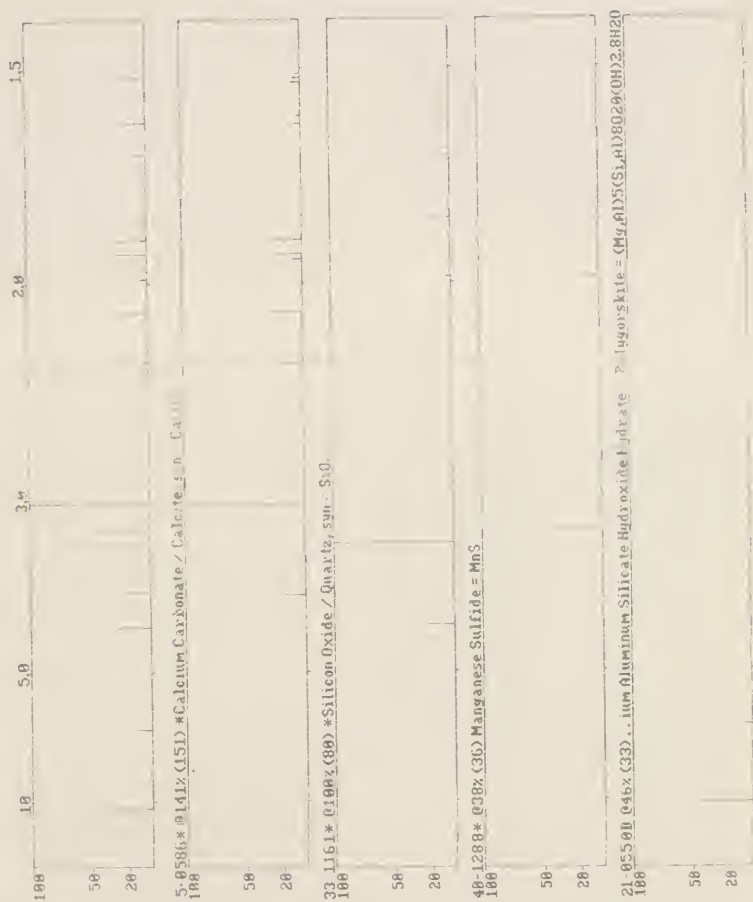
Munsell: 5YR 7/4

Surface is not smooth and is very irregular. Several cracks. Surface hard to the touch and is even in color. Nodules and aggregates completely embedded in the soil matrix.

Great Amount of inactive insect and animal activity (webs, cocoons, insect nests, insects skeletons).



C2: Additional Data from X-ray Diffraction



Data from X-ray diffraction of caliche fines (passed #200)

31-0783

Wavelength= 1.5418

Mg₅(Si₄Al)8O₂₀(OH)₂·8H₂O

2θ Int h k l

Magnesium Aluminum Silicate Hydroxide Hydrate

8.502 100 1 1 0
13.924 14 2 0 0
16.415 10 1 3 0

Palygorskite

19.862 20 0 4 0

Rad.: CuKα λ: 1.5418 Filter: Ni Beta d-sp:

20.852 20 1 2 1

Cut off: Int.: Diffract. I/Icor

21.516 2 3 1 0

Ref: Christ, Hathaway, Hostettler, Shepard, Am. Mineral., 54, 198 (1969)

24.184 16 2 2 1
25.900 2 1 5 0
26.808 8 2 3 1

Sys.: Orthorhombic S.G.: P

28.059 12 4 0 0

a: 12.725 b: 17.872 c: 5.242 A: 0.7120 C: 0.2933

28.799 16 3 2 1

α: β: γ: Z: 2 mp:

30.953 4 3 3 1

Ref: Ibid.

33.447 8 2 5 1
34.646 10 0 6 1
34.953 12 1 0 2
35.351 20 1 6 1Dx: 2.370 Dm: SS/FOM: F₁₆ = 13 (.0186, 65)

Specimen from Sapillo, New Mexico, USA Sepiolite group, palygorskite subgroup. PSC: oP122 To replace 21-550. Volume[CD]: 1192.14


© 1997 JCPDS-International Centre for Diffraction Data. All rights reserved
PCPDFWIN v. DEMO

31-0783

Wavelength= 1.5418

Mg₅(Si₄Al)8O₂₀(OH)₂·8H₂O

d(A) Int h k l

Magnesium Aluminum Silicate Hydroxide Hydrate

10.40 100 1 1 0
6.36 14 2 0 0
5.40 10 1 3 0

Palygorskite

4.47 20 0 4 0

Rad.: CuKα λ: 1.5418 Filter: Ni Beta d-sp:

4.26 20 1 2 1

Cut off: Int.: Diffract. I/Icor.

4.13 2 3 1 0

Ref: Christ, Hathaway, Hostettler, Shepard, Am. Mineral., 54, 198 (1969)

3.68 16 2 2 1
3.44 2 1 5 0
3.35 8 2 3 1
3.18 12 4 0 0
3.10 16 3 2 1

Sys.: Orthorhombic S.G.: P

2.899 4 3 3 1

a: 12.725 b: 17.872 c: 5.242 A: 0.7120 C: 0.2933

2.679 8 2 5 1

α: β: γ: Z: 2 mp:

2.589 10 0 6 1
2.567 12 1 0 2
2.539 20 1 6 1

Ref: Ibid.

Dx: 2.370 Dm: SS/FOM: F₁₆ = 13 (.0186, 65)

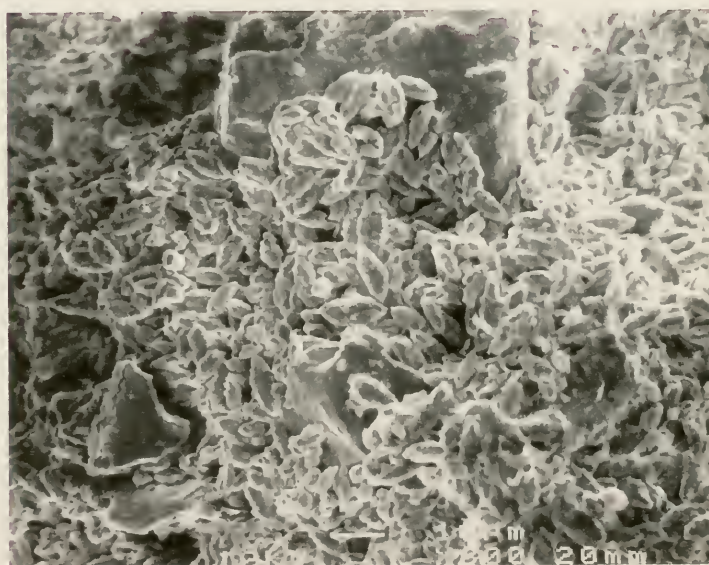
Specimen from Sapillo, New Mexico, USA Sepiolite group, palygorskite subgroup. PSC: oP122 To replace 21-550. Volume[CD]: 1192.14


© 1997 JCPDS-International Centre for Diffraction Data. All rights reserved
PCPDFWIN v. DEMO

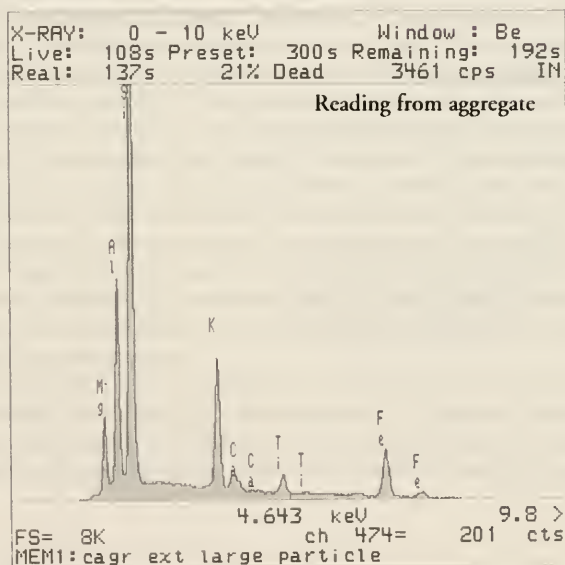
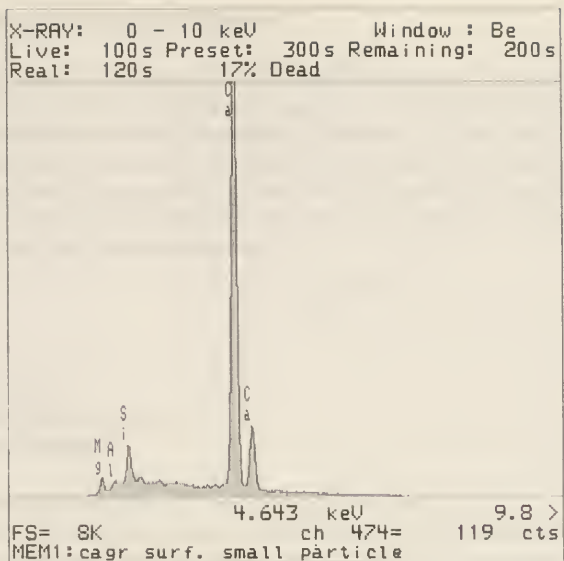
Data from X-ray diffraction for clay identification



Electron dot mapping. Reading of Mg, Al, Si, K, Ca and Fe for sample CAGR Ext



SEM photograph of CAGR Ext used for electron dot mapping. Bar is 10μm. Mag.: 800X.



Electron dot mapping. Reading of different particles of caliche (aggregates and from the matrix).

C3: Acid Soluble (Carbonate) Content

The procedure selected for these tests are a modified version of experiment No. 21 from "A Laboratory Manual for Architectural Conservators" (Teutonico, 1988) which basically follows the acid-soluble weight loss method (Channey et al. 1981, 10-11).

In brief⁵ the method consists of: (1) treatment of specimen of known dry weight with dilute HCl until all visible reactions are complete, (2) washing the specimen with de-ionized water, and (3) drying the specimen and weight recording. The percent of CaCO₃ is calculated using the following formula:

$$C = \frac{W_i - W_f}{W_i} \times 100$$

where:

C = CaCO₃ percent

W_i = initial dry weight (g), and

W_f = final dry weight (g)

Procedure of Acid Digestion of the Complete Samples

1. Samples CAGR A, CAGR B and CAGR C were dried in oven at 110°C for 24 hours until constant weight and their weight recorded.
2. Each sample was placed in a beaker, moistened with de-ionized water and then a 14% hydrochloric acid solution was poured onto the sample. The sample was left in the HCl solution until all the calcium carbonate was dissolved (no further reaction when more HCl solution added). All observations and reactions were recorded. During the digestion process, each sample was stirred daily and the soil was broken with a glass stirring bar. When needed, more fresh 14% solution of hydrochloric acid was added to the samples in order to reactivate the reaction. After the first two days of the digestion process, it was noticed that the hard nodules of caliche were still not dissolved and no fizzing was observed when adding more HCl solution. For this reason, the nodules of each sample were transferred to a 30% solution of HCl⁶ until all nodules were dissolved (approximately after 24 hours). Once the reaction was completed, the material obtained from the nodules was added to the digested material from their respective samples.
3. Then, all material left was washed⁷ and oven dried at 110°C for 24 hours until constant weight. Both weights, before and after acid digestion of the samples, were compared. The amount of CaCO₃ present in the sample before the acid digestion is represented by the loss of weight, which was converted to weight percent.

⁵ The acid-soluble weight loss method has been described in detail in Twenhofel 1941.

⁶ Immediate fizzing was recorded when the nodules of *caliche* were transferred to the 30% solution of HCl.

⁷ No filtering was required. Water was added, the material was let sit and the liquid was removed. This procedure was repeated until most HCl was washed away.

Acid Digestion Charts

NAME OF SAMPLE		CAGR A
DATE		March 1997
ORIGIN OF SAMPLE	From the outer section of original fragment, that is approximately between 0 and 10 cm. (between 0 and 1/3 depth of sample). This area corresponds to the layer of material located approximately in the outer 10 cm. of the Great House walls. This sample contains the characteristic reddish surface of the outer or exposed side of the walls.	
VISUAL DESCRIPTION OF SAMPLE	Very well cemented sample. Dense, not crumbly. Very hard to cut/brake in pieces. Hard nodules of different shapes and sizes.	
OBSERVATIONS: DISSOLUTION OF CAC03, COLOR OF LIQUID, ETC.	Took 3 days for complete digestion. Nodules very hard to dissolve. Thus, they were separated and a stronger solution of HCl was used to digest them. 24 additional hours for nodules to digest in stronger solution of HCl. Color of HCl solution after digestion: Very intense yellow color.	
CONCENTRATION OF HCL	14% HCl solution for the entire sample. 30% HCl solution for nodules.	
CALCIUM CARBONATE CONTENT ANALYSIS	Test # 21 modified/from: <i>A Laboratory Manual for Architectural Conservators.</i>	

**WT.OF SAMPLE
BEFORE HCL
DIGESTION (W1)**

**WT. OF SAMPLE
AFTER HCL
DIGESTION (W2)**

**WT. LOSS (W3 = W1 -
W2)**

**% WT. LOSS
(CAC03 CONTENT)**

$\frac{W1 - W2}{W1} \times 100$

342.90 g.

241.84 g.

101.06 g.

29.47 %

CAC03 CONTENT OF SAMPLE CAGR. A


**CAC03
CONTENT**

**REST OF
SAMPLE**

NAME OF SAMPLE		CAGR B
DATE		March 1997
ORIGIN OF SAMPLE	From the middle section of original fragment, that is approximately between 10 and 20 cm.(between 1/3 and 2/3 depth of sample). This area corresponds to the layer of material located approximately between 10 and 20 cm. deep in the exterior side of the Great House walls.	
VISUAL DESCRIPTION OF SAMPLE	Sample not as dense as CAGR A. More crumbly, specially during cutting of sample. Hard nodules of different shapes and sizes.	
OBSERVATIONS: DISSOLUTION OF CAC03, COLOR OF LIQUID, ETC.	Took 3 days for complete digestion. Nodules very hard to dissolve. Thus, they were separated and a stronger solution of HCl was used to digest them. 24 additional hours for nodules to digest in stronger solution of HCl. Color of HCl solution after digestion: Less intense yellow color than CAGR. A.	
CONCENTRATION OF HCL	14% HCl solution for the entire sample. 30% HCl solution for nodules.	
CALCIUM CARBONATE CONTENT ANALYSIS	Test # 21 modified/from: <i>A Laboratory Manual for Architectural Conservators</i>	

WT.OF SAMPLE BEFORE HCL. DIGESTION (W1)	344.64 g.
WT. OF SAMPLE AFTER HCL. DIGESTION (W2)	252.61 g.
WT. LOSS (W3 = W1 - W2)	92.03 g.
% WT. LOSS (CAC03 CONTENT) $\frac{W1 - W2}{W1} \times 100$	<u>26.70%</u>

CAC03 CONTENT OF SAMPLE CAGR. B



CAC03
CONTENT

REST OF
SAMPLE

NAME OF SAMPLE		CAGR C
DATE		March 1997
ORIGIN OF SAMPLE	From the back section of original fragment, that is approximately between 20 and 30 cm. (between 2/3 and 3/3 depth of sample). This area corresponds to the layer of material located approximately between 20 and 30 cm. deep in the exterior side of the Great House walls.	
VISUAL DESCRIPTION OF SAMPLE	Sample not as dense as CAGR A and CAGR B. Very crumbly, specially during cutting of sample. Hard nodules of different shapes and sizes.	
OBSERVATIONS: DISSOLUTION OF CAC03, COLOR OF LIQUID, ETC.	Took 2 days for complete digestion. Nodules very hard to dissolve. Thus, they were separated and a stronger solution of HCl was used to digest them. 24 additional hours for nodules to digest in stronger solution of HCl. Color of HCl solution after digestion: Light yellow color.	
CONCENTRATION OF HCL	14% HCl solution for the entire sample. 30% HCl solution for nodules.	
CALCIUM CARBONATE CONTENT ANALYSIS		Test # 21 modified/from: <i>A Laboratory Manual for Architectural Conservators.</i>

WT.OF SAMPLE
BEFORE HCL
DIGESTION (W1)

316.30g.

WT. OF SAMPLE
AFTER HCL
DIGESTION (W2)

289.95g.

WT. LOSS (W3 = W1 -
W2)

26.35 g.

% WT. LOSS
(CAC03 CONTENT)
 $\frac{W1 - W2}{W1} \times 100$

8.33%

CAC03 CONTENT OF SAMPLE CAGR. C

CAC03
CONTENT

REST OF
SAMPLE

Procedure of Acid Digestion of Samples by Particle Size

Samples CAGR. B and CAGR. C were dried in an oven at 110°C for 24 hours until constant weight. In order to divide each sample by its particle size content, a sieving procedure was used. After a failed attempt, dry sieving proved to be unsatisfactory for dividing the caliche. It was very difficult to disintegrate the solid sample without disintegrating the softer nodules of small size. The disintegration or breakage of any nodule would have given a particle size distribution not representative of the caliche. Therefore, sieving of the wet sample, or wet sieving, was used instead. The wet sieving procedure was performed in all samples according to the following steps:

1. Each sample, previously oven dried and weighed, was immersed in de-ionized water for at least 3 hours in order to soften and disintegrate the caliche. Sample CAGR B was left for a longer period (overnight) because it proved more difficult to disintegrate.
2. After disintegration, each sample was poured onto a stack of sieves (that varied according to each sample)⁸ to separate the samples by particle size. The sieves used for the test were as follows: #4 (ASTM, 4.75mm), #8 (ASTM, 2.36mm), #16 (1.18mm), #30 sieve (ASTM, 600µm), #50 (ASTM, 300µm), #100 (ASTM, 150µm), #200 (ASTM, 75µm) and pan (<75µm). A de-ionized water jet and some gentle finger pressure was used in order to ease the sieving procedure. This procedure was repeated with all the sieves in the stack. All material passed sieve #30 (in the case of sample CAGR C) and passed #200 (in the case of sample CAGR B) were collected.
3. After the sieving procedure was completed, the material retained in each sieve was transfer (by backwashing) to an evaporating dish and let it stand for a short period of time until the top of the suspension became clear. Most of the clear water was poured off and the material was oven dried for 24 hours at 110° C until constant weight. Weights were compared to the initial total weight of the samples.
4. All fractions were mixed and re-sieved in dry to obtain accurate particle size distribution.
5. The dry weight of each fraction of the sample was recorded and the dry weights of all the fractions were compared again to the initial weight of the sample at the beginning of the experiment. Each fraction of sample was named according to the sieve size: #4, #8, #16, retained #30, passed #30, #50, #100, #200 and passed #200.
6. Each fraction of sample was placed in a beaker, some de-ionized water added, and then a 14% HCl solution was added to each fraction. A 30% HCl solution⁹ was used for the larger particles, #4 and #8, in order to dissolve the large nodules strongly cemented by CaCO₃. When needed, fresh HCl solution was added in order to reactive the reaction. After the reaction was completed (1 to 2 days), the remaining material of each fraction was washed, filtered and, oven dried at 110°C for 24 hours until constant weight. Both weights, before and after acid digestion, were compared. The amount

⁸ CAGR. B according to the following sieves: #30 (particles from > 4.75mm to = 600µm), #50, #100, #200 and passed #200; and sample CAGR. C according to #4, #8, #16, #30 and passed #30 (particles = 300µm to < 75µm).

⁹ 30% HCl solution proved to be satisfactory to dissolve the larger nodules in the previous test.

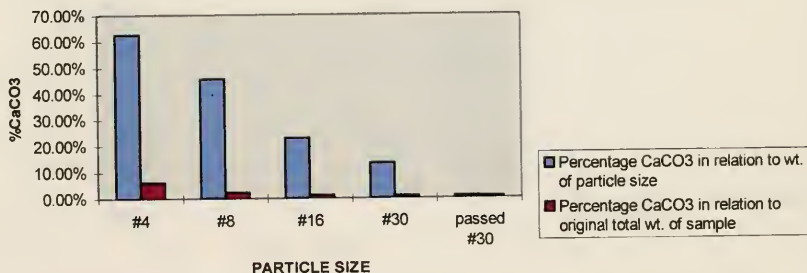
of CaCO_3 present in the sample before the acid digestion was represented by the loss of weight, which was converted to weight percent.

NAME OF SAMPLE	CAGR C	DATE	March 1997
ORIGIN OF SAMPLE	Material retained #4, #8, #16, #30 and passed #30 from caliche between 20-30 cm. of original fragment.		
VISUAL DESCRIPTION OF SAMPLE	The different particles sizes are composed by particles of various shapes and sizes. In general, there is a decrease of nodules with the decrease of particles size. Very little content of nodules in material passed #30.		
OBSERVATIONS: DISSOLUTION OF CaCO_3 , COLOR OF LIQUID	Reaction completed after 2 days. Color of HCl solution after digestion: intense yellow color for #4, #8 and #16; less intense yellow for #30 and passed #30.		
CONCENTRATION OF HCL	30% HCl solution of material retained #4, #8 and #16. 14% HCl solution for material retained #30 and passed #30.		
CALCIUM CARBONATE CONTENT BY PARTICLE SIZE	Test # 21 modified from: <i>A Laboratory Manual for Architectural Conservators.</i>		

SIEVING AND HCL DIGESTION RESULTS

ORIGINAL WEIGHT OF SAMPLE		233.73 g.				
TOTAL CONTENT OF CaCO_3 OF SAMPLE		11.52%				
SIEVE #	SIEVE SIZE	W_i = WT. MATERIAL RETAINED BEFORE HCL DIGESTION (g)	W_f = WT. MATERIAL AFTER HCL DIGESTION (g)	$W_i - W_f$ = WT. LOSS (g)	% CaCO_3 CONTENT BY PARTICLE SIZE	% CaCO_3 CONTENT ACCORDING TO ORIGINAL TOTAL WEIGHT OF SAMPLE
4	4.75	22.91	8.54	14.37	62.72%	6.15%
8	2.36	12.34	6.70	5.64	45.70%	2.41%
16	1.18	13.80	10.61	3.19	23.11%	1.36%
30	600 μm	16.23	14.04	2.19	13.49%	0.93%
passed 30	<600 μm	168.45	166.91	1.54	0.91%	0.65%

PERCENTAGE OF CaCO_3 CONTENT BY PARTICLE SIZE FOR SAMPLE CAGR. C

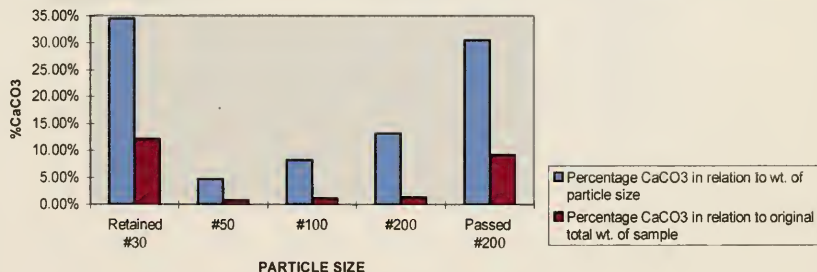


NAME OF SAMPLE	CAGR B	DATE	March 1997
ORIGIN OF SAMPLE	Material retained #4, #8, #16, #30, #50, #100, #200, and passed #200 from caliche material between 10-20 cm. of original fragment.		
VISUAL DESCRIPTION OF SAMPLE	Material retained #30: Particles of various sizes and shapes. Mostly nodules of different sizes and shapes. Material retained #50, #100, #200 and passed #200: Particles of various shapes and sizes. Decrease in content of nodules with the decrease of particle size. Particles #200 and passed #200 had no nodules.		
OBSERVATIONS: DISSOLUTION OF CaCO_3 , COLOR OF LIQUID	Reaction completed after 2 days. Color of HCl solution after digestion: intense yellow color for #4, #8, #16 and #30; less intense yellow for rest of the particles sizes.		
CONCENTRATION OF HCL	30% HCl solution of material retained #4, #8, and #16. 14% HCl solution for rest of the particle sizes.		
CALCIUM CARBONATE CONTENT BY PARTICLE SIZE	Test # 21 modified/from: <i>A Laboratory Manual for Architectural Conservators.</i>		

SIEVING AND HCL DIGESTION RESULTS

TOTAL WEIGHT OF SAMPLE				198.835g		
TOTAL CONTENT OF CaCO_3 SAMPLE				24.70%		
SIEVE #	SIEVE SIZE	W_i = WT. MATERIAL RETAINED BEFORE HCL DIGESTION (g)	W_f = WT. MATERIAL AFTER HCL DIGESTION (g)	$W_i - W_f$ = WT. LOSS (g)	% CaCO_3 CONTENT BY PARTICLE SIZE	% CaCO_3 CONTENT ACCORDING TO ORIGINAL TOTAL WEIGHT OF SAMPLE
retained 30		70.355	46.07	24.285	34.51%	12.21%
50	300 μm	21.57	19.93	1.64	4.63%	0.82%
100	150 μm	27.51	25.23	2.28	8.28%	1.15%
200	75 μm	19.21	16.67	2.54	13.22%	1.28%
passed 200	<75 μm	60.19	41.82	18.37	30.52%	9.24%

PERCENTAGE OF CaCO_3 CONTENT BY PARTICLE SIZE FOR SAMPLE CAGR. B



C4: Particle Size Analyses (ASTM 422-63)

Procedure of Particle Size Analysis Without Acid Digestion

Samples CAGR B and CAGR C were oven dried for 24 hours at 110°C until constant weight. Weights of samples were recorded after oven drying was completed. Then, the test was performed according to the procedure detailed in “A Laboratory Manual for Architectural Conservators” (Teutonico, 1988), experiment 18A.

Procedure of Particle Size Analysis With Total Acid Digestion

1. Samples CAGR. B and CAGR. C were entirely digested in Hydrochloric acid in order to remove all calcium carbonate content, both from the matrix of the caliche and from the nodules. Acid digestion was performed according to the test procedure of “acid digestion of the complete sample”, using a 30% solution of hydrochloric acid in order to disintegrate the hard nodules.
2. After acid digestion was completed, the remaining material was washed and filtered. All material was dried slowly in order to prevent binding of the fine particles (particularly clays), which would have ruined the particle size analysis test. For this reason, all digested material, coarse and fine, was mixed and then let it dry at room temperature for several days. The material collected in the filters was also dried at room temperature and when it was dried enough to, it was carefully piled off the filters. The drying process was completed with a heat lamp avoiding fast drying or close exposure to the lamp. All material was mixed several times during heat-lamp drying.¹⁰
3. Oven drying was used at the very end of the drying process. The temperature of the oven proved to be satisfactory at 65°C. The material was dried until constant weight was reached.
4. Sieving was performed following the procedure detailed in Experiment 18A (Teutonico 1988, 73)

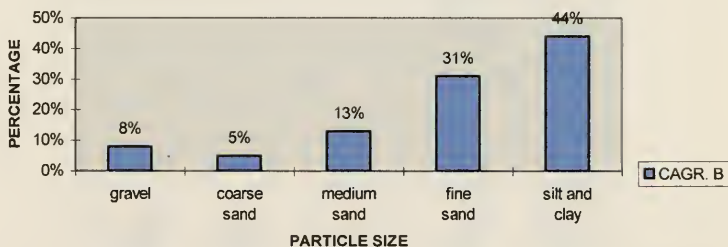
¹⁰ It was found extremely important to avoid fast heating and continuously mix the fines obtained from filtering with the rest of the coarse material. Otherwise, clays tend to bind strongly in small conglomerates, which are almost impossible to desegregate for sieving.

Particle Size Analysis Charts

Particle Size Analysis With No Acid Digestion

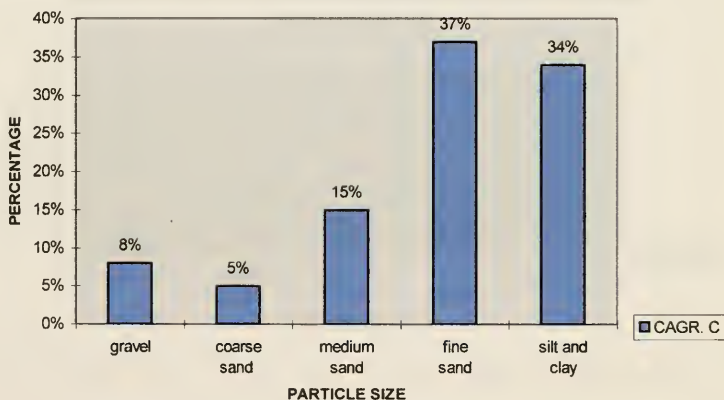
SAMPLE	CAGR B NO ACID DIGESTION	DATE	February 1997
ORIGIN OF SAMPLE		From the middle section of original fragment, that is approximately between 10 and 20 cm. (between 1/3 and 2/3 depth of sample). This area corresponds to the layer of material located approximately between 10 and 20 cm. deep in the exterior side of the Great House walls.	
SAMPLE PREPARATION		Material was prepared accordingly with the instructions from "A Laboratory Manual for Architectural Conservators" Experiments 18A and 18B	
TEST		D 422-63 <i>Standard Method for Particle Analysis of Soils</i>	
WEIGHT TOTAL SAMPLE (g):		257.97	
SIEVE #	WT. RETAINED (g)	% RETAINED	% PASSING
4	19.66	7.62	92.38
8	13.10	5.08	87.30
16	13.87	5.38	81.92
30	19.15	7.42	74.50
50	30.86	11.96	62.54
100	29.52	11.44	51.11
200	18.62	7.22	43.89
passed 200	113.19	43.88	

SAMPLE CAGR.B - PARTICLE SIZE ANALYSIS WITHOUT ACID DIGESTION



SAMPLE	CAGR C NO ACID DIGESTION	DATE	February 1997
ORIGIN OF SAMPLE		From the back section of fragment sample, that is approximately between 20 and 30 cm.(between 2/3 and 3/3 depth of sample). This area corresponds to the layer of material located approximately between 20 and 30 cm. deep in the exterior side of the Great House walls.	
SAMPLE PREPARATION		Material was prepared accordingly with the instructions from "A Laboratory Manual for Architectural Conservators" Experiments 18A and 18B	
TEST		D 422-63 <i>Standard Method for Particle Analysis of Soils</i>	
WT. TOTAL SAMPLE (g):		243.62	
SIEVE #	WT. RETAINED (g)	% RETAINED	% PASSING
4	20.53	8.43	91.57
8	12.60	5.17	86.40
16	16.34	6.71	79.69
30	20.55	8.43	71.26
50	36.21	14.86	56.40
100	34.48	14.15	42.25
200	20.24	8.31	33.94
passed 200	82.67	33.93	

SAMPLE CAGR. C - PARTICLE SIZE ANALYSIS WITHOUT ACID DIGESTION



Particle Size Analysis With Total Acid Digestion

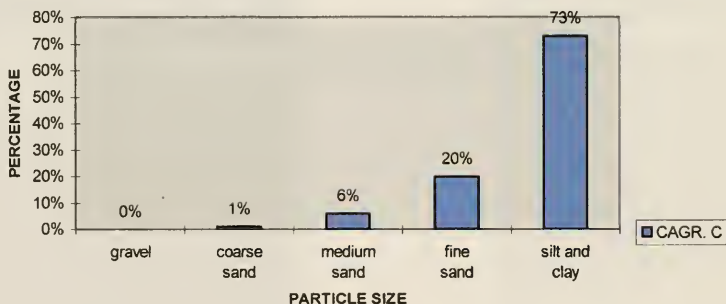
SAMPLE		CAGR B WITH TOTAL ACID DIGESTION	DATE	February 1997
ORIGIN OF SAMPLE			From the middle section of original fragment, that is approximately between 10 and 20 cm. (between 1/3 and 2/3 depth of sample). This area corresponds to the layer of material located approximately between 10 and 20 cm. deep in the exterior side of the Great House walls.	
SAMPLE PREPARATION			30% HCl solution used for digestion, especially for the hard nodules. Took 2 days for complete digestion. Color of HCl solution after digestion: Intense yellow.	
TEST			D 422-63 <i>Standard Method for Particle Analysis of Soils</i> and acid digestion of complete sample.	
WT. TOTAL SAMPLE (g)			470.46	
SIEVE #	WT. RETAINED (g)	% RETAINED	% PASSING	
4	2.27	0.48	99.52	
8	5.03	1.07	98.45	
16	9.48	2.01	96.44	
30	18.10	3.85	92.59	
50	29.87	6.35	86.24	
100	30.34	6.45	79.79	
200	21.71	4.61	75.18	
passed 200	353.66	75.17		

SAMPLE CAGR. B - PARTICLE SIZE ANALYSIS WITH TOTAL ACID DIGESTION

PARTICLE SIZE	PERCENTAGE
gravel	0%
coarse sand	1%
medium sand	6%
fine sand	17%
silt and clay	75%




SAMPLE	CAGR. C WITH TOTAL ACID DIGESTION	DATE	February 1997
ORIGIN OF SAMPLE		From the back section of original sample, that is approximately between 20 and 30 cm. (between 2/3 and 3/3 depth of sample). This area corresponds to the layer of material located approximately between 20 and 30 cm. deep in the exterior side of the Great House walls.	
SAMPLE PREPARATION		30% HCl solution used for digestion, especially for the hard nodules. Took 1-2 days for complete digestion. Color of HCl solution after digestion: Intense yellow.	
TEST		D 422-63 <i>Standard Method for Particle Analysis of Soils</i> and acid digestion of complete sample.	
WT. TOTAL SAMPLE (g)		477.02	
SIEVE #	WT. RETAINED (g)	% RETAINED	% PASSING
4	0.68	0.14	99.86
8	4.46	0.93	98.93
16	10.96	2.28	96.65
30	18.33	3.84	92.81
50	35.40	7.42	85.39
100	39.61	8.30	77.09
200	19.00	3.98	73.11
passed 200	348.58	73.07	

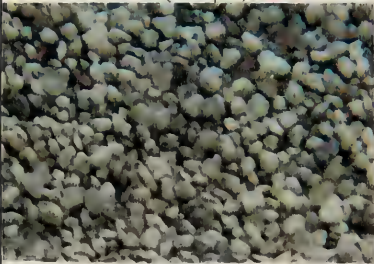



**SAMPLE CAGR. C - PARTICLE SIZE ANALYSIS WITH TOTAL
ACID DIGESTION**



C5: Observations of Caliche Soil Particles

Photographs taken with a Canon AE-1 with a 50mm lens and a macro lens. Magnification: +10.

Particles retained #	Color (Munsell notation)	Observations
#4 ($\geq 4.75\text{mm}$) 	5YR 8/2 pinkish white	Approximately 90% of these particles are composed of caliche nodules. Non-nodule particles are represented by quartz rich particles, mostly white, light gray and yellowish in color. Grain shapes are mostly rounded and subangular. Some of the non-nodule particles are glued together by a thin coating of calcium carbonate. High effervescence under a drop of 30% HCl.
#8 ($\geq 2.36\text{mm}$) 	5YR 8/2 pinkish white	Approximately 80% of these particles are composed of caliche nodules. Non-nodules particles are represented by quartz rich particles, mostly white, light gray and yellowish in color. Shapes are mostly rounded to subangular. Non-nodule particles are mostly subrounded to angular. Some nodules are formed by particles glued together and covered by calcium carbonate matrix. High effervescence under a drop of 30% HCl.
#16 ($\geq 1.18\text{mm}$) 	5YR 7/2 pinkish gray	Approximately, 50-60% of these particles are composed by caliche nodules. Non nodules particles are represented by quartz rich particles, mostly white, light gray and yellowish in color. Grains have various shapes from rounded (mainly nodules) to angular. Medium effervescence under a drop of 30% HCl.

Particles retained #	Color (Munsell notation)	Observations
#30 ($\geq 600\mu\text{m}$) 	5YR 7/3 pink	Approximately 50% of these particles are represented by caliche nodules, mostly rounded to angular. Non-nodules particles are mainly quartz rich particles, white, gray and yellowish in color, from rounded to angular, and present traces of calcium carbonate matrix on their surface. Medium effervescence under a drop of 30% HCl.
#50 (300 μm) 	5YR 7/3 pink	Approximately 40% of these particles are represented by caliche nodules, mainly subangular to angular. Non-nodules particles are mainly quartz rich particles, white, gray and yellowish in color, subrounded to angular. Medium effervescence under a drop of 30% HCl.
#100 (150 μm) 	5YR 7/3 pink	Approximately 30% of these particles are represented by caliche nodules, mainly subangular to angular. Non-nodules particles are mainly quartz rich particles, white, gray and yellowish in color, subangular to angular. Low effervescence under a drop of 30% HCl.
#200 (75 μm) 	5YR 7/3 pink	Approximately 20-25% of these particles are represented by caliche nodules, mainly subangular to angular. Non-nodules particles are mainly quartz rich particles, white, gray and yellowish in color, mainly subangular to angular. Low effervescence under a drop of 30% HCl.

C6: Atterberg Limits (Plastic and Liquid Limits) (ASTM D4318)

Sample: CAGR A no HCl digestion

Soil Description: From the outer section of original fragment, that is approximately between 0 and 10 cm. (between 0 to 1/3 depth of fragment). This area corresponds to the layer of material located approximately in the outer 10 cm. of the Great House walls. This sample contains the characteristic reddish surface of the outer or exposed side of the walls.

Sample Preparation: Follow Procedure from *A Laboratory Manual for Architectural Conservators*, Experiments 19 and 20

Observations: Sample hardly cemented. Compact, dense. Very difficult to prepare (sieving) for the test.

PLASTIC LIMIT

Test number	1	2	3	4	5	Average
Container number.	1	2	3	4	5	
Wet soil & container (M2) g	9.83	9.71	9.81	8.79	8.78	
Dry soil & container (M3) g	7.98	7.95	8.03	6.98	7.03	
Moisture loss (M2 - M3) g	1.85	1.76	1.78	1.81	1.75	
Container (M1) g	1.65	1.65	1.64	0.67	0.66	
Dry soil (M3 - M1) g	6.33	6.30	6.39	6.31	6.37	
MOISTURE CONTENT W %	29.22	27.93	27.85	28.68	27.47	28.23

LIQUID LIMIT

Test number	1	2	3	4	5	6
Container number	1	2	3	4	5	6
Number of drops	4	5	13	9	4	4
Wet soil & container (M2) g	12.95	15.78	15.72	23.65	19.68	24.09
Dry soil & container (M3) g	10.09	12.40	12.57	20.60	15.34	18.57
Moisture loss (M2 - M3) g	2.86	3.38	3.15	3.05	4.34	5.52
Container (M1) g	1.65	1.63	1.61	10.37	1.66	1.65
Dry soil (M3 - M1) g	8.44	10.77	10.96	10.23	13.68	16.92
MOISTURE CONTENT W %	33.88	31.38	28.74	29.81	31.72	32.62

Liquid Limit (LL): 22
Plastic Limit (PL): 29
Plastic Index (PI): NP (non plastic)

Sample: CAGR B no HCl digestion

Soil Description: From the middle section of original fragment, that is approximately between 10 and 20 cm. (between 1/3 and 2/3 depth of fragment). This area corresponds to the layer of material approximately located between 10 and 20 cm. deep in the exterior side of the Great House walls.

Sample Preparation: Follow Procedure from *A Laboratory Manual for Architectural Conservators*, Experiments 19 and 20.

Observations: Sample more crumbly. Easy to disintegrate.

PLASTIC LIMIT

Test number	1	2	3	4	5	Average
Container number.	1	2	3	4	5	
Wet soil & container (M2) g	8.55	7.62	7.95	8.13	8.43	
Dry soil & container (M3) g	7.18	6.25	6.46	6.67	6.88	
Moisture loss (M2 - M3) g	1.37	1.37	1.49	1.46	1.55	
Container (M1) g	1.64	0.68	0.68	0.68	0.68	
Dry soil (M3 - M1) g	5.54	5.57	5.78	5.99	6.20	
MOISTURE CONTENT W %	24.72	24.59	25.77	24.37	25.00	24.89

LIQUID LIMIT

Test number	1	2	3	4	5	6
Container number	1	2	3	4	5	6
Number of drops	8	14	32	39	37	5
Wet soil & container (M2) g	25.59	26.42	23.33	26.10	22.33	25.64
Dry soil & container (M3) g	20.98	21.95	19.76	21.97	19.17	20.82
Moisture loss (M2 - M3) g	4.61	4.47	3.57	4.13	3.16	4.82
Container (M1) g	8.50	8.34	8.47	8.43	8.46	8.44
Dry soil (M3 - M1) g	12.48	13.61	11.29	13.54	10.71	12.38
MOISTURE CONTENT W %	36.93	32.84	31.62	30.50	29.50	38.93

Liquid Limit (LL): 34
Plastic Limit (PL): 24.89
Plasticity Index (PI): 9.11

Sample: CAGR C no HCl digestion

Soil Description: From the back section of original fragment, that is approximately between 20 and 30 cm. (between 2/3 and 3/3 depth of fragment). This area corresponds to the layer of material approximately between 20 and 30 cm. deep in the exterior side of the Great House walls.

Sample Preparation: Follow Procedure from "A Laboratory Manual for Architectural Conservators" Experiments 19 and 20.

Observations: Sample more crumbly. Easy to disintegrate.

PLASTIC LIMIT

Test number	1	2	3	4	5	Average
Container number.	1	2	3	4	5	
Wet soil & container (M2) g	8.18	7.65	8.68	7.68	8.15	
Dry soil & container (M3) g	6.65	6.19	6.25	6.27	6.52	
Moisture loss (M2 - M3) g	1.53	1.46	2.43	1.41	1.63	
Container (M1) g	0.68	0.68	0.68	0.69	0.68	
Dry soil (M3 - M1) g	5.97	5.51	5.57	5.58	5.84	
MOISTURE CONTENT W %	25.62	26.49	43.62*	25.26	27.91	26.32

*This result was discharged from the average value calculation

LIQUID LIMIT

Test number	1	2	3	4	5	6
Container number	1	2	3	4	5	6
Number of drops	9	28	8	9	25	31
Wet soil & container (M2) g	22.30	10.92	11.69	12.77	10.92	17.94
Dry soil & container (M3) g	18.40	8.61	8.28	9.85	8.51	13.98
Moisture loss (M2 - M3) g	3.90	2.31	3.41	2.92	2.41	3.96
Container (M1) g	8.43	2.62	1.64	2.64	1.69	2.63
Dry soil (M3 - M1) g	9.97	5.99	6.64	7.21	6.82	11.35
MOISTURE CONTENT W %	39.11	38.56	51.35	40.49	35.33	34.88

Liquid Limit (LL): 40
Plastic Limit (PL): 26.32
Plasticity Index (PI): 13.68

Sample: CAGR A with HCl digestion

Soil Description: From the outer section of original fragment, that is approximately between 0 and 10 cm. (between 0 to 1/3 depth of fragment). This area corresponds to the layer of material located approximately in the outer 10 cm. of the Great House walls. This sample contains the characteristic reddish surface of the outer or exposed side of the walls.

Sample Preparation: Follow Procedure from *A Laboratory Manual for Architectural Conservators*, Experiments 19 and 20.

Observations: Sample hardly cemented. Compact, dense. Very difficult to prepare (sieve) for the test. Sample digested in 14% solution of HCl.

PLASTIC LIMIT

Test number	1	2	3	4	Average
Container number.	1	2	3	4	
Wet soil & container (M2) g	6.62	6.60	6.67	6.67	
Dry soil & container (M3) g	5.08	5.06	5.11	5.12	
Moisture loss (M2 - M3) g	1.54	1.54	1.56	1.55	
Container (M1) g	0.70	0.70	0.70	0.71	
Dry soil (M3 - M1) g	4.38	4.36	4.41	4.41	
MOISTURE CONTENT W %	35.15	35.32	35.37	35.12	35.24

LIQUID LIMIT

Test number	1	2	3	4	5
Container number	1	2	3	4	5
Number of drops	21	12	11	13	15
Wet soil & container (M2) g	14.14	12.39	13.83	12.45	13.68
Dry soil & container (M3) g	10.12	8.98	9.88	8.98	9.92
Moisture loss (M2 - M3) g	4.02	3.41	3.95	3.47	3.76
Container (M1) g	0.74	0.71	0.70	0.71	0.71
Dry soil (M3 - M1) g	9.38	8.27	9.18	8.27	9.21
MOISTURE CONTENT W %	42.85	41.23	43.02	41.95	40.82

Liquid Limit (LL): 43
Plastic Limit (PL): 35.24
Plasticity Index (PI): 7.76

Sample: CAGR B with HCl digestion

Soil Description: From the middle section of original fragment, that is approximately between 10 and 20 cm. (between 1/3 and 2/3 depth of fragment). This area corresponds to the layer of material approximately located between 10 and 20 cm. deep in the exterior side of the Great House walls.

Sample Preparation: Follow Procedure from *A Laboratory Manual for Architectural Conservators*, Experiments 19 and 20.

Observations: Sample more crumbly. Easy to disintegrate. Sample digested in 14% solution of HCl.

PLASTIC LIMIT

Test number	1	2	3	4	Average
Container number.	1	2	3	4	
Wet soil & container (M2) g	4.83	4.78	4.72	4.75	
Dry soil & container (M3) g	3.76	3.65	3.63	3.63	
Moisture loss (M2 - M3) g	1.07	1.13	1.09	1.12	
Container (M1) g	0.71	0.70	0.72	0.70	
Dry soil (M3 - M1) g	3.05	2.95	2.91	2.93	
MOISTURE CONTENT W %	35.08	38.30	37.45	38.22	37.26

LIQUID LIMIT

Test number	1	2	3	4	5	6
Container number	1	2	3	4	5	6
Number of drops	10	13	15	12	16	19
Wet soil & container (M2) g	17.93	17.30	15.74	15.93	16.29	16.06
Dry soil & container (M3) g	12.94	12.50	11.42	11.62	11.96	11.84
Moisture loss (M2 - M3) g	4.99	4.80	4.32	4.31	4.33	4.22
Container (M1) g	0.69	0.72	0.70	0.70	0.70	0.70
Dry soil (M3 - M1) g	12.25	11.78	10.72	10.92	11.26	11.14
MOISTURE CONTENT W %	40.73	40.74	40.29	39.46	38.45	37.88

Liquid Limit (LL): 35
Plastic Limit (PL): 37.26
Plasticity Index (PI): NP (non plastic)

Sample: CAGR C with HCl digestion

Soil Description: From the back section of original fragment, that is approximately between 20 and 30 cm. (between 2/3 and 3/3 depth of fragment). This area corresponds to the layer of material approximately between 20 and 30 cm. deep in the exterior side of the Great House walls.

Sample Preparation: Follow Procedure from *A Laboratory Manual for Architectural Conservators*, Experiments 19 and 20.

Observations: Sample more crumbly. Easy to disintegrate. Sample digested in 14% solution of HCl.

PLASTIC LIMIT

Test number	1	2	3	4	Average
Container number.	1	2	3	4	
Wet soil & container (M2) g	6.51	6.27	6.55	6.63	
Dry soil & container (M3) g	4.83	4.68	4.83	4.90	
Moisture loss (M2 - M3) g	1.68	1.59	1.72	1.73	
Container (M1) g	0.71	0.71	0.70	0.70	
Dry soil (M3 - M1) g	4.12	3.97	4.13	4.20	
MOISTURE CONTENT W %	40.77	40.05	41.64	41.19	40.91

LIQUID LIMIT

Test number	1	2	3	4	5
Container number	1	2	3	4	5
Number of drops	12	13	16	11	15
Wet soil & container (M2) g	14.18	13.05	15.83	16.79	12.76
Dry soil & container (M3) g	9.82	9.06	10.99	11.72	8.99
Moisture loss (M2 - M3) g	4.36	3.99	4.84	5.07	3.77
Container (M1) g	0.71	0.70	0.70	0.71	0.71
Dry soil (M3 - M1) g	9.11	8.36	10.29	11.01	12.66
MOISTURE CONTENT W %	47.85	47.72	47.03	46.04	29.77

Liquid Limit (LL): undetermined

Plastic Limit (PL): 40.91

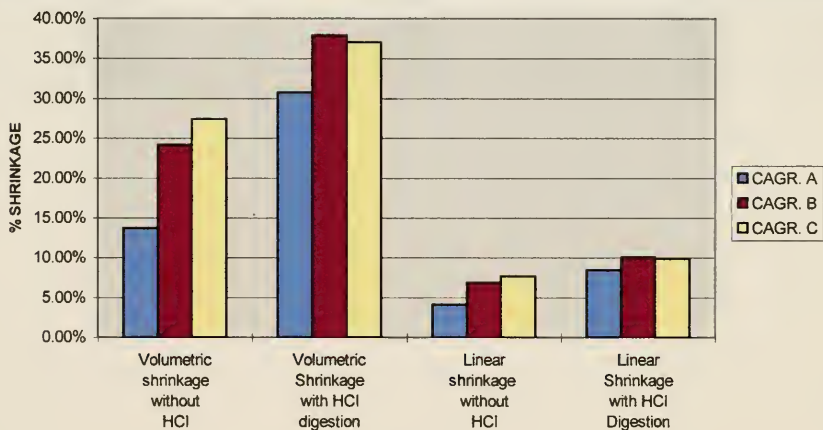
Plasticity Index (PI): undetermined

C6: Linear and Volumetric Shrinkage (ASTM D4943)

The technique for determining volumetric shrinkage involves: (1) the moisture content of a pat of wet soil is determined, (2) then the moisture-content loss to dry the soil to a constant volume is determined and subtracted from the initial moisture content to calculate the shrinkage limit, and (3) the volume of the dry soil pat is determined from its mass in air and its indicated mass when submerged in water (a coating of wax is used to prevent water absorption by the dry soil sample).

SHRINKAGE WITHOUT HCl DIGESTION			SHRINKAGE WITH HCl DIGESTION		
SAMPLE	VOLUMETRIC SHRINKAGE	LINEAR SHRINKAGE	SAMPLE	VOLUMETRIC SHRINKAGE	LINEAR SHRINKAGE
CAGR. A 1	17.45 %	5.16%	CAGR. A 1	35.84%	9.61%
CAGR. A 2	10.04%	3.10%	CAGR. A 2	34.12%	9.23%
CAGR. A 3	12.67%	3.86%	CAGR. A 3	25.64%	7.25%
CAGR. A MEAN VALUE	13.74%	4.13%	CAGR. A MEAN VALUE	30.74%	8.43%
CAGR. B 1	24.02%	6.85%	CAGR. B 1	39.61%	10.42%
CAGR. B 2	21.48%	6.21%	CAGR. B 2	36.34%	9.72%
CAGR. B 3	26.85%	7.54%	CAGR. B 3	39.63%	10.43%
CAGR. B MEAN VALUE	24.16%	6.87%	CAGR. B MEAN VALUE	37.98%	10.07%
CAGR. C 1	28.79%	8.01%	CAGR. C 1	36.02%	9.65%
CAGR. C 2	28.26%	7.88%	CAGR. C 2	38.11%	10.10%
CAGR. C 3	26.0	7.34%	CAGR. C 3	36.66%	9.79%
CAGR. C MEAN VALUE	27.39%	7.67%	CAGR. C MEAN VALUE	37.06%	9.87%

VOLUMETRIC AND LINEAR SHRINKAGE WITH AND WITHOUT HCl DIGESTION



C7: Determination of Moisture and Soluble Salt Content (Charola 1997) and Qualitative Analysis of Water-Soluble Salts (Teutonico 1988)

Procedure to Determine Moisture and Soluble Salt Content

1. Three samples of the caliche, CAGR A, CAGR B and CAGR C¹¹; were selected for determining moisture and soluble salt contents.
2. The solid samples were weighed and then dried in an oven at 105°C for at least 24 hours until constant weight was achieved. The weights of the dried samples were recorded and the moisture content of each sample was calculated.
3. For the soluble salt content, each dry sample was ground in an agate mortar until a uniform coarse powder was obtained. After grinding, the weights of the samples were recorded and then the samples were dried in an oven (set at 110°C) for at least two hours until constant weight. Then, each sample was placed in a beaker with sufficient de-ionized water and a magnetic stirring bar was added.
4. The beaker containing the sample was placed on a magnetic stirrer for two hours. Then, the suspension was left to settle overnight. The sample was filtered and the solid was dried in an oven for 24 hours until constant weight.
5. The weight of each sample was recorded and the soluble salt content was calculated. The solutions obtained from the filtration were dried and weighed as a confirmation of the above calculations and then used to identify the ions present by semi-micro chemical reactions or spot tests according to Experiment 16 in *A Laboratory Manual for Architectural Conservators* (Teutonico 1988, 58)

SAMPLE	MOISTURE % W/W	SOLUBLE SALT % W/W
CAGR A	1.56%	1.36%
CAGR B	1.50%	0.94%
CAGR C	1.48%	1.01%
AVERAGE	1.51%	1.10%

¹¹ The *caliche* material for the samples was selected following the same procedure that has been previously explained.

Procedure for Qualitative Analysis of Water-Soluble Salts (Teutonico 1988)

A drop of reagent was added to a test tube filled with 5ml of test solution (salts from caliche). Two controls were used for each test, de-ionized water and a 0.1M solution containing the anion tested. Control solutions used were: sodium sulfate (Na_2SO_4), sodium chloride (NaCl); sodium nitrate (NaNO_3), and sodium phosphate (Na_2HPO_4). Every positive test was confirmed with another reagent.

Results

ANION	CAGR. A	CAGR. B	CAGR. C
Sulfates (SO_4^{-2})	++	+++	+++
Chlorides (Cl^{-1})	++	+++	+++
Nitrites (NO_2^{-1})	+	++	++
Carbonates (CO_3^{-2})	++	++	+++

+ = presence of the ion; ++ = presence of the ion in notable quantity, and +++ = presence of the ion as the principal component.

C8: Water Related Tests

Procedure of Wet/Dry Cycling (ASTM D559 Modified)

1. All samples were oven dried at 110°C for 24 hours until constant weight. Then, they started a series of wet/dry cycles described as follows:
2. The samples were first immersed in de-ionized water for one minute, and all observable changes recorded. Following immersion, they were left to dry at room temperature for 24 hours and then weighed again.
3. Samples were then placed in oven and dried for 24 hours at 110°C temperature until constant weight. After oven drying, the samples were removed from oven and allowed to cool inside a desiccating chamber.
4. After cooling, they were weighed again. This procedure was repeated 12 times (cycles) and the time of immersion was doubled each cycle. The time of immersion of the last cycle was 34 hours and 4 minutes.
5. Observations were recorded throughout the entire procedure. At the end of the experiment, all samples¹² were dried in at 110°C for 24 hours until constant weight. The final weight of the samples was recorded.

The resistance to wet/dry cycling is expressed by both (1) the rate of loss of material during the experiment (see table # and graphic #) and (2) the percentage of material loss after the experiment.

SAMPLE #	WEIGHT OF SAMPLE BEFORE 12 CYCLES OF WATER IMMERSION/DRYING (g)	WEIGHT OF SAMPLE AFTER 12 CYCLES OF WATER IMMERSION/DRYING (g)	% W/W OF TOTAL LOSS OF MATERIAL (BASED ON ORIGINAL WEIGHT OF SAMPLE)
CAGR Int- Ext	786.50	259.8	66.96
CAGR Ext 1	119.50	116.0	2.92
CAGR Ext 2	101.37	65.9	34.99
CAGR Int 1	126.69	62.5	50.66
CAGR Int 2	100.34	0	100

Table #: Percentage of loss according to original weight of sample

¹² Except sample CAGR. Int. 2 which was lost during cycle 8.

Procedure for Capillary Water Absorption Test (NORMAL 11/85)¹³

1. The samples were dried in oven at 110°C for 24 hours until constant weight. Weights of samples were recorded. Each sample was set into a container on a porous support constituted by a pack (1cm. in thickness) of circular filter paper of the fast-filtering type (Whatman n° 4). The set of samples CAGR Ext. were placed with their reddish surface in contact with the filter paper.
2. De-ionized water was poured in slowly until the filter paper was totally wetted but keeping the water level below the top surface of the filter paper pack. In order to reduce the evaporation of the water and the influence of any changes in the thermohygrometric ambient conditions, the top of the container was closed with clear plastic wrap.¹⁴
3. At given time intervals the samples were taken out of the container, the wet surface patted dry with a damp cloth, and then weighed. After recording the weights, the samples were put back into the container. This procedure was continued until the variation in the amount of absorbed water between two successive weights, at a 24-hour interval, was $\leq 1\%$ of the amount of water absorbed. The experimental values obtained were plotted in a "capillary absorption curve", that is the amount of water absorbed per unit surface as a function of \sqrt{t} .
4. The amount of water absorbed by the sample per unit surface (M_i) at a time t_i , was calculated with the following equation:

$$M_i = [m_i - m_0] / S$$

where:

m_i = weight of the sample at time t_i (g);

m_0 = weight of the dry sample (g);

S = surface of the sample in contact with the porous support (cm^2)
given with a 5 % precision.

The average values M_i for each series were calculated and plotted in a graph as a function of \sqrt{t} , where time t is given in seconds.

¹³ This same procedure is also explained in Hennessy et al. 1983, 723.

¹⁴ Special care was taken in order to avoid that drops from water condensed on the clear plastic wrap fall on the samples.

Results for Capillary Water Absorption

AVERAGE CAPILLARY WATER ABSORPTION RESULTS M/S (10^{-2} g/cm ²)		
TIME t_t (IN MINUTES)	CAGR. EXT. (g/cm ²)	CAGR. INT. (g/cm ²)
15	1.05	2.22
45	1.65	2.61
120	1.66	2.78
240	1.70	Complete disintegration of samples due to excessive and rapid absorption.
1020	1.76	
2460	1.81	
3900	1.84	
5340	1.89	
6780	1.88	
8220	1.95	
9660	1.95	

INDEX

allothiic 71
argillic 8
Aridisols 7, 8
authigenic 41
birefringence 75, 76
borrow 22, 24
brecciation 40
bursage 12
calcaire 36
calcareous 35
calciorthids 9
calcite 79
calcrete 36
calix 35
calizo 35
cleavage 69
cob 27, 28, 203
Coolidge 1, 8, 9
creosote 12
croute 36

cryptocrystalline 67, 71, 72, 75, 76

Dateland 8

Denure-Laveen 8

detrital 39

disorthic 71

duricrust 36

duripan 8

epipedon 8

hardpan 36

Hohokam 1, 21, 22, 44

horizon 41, 42, 73

hyperthermic 9

interfluves 7

iodineweed 12

joint 144, 146, 147, 171

kankar 36

lens 29, 110, 144, 167, 168, 169

limewater 197, 198

lithification 73

loess 40

lozenge 80

McClellan 7

mesquite 12, 14

metate 22

micritic 65, 76, 77, 79, 80, 82

micrititization 40

microcrystalline 67, 72, 73, 74

micropedology 61

microsparitic 65, 82

Mozarabic 35

nari 36

nodule 42, 68, 69, 71, 72, 73, 74, 76, 84, 89, 92, 96, 97, 98, 99, 101, 192, 203

ondulatory 69

osmosis 82

palygorskite 55, 58, 59, 60, 81, 82, 104, 150

pedogenic 39

pedological 62

pedon 10

petrocalcic 8

phreatophytes 12

Pinal 5, 8

pise 27

poikilitic 74, 76

puddled 28, 29, 125, 168, 202

puddling 23, 24

saltcedar 12

saltgrass 12

sabach 36

seam 29, 144, 145, 146, 175, 176, 182, 183

shelter 31, 33

tepetate

tier 15, 17, 21, 144, 175, 176, 180, 182, 183, 184, 186,

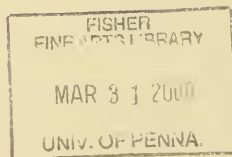
xerophytes 12

Anne & Jerome Fisher

FINE ARTS LIBRARY

University of Pennsylvania

Please return this book as soon as you have finished with it. It must be returned by the latest date stamped below.



3 1198 02651 6018



N/1198/02651/6018X

3 1198 02651 6018



N/1198/02651/6018X